UNIVERSITY OF CALIFORNIA, SAN DIEGO

Design and Syntheses of Nonnatural Amino Acids and Their Incorporation into Somatostatin and RGD Analogs

A dissertation submitted in partial satisfaction of the

requirements for the degree Doctor of Philosophy

in

Chemistry

by

Audrey Kelleman

Committee in charge:

Professor Michael S. VanNieuwenhze, Chair
Professor J. Andrew McCammon
Professor Daniel T. O'Connor
Professor Charles L. Perrin
Professor Emmanuel A. Theodorakis

2007

The Dissertation of Audrey Kelleman is approved, and it is acceptable in quality and form for publication on microfilm:

_____

_____

_____

_____

_____

Chair

UNIVERSITY OF CALIFORNIA, SAN DIEGO

2007

Dedication

For my grandparents,

Anna and Andrew Kelleman

and

Josephine and Stanley Krawiec

Thank you for teaching me, encouraging me, and indulging my endless curiosity. I never would have made it this far had you not been such a huge part of my life. Your love and support are with me always.

For my mentor,

Dr. Murray Goodman

I could not have chosen a better advisor. You taught me so much about chemistry and professionalism. You embraced my enthusiasm; instead of stifling it, you showed me how to utilize it. Thank you for accepting me into the "family".

You all left me too soon and are deeply missed.

Table of Contents

Signature Page iii

Dedication iv

Table of Contents v

List of Abbreviations ix

List of Figures xiv

List of Schemes xxi

List of Tables xxv

Acknowledgements xxvi

Vita xxxii

Publications xxxiii

Abstract of the Dissertation xxxiv

Chapter 1 1

1. Introduction and Overview 1

    1.1 Introduction 2

    1.2 Unnatural amino acids as conformational scaffolds 5

    1.3 Unnatural α-amino acid building blocks 6

    1.4 Cyclic peptides incorporating unnatural amino acid bridges 6

Chapter 2 8

2. Dibenzofuran-Scaffolded Somatostatin Analogs 8

    2.1 Introduction 9

2.1.1 Somatostatin: Discovery of a peptide hormone 9
2.1.2 Somatostatin receptors and their functions 12
2.1.3 Early structure-activity relationship studies of somatostatin 19
2.2 Synthetic analogs of somatostatin 21
2.2.1 Peptidic somatostatin analogs 21
2.2.2 Clincal use of peptidic somatostatin analogs 28
2.2.3 Somatostatin analogs which contain unnatural amino acids 30
2.2.4 Non-peptidic somatostatin analogs 43
2.3 Design and synthesis of scaffold-constrained SRIF-14 analogs 50
2.3.1 Type II' β-turns 50
2.3.2 Somatostatin analogs containing a dibenzofuran scaffold 56
2.3.2.1 Design of the compounds 56
2.3.2.2 Synthesis of the dibenzofuran scaffold 59
2.3.2.3 Synthesis of the dipeptides and coupling to the scaffold 63
2.3.2.4 NMR analysis 71
2.3.2.5 Results of binding assays 73
2.4 Conclusions 74
2.5 Experimental 77
2.5.1 General 77
2.5.2 Synthesis of the dibenzofuran scaffold 79
2.5.3 Syntheses of the dipeptides 89
2.5.4 Preparation of the final compounds 100

2.6 References 115

Chapter 3 125

3. Nonnaturally Occurring Nitrogen-Containing, Fused 5,6-Heterocyclic, Aromatic α-Amino Acids 125

3.1 Introduction 126

3.1.1 The use of nonnatural amino acids in peptides 126

3.1.2 Known modifications to the Trp^8 residue of somatostatin 127

3.2 The design and syntheses of nitrogen-containing heterocyclic α-amino acids 139

3.3 Incorporation of synthesized amino acids into peptides 163

3.4 Conclusions 168

3.5 Experimental 170

3.5.1 General 170

3.5.2 Syntheses of amino acids 172

3.5.3 Syntheses of peptides 202

3.6 References 211

Chapter 4 213

4. Thioether-Bridged Amino Acids and Their Incorporation into Cyclic RGD-Containing Integrin Peptide Ligands 213

4.1 Introduction 214

4.1.1 The integrin cell surface receptors 214

4.1.2 Discussion of specific integrins 217

4.1.3 Structure-activity relationship studies of the RGD peptide 220
4.2. The incorporation of thioether building blocks into $\alpha v\beta 3$-specific peptides 223
4.2.1. Design of the thioether building blocks 223
4.2.2. Methods to synthesize thioether bridges 226
4.2.3. The syntheses of the thioether building blocks and their incorporation into peptides 229
4.2.4. Results of the receptor binding assays 235
4.3 Conclusions 237
4.4 Acknowledgements 239
4.5 Experimental 239
4.5.1 General 239
4.5.2 Syntheses of building blocks 241
4.5.3 Peptide synthesis 254
4.5.4 Binding assays 257
4.6 References 259

List of Abbreviations

Å	Angstrom
δ	Chemical shift
μM	Micromolar
°C	Degrees, Celcius
^{1}H	Proton
abi	Azabenzimidazole
ACN	Acetonitrile
AcOH	Acetic acid
Ar	Argon
bi	Benzimidazole
Boc	*tert*-Butyloxycarbonyl
Boc_2O	Di-*tert*-butyl dicarbonate
bt	Benzotriazole
t-But	*tert*-Butyl
Cbz	Benzyloxycarbonyl
$CDCl_3$	Deuterated Chloroform
Cs_2CO_3	Cesium carbonate
DBF	Dibenzofuran
DCHA	Dicyclohexylamine
DCM	Dichloromethane

DEPBT	3-(Diethoxyphosphoryloxy)-1,2,3-benzotriazin-4-(3*H*)-one
DIC	Diisopropylcarbodiimide
DIEA	*N*,*N*'-Diisopropylethylamine (Hünig's base)
DMAP	Dimethylaminopyridine
DMF	*N*,*N*'-Dimethylformamide
DMSO-d_6	Deuterated dimethyl sulfoxide
ECD	Extracellular matrix
EDC	1-(3-Dimethylaminopropyl)-3-ethylcarbodiimide hydrochloride
eq.	Equivalents
Et_2O	Diethyl ether
EtOAc	Ethyl acetate
EtOH	Ethanol
Fmoc	9-Fluorenylmethoxycarbonyl
g	Gram
GCMS	Gas chromatography mass spectrometry
H_2	Hydrogen gas
H_2O	Water
h	Hour
HATU	*O*-(7-Azabenzotriazole-1-yl)-*N*,*N*,*N*',*N*'-tetramethyluronium hexafluorophosphate
HCl	Hydrochloric acid
hex	Hexanes

HF	Hydrofluoric acid
Hz	Hertz
ind	Indazole
K_2CO_3	Potassium carbonate
K_i	Dissociation constant
HOBt	1-Hydroxybenzotriazole
IC_{50}	Concentration which produces half-maximal inhibition
LiCl	Lithium chloride
LiOH	Lithium hydroxide
MeOH	Methanol
mg	Milligram
$MgSO_4$	Magnesium sulfate
MHz	Megahertz
min	Minutes
mL	Milliliter
mmol	Millimole
mol %	Mole percent
MS	Mass spectrometry
$NaBH_4$	Sodium borohydride
NaH	Sodium hydride
$NaHCO_3$	Sodium bicarbonate
$NaHSO_3$	Sodium bisulfite

$NaHSO_4$	Sodium bisulfate
NaOH	Sodium hydroxide
Na_2SO_3	Sodium sulfite
$Na_2S_2O_3$	Sodium thiosulfate
nm	Nanometers
nM	Nanomolar
NMR	Nuclear magnetic resonance
OcHx	Cyclohexyl ester
Pal	3-(3-Pyridyl)-Alanine
Pd/ C	Palladium on carbon
Pmp	Pentamethylphenylalanine
ppt	Precipitate
psi	Pounds per square inch
pur	Purine
RP-HPLC	Reverse phase high performance liquid chromatography
r_t	Retention time
r.t.	Room temperature
SAR	Structure activity relationship
$SOCl_2$	Thionyl chloride
SRIF	Somatotropin release inhibiting factor (somatostatin)
TEA	Triethylamine
TFA	Trifluoroacetic acid

TEMPO	2,2,6,6-Tetramethylpiperidinyl-1-oxy
THF	Tetrahydrofuran
TLC	Thin layer chromatography
Trt	Trityl
p-TsOH·H_2O	*para*-Toluenesulfonic acid
uv	ultra violet light
Z	Benzyloxycarbonyl

List of Figures

Figure 2-1: Structures of the two native forms of somatostatin; SRIF-14 and SRIF-28 9

Figure 2-2: The primary amino acid sequence of prosomatostatin 10

Figure 2-3: Principal actions of somatostatin 11

Figure 2-4: Model of the orientation of GPCR hsst2 within the cellular membrane, including the possible arrangement of the seven transmembrane domains (TM1-TM7). Both models are based on the known structure of rhodopsin 14

Figure 2-5: The cyclic hexapeptide L-363,301 developed by Veber and coworkers 22

Figure 2-6: The cyclic hexapeptide MK678/ seglitide 23

Figure 2-7: The structure of disulfide-bridged octreotide, a somatostatin analog which is used in the clinic 24

Figure 2-8: The structures of RC-121 and RC-160 (octastatin), cyclic octapeptide analogs of octreotide 25

Figure 2-9: The structure of disulfide-bridged lanreotide which contains a D-naphthylalanine at the *N*-terminus 26

Figure 2-10: Octreotide analogs, OctreoScan [**2-10**] and OctreoTher [**2-11**] can both coordinate radioactive isotopes for use in imaging and treating sst2-positive tumors 29

Figure 2-11: SRIF-14 analogs containing *gem*-diamino and malonyl structures (highlighted in boxes) which result in retro-inverso peptides 31

Figure 2-12: An analog of L-363,301 which contains (2*R*,3*S*)-β-methyl tryptophan[8] 33

Figure 2-13: A model of the somatostatin pharmacophore with the spatial and distance requirements of the functional groups needed for receptor binding 35

Figure 2-14: A lanthionine-bridged analog of octreotide 36

Figure 2-15: The *N*-alkylated peptoid residues which were incorporated into the Pro^6 position of L-363,301 were conceptualized from the breaking of the bond between α- and β- carbons of Phe^6 37

Figure 2-16: The incorporation of acidic and basic *N*-alkylated peptoid residues into position 6 of L-363,301 38

Figure 2-17: The cyclic hexapeptide SOM230 displays a universal somatostatin receptor binding profile 41

Figure 2-18: Structures of first generation somatostatin peptidomimetics and their reported binding affinities to the multiple receptors within isolated rat cortex membranes 44

Figure 2-19: Ellman and coworkers' β-turn mimetic scaffold and their most potent somatostatin analog 45

Figure 2-20: Small molecule SRIF peptidomimetics with nM receptor binding 46

Figure 2-21: The lead compounds discovered by researchers at Merck and their hsst receptor binding affinity, K_i (nM), at their preferred receptor subtype 47

Figure 2-22: Important features of a typical β-turn depicted on L-363,301 [**2-4**] include the torsion angles Φ and Ψ, less than 7 Å between the α-Cs of the *i* and the *i* + 3 residues, and the possible presence of a hydrogen bond between the carbonyl of the *i* residue and the NH of the *i* + 3 residue 50

Figure 2-23: Examples of β-turn-inducing structures which have been incorporated into various cyclic peptides 52

Figure 2-24: The *N,N′*-diphenylurea and biphenyl containing analogs of MK678 which were designed, synthesized, and evaluated in the DeGrado laboratories 53

Figure 2-25: The sugar amino acid scaffolded somatostatin analogs designed and synthesized by Kessler and coworkers 55

Figure 2-26: The lowest energy conformation of the dibenzofuran-based compound is the closest topological match to that of L-363,301 [**2-4**] 57

Figure 2-27: Kelly's dibenzofuran based scaffold was designed to array β-sheet structures 58

Figure 2-28: Two dibenzofuran constrained somatostatin analogs based on the classical somatostatin hexapeptides, L-363,301 [**2-4**] and MK678 [**2-5**] 59

Figure 2-29: ROE data for the Phe-D-Trp-Lys-Thr analog [**2-48**] demonstrates the strong D-Trp α-H-Lys NH ROE and the medium Lys NH-Thr NH ROE, both of which support the presence of a type II' β-turn 71

Figure 2-30: ROE data for the Tyr-D-Trp-Lys-Val analog [**2-49**] demonstrates the strong D-Trp α-H-Lys NH ROE and the medium Lys NH-Val NH ROE, both of which support the presence of a type II' β-turn 72

Figure 3-1: The structure of SRIF-14 and the substituted tryptophan analogs which were incorporated into the peptide in place of Trp^8 129

Figure 3-2: An analog of RC-121 [**2-7**] which contains 3-(3-Pyridyl)-D-Alanine (D-Pal^8) in place of the Trp^8 residue..... 133

Figure 3-3: Des-AA ^{1,2,5}-somatostatin analogs with $IAmp^9$ and additional substitutions of Trp^8 134

Figure 3-4: Substitution of the Trp^8 position of the cyclic octapeptide ODT-8 with D-2-Nal and betidamino acids 135

Figure 3-5: An analog of L-363,301 which contains (2*R*,3*S*)-β-methyl $Tryptophan^8$ 137

Figure 3-6: Nitrogen-containing, fused 5,6-heterocyclic, aromatic α-amino acids and the heterocycles from which they are derived..... 140

Figure 3-7: The aromatic ring of the 2-substituted benzotriazole analog has only two signals in the aromatic region of the ^{1}H NMR spectrum 151

Figure 3-8: The aromatic ring of the 1-substituted benzotriazole analog has many signals in the aromatic region of the ^{1}H NMR spectrum..... 151

Figure 3-9: 2D-NOESY NMR spectra of N9-substituted purine analog [**3-54**] do not have an NOE between the β-hydrogens (**d**) and N3 because there are no protons on the nitrogen. There are also no NOEs between the β-hydrogens (**d**) and the purine H6 (**g**) because they are too far away from each other 155

Figure 3-10: 2D-NOESY NMR spectra of N7-substituted purine analog [**3-55**] shows an NOE between the β-hydrogens (**d**) and the purine H6 (**g**).. 156

Figure 3-11: The aromatic regions of the ^{1}H NMR spectra of the N9-substituted purine alcohol [**3-58**] and N7-substituted purine alcohol [**3-59**]. The signal of H8 for compound [**3-58**] (8.429 ppm) is shifted upfield relative to the corresponding signal of H8 for compound [**3-59**] (8.556 ppm). This upfield shift supports the structural assignments of the regioisomers..... 157

Figure 3-12: 2D-NOESY NMR spectra of N3-substituted 4-azabenzimidazole analog [**3-60**] do not have an NOE between the β-hydrogens (**d**) and N4 because there are no protons on the nitrogen. There are also no NOEs between the β-hydrogens (**d**) and the

4-azabenzimidazole H7 (**h**) because they are too far away from each other..... 160

Figure 3-13: 2D-NOESY NMR spectra of N1-substituted 4-azabenzimidazole analog [**3-61**] shows an NOE between the β-hydrogens (**d**) and 4-azabenzimidazole H7 (**h**) 161

Figure 3-14: The aromatic regions of the ^{1}H NMR spectra of the N3-substituted 4-azabenzimidazole amino acid [**3-62**] and N1-substituted 4-azabenzimidazole amino acid [**3-63**]. The signal of H2 for compound [**3-62**] (8.966 ppm) is shifted upfield relative to the corresponding signal of H2 for compound [**3-63**] (9.182 ppm). This upfield shift supports the structural assignments of the regioisomers 162

Figure 3-15: An analytical RP-HPLC trace of the crude linear hexapeptide [**3-63**] after cleavage from the resin 165

Figure 3-16: The cyclic hexapeptide analogs of L-363,301 which contain the synthesized unnatural amino acids in place of the D-Trp residue: benzimidazole-containing [**3-67**], 1-benzotriazole-containing [**3-68**], and indazole-containing [**3-69**]..... 167

Figure 4-1: The tripeptide integrin recognition sequence Arg-Gly-Asp, or RGD 214

Figure 4-2: Diagram of the integrin family showing subunit associations and known ligand specificities 215

Figure 4-3: Schematic illustration of integrins and their interactions with some proteins within the cellular domain 217

Figure 4-4: Structures of disulfide-bridged RGD peptides which selectively bind to integrin $\alpha v\beta 3$ 224

Figure 4-5: Thioether building blocks based on alkylated cysteine and homocysteine 225

Figure 4-6: Thioether bridged RGD peptide analogs: c[(*S*-Ac-C) RGDD(*t*BuG)C]-NH_2 [**4-7**], c[(*S*-Pr-C)RGDD(*t*BuG)C]-NH_2 [**4-8**],c[(*S*-Ac-hC)RGDD(*t*BuG)C]-NH_2 [**4-9**], and c[(*S*-Pr-hC) RGDD(*t*BuG)C]-NH_2 [**4-10**] 226

Figure 4-7: Problematic methods for the synthesis of thioether bridges include sulfur extrusion, Michael addition of cysteine to dehydroalanine, and the Vederas lactone 227

Figure 4-8: Attack of *N*-trityl-3-iodoalanine benzyl ester by cysteine derivatives in solution provides lanthionines and an aziridine by-product 228

List of Schemes

Scheme 2-1: Synthesis of the dibenzofuran-based scaffold includes two Heck cross-coupling reactions 60

Scheme 2-2: The continued synthesis of the dibenzofuran-based scaffold which highlights the use of a Hoffman rearrangement to provide the Boc-protected amino acid..... 62

Scheme 2-3: Syntheses of the two Lysine-containing dipeptides 64

Scheme 2-4: Synthesis of an orthogonally protected D-Trp analog which was not commercially available..... 65

Scheme 2-5: Syntheses of the two D-Tryptophan-containing dipeptides..... 66

Scheme 2-6: Coupling of the L-363,301 [**2-4**]-analogous dipeptides to the dibenzofuran scaffold 67

Scheme 2-7: Cyclization and final deprotection of Phe-D-Trp-Lys-Thr-dibenzofuran analog [**2-48**] 68

Scheme 2-8: Coupling of the MK678 [**2-5**]-analogous dipeptides to the dibenzofuran scaffold 69

Scheme 2-9: Cyclization and final deprotection of Tyr-D-Trp-Val-Thr-dibenzofuran analog [**2-49**] 70

Scheme 3-1: Reaction of deprotonated benzimidazole with Trt-3-iodoalanine-OBzl provides dehydroalanine as the exclusive product..... 141

Scheme 3-2: The OBO ester of Z-Serine was unstable and decomposed within one to two days..... 142

Scheme 3-3: The reaction of various protected serine derivatives with benzimidazole under Mitsunobu conditions did not provide any product 143

Scheme 3-4: Reductive amination of benzimidazole with propionaldehyde provided no product. Only starting material was recovered..... 143

Scheme 3-5: Synthesis of the Boc-protected tosyl-oxazolidine intermediate [**3-39**] from L-Serine..... 144

Scheme 3-6: Displacement of the tosylate with benzimidazole, followed by ring opening and oxidation to the Boc-protected amino acid 145

Scheme 3-7: Synthesis of Cbz-protected tosylate oxazolidine intermediate..... 146

Scheme 3-8: Opening of the oxazolidine ring and the final oxidation of the alcohol to the carboxylic acid provided the Cbz-protected benzimidazole amino acid 147

Scheme 3-9: The displacement of the tosylate by benzotriazole provided two regioisomers which are isolated and oxidized separately to the corresponding Cbz-protected amino acids 149

Scheme 3-10: The synthesis of the indazole amino acid from the tosyl-oxazolidine intermediate 152

Scheme 3-11: The syntheses of N9- and N7-substituted purine amino acids from a common tosyl-oxazolidine intermediate..... 153

Scheme 3-12: The syntheses of N3- and N1-substituted 4-azabenzimidazole amino acids from a common tosyl-oxazolidine intermediate..... 158

Scheme 3-13: The coupling of the building blocks to the resin bound pentapeptide and subsequent cleavage from the resin, using the benzimidazole amino acid [**3-47**] as a representative example 164

Scheme 3-14: Cbz-deprotection of the amine terminus, macrocyclization, and final deprotection with TFA provided cyclic hexapeptide [**3-67**] 166

Scheme 4-1: Syntheses of Fmoc-protected, *S*-alkylated cysteine analogs 231

Scheme 4-2: Syntheses of Fmoc-protected, *S*-alkylated homocysteine analogs 232

Scheme 4-3: Synthesis of *S*-*t*butyl acetyl cysteine peptide [**4-4**] is representative of the syntheses of all four thioether-bridged peptide analogs 234

List of Tables

Table 2-1: Established sst receptor-activity correlations 17

Table 2-2: Binding affinities (K_i in nM) of selected peptidic somatostatin analogs for the five somatostatin receptor subtypes, sst1-5 27

Table 2-3: Binding affinities (IC_{50} in nM) of selected β-methyl tryptophan analogs for all five human somatostatin receptor subtypes, hsst1-5..... 34

Table 2-4:..... *In vitro* binding affinities (K_i in nM) of peptoid analogs of L-363,301 for the individual human somatostatin receptor subtypes, hsst1-5..... 40

Table 2-5: Binding affinities (IC_{50}, nM) of SRIF-14, octreotide, and SOM230 for the human somatostatin receptor subtypes 42

Table 2-6: The idealized dihedral angles of common β-turns 51

Table 2-7: Sst receptor subtype binding affinities of DeGrado's compounds (IC_{50}, nM) were measured in human (hsst) and mouse (msst) cloned receptors..... 54

Table 2-8: Binding affinities (K_i in nM) of synthesized somatostatin analogs for the five human somatostatin receptor subtypes hsst1-5..... 73

Table 3-1: The relative inhibitory potencies of SRIF-14, D-Trp^8-SRIF-14 and D-Tyr^8-SRIF-14 against insulin, glucagon, and GH..... 128

Table 3-2: Comparison of gastric acid,[11] glucagon,[11] insulin,[11] and GH[12] inhibitory potencies of somatostatin analogs containing Trp[8] modified residues relative to SRIF-14 [**2-1**] 131

Table 3-3: Comparison of insulin, glucagon, and GH inhibitory potencies L-363,301 [**2-4**] and Trp[8] modified analogs of L-363,301 relative to SRIF-14 [**2-1**] 132

Table 3-4: Binding affinities of ODT-8 and analogs containing 2-Nal[8] and betidamino acids and for the somatostatin receptor subtypes (IC_{50}, nM) 136

Table 4-1: Binding affinities of the parent compound and the thioether-bridged RGD peptides for integrins $\alpha v\beta 3$, $\alpha v\beta 5$, $\alpha 5\beta 1$, and $\alpha IIb\beta 3$ (IC_{50}, nM) 235

Acknowledgements

My deepest gratitude to Professor Murray Goodman, with whom this body of work was completed. I could not have chosen a better mentor to train with and to launch my career. Thank you for all of your guidance, support, and help through the years. I have countless fond memories of the time that I spent with you. You gave me so many unprecedented opportunities to meet and interact with so many wonderful people. I will be forever thankful for being a part of the Goodman family. I only wish you were here to witness the completion of my work.

I have great admiration for Mrs. Zelda Goodman. You have been such a strong role model for me. Thank you for your friendship, guidance, and for always opening your home to all of us.

Thank you to Joseph Taulane for being a sounding board and for helping me to arrive at the end. I am indebted to you for reading my dissertation and offering so much advice. Thank you for maintaining all of the equipment in the laboratories and for spending so much time showing me all the tricks to keep them working. I learned so much from you.

Robyn Swanland always offered a smile and an often much needed piece of chocolate. I enjoyed all of our daily chats. Thank you for always going out of your way to help me get the job done.

Professor Michael VanNieuwenhze, if you had not stepped up and offered your help and support in the toughest, saddest time of my graduate career, I never would

have made it through to the end. Thank you for your guidance and for taking a chance on me.

I do not know how to begin to thank William Fuller of Senn Chemicals, U.S.A. Thank you for donating so many materials for my research projects; though you barely knew me back then. The past 15 months have been the most difficult of my life, yet because of you, they have also been some of the most challenging, interesting, fulfilling, and fun. Thank you for believing in me, supporting me, and for giving me the space I needed to get through everything that has happened. You are a fantastic mentor and friend.

I owe so much to Dr. Mark Yeager. Thank you for all of your guidance and advice. I never would have made it through this without your support. Thank you so very much for all the time you took from your terribly busy schedule to edit my posters and to answer so many of my biology questions. You have been a true mentor and friend.

Aaron Wholrab followed me through undergraduate, out to San Diego, and into the Goodman laboratory. I am forever grateful that with so many near misses, our paths finally crossed. I owe you so much for all of the time that you took out of your schedule to help me finish up my work. I have never met a more generous and helpful person. You always had a smile for me. You're next Jersey boy, and I will be there for you to help you too.

I was so lucky to work with Mika Tomioka for so many years. We may have been opposites, but we became the best of friends. Thank you for all the years of

discussion, chats, fun, and support. Since you left, I have missed you every day. An ocean may separate us, but you will always be near and dear to my heart.

Dr. Christoph Zapf indoctrinated me into the Goodman laboratory and became one of my closest friends. Thank you for so many insightful, helpful conversations and especially for pushing me so hard when I thought about giving up. I have so many memories of the fun we had. I look forward to the years to come.

I was fortunate to have Molly Milner work for me as an undergraduate researcher. Thank you for all of your help bringing starting material forward. I had such a great time mentoring you and I am so proud of you and all of your accomplishments!

Dr. Ralph-Heiko Mattern was integral to the work described in Chapter 4. Thank you for providing so much guidance during my many months bouncing back and forth between UCSD and Integra. I am so glad that I got to know you and your family and look forward to many years of friendship with all of you.

I never would have gone to graduate school had it not been for Dr. Kenneth Overly's encouragement. I did not even know graduate school in chemistry existed until you told me about it. Thank you for all of the time that you spent teaching me in undergraduate and for taking a special interest in my success.

Dr. Melissa Rewolinski gave me a special opportunity to intern at Agouron Pharmaceuticals for the summer before I started graduate school. You taught me so much and really helped prepare me for the rigors of research. You weren't kidding when you said grad school was an endurance test!

I have to give a shout out to my best friend in the world, Mrs. Stephanie Noss Schleckser. Had it not been for you, I'd still be working at Ron Jon's. Thank you for dragging me back to college. For 28 years, you never once doubted me. Words cannot express my gratitude for all that you have done to help me through some of the most difficult times of my life. I only wish we were closer to share every moment together.

A big thank you goes to Kane Hanson who uprooted his life to help me follow my dreams. You have grown with me and supported me through many of the difficult times. Thank you for taking care of me so often by making sure I had everything that I needed to survive and be successful. You were the only one who believed I would finish. I needed that support to get here.

My mother Doreen Kelleman has always provided me with unconditional love. Thank you for pushing me so hard to do well in school and for helping me to realize my potential. Your doing so provided me with the foundation I needed to make all of the decisions that I have about my life. I know I did not choose the path that you hoped I would, but I know that you are proud of all that I have accomplished. I wish that you were able to be here with me for the end of my graduate school career. I miss you very much.

I thank my father, Andrew Kelleman, for working to provide for us when we were young. Thank you for the times when you believed in me and when you were proud of me. I have many fun memories of the time I spent with you.

I would not be here had it not been for my brothers, Andrew S. and Daniel John P. Kelleman. All of our adventures together shaped who I am today. I never could

have completed this journey without knowing you supported me. I am so proud of both of you and of all that you have become. Thank you for always listening, always taking my side, and for loving me.

I thank my extended family, Robert, Linda, Tammy, Keri-Lyn, Daniel, and Peter, for continuously stepping up to help out throughout my life. I have always known I could call on all of you for anything. Thank you for taking care of so much over the years.

Thank you to my graduate committee Professor Charles Perrin, Professor Emmanuel Theodorakis, Professor J. Andrew McCammon, and Professor Daniel O'Connor for your patience and advice during this long, winding journey. Thank you for taking time out of your schedules to attend my examinations and for reading my dissertation.

Chapter 4 is based upon material in: Incorporation of thioether building blocks into an $\alpha_v\beta_3$-specific RGD peptide: synthesis and biological activity. Kelleman, Audrey; Mattern, Ralph-Heiko; Pierschbacher, Michael D.; Goodman, Murray. *Biopolymers*. **2003**, *71*, 686-695. The dissertation author was the primary investigator and author of this paper.

I would like to thank Dr. Shaokai Jiang for his help in modeling the scaffolded peptides described in Chapter 2.

Dr. Giuseppe Malacini and Hao Huang of McMaster University collaborated with us on the 2D NMR spectroscopy of the final compounds described in Chapter 2. Thank you for your effort and for taking time to answer all of my questions.

Ujendra Kumar and Michael Grant of McGill University performed the biological assays described in Chapter 2.

I would like to thank the National Institute of Health for financial support of the projects that I worked on. Chapter 2 and 3 were funded by NIH DK15410 while Chapter 4 was funded by NIH DK1540 (M. Goodman) and DK51938 (R. Mattern).

Vita

April, 1991 – May, 1999	Store Manager and Department Head of Merchandising Ron Jon Surf Shop Ship Bottom, New Jersey
September, 1997 – May, 1999	Teaching Assistant Department of Chemistry and Biochemistry Richard Stockton College of New Jersey
May, 1999	Bachelor of Science, Richard Stockton College of New Jersey
June, 1999 – September, 1999	Intern, Chemical Development Agouron Pharmaceuticals La Jolla, California
September, 1999 – December, 2004	Teaching Assistant Department of Chemistry and Biochemistry University of California, San Diego
September, 1999 – December, 2005	Research Assistant Department of Chemistry and Biochemistry University of California, San Diego
January, 2001	Master of Science, University of California, San Diego
January, 2006 – Present	Research Scientist, Research and Development Senn Chemicals, U.S.A San Diego, California
March, 2007	Doctor of Philosophy, University of California, San Diego

Publications

Kelleman, Audrey; Mattern, Ralph-Heiko; Pierschbacher, Michael D.; Goodman, Murray. Incorporation of thioether building blocks into an $\alpha_v\beta_3$-specific RGD peptide: synthesis and biological activity. *Biopolymers*. **2003**, *71*, 686-695.

Haddach, Aubrey A.; Kelleman, Audrey; Deaton-Rewolinski, Melissa V. An efficient method for the N-debenzylation of aromatic heterocycles. *Tetrahedron Letters*. **2002**, *43*, 399-402.

Synthesis of novel heterocyclic amino acids and their incorporation into somatostatin analogs. Poster presented at the 230th American Chemical Society National Meeting, August, 2005, Washington, D.C.

Design and synthesis of type II' β-turn constrained somatostatin analogs. Poster presented at the 19th American Peptide Society Symposium, June, 2005, San Diego, CA.

Mild and efficient methods for the N-debenzylation of aromatic heterocycles. Poster presented at the 221st American Chemical Society National Meeting, April, 2001, San Diego, CA.

ABSTRACT OF THE DISSERTATION

Design and Syntheses of Nonnatural Amino Acids and Their Incorporation into Somatostatin and RGD Analogs

by

Audrey Kelleman

Doctor of Philosophy in Chemistry

University of California, San Diego, 2007

Professor Michael VanNieuwenhze, Chair

The peptide hormone somatostatin has been the focus of ongoing research in our laboratories. In an effort to constrain the tetrapeptide pharmacophore of somatostatin in a rigid type II' β-turn, we synthesized the 4,6-substituted dibenzofuran amino acid, 4-(2-aminoethyl)-6-(2-carboxyethyl)-dibenzofuran (DBFaa). Two sets of dipeptides, Z-Lys(Boc)-Thr(*t*-But)-OH and H-Phe-D-Trp(Boc)-OMe, and Z-Lys(Boc)-Val-OH and H-Tyr(*t*-But)-D-Trp(Boc)-OMe were synthesized and then coupled to the dibenzofuran amino acid scaffold to provide c[Phe-D-Trp-Lys-Thr-DBFaa] and c[Tyr-D-Trp-Lys-Val-DBFaa]. 2D-NMR spectroscopy of both compounds provided ROEs which supported the presence of a type II' β-turn spanning the D-Trp-Lys residues. The binding affinities of both

scaffolded somatostatin analogs were evaluated for potency and selectivity for each subtype of the hsst receptors in binding assays. Neither compound showed any affinity for hsst1 or hsst4. The c[Phe-D-Trp-Lys-Thr-DBFaa] compound was slightly selective for hsst2 (2 μM) over hsst3 (4.2 μM) and hsst5 (3.5 μM). The c[Tyr-D-Trp-Lys-Val-DBFaa] analog did not display any affinity for hsst5, but was selective for hsst2 (2.2 μM) over hsst3 (5.5 μM).

In an effort to incorporate analogs of naturally occurring tryptophan into somatostatin compounds, we designed and synthesized eight unnatural nitrogen-containing, fused 5,6-heterocyclic, aromatic α-amino acids. The target compounds include Z-D-1*H*-benzimidazole-yl alanine, Z-D-1*H*- and Z-D-2*H*-benzotriazole-yl alanine, Z-D-1*H*-indazole-yl alanine, Z-D-9*H*- and Z-D-7*H*-purine-yl alanine, and Z-D-3*H*- and Z-D-1*H*-(4-azabenzimidazole-yl) alanine. The key step of the syntheses of the amino acids involved the nucleophilic displacement of the tosylate of Garner's alcohol, which enabled us obtain the desired D-amino acids in good yields. Three of the amino acids, Z-D-1*H*-benzimidazole-yl alanine, Z-D-1*H*-benzotriazole-yl alanine, and Z-D-1*H*-indazole-yl alanine were incorporated into the pentapeptide, H-Lys(Boc)-Thr(*t*-But)-Phe-Pro-Phe, cyclized, and were obtained cleanly and in good yields.

Another area of research in our laboratories involved the synthesis of RGD-containing integrin ligands. We designed and synthesized a family of unnatural thioether amino acids; Fmoc-*S*-(*t*-butoxycarbonylmethyl)-cysteine, Fmoc-*S*-(*t*-butoxycarbonylethyl)-cysteine, Fmoc-*S*-(*t*-butoxycarbonylmethyl)-homocysteine, and Fmoc-*S*-(*t*-butoxycarbonylethyl)-homocysteine. These compounds

were designed to replace the mercaptopropionic acid-cysteine disulfide bridge of the integrin $\alpha v\beta 3$-specific compound c[(Mpa)RGDD(*t*BuG)C]-NH_2. The syntheses of the thioether building blocks were scalable and produced the desired products in good yields. Of the series, the peptide c[NH-Arg-Gly-Asp-Asp-(tBuG)-(S-Ac-C)]-NH_2 demonstrated potent affinity for the $\alpha v\beta 3$ and $\alpha 5\beta 1$ receptors while having reduced affinity for integrin αIIb$\beta 3$.

CHAPTER 1

1. INTRODUCTION AND OVERVIEW

1.1 Introduction

During the past 60 years, a large number of biologically active peptides have been discovered and knowledge of the structures, properties, and functions of these peptides has grown considerably. These compounds are important in normal and disease physiology acting as hormones, neurotransmitters, and modulators of cell surface receptors and numerous other biological activities. All of these functions imply important therapeutic applications. In some cases, such as insulin and oxytocin, native peptides have proven to be useful as therapeutic agents. However, in many cases, peptidic structures are not suitable for use as drugs. Poor oral availability is a major limitation and problems arise from short durations of action. Enzymes rapidly degrade peptides by cleaving peptide bonds which ultimately leads to a loss of biological activity. Peptides can also often interact with more than one receptor or subtype which results in unsatisfactorily low selectivity and associated side effects.

Recently, researchers have overcome many of the above limitations of peptides as therapeutics through the development of mimetics of natural amino acid building blocks. This research led to new structures known as peptidomimetics. Theoretically, the scope of peptidomimetics extends from peptides where single amino acid residues or peptide bonds have been altered, all the way to the transformation of a peptide into a small, non-peptidic molecule. In the development of peptidomimetics, the search for initial leads can be entirely empirical, simply involving deletion, addition, or replacement of one or more amino acid residues of the endogenous ligands. Once an initial structure-activity relationship (SAR) is established, more sophisticated

structural changes can be made, such as the use of unusual amino acids, modification of the peptide backbone, cyclization of peptides, and mimicry of secondary structural features such as helices or reverse turns, through the inclusion of heterocyclic structures which act as templates or scaffolds. The ultimate goal of the incorporation of these mimetic structures into peptides is to prepare more metabolically stable, less-peptidic molecules which hold the pharmacophore in the proper conformational array and result in analogs which exhibit increased potency, receptor selectivity, and improved pharmacological properties.

Synthetic building blocks can be considered conformational probes which provide insight into the bioactive conformations of parent peptides and of the topospace within the binding pocket of the receptor. This information helps to ultimately identify the required pharmacophoric groups to discover potent and receptor specific ligands. Such tools can also protect the global molecular structures from metabolic degradation by introducing structures which the enzymes can not recognize.

Unnatural amino acids utilized as building blocks, conformational constraints, or molecular scaffolds, represent an array of diverse structural elements for the development of new peptidic and non-peptidic lead compounds. The major focus of this dissertation is the design and synthesis of nonnaturally occurring amino acid building blocks which, when incorporated into peptides, could provide additional information about the topological requirements for receptor binding and specificity. In our laboratories, we were interested in a number of bioactive peptides including

somatostatins and RGD-containing ligands of the integrin receptors. Both classes of compounds have potential therapeutic value in cancer treatment, diabetes, and other areas of disease. We hoped that incorporating our rationally designed building blocks into these classes of biological ligands would provide us with additional structure-activity relationships to aid in the design of clinically useful compounds.

Over the years, the Goodman laboratories developed an interdisciplinary approach to study biologically active molecules. We have synthesized families of target molecules involving systematic compositional modifications. We then examined the conformational effects of these structural alterations using high resolution NMR spectroscopy and molecular modeling simulations. In collaborating laboratories, bioassays were carried out to determine the bioactivity profiles of our candidate molecules. Collectively, this information has enabled us to refine our understanding of structure-activity relationships of peptides and to design and synthesize new target molecules.

The research in this dissertation focuses on the synthetic aspects of the research programs in our laboratories. Our efforts in the design and synthesis of novel unnatural amino acids will be discussed, as well as our incorporation of these compounds into bioactive molecules in the areas of somatostatin and RGD-containing integrin ligands.

1.2 Unnatural amino acids as conformational scaffolds

The secondary structure of peptides is crucial for receptor binding and biological activity. Incorporation of peptidomimetic building blocks, such as conformationally constrained amino acids, into the sequences of biologically active peptides restricts the rotation of the bonds and/ or side chain conformations. This approach can minimize the number of possible conformations of a particular peptide and provide insight into the receptor bound conformation of a receptor ligand.

One of the most important secondary structural features of peptides is the β-turn. This feature often plays a key role in molecular recognition in biological systems. Great efforts have been undertaken to design scaffolds or templates which can be used as β-turn mimetics.

Chapter 2 describes our efforts to design somatostatin pharmacophore tetrapeptides constrained on an aromatic amino acid scaffold capable of inducing a rigid type II' β-turn about the peptide. Molecular dynamics simulations of a variety of candidates lead us to a dibenzofuran-based amino acid, which constrained the peptide in a conformation closest to that exhibited by a known potent compound. We synthesized the scaffold and incorporated it into two somatostatin pharmacophoric tetrapeptides. The conformation was then studied in solution by 2D-NMR techniques and the somatostatin receptor subtype binding affinities were measured.

1.3 Unnatural α-amino acid building blocks

The incorporation of unnaturally occurring α-amino acids into a peptide sequence may add or reduce conformational constraints within molecules, while others may affect hydrogen-bonding capacities and change electronic interactions. Nonnaturally occurring amino acid side chain moieties can provide information about receptor interactions and specificities. They may also increase the metabolic stability of an analog by introducing groups that can not be recognized by enzymes. The study of structure-activity relationships make it possible to design peptidomimetics based on native peptide structures.

Chapter 3 describes our design and synthesis of a class of nitrogen-containing, fused 5,6-heterocyclic, aromatic α-amino acids. The eight novel α-amino acids were synthesized from a scalable common intermediate and are based on the heterocycles benzimidazole, benzotriazole, azabenzimidazole, indazole, and purine. These compounds were designed to replace the D-Trp residue of a potent somatostatin analog in order to gain further insight into the requirements of the somatostatin receptor for the side chain of the position 8 residue for binding affinity and subsequent biological activity.

1.4 Cyclic peptides incorporating unnatural amino acid bridges

Naturally occurring cyclic structures exist in many native peptides such as somatostatin, oxytocin, and insulin. There are several different routes to obtain cyclic peptides including: cyclization from *N*-terminus to *C*-terminus of a peptide chain,

cyclization from main chain to side chain, or side chain to side chain, such as the formation of a disulfide bridge between the side-chains of two cysteine residues. An advancement made in our laboratories involves the incorporation of lanthionine and thioether bridges in place of disulfides because they are more stable toward enzymatic degradation.

Chapter 4 discusses our design and synthesis of four unnatural thioether-containing amino acids based on cysteine and homocysteine. We incorporated these amino acids into a small, cyclic RGD-containing integrin peptide ligand which bound potently and selectively for an integrin involved in angiogenesis. The parent compound was cyclized via a disulfide bridge between two cysteine residues. The thioether amino acids were designed to replace the disulfide in order to decrease the susceptibility of the compounds to enzymatic degradation, as well as explore the structure-activity relationships of chain length in the bridging region. The synthesized thioether-bridged peptides were evaluated for receptor binding and selectivity against four related integrins.

CHAPTER 2

2. DIBENZOFURAN-SCAFFOLDED SOMATOSTATIN ANALOGS

2.1 Introduction

2.1.1 Somatostatin: Discovery of a peptide hormone

Somatostatin (also known as somatotropin release-inhibiting factor, SRIF) is a regulatory peptide-hormone which was first isolated, purified, and characterized from ovine hypothalamus in 1973.[1] Somatostatin occurs systemically in two native forms, a 14- and a 28-amino acid peptide, which are similar in biological activity but display slightly different potencies depending on the tissue in question.[2] The sequence of somatostatin-28 (SRIF-28) [**2-2**] is identical to that of somatostatin [**2-1**], but is extended by fourteen amino acids at the *N*-terminus,[3] as depicted in Figure 2-1. Both forms of somatostatin are cyclized through a disulfide bridge formed between the sulfurs of the two cysteine side chains.

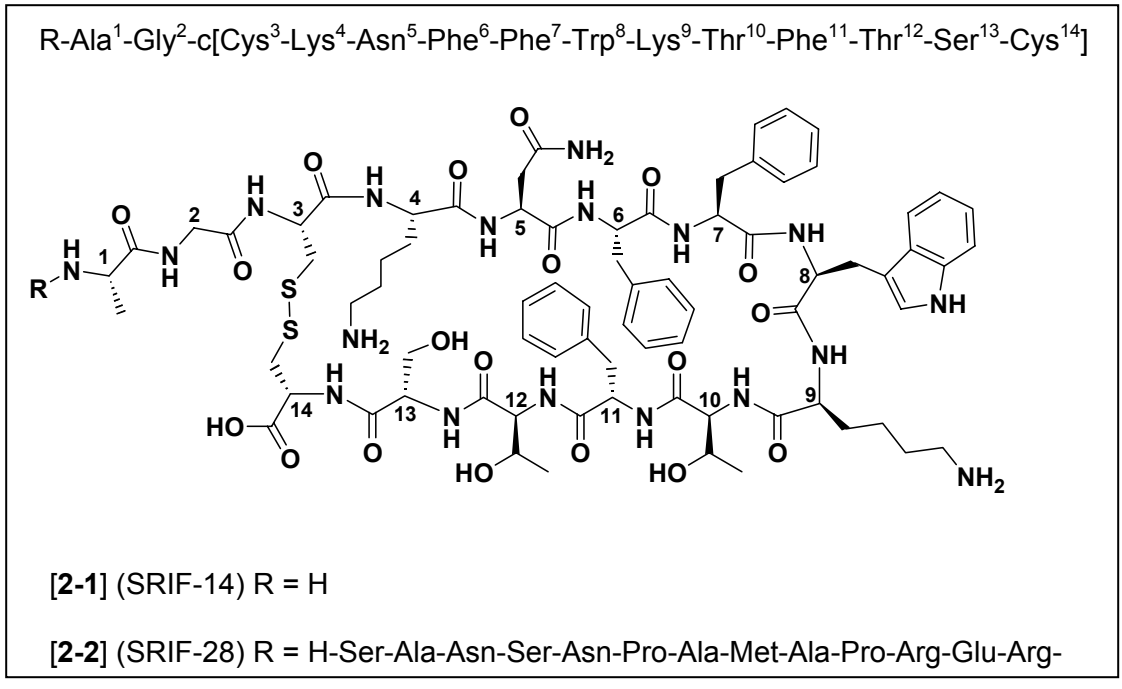

Figure 2-1: Structures of the two native forms of somatostatin; SRIF-14 and SRIF-28.

Both forms of somatostatin are generated in mammals from prosomatostatin (pro-SRIF) [**2-3**] (Figure 2-2), a 92-amino acid peptide which is identical in humans, pigs, and sheep.[4] Somatostatin comprises the COOH-terminal 14 residues. Proteolytic processing of pro-SRIF between di- and monobasic amino acid residues generates somatostatin and SRIF-28, respectively.[5,6]

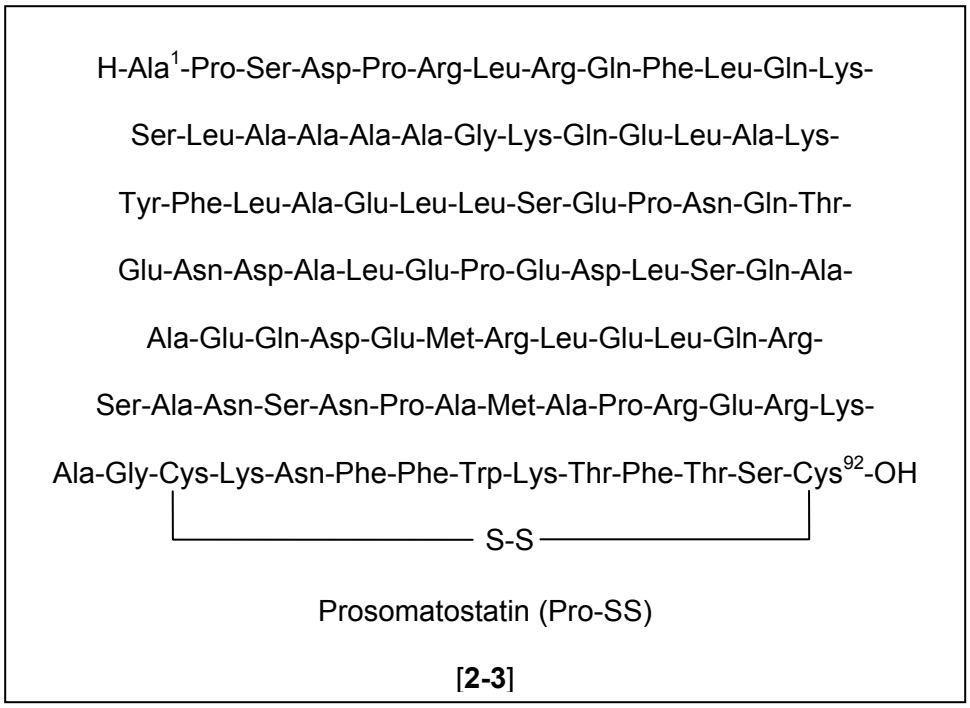

Figure 2-2: The primary amino acid sequence of prosomatostatin.

Extensive structure-activity relationship studies on somatostatin and its derivatives have shown that the tetrapeptide fragment, Phe^{7}-Trp^{8}-Lys^{9}-Thr^{10} (the superscript numbers refer to the sequence of SRIF-14 [**2-1**], Figure 2-1), is the pharmacophore essential for biological activity.[7] NMR studies also indicated that those four residues adopt a type II' β-turn conformation.[8]

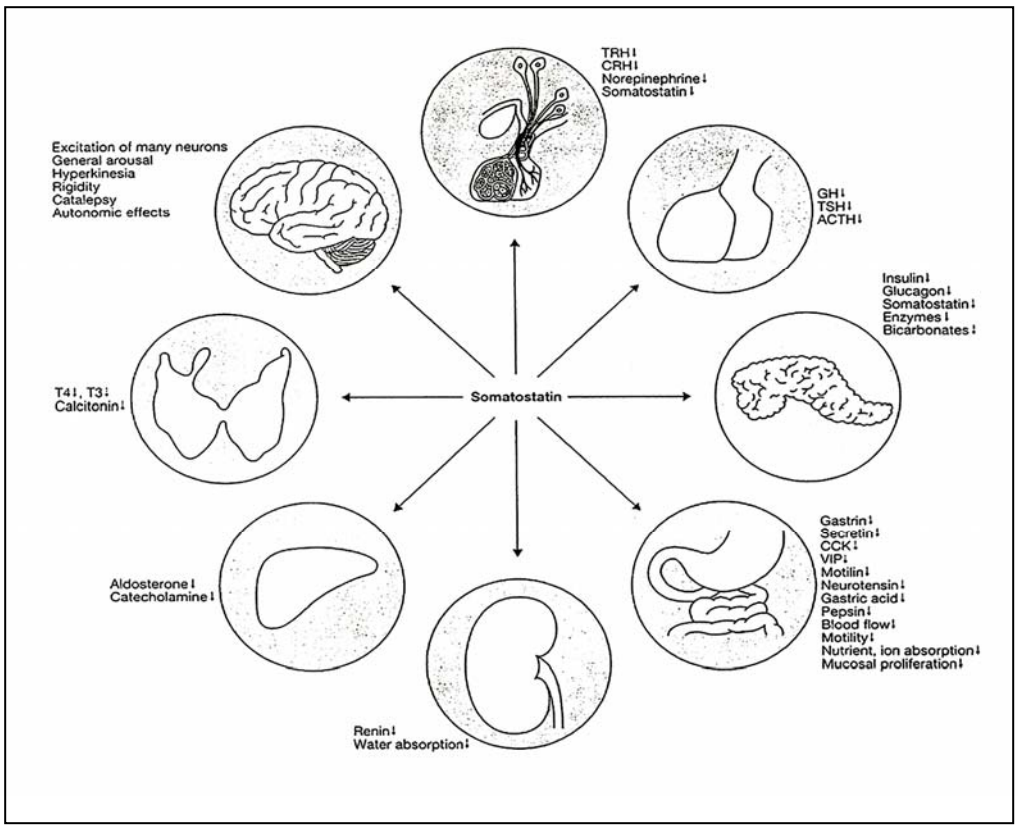

Figure 2-3: Principal actions of somatostatin.[9]

Somatostatin was originally isolated as an inhibitor of growth hormone (GH) release from the hypothalamus.[1] Subsequent studies revealed that it has very broad activities.[10,11] As depicted in Figure 2-3, somatostatin acts on multiple targets including the brain, intestine, pituitary, endocrine and exocrine pancreas, adrenals, thyroid, and kidneys.[9] Somatostatin is widely distributed in the brain and spinal cord where it is thought to act as a neurotransmitter[12] or a modulator of cognitive functions.[13] The hormone is also found in areas of the gastrointestinal tract[10] where it regulates the release of glucagon as well as insulin from the pancreas,[14] as well as the secretion of gastrin and gastric acid by the gut.[15] These actions are mediated through

high-affinity membrane-bound protein receptors that occur in varying densities in all target tissues. The wide physiological roles of somatostatin make it of considerable importance in the pathology of diseases such as GH related tumors, acromegaly, diabetes mellitus, Alzheimer's and Huntington's disease, and epilepsy.[10,16-18]

The early evaluation of somatostatin analogs *in vitro* was carried out utilizing isolated tissue which elicited a biological response. For example: The pituitary cells of rats were isolated and used to analyze the inhibitory effects of somatostatin on the secretion of growth hormone.[19] The advantage of this approach was that biological responses could be measured directly. Unfortunately, not all of the biological effects of somatostatin and its analogs could be measured so easily using *in vitro* methods. Studies of the inhibition of insulin and glucagon secretion were carried out *in vivo* by measuring levels in rat blood serum[20,21] while inhibition of gastric acid secretion was carried out in dogs.[22]

2.1.2 Somatostatin receptors and their function

While it was originally noted that somatostatin triggered a variety of biological responses, the idea that somatostatin interacted with more than one receptor in the cellular membrane (receptor heterogeneity) did not evolve until the 1980s. Isolated rat cortex was treated with [^{125}I]-somatostatin whose specific binding was then displaced with octreotide (an octapeptide analog of SRIF-14). The results were bimodal, indicating that two different receptors were involved. The sites with nanomolar affinity for octreotide were named SRIF-1 and those with micromolar affinity for

octreotide were named SRIF-2.[23] Additional pharmacological and binding studies with other synthetic somatostatin analogs confirmed that there were more than one type of somatostatin receptor.[24-27] The final proof for somatostatin receptor heterogeneity came with the cloning of five somatostatin receptor genes which coded for the five subtypes, sst1-5. Based on amino acid sequences and bonding similarities, it has been proposed that the cloned somatostatin receptors can be viewed as subfamilies, with sst2, 3, and 5 comprising family SRIF-1 and sst1 and sst4 comprising family SRIF-2.[28]

All five human somatostatin (hsst) receptors belong to the super family of guanine nucleotide binding protein-coupled receptors (GPCRs).[29-32] Because GPCRs are membrane bound, it is difficult to determine their structure by either NMR spectroscopy and X-ray crystallography. Therefore, the model of the organization of the membrane spanning α-helical segments is based on rhodopsin, a structurally related protein whose structure was obtained by two-dimensional crystallography to a resolution of 2.5 Å.[33,34] A model of human somatostatin receptor hsst2 orientated within the cell membrane is shown in Figure 2-4. All five hsst receptor subtypes are speculated to have similar structures.

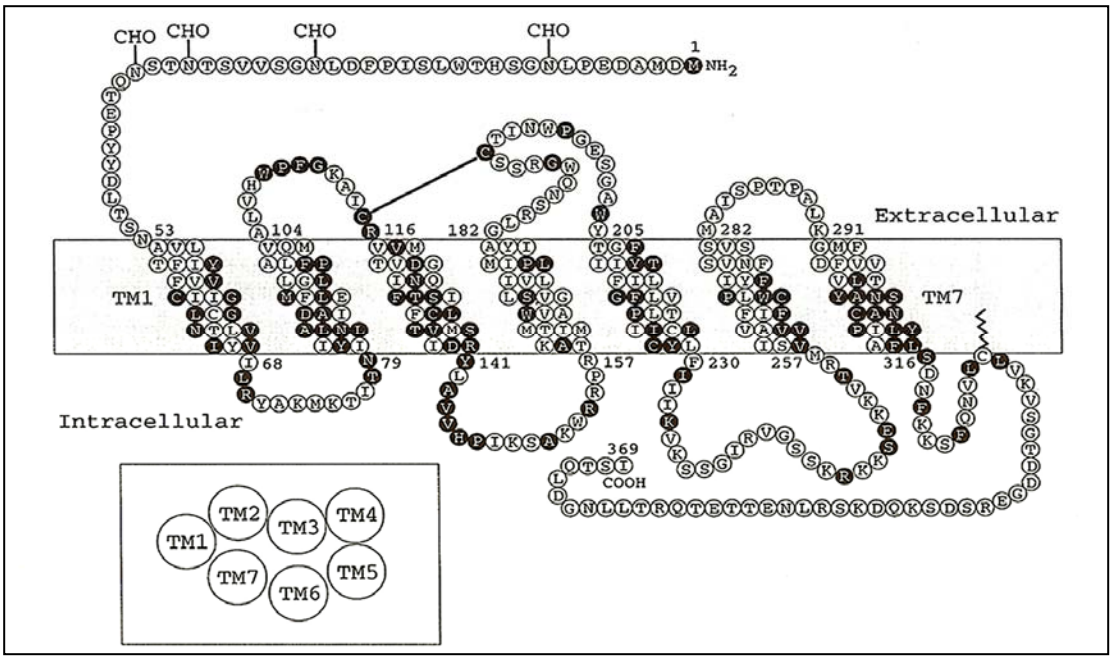

Figure 2-4: Model of the orientation of GPCR hsst2 within the cellular membrane, including the possible arrangement of the seven transmembrane domains (TM1-TM7). Both models are based on the known structure of rhodopsin.[35]

From the primary amino acid sequence it was concluded that, like other GPCRs, the sst receptors are defined by seven transmembrane segments.[36] The transmembrane regions consist of α-helices which connect four intracellular and three extracellular loops. The inset in Figure 2-4 shows the possible arrangement of the seven transmembrane domains (TM1-TM7), based on the structure of rhodopsin. Intracellular Cys^{328} is theorized to be palmitoylated, as in the β_2-adrenergic receptor,[37] which would anchor the region to the membrane and create the fourth intracellular loop. A disulfide bond is predicted to link Cys^{115} to Cys^{193}. The darkened circles indicate the amino acids which are invariant among all five subtypes. The four

extracellular asparagine residues labeled with 'CHO' denote potential sites of glycosylation which is implied in molecular recognition.

Human, mouse, and rat somatostatin receptors possess a remarkable sequence homology among the species. Receptors sst1 and sst2 have a homology of greater than 93% among the species, whereas receptors sst3-5 are slightly less conserved with a homology of 82-88%. Among each other, however, receptors sst1-5 only show a homology of 39-57%.[35] This low homology can be utilized for the design of ligands which can bind selectively to one receptor subtype over the others.

In the 1990s, all five human somatostatin (hsst) receptors became available through molecular cloning techniques,[38-41] along with the receptor subtypes of the rat (rsst)[23,42-45] and the mouse (msst).[38,46,47] Of the five sst receptors, only sst2 occurs in two isoforms, which differ in length at the *C*-terminus of the protein. Receptor sst2A contains 369 amino acids, while sst2B, with 356 amino acids, is slightly shorter.[48] The two isoforms of sst2 have similar ligand selectivities and cannot be distinguished by pharmacological agents.[49]

Each receptor subtype can be expressed in the membranes of cell lines such as Chinese hamster ovaries (CHO cells),[50,51] Chinese hamster lung fibroblast cells (CCL39),[52] monkey kidney cells (COS-1),[46] or mouse fibroblast (Ltk-cells).[53] The availability of separate receptor subtypes made it an attractive research goal to design and synthesize subtype selective analogs and to study their effects on biological function. The correlation between each receptor subtype and biological response has

not been entirely elucidated, although certain correlations based on *in vivo* and *in vitro* binding assays have been established.

The somatostatin receptors are critical for the biological effects of somatostatin to be elicited. As with other hormone receptors, the somatostatin receptors have two functions; to recognize the ligand and bind it with high affinity and specificity, and to generate a transmembrane signal that evokes a biological response. In order to explore the function of each of the receptors, molecular cloning techniques were employed to express individual receptors in host cells. The binding of somatostatin analogs to each of the receptors was then determined. The study of receptor subtype-selective ligands could also be carried out in the presence of different receptor subtypes. Subtype specific compounds were subjected to functional assays and *in vivo* studies to determine the biological response garnered from the binding of that compound to a specific receptor while in the presence of other receptor subtypes.

Native somatostatin binds to all five sst receptors with nanomolar affinity while most of the synthetic analogs, such as L-363,301 [**2-4**] (Figure 2-5) and octreotide [**2-6**] (Figure 2-7) bind to sst2, 3, and 5.[54] Few synthetic analogs bind selectively to only one of the receptor subtypes. The relationship of ligand binding at a given receptor to specific biological activity has not been totally elucidated because of the lack of subtype-selective analogs.[55,56] Table 2-1 summarizes some of the reported findings.

Table 2-1: Established sst receptor-activity correlations.

Receptor	Relevance	Ref.
sst1	Inhibition of Actin Stress Fiber Assembly	57
sst1	Inhibition of Cell Migration	57
sst2	Inhibition of Growth Hormone Release	58,59
sst2	Inhibition of Glucagon	59
sst2	Gastrin and Gastric Acid Inhibition	60
sst3	Induction of Apoptosis	61
sst3	Regulation of Gastric Smooth Muscle Contraction	62
sst4	Reduction of Intraocular Pressure (?)	63
sst5	Inhibition if Insulin Release	55,59
sst5	Amylase Inhibition	55

Receptor sst1 has been shown to regulate the inhibition of actin stress fiber assembly. Cells expressing sst1 and sst2 were each treated with thrombin and then incubated with SRIF-14. Only the cells expressing sst1 receptors inhibited fiber formation. The study also demonstrated that thrombin-stimulated cell migration is inhibited through sst1.[57]

Both peptides[58] and non-peptides[59] possessing a high degree of selectivity for sst2 have been utilized to demonstrate that sst2 is involved in the regulation of growth hormone release. Non-peptidic ligands which selectively bound to sst2 inhibited the

release of glucagon from pancreatic cells.[59] A cyclic octapeptide which was selective for sst2 inhibited the release of gastrin and gastric acid in dogs.[60]

By expressing sst receptors individually in CHO cells and treating them with octreotide [**2-6**] (Figure 2-7) it was shown that apoptosis is signaled *via* sst3, suggesting that sst3 selective analogs could be of great value in treating tumors.[61] Utilizing ^{125}I-labeled SRIF-14, it was shown that sst3 is involved in the relaxation of gastric smooth muscle cells as well.[62]

Very little information is available about the significance of sst4. It's RNA was detected in the rat eye and it was speculated that the activation of sst4 could reduce intraocular pressure, rendering sst4 an interesting target receptor for anti-glaucoma drugs.[63]

Utilizing the sst5 selective linear peptide, D-Phe-Phe-Phe-D-Trp-Lys-Thr-Phe-Thr-NH_2, it was concluded that sst5 is involved in insulin and amylase inhibition.[55] Receptor sst5 selective non-peptide somatostatin analogs were also employed to confirm the inhibition of glucagon through sst5.[59] It has also been proposed that sst5 is related to the anti-tumor activities of somatostatin.[64]

Several review articles have been published over the last decade which summarize the structural, physiological, and molecular-biological background of the somatostatin receptor families in detail.[35,48,65-68]

2.1.3 Early structure-activity relationship studies of somatostatin

The biological characterization of somatostatin began with structure-activity relationship (SAR) studies. These studies included the systematic deletion of single residues, the progressive shortening of the somatostatin peptide from the *N*- and *C*-termini, and the replacement of single residues by alanine (an alanine scan).[19] A first conclusion from the studies was that the loss of the disulfide bond between Cys^3 and Cys^{14} by replacement of either residue with alanine resulted in a linear peptide with only 0.5% of the activity of somatostatin. Incorporation of methionine in either position also prevented disulfide cyclization and resulted in complete loss of biological activity. These findings suggested that the cyclic structure of somatostatin was mandatory for biological activity and probably arrayed the essential residues into a biologically active conformation.

The alanine scan also established the importance of the Trp^8 residue, as well as the surrounding aromatic residues, for biological activity. Further analysis of the tryptophan revealed that incorporation of the enantiomeric D-Trp at position 8 led to an analog which was 6-8 times more active *in vivo* and *in vitro* compared to the parent hormone.[20] The enhanced *in vivo* activity was attributed to an optimization of the conformation of the peptide as well as a reduction in the susceptibility to enzymatic degradation because of the D-configuration. The majority of somatostatin analogs synthesized since have incorporated D-Trp^8.

The importance of Phe^6, Phe^7, Lys^9, and Phe^{11} was also demonstrated with the alanine scan. Replacement of any of those residues led to compounds without any

activity with respect to inhibition of growth hormone.[69] Replacement of Asn^5 and Thr^{10} with alanine led to mixed results in bioassays.[19,69]

An additional SAR study revealed the importance of the Trp^8-Lys^9 portion of the hormone. The Lys^9 residue was replaced with *S*-β-(aminoethyl)-cysteine, ornithine, arginine, histidine, *p*-amino-phenylalanine, and γ- and δ-fluoro lysine. In all cases, the synthesized analogs were significantly less potent than L-363-301 [**2-4**] (Figure 2-5), a potent cyclic somatostatin analog, underlining the importance of the lysine side chain.[70]

Replacement of Cys^{14} with D-Cys^{14} resulted in a compound which was 2-3 times more potent *in vivo* than somatostatin and had a 10-fold increase in selectivity for inhibition of growth hormone (GH) and glucagon over insulin.[21] Incorporation of D-Trp^8 into that compound decreased selectivity 5-7-fold, but increased inhibition of growth hormone and glucagon 6-9 times more than somatostatin.[71] These two compounds raised the expectations of finding clinically significant analogs for the treatment of diabetes.[72] Many more somatostatin analogs were synthesized and studied, several of which exhibited impressive biological profiles with regard to increased affinity and selectivity.[69] A selection of the most important compounds will be discussed in the next section.

2.2 Synthetic analogs of somatostatin

2.2.1 Peptidic somatostatin analogs

The variety of biological functions regulated by somatostatin makes it a highly attractive drug target. Unfortunately, several factors have prevented the direct use of somatostatin for therapeutic purposes. The half-life of somatostatin in the blood stream is about three minutes; not long enough to be very useful as a therapeutic agent.[73] The liver and kidneys rapidly inactivate circulating somatostatin. The peptide is also not orally available and must be administered intravenously. Orally available somatostatin analogs would be advantageous for clinical applications.

The earliest reported SRIF-14 analogs displayed only agonist activity, (the analogs resulted in the same biological effects as the native peptide), but were generally less biologically effective than the native peptide. Both agonists and antagonists (which bind to the receptor and block a specific response) were desirable compounds. While an enormous amount of research has been devoted to the design, synthesis, and evaluation of somatostatin analogs, the majority of compounds that have been synthesized are agonists. Potent and selective antagonists for each of the receptors remain elusive.

The initial search for a clinically useful somatostatin analog began when Veber and coworkers at Merck published their first synthetic analog. Peptide [**2-4**], known as L-363,301 (Figure 2-5) is a hexapeptide containing the SRIF-14 pharmacophore cyclized by a Phe-Pro dipeptide. Several dipeptide sequences were investigated for the cyclization, but the Phe-Pro sequence provided the compound with the best binding

properties and was twice as effective as somatostatin at inhibiting growth hormone release.[74] Compound [**2-4**] was shown to be quite resistant to enzymatic hydrolysis with trypsin. NMR studies confirmed the structure to be rigid and to array the pharmacophore about a type II' β-turn,[8] while the Phe^{11}-Pro^{6} dipeptide spans a type VI β-turn and includes a cis peptide bond between the two residues.[75] This dipeptide unit, known as the bridging region, is important in maintaining the proper orientation of the tetrapeptide pharmacophore.

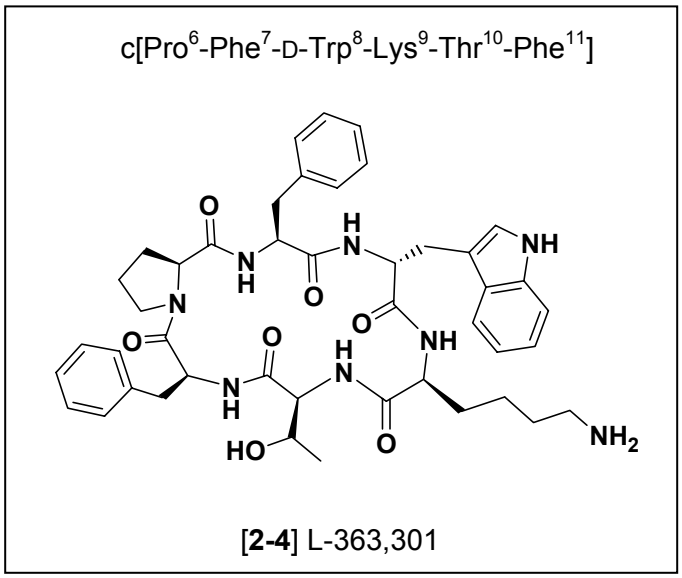

Figure 2-5: The cyclic hexapeptide L-363,301 developed by Veber and coworkers.

Further derivatization of L-363,301 led Merck researchers to develop somatostatin analog [**2-5**], known as MK678 or seglitide (Figure 2-6). MK678 is also a cyclic hexapeptide, but replaces Pro^{6} with *N*-methyl-Ala, Phe^{7} with Tyr, and Thr^{10} with Val.[76] Analog [**2-5**] is 50-100 times more potent than SRIF-14 in inhibiting

insulin, glucagon, and growth hormone release *in vivo* and showed at least 10-fold greater potency than the parent compound, L-363,301 [**2-4**], in all biological tests.

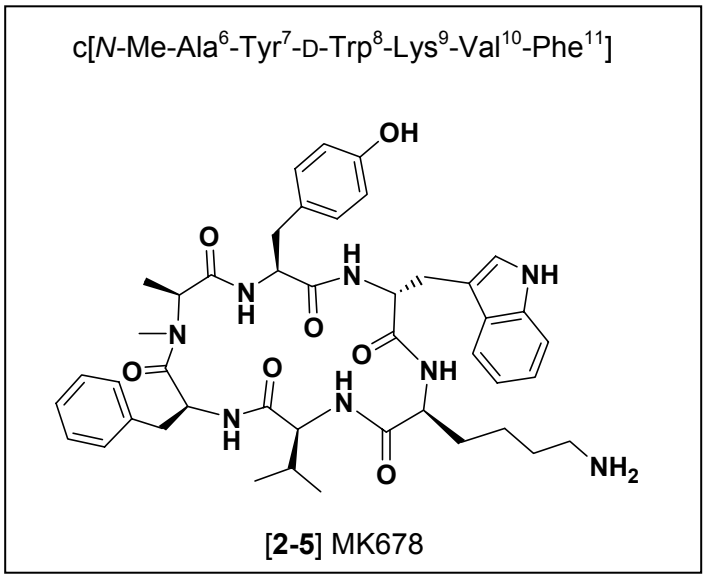

Figure 2-6: The cyclic hexapeptide MK678/ seglitide.

During the same time period, scientists at Sandoz also carried out research in the area of small, cyclic, peptidic somatostatin analogs and developed octreotide [**2-6**] (also known as SMS 201-995 and Sandostatin, Figure 2-7). The octapepide was reported to be selective for inhibition of growth hormone and glucagon secretion over insulin secretion and was 20 times more potent than somatostatin in rats and monkeys. In octreotide, the somatostatin pharmacophore is conformationally restricted by a disulfide bridge formed between the side-chains of the flanking cysteine resides. The reduced *C*-terminus of the α-hydroxylmethyl Threonine residue decreases the likelihood of enzymatic degradation.[77] Octreotide is remarkable in its high resistance

to enzymatic degradation, with a plasma half-life of 1.5 hours, making it orally available and resulting in its investigation in clinical trials.

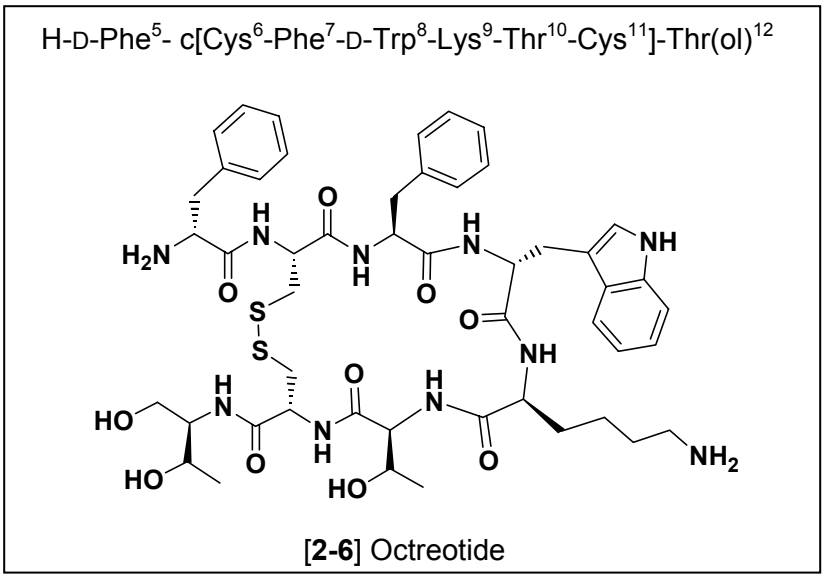

Figure 2-7: The structure of disulfide-bridged octreotide, a somatostatin analog which is used in the clinic.

The biological profile of octreotide encouraged researchers to optimize the binding affinity and selectivity of the octapeptide. The synthesis and biological evaluation of two octreotide analogs, named RC-121 [**2-7**] and RC-160 [**2-8**] (also known as octastatin, Figure 2-8) were reported. Both compounds differ from octreotide through the substitution of Tyr for Phe^7 and Val for Thr^{10}, making them somewhat analogous to MK678. The compounds differ from octreotide and each other in the *C*-terminus where RC-121 [**2-7**] contains a threonine amide and RC-160 [**2-8**] contains a tryptophan amide. RC-121 [**2-7**] was found to be 177 times more potent than SRIF-14 in inhibiting growth hormone secretion in rats, while RC-160 was

113 times more potent. Both analogs were determined to be 4-10 times more potent than SRIF-14 in inhibiting insulin, glucagon, and gastric acid release in dogs.[78]

H-D-Phe^5- c[Cys^6-Tyr^7-D-Trp^8-Lys^9-Val^{10}-Cys^{11}]-Thr^{12}-NH_2

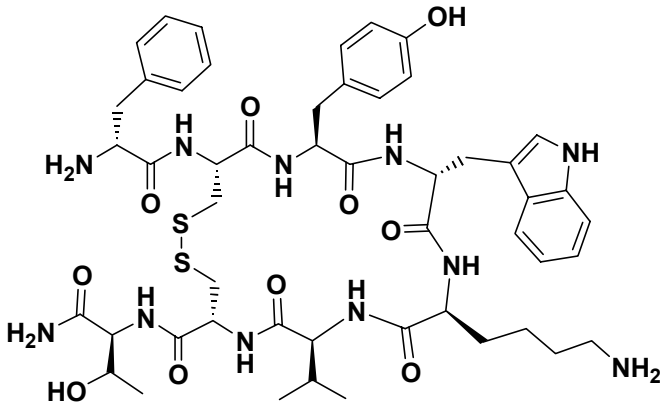

[**2-7**] RC-121

H-D-Phe^5- c[Cys^6-Tyr^7-D-Trp^8-Lys^9-Val^{10}-Cys^{11}]-Trp^{12}-NH_2

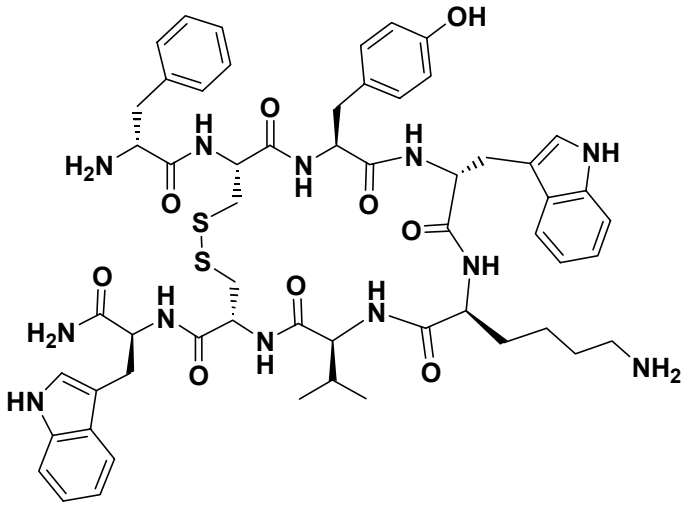

[**2-8**] RC-160

Figure 2-8: The structures of RC-121 and RC-160 (octastatin), cyclic octapeptide analogs of octreotide.

Further derivatization of RC-121 [**2-7**] by scientists at Biomeasure allowed them to develop the cyclic octapeptide, lanreotide [**2-9**] (also known as BIM23014, Figure 2-9). Lanreotide [**2-9**] differs from RC-121 [**2-7**] only in the *N*-terminal residue through incorporation of a D-naphthylalanine. This small change produced a compound which inhibited growth hormone secretion in rats 10,000 times more effectively than SRIF-14. Lanreotide was shown to be half as effective as SRIF-14 in the inhibition of glucagon release and comparable in the inhibition of insulin release.[79] Mice implanted with a tumor cell line were treated with lanreotide which retarded the tumor growth *in vivo*. Lanreotide also inhibited tumor growth *in vitro*, presumably through an antiproliferative effect, rather than through cytotoxicity.[80] These exciting results led to the investigation of lanreotide in clinical trials.

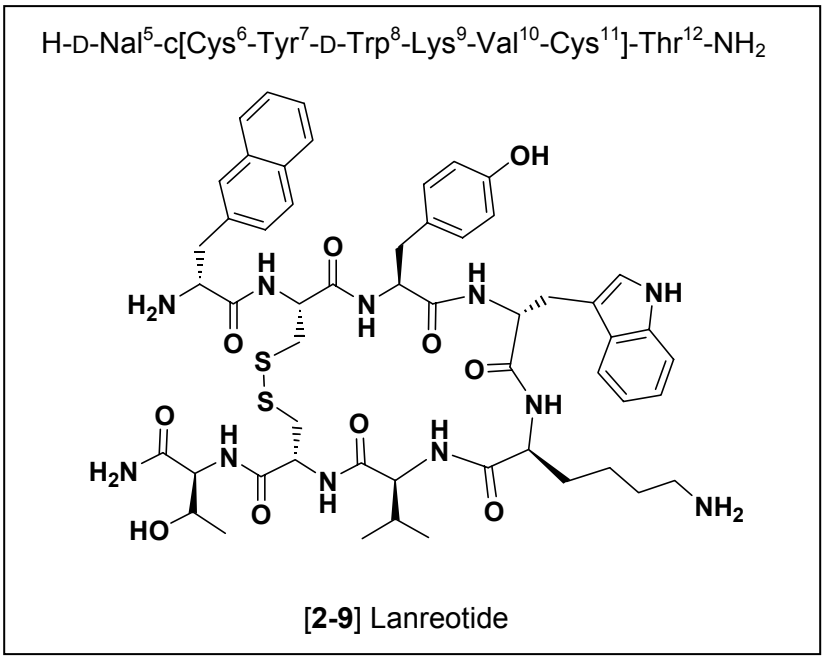

Figure 2-9: The structure of disulfide-bridged lanreotide which contains a D-naphthylalanine at the *N*-terminus.

Table 2-2 summarizes the binding affinities of the previously mentioned peptidic somatostatin analogs for all five of the receptor subtypes. These compounds are considered to be milestones in the area of somatostatin research because they provided insight into the biological function of the receptors and were the basis for the design of more potent and selective analogs. At the time of the discovery of the analogs, the individual receptor subtypes were not known or available. The listed references provide the separate receptor subtype binding data for the compounds. Table 2-2 also highlights the lack of subtype selectivity displayed by the two native forms of the hormone.

Table 2-2: Binding affinities (K_i in nM) of selected peptidic somatostatin analogs for the five somatostatin receptor subtypes, sst1-5.

Compound	sst1	sst2	sst3	sst4	sst5	Ref.
Somatostatin [**2-1**]	0.38	0.04	0.66	1.78	2.32	[68]
Somatostatin-28 [**2-2**][a]	0.63	0.20	0.32	0.79	0.40	[54]
L-363,301 [**2-4**]	>1000	5.1	129	>1000	25	[81]
MK678 [**2-5**]	>1000	1.5	27	127	2	[82]
Octreotide [**2-6**]	875	0.57	26.8	>1000	6.78	[83]
RC-121 [**2-7**]	>1000	1.7	>1000	>1000	13.1	[84]
RC-160 [**2-8**]	>1000	5.4	31	45	0.7	[82]
Lanreotide [**2-9**]	>1000	1.8	43	66	0.62	[82]

[a] calculated from ref.[54].

2.2.2 Clinical use of peptidic somatostatin analogs

It has been a challenge to develop somatostatin analogs with minimal side effects. Only three of the analogs, namely octreotide [**2-6**], lanreotide [**2-9**], and RC-160 [**2-8**], were introduced for routine hormone secretion therapies in humans. Their approved medical indications include acromegaly, TSH-secreting pituitary tumors, neuroendocrine tumors of the gastrointestinal tract, some refractory diarrhoeas (such as chemotherapy and AIDS-related diarrhoea), prevention and treatment of pancreatic surgery complications, and malignant bowel obstruction.[85-87] Unfortunately, the clinical administration of somatostatin analogs has been limited because side effects, such as gallstone formation, occur because the secretion of hormones other than the target are also inhibited which interferes with gallbladder function.[88]

Receptor scintigraphy using radiolabeled SRIF-14 analogs has become a routine procedure for the visualization of hsst-positive tumors. Octreotide, conjugated to diethylenetriamine pentaacetic acid (DTPA) and labeled with ^{111}In ([^{111}In-DTPA] octreotide or OctreoScan, [**2-10**], Figure 2-10) is the most commonly used agent. It exhibits a high affinity and selectivity for hsst2, the most abundant sst receptor subtype in human tumors expressing sst receptors. Somatostatin receptor imaging has clinical importance in the localization of several neuroendocrine tumors as well as in Hodgkin's disease.[89]

Recently, this approach was extended to therapeutic applications. The demonstration of effective internalization of the somatostatin receptor complex by human tumors encouraged researchers to couple cytotoxic agents to somatostatin

analogs.[90] DTPA was replaced with 1,4,7,10-tetraazacyclododecan-1,4,7,10-tetraacetic acid (DOTA), which chelates ^{90}Y (in addition to ^{111}In). The β-emitting isotope can kill tumor cells within a few millimeters. The resulting compound, [^{90}Y-DOTA-D-Phe^{1}-Tyr^{3}]octreotide [**2-11**] (also known as OctreoTher, Figure 2-10) has high affinity for hsst2 and is being tested in clinical trials for the treatment of hsst2-positive tumors.[91]

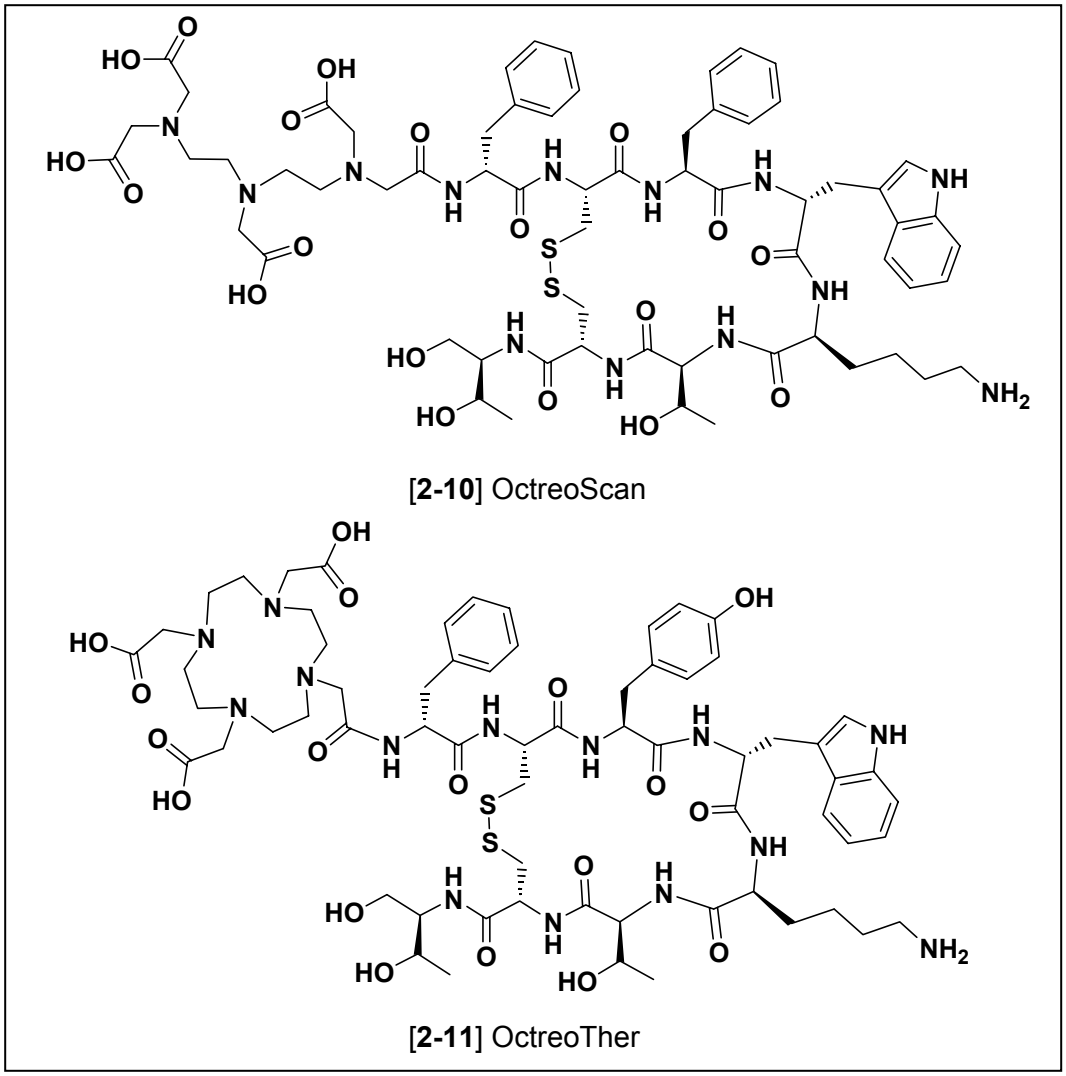

Figure 2-10: Octreotide analogs, OctreoScan [**2-10**] and OctreoTher [**2-11**] can both coordinate radioactive isotopes for use in imaging and treating sst2-positive tumors.

While potency is not an issue with the classical SRIF-14 drugs, (which are active in the nanomolar range), new SRIF-14 analogs which are orally available and possess longer duration of action in the blood would certainly offer an alternative to the currently available injectable treatments. Research which continues to probe the topochemical and conformational requirements of somatostatin analogs for biological activity and selectivity will contribute to the exploitation of somatostatin's regulatory functions for therapeutic applications.

2.2.3 Somatostatin analogs which contain unnatural amino acids

Replacing amino acid residues within a peptide with nonnaturally occurring amino acids or amino acid derivatives can provide a wealth of information about the peptide and its cellular receptors. By incorporating such residues, the stability of the compound against enzymatic degradation is often enhanced because enzymes are unable to recognize the residues. Additional SAR information from positive and negative biological results provides further insight into the bioactive conformation of the compound as well as the chemical and topological space of the binding pocket of the receptor. Numerous non-natural amino acids and amino acid derivatives have been synthesized and incorporated into SRIF-14 [**2-1**] and its classical, smaller analogs.

The amide bonds between Phe^7-Trp^8 and Trp^8-Lys^9 of SRIF-14 were thought to be particularly prone to enzymatic cleavage.[92,93] To increase the enzymatic stability, Goodman and coworkers employed retro-inverso modifications to those bonds by incorporating *g*Phe^7-*m*Trp^8 and *g*Trp^8-*m*Lys^9 (*g* denoting the *gem*-diamino derivative,

and *m* denoting the malonyl derivative) residues into the respective positions in SST-14 (Figure 2-11).

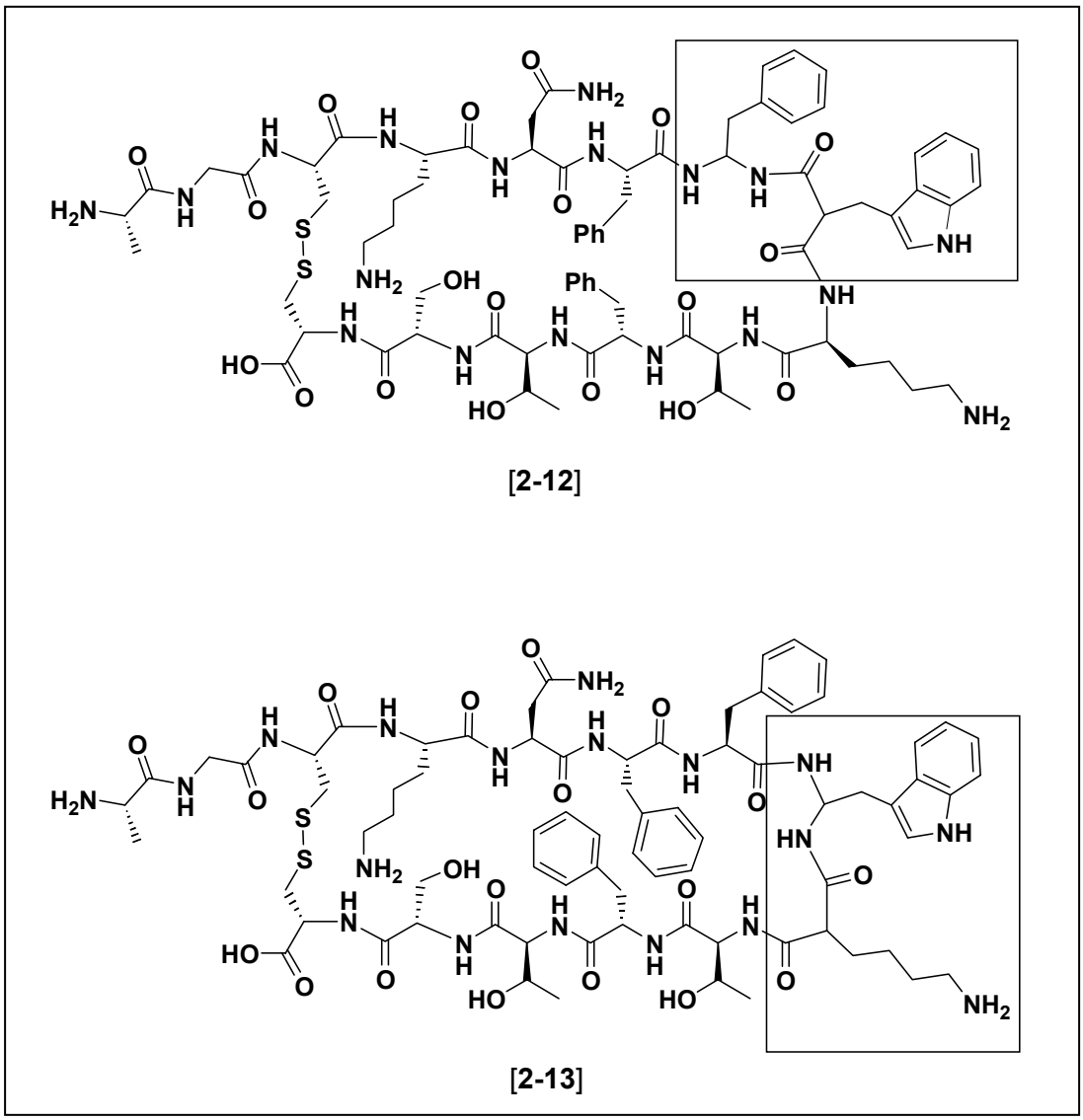

Figure 2-11: SRIF-14 analogs containing *gem*-diamino and malonyl structures (highlighted in boxes) which result in retro-inverso peptides.

The *g*Phe^7-*m*Trp^8 compound [**2-12**] inhibited growth hormone release only slightly less effectively than the native peptide, while the *g*Trp^8-*m*Lys^9 compound [**2-13**] was less effective by two orders of magnitude.[94] The difference in activity was attributed to the ability of the *g*Phe^7-*m*Trp^8 compound [**2-12**] to array the pharmacophore in a topography closer to that of a β-turn.

Analogs of L-363,301 containing retro-inverso residues were also synthesized.[95] Conformational analysis of the retro-inverso cyclic hexapeptides provided information which led to the incorporation of α- and β-methylated amino acids into the cyclic hexapeptide structure. Additional methyl groups within the side-chain of the amino acids reduce the rotational freedom of flexible parts of the molecules. The rotational restriction forces the compound to reside in specific rotamers which facilitates the probing of bioactive conformations.

Researchers in the Goodman laboratories prepared all four diastereomers of β-methyl tryptophan as enantionmerically pure compounds and incorporated them into L-363,301.[96] Substitution of D-Trp with (2*R*,3*S*)-β-methyl tryptophan produced compound [**2-14**] (Figure 2-12) which was more biologically active than the parent hexapeptide. The compound containing the (2*S*,3*R*)-diastereomer was less active by 10-fold, while the (2*R*,3*R*)- and (2*S*,3*S*)-diastereomers were about 100-fold less active than L-363,301 *in vitro*. Conformational searches were then performed which were consistent with the data from NMR spectroscopy. The resulting conformations could be divided into two families; 'folded' and 'flat', referring to the overall topology of the compounds. Further studies of analogs containing α-methyl-Phe^7 suggested the

'folded' conformation to be the bioactive one.[96] These findings by Goodman refute those of Veber and coworkers, who demonstrated that L-363,301 adopts a flat and folded conformation, but suggested the flat topology to be the bioactive form.[7]

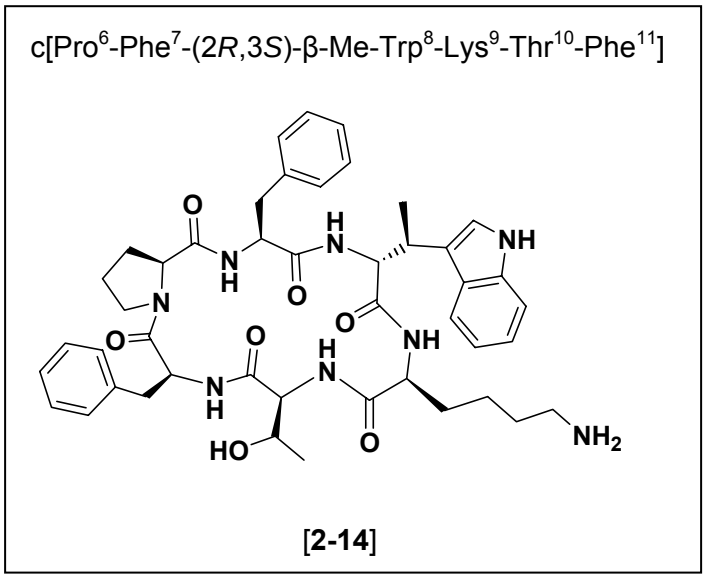

Figure 2-12: An analog of L-363,301 which contains (2*R*,3*S*)-β-methyl tryptophan[8].

The binding of each of the four of the β-methyl tryptophan containing peptides was compared to that of L-363,301 utilizing a mixture of all five receptor subtypes which did not allow for the determination of subtype selectivity.[96] The original assays found the IC_{50} of L-363,301 to be 1 nM, of the (2*R*,3*S*)-β-methyl tryptophan compound to be less than 1 nM, of the (2*S*,3*R*)-β-methyl tryptophan analog to be 10 nM. The (2*R*,3*R*)- and (2*S*,3*S*)-β-methyl tryptophan compounds were inactive. The (2*R*,3*S*)- and (2*R*,3*R*)-β-methyl tryptophan compounds were recently resynthesized so that the binding affinities for all five of the hsst receptors could be measured.[97] While

the (2*R*,3*R*)-analog was originally thought to be inactive, the recent data suggests it binds to hsst2 with at least 100-fold selectively over the other receptors and an IC_{50} of 7.2 nM, comparable to SRIF-14. The (2*R*,3*S*)-β-methyl tryptophan analog [**2-14**] was more potent at hsst2 with an IC_{50} of 0.23 nM. Table 2-3 summarizes the results of those biogical tests.

Table 2-3: Binding affinities (IC_{50} in nM) of selected β-methyl tryptophan analogs for all five human somatostatin receptor subtypes, hsst1-5.

Compound	hsst1	hsst2	hsst3	hsst4	hsst5
Somatostatin [**2-1**]	0.17	1.2	0.11	0.14	0.53
L-363,301 [**2-4**]	897	0.16	917	756	39
(2*R*,3*S*)-analog [**2-14**]	969	0.23	>1000	242	68
(2*R*,3*R*)-analog	915	7.2	>1000	936	>1000

The incorporation of α-methyl-Val[10] in place of Thr[10] or of β-methyl-Phe[11] in place of Phe[11] in L-363,301 analogs did not lead to any enhancement in biological activity but did provide valuable insight into biologically relevant conformations.[98] The aforementioned results led the Goodman laboratories to develop a model of the special and side-chain requirements of the somatostatin pharmacophore for receptor binding. This model was subsequently refined using data from the analysis of lanthionine bridged octreotide analogs. The model depicted in Figure 2-13 provides the distances required between the functional groups thought to be essential for

binding to the somatostatin receptors.[96,99] The distance values indicated in the model were calculated from NMR spectroscopic analysis of lanthionine [**2-15**] (Figure 2-14) whereas the distances in parentheses were obtained from spectroscopic analysis of the β-methyl-tryptophan containing hexapeptides.

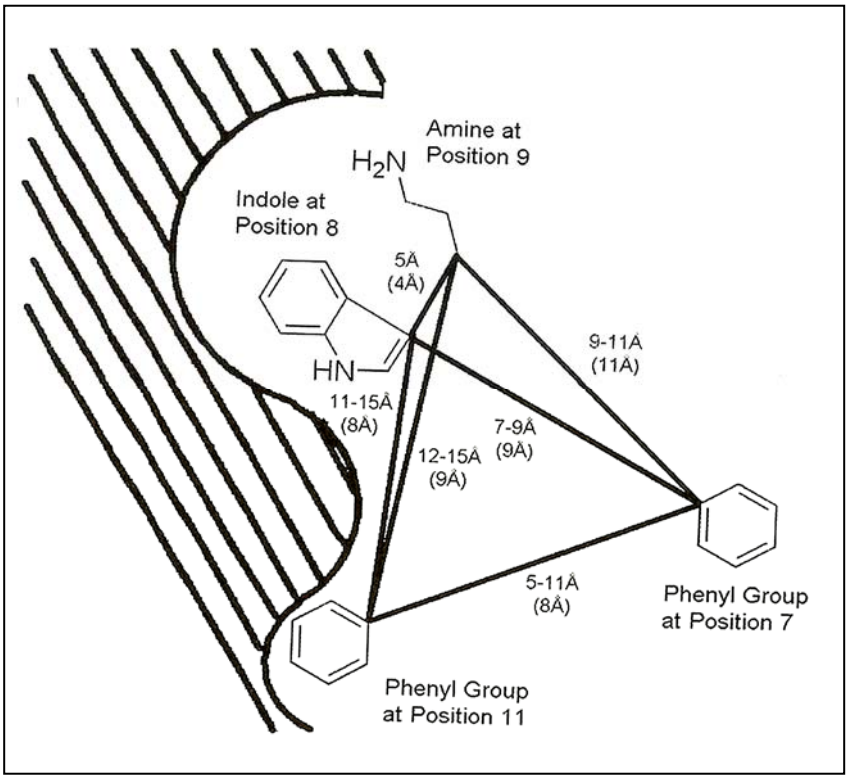

Figure 2-13: A model of the somatostatin pharmacophore with the spatial and distance requirements of the functional groups needed for receptor binding.

The previously mentioned lanthionine-bridged octreotide analogs were synthesized using solid phase techniques and were evaluated *in vivo* using expressed somatostatin receptors. Of the several octreotide analogs synthesized, compound

[**2-15**] (Figure 2-14) displayed 3-fold selectivity for hsst5 over hsst2, noteworthy because octreotide binds with equal potency to both. However, substrate [**2-15**] was five to six times weaker in binding affinity than somatostatin and octreotide. Enzymatic degradation studies using rat brain homogenates showed the lanthionine bridged analog [**2-15**] to have a three times longer half-life than octreotide.[100]

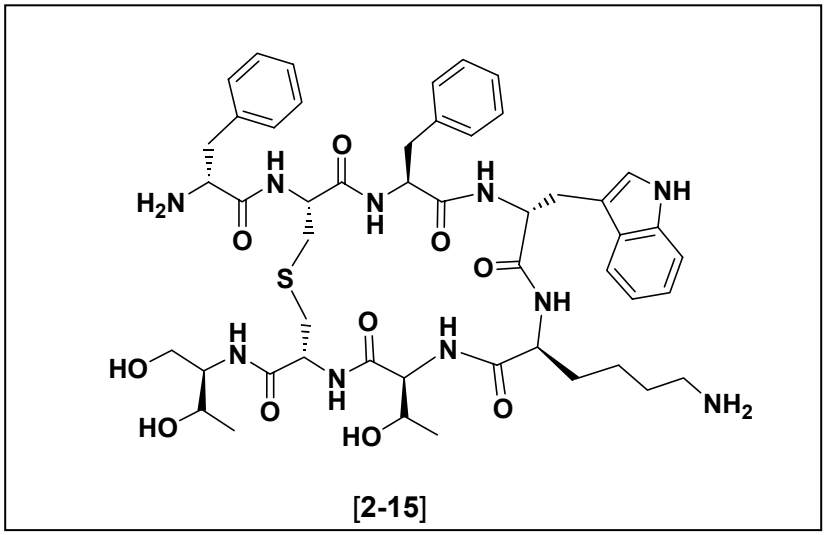

Figure 2-14: A lanthionine-bridged analog of octreotide.

It has been shown that oligomers containing peptoid residues are virtually untouched by a variety of proteases and display reduced susceptibility toward enzymatic degradation.[101] In an effort to develop analogs of L-363,301 with increased enzymatic stability and to further derivatize the bridging region, the Goodman laboratory synthesized new analogs which contained *N*-alkyl glycine derivatives in the Pro^6 position.[102,103] As demonstrated in Figure 2-15, the target peptoid residues were

conceptualized from the opening of the Pro^6 ring of L-363,301 between the α- and β-carbons.

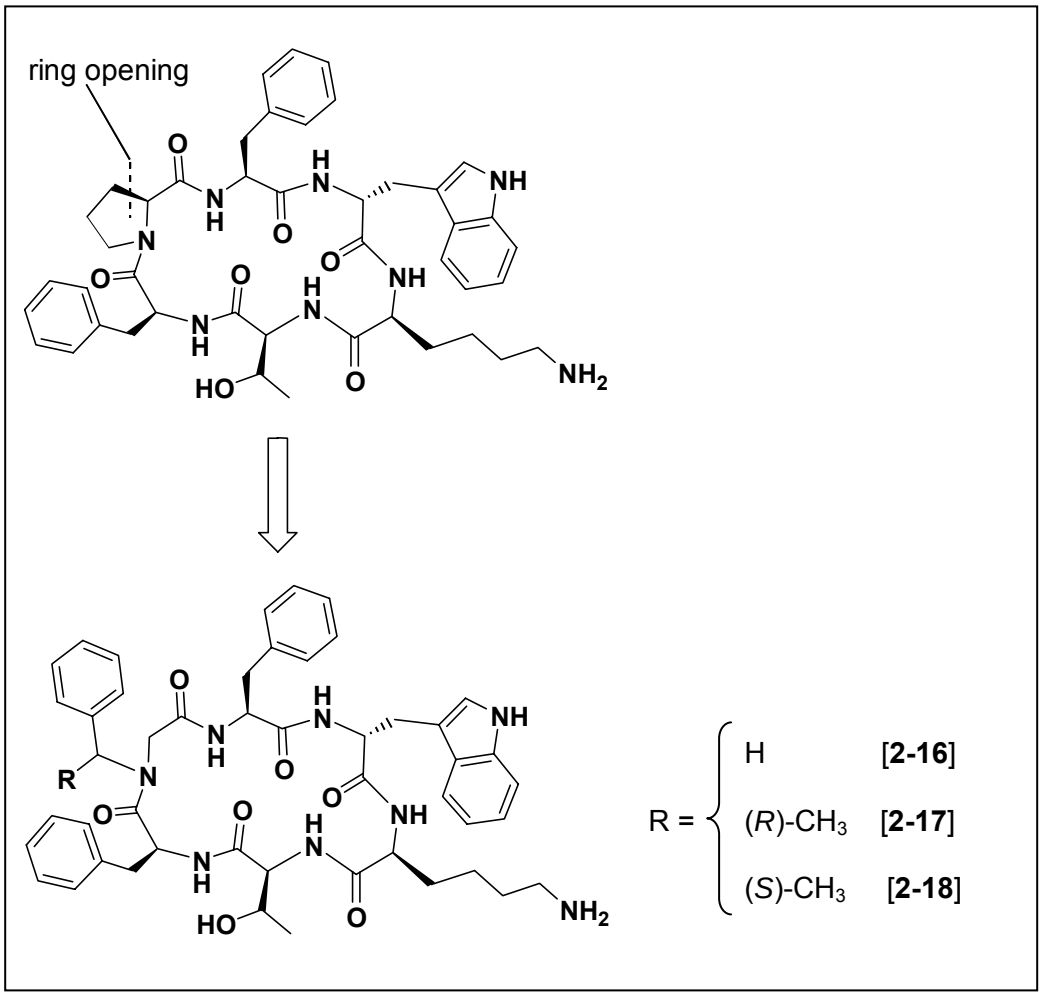

Figure 2-15: The *N*-alkylated peptoid residues which were incorporated into the Pro^6 position of L-363,301 were conceptualized from the breaking of the bond between α- and β-carbons of Phe^6.

Based on this design, the *N*-benzyl-Gly (*N*Phe) analog [**2-16**] and both enantiomers of β-methyl-*N*Phe, [**2-17**] and [**2-18**], were synthesized, evaluated for

receptor subtype selectivity,[81] and characterized by NMR spectroscopyand molecular modeling.[104] Within the series, (*R*)-β-Me-*N*Phe analog [**2-17**] displayed the highest selectivity for hsst2 by three orders of magnitude over hsst1 and hsst4, and two orders of magnitude over hsst3 and hsst5.

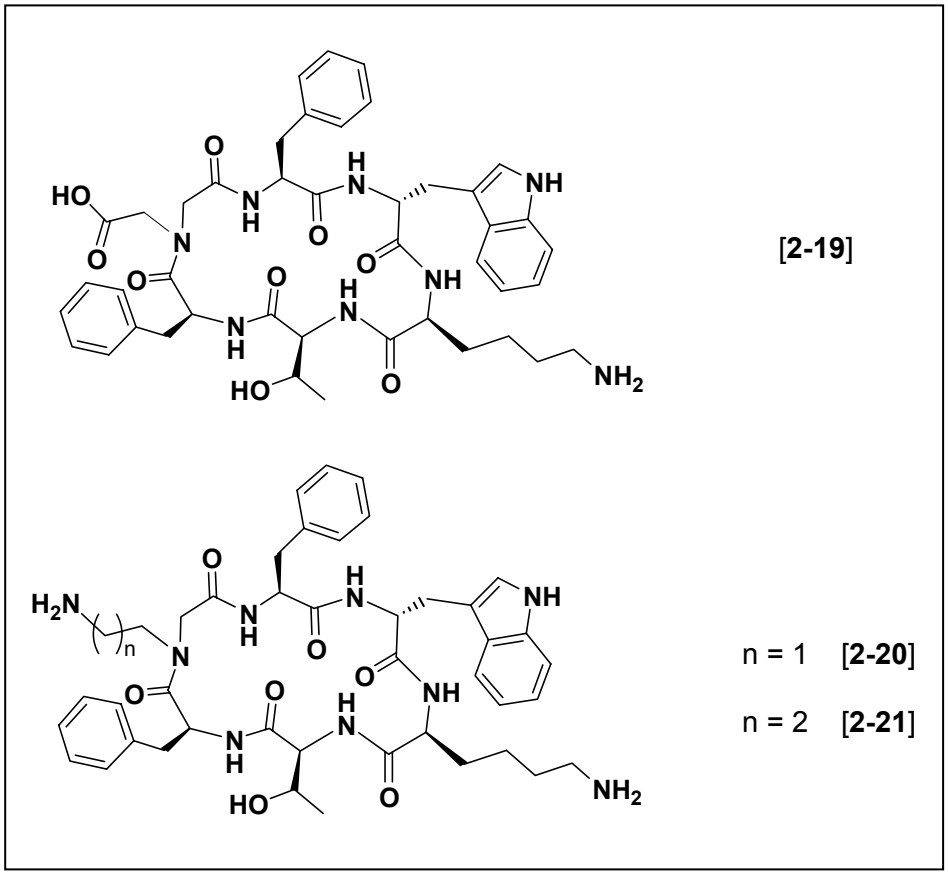

Figure 2-16: The incorporation of acidic and basic *N*-alkylated peptoid residues into position 6 of L-363,301.

Because the incorporation of hydrophobic, aromatic peptoid residues into the bridging region of L-363,301 resulted in a decrease in binding, researchers in the

Goodman laboratories incorporated a series of polar peptoid residues to further study the requirements for receptor binding. Specifically, *N*-(2carboxyethyl) glycine (*N*Asp) [**2-19**], *N*-(2-aminoethyl) glycine (*N*Dab) [**2-20**], and *N*-(2-aminobutyl) glycine (*N*Lys) [**2-21**] were incorporated into the Phe^6 position of hexapeptide L-363,301 (Figure 2-16).

The compounds were assayed for binding at the cloned receptors, *in vitro*. The binding affinities for the peptoid-containing analogs of L-363,301 synthesized in the Goodman laboratories are summarized in Table 2-4. The incorporation of the acidic group in compound [**2-19**] resulted in loss of binding at hsst 3 and hsst5, and a 100-fold decrease in affinity for hsst2 as compared to L-363,301. The incorporation of the basic aminoalkyl side chains led to a slight increase in binding affinity for hsst2 and a substantial increase in affinity for hsst3. Compound [**2-20**] was interesting because it was about six times more selective for hsst2 over hsst5 as compared to L-363,301, whereas compound [**2-21**] possessed hsst2 and hsst5 selectivity similar to that of L-363,301.[105] The longer side chain of [**2-21**] resulted in improved binding to hsst5 over L-363,301 which was not observed with compound [**2-20**].

Table 2-4: *In vitro* binding affinities (K_i in nM) of peptoid analogs of L-363,301 for the individual human somatostatin receptor subtypes, hsst1-5.

Compound	hsst1	hsst2	hsst3	hsst4	hsst5
L-363,301 [**2-4**]	>1000	5.10	129	>1000	20.3
Phe^{11}-*N*Phe^{6}-Phe^{7} [**2-16**]	>1000	6.98	253	>1000	100.7
Phe^{11}-(*R*)-β-Me-*N* Phe^{6}-Phe^{7} [**2-17**]	>1000	2.33	425	>1000	33.5
Phe^{11}-(*S*)-β-Me-*N* Phe^{6}-Phe^{7} [**2-18**]	>1000	29.5	797	>1000	87
Phe^{11}-*N*Asp^{6}-Phe^{7} [**2-19**]	>1000	157	>1000	>1000	>1000
Phe^{11}-*N*Dab^{6}-Phe^{7} [**2-20**]	>1000	4.2	40.4	>1000	102
Phe^{11}-*N*Lys^{6}-Phe^{7} [**2-21**]	>1000	4.6	53.4	>1000	15.3

Scientists at Novartis recently shifted focus away from the quest for hsst receptor subtype selective somatostatin analogs and synthesized an analog with a more universal binding profile but with enhanced metabolic stability compared to SRIF-14. SOM230 [**2-22**] (Figure 2-17) is a cyclic hexapeptide which structurally resembles L-363,301 [**2-4**], but contains non-natural amino acids in the bridging region and within the pharmacophore itself. Pro^{6} is replaced with a substituted hydroxylproline, Phe^{7} is replaced with phenylglycine, and Thr^{10} is replaced with a benzylated tyrosine. SOM230 binds with high affinity to sst1-3 and sst5 *in vitro* and inhibits growth hormone release from rat pituitary cells with an IC_{50} of 0.4 nM.[106]

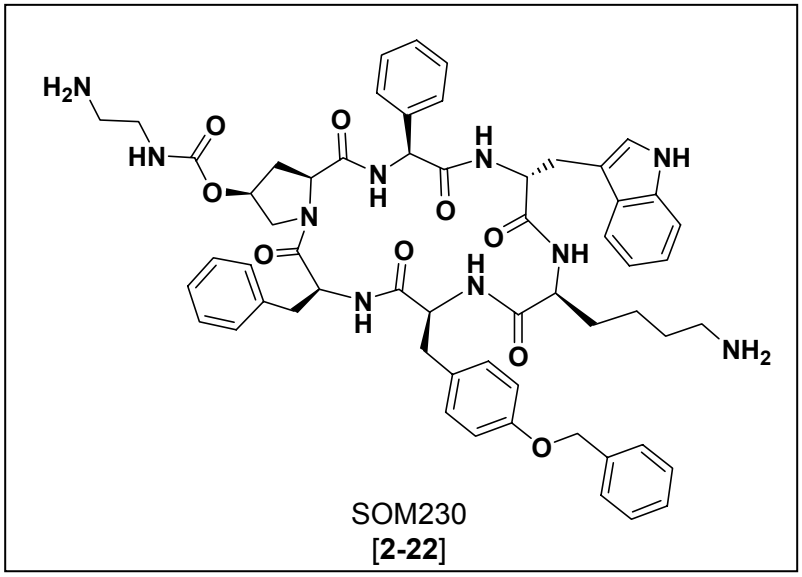

Figure 2-17: The cyclic hexapeptide SOM230 displays a universal somatostatin receptor binding

Though not structurally similar, the biological profile of SOM230 was compared to that of octreotide [**2-6**]. SOM230 binds with much higher affinity to hsst1, hsst3, and hsst5, but is comparable to octreotide in its binding to hsst2. With a blood plasma half-life of 23 hours, SOM230 effectively inhibits growth hormone release *in vivo* for an extended time period over octreotide, whose half-life is only two hours. Insulin secretion inhibition was observed in rats, however long term diabetogenic effects were not observed, even after four months of administration of SOM230. SOM230 [**2-22**] is currently under investigation for clinical use in humans.

Table 2-5: Binding affinities (IC_{50}, nM) of SRIF-14, octreotide, and SOM230 for the human somatostatin receptor subtypes.[106]

Compound	sst1	sst2	sst3	sst4	sst5
Somatostatin [**2-1**]	0.98	0.15	0.56	1.5	0.29
Octreotide [**2-6**]	280	0.38	7.1	>1000	6.3
SOM230 [**2-22**]	9.3	1.0	1.5	>100	0.16

Very little has been published about potent or selective somatostatin analogs which contain modifications to the D-Trp^8-Lys^9 dipeptide portion of the pharmacophore. Non-naturally occurring amino acid substitutions of D-Trp^8 have included the incorporation of D-naphthylalanine and a few halogenated D-Tryptophans. These compounds will be discussed in greater detail in Chapter 3.

Many different types of non-naturally occurring amino acids have been successfully incorporated into SRIF-14, L-363,301, and octreotide analogs. These compounds have provided insight into the required conformation for receptor subtype binding, selectivity, and biological activity. A model for the topological distances and pharmacophoric requirements for receptor binding was developed from the acquired data which will aid in the design of future somatostatin peptides and peptidomimetics. Scientists at Novartis incorporated numerous non-natural amino acid residues which resulted in a potent compound with enhanced metabolic stability and universal binding to all five hsst receptors with potency similar to that of SRIF-14.

2.2.4 Non-peptidic somatostatin analogs

Peptides play an important role in biological systems. In some cases, native peptides such as insulin and oxytocin can be used directly as therapeutic agents. In most cases, though, the lack of metabolic stability and selectivity limits the therapeutic use of peptides. To overcome these drawbacks, much effort has been expended to develop peptidomimetics; non-peptidic analogs of a peptide which can properly array the pharmacophores of the peptide to participate in biological recognition and response.

One of the first somatostatin peptidomimetic structures reported was the Hirschmann-Nicolaou β-D-glucose scaffold [**2-23**] (Figure 2-18). The glucose derivative was reported to act as an agonist and inhibited growth hormone release in a functional assay with an IC_{50} of 3 μM.[107,108]

Following the lead of Hirschmann and Nicolaou, other scaffolds were examined which led to the development of a xylofuranose-based analog [**2-24**],[109] benzodiazepinone [**2-25**], [110] and the azepine-based analog [**2-26**].[111] Figure 2-18 shows the structures of these peptidomimetics and lists their reported binding affinities (IC_{50} in μM) to the multiple somatostatin receptor subtypes located within isolated rat cortex membranes. While it was impressive that somatostatin activity could be obtained without a peptide backbone, these first generation peptidomimetics were not potent compared to SRIF-14 and its classical analogs. The binding affinities of SRIF-14 [**2-1**], L-363,301 [**2-4**], and MK678 [**2-5**] are also included in Figure 2-18 for comparison.

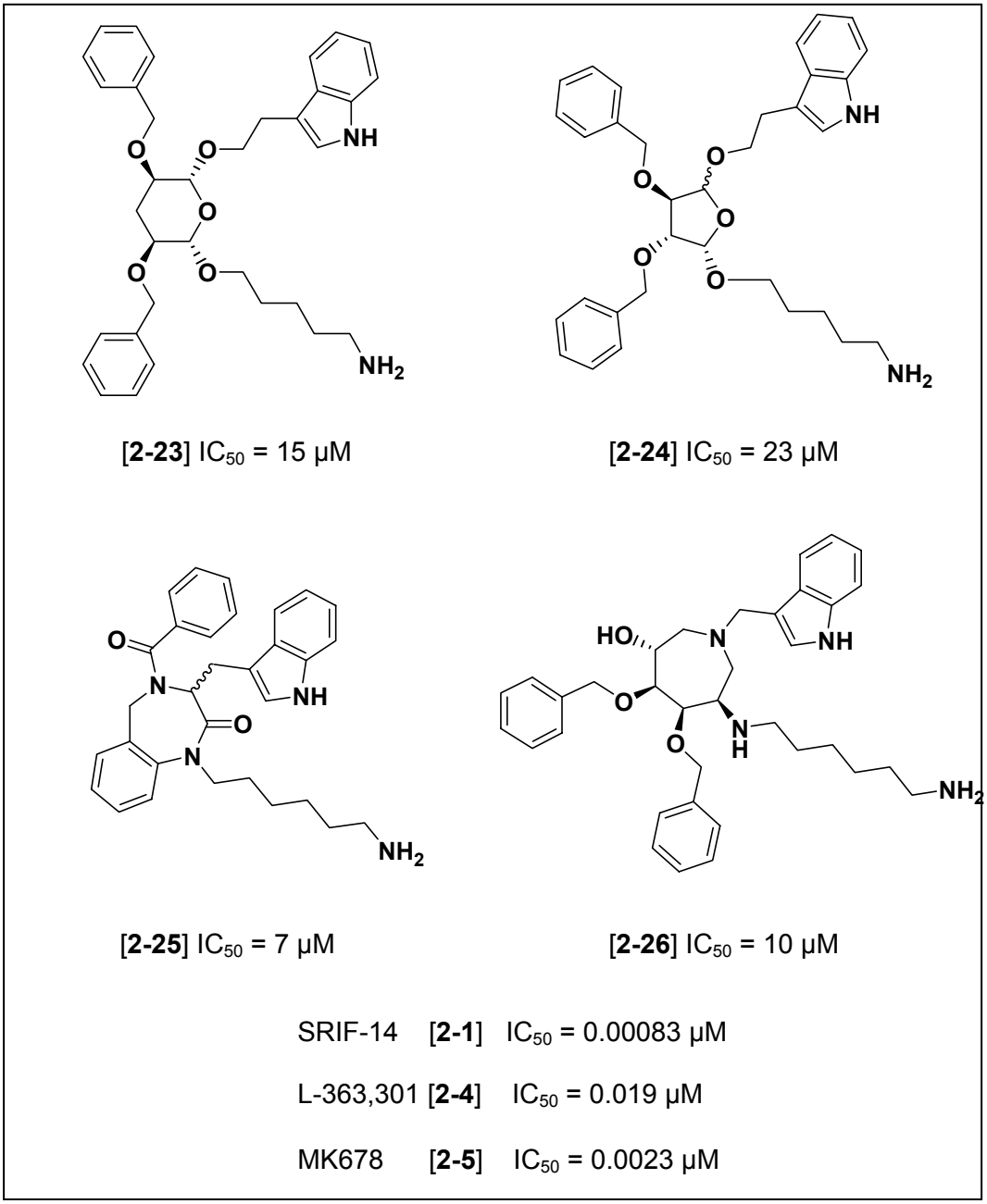

Figure 2-18: Structures of first generation somatostatin peptidomimetics and their reported binding affinities to the multiple receptors within isolated rat cortex membranes.

In an effort to develop small molecule β-turn mimetics, Ellman and coworkers designed scaffold [**2-27**] (Figure 2-19). A small library of compounds was synthesized and thioether [**2-28**] was found to be the most hsst5 selective with an IC_{50} of 87 nM; 5-fold selective over hsst1 and at least 10-fold selective over hsst2-4.[112] The indole and amine functionalities were thought to be arrayed in a β-turn type conformation.

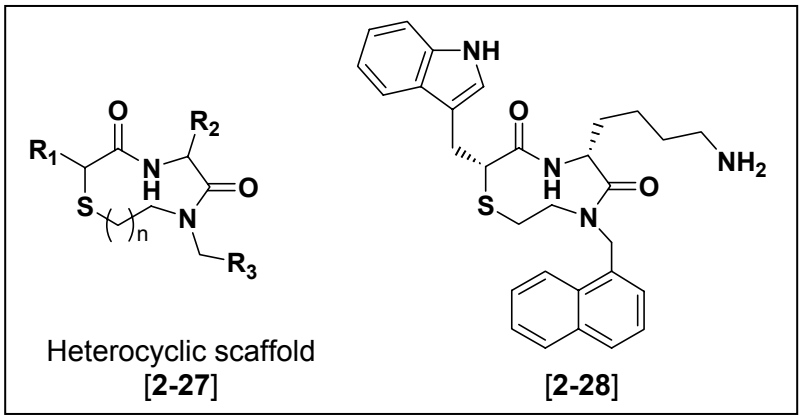

Figure 2-19: Ellman and coworkers'β-turn mimetic scaffold and their most potent somatostatin analog .

The previously described peptidomimetics all contained residues reminiscent of the pharmacophore of somatostatin, i.e. an indole ring, an aromatic group, and an alkyl amine. The advent of high throughput screening allowed researchers the ability to create large libraries of small molecules and to assay them for biological activity. This technique enabled additional probing of topological space and provided potent somatostatin analogs which did not contain the obvious pharmacophores.

The selective sst4 agonist, NNC 26-9100 [**2-29**] (Figure 2-20),[113] contains a thiourea backbone with pendant imidazole, benzyl, and pyridyl groups. This thiourea selectively bound to hsst4 with a K_i of 6 nM and decreased cAMP levels in additional functional assays which indicated that hsst4 agonists could lower intraocular pressure and be potential useful in the treatment of glaucoma.[114]

High throughput parallel synthesis was employed to create a series of imidazole derivatives which were selective agonists for hsst3. BN81674 [**2-30**] (Figure 2-20) was the lead structure and was more than 10,000-fold selective for hsst3 with a K_i of 0.92 nM.[115]

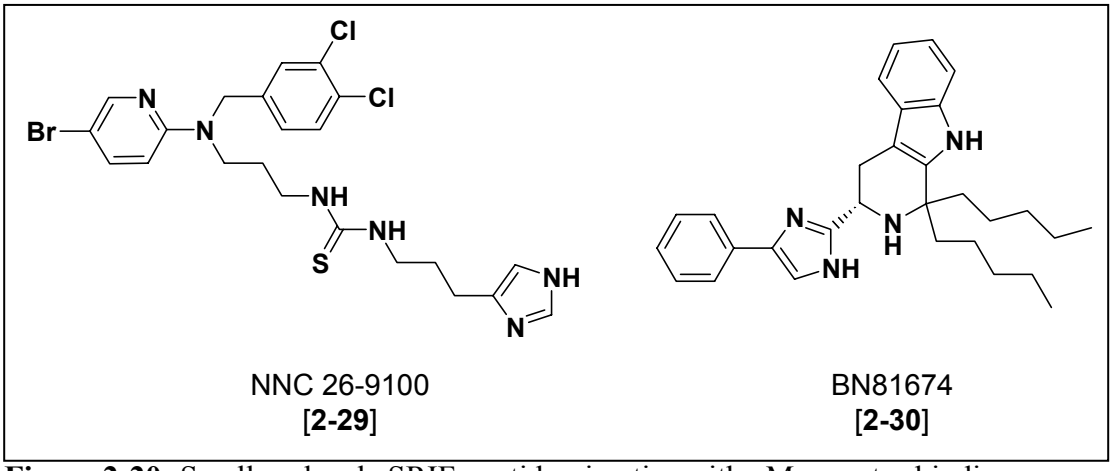

Figure 2-20: Small molecule SRIF peptidomimetics with nM receptor binding.

Merck Research Laboratories conducted a substantial effort toward the design and synthesis of non-peptide somatostatin receptor agonists using a combinatorial approach.[59,116] Lead compounds were discovered which were potent and selective for each of the five hsst receptors, and are shown in Figure 2-21.

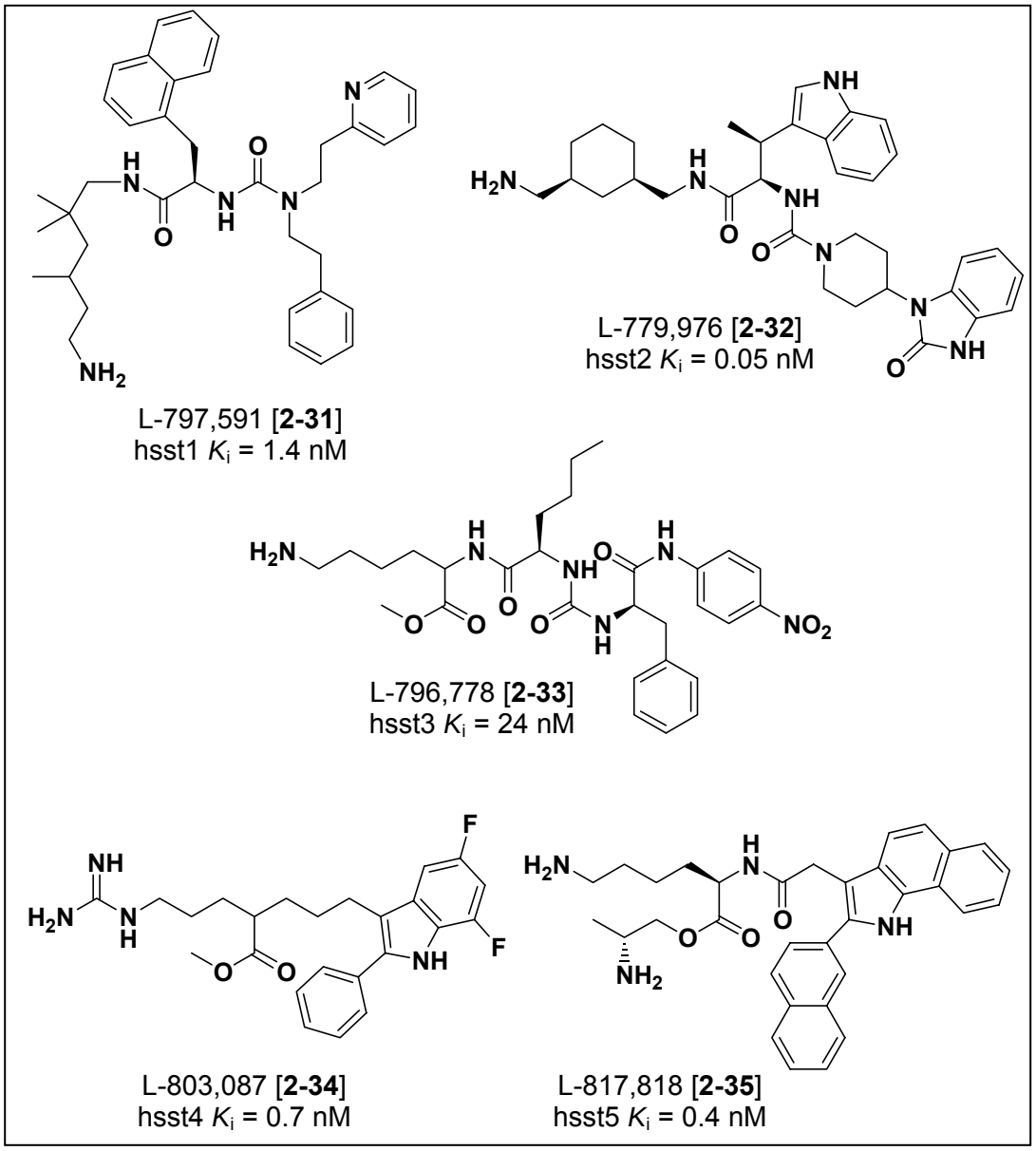

Figure 2-21: The lead compounds discovered by researchers at Merck and their hsst receptor binding affinity, K_i (nM), at their preferred receptor subtype.

While naphthylalanine derivative [**2-31**] was selective for hsst1 and compound [**2-33**] was selective for hsst3, both were greater than 100-fold selective over the other

receptors. β-Methyl tryptophan analog [**2-32**] was greater than 10,000 times more selective for hsst2 over the other receptors and was investigated further in functional assays for inhibition of growth hormone release.[117] Guanidine [**2-34**] was greater than 1000-fold selective for hsst4. Compound [**2-35**] was the least selective of the series showing only 10-fold selectivity for hsst5 over hsst1, and 100-fold selectivity over hsst2-4.

The small molecule somatostatin peptidomimetics discussed herein are a small sampling of the most potent analogs described in the literature. Libraries of thousands of these types of compounds have been synthesized, characterized and tested for somatostatin bioactivity. However, no somatostatin peptidomimetics have demonstrated clinical significance to date.

Since its discovery over 30 years ago, much progress has been made in the understanding of the structure of the peptide hormone, somatostatin, and its interaction with GPCRs through which its biological regulatory functions are mediated. The five human somatostatin receptor subtypes have been cloned and individually expressed in host cell lines. Because of the short half-life in blood serum and its lack of appreciable selectivity for the different receptor subtypes, the direct application of somatostatin as a therapeutic agent is limited. A wide variety of peptidic somatostatin analogs have been designed and synthesized. In many instances, the biological profiles of the designed compounds are greatly improved with respect to activity and selectivity and a few of them, such as octreotide [**2-6**], lanreotide [**2-9**], and RC-160 [**2-8**] are being used in the clinic to treat various diseases.

The incorporation of unnatural building blocks into peptide-based structures has led to compounds with greater enzymatic stability and longer duration of action as exemplified by SOM230. Much progress has also been made in the area of non-peptidic peptidomimetics as well. However, the clinical relevance of those compounds remains unknown.

The vast wealth of information gathered from 30 years of somatostatin research led us to design, synthesize, and evaluate novel scaffold-constrained semi-peptidic analogs. It was our hope that constraining the tetrapeptide pharmacophore into a rigid type II' β-turn would lead to enhanced potency and selectivity while providing further insight into the bioactive conformation and the topological space of the cellular receptors.

2.3 Design and synthesis of scaffold-constrained SRIF-14 analogs

2.3.1 Type II' β-turns

Utilizing structure-activity relationship studies Veber and coworkers proposed that somatostatin adopts a type II' β-turn about the Phe[7]-Trp[8]-Lys[9]-Thr[10] residues, providing the biologically active conformation.[7,8,118,119] Additional conformational studies of L-363,301 [**2-4**][8] and subsequent active analogs,[98,99,120-123] confirmed the type II' β-turn about the pharmacophore as well as the VI β-turn about the bridging region.

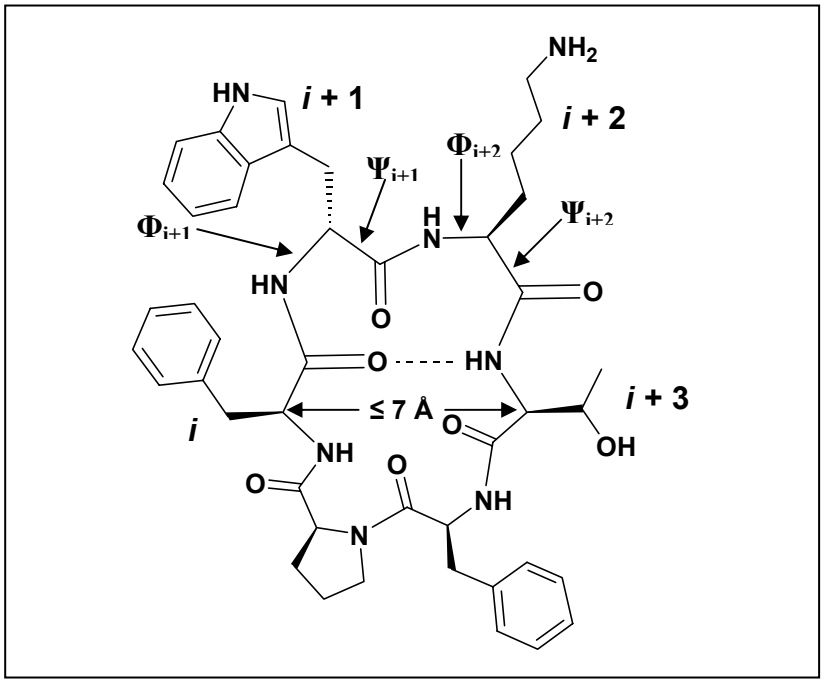

Figure 2-22: Important features of a typical β-turn depicted on L-363,301 [**2-4**] include the torsion angles Φ and Ψ, less than 7 Å between the α-Cs of the *i* and the *i* + 3 residues, and the possible presence of a hydrogen bond between the carbonyl of the *i* residue and the NH of the *i* + 3 residue.

Figure 2-22 depicts a β-turn about the somatostatin pharmacophore of L-363,301 [**2-4**]. A β-turn is characterized by four amino acids in a turn in which the α-carbons of the *i* and *i+3* residues are less than 7 Å apart and a hydrogen bond usually exists between the carbonyl of the *i* residue and the NH of the *i+ 3* residue. The dihedral angles Φ and Ψ about residues *i+1* and *i+2* designate which type of β-turn exists. Table 2-6 summarizes the idealized dihedral angles of the most common types of β-turns.[124]

Table 2-6: The idealized dihedral angles of common β-turns.[124]

Turn Type	Φ_{i+1}	Ψ_{i+1}	Φ_{i+2}	Ψ_{i+2}
I	-60	-30	-90	0
I'	60	30	90	0
II	-60	120	80	0
II'	60	-120	80	0

Peptide cyclization can constrain a short amino acid sequence into a turn conformation. The β-turn is the most common type of nonrepetitive structural motif recognized in proteins. Macrocyclization has been an effective approach for restricting the conformation of a turn sequence. One of the simplest strategies involves backbone cyclization with dipeptide sequences in the bridging region, such as the Phe^{11}-Pro^{6} sequence of L-363,301 [**2-4**] or the previously discussed *N*-alkyl glycine derivatives

employed by Goodman. This concept has been expanded further by replacing one of the turns of a cyclic peptide with a synthetic compound which can either mimic the turn itself or serve as a structurally-constrained template to array the remaining peptide in a β-turn conformation. The peptide content of a cyclic peptide is also decreased using this approach, which should increase enzymatic stability. A number of different compounds have been suggested as potential linkers for fixing the conformation of cyclic peptides. Examples of scaffolds which have been incorporated into various cyclic peptides to induce β-turns are depicted in Figure 2-23. (For references, please see: [**2-36**],[125] [**2-37**],[126] [**2-38**],[127] [**2-39**],[128] [**2-40**],[129] [**2-41**],[130] and [**2-42**].[131])

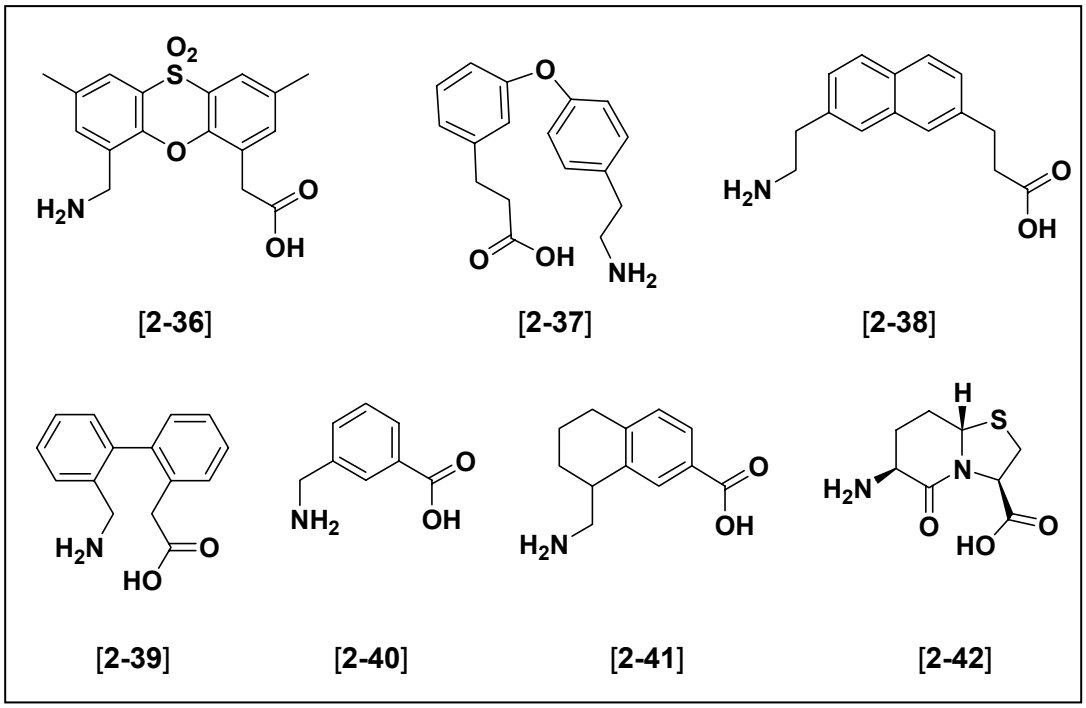

Figure 2-23: Examples of β-turn-inducing structures which have been incorporated into various cyclic peptides.

The scaffolds depicted in Figure 2-23 have not been incorporated into somatostatin analogs. However, there are a handful of examples in the literature in which this approach has been applied to the somatostatin tetrapeptide pharmacophore. DeGrado and coworkers utilized molecular modeling techniques to design *N*,*N*′-diphenylurea compound DJS631 [**2-43**] and biphenyl analog DJS811 [**2-44**]. Both scaffolds were utilized to constrain the MK678 [**2-5**] pharmacophore Tyr^{7}-D-Trp^{8}-Lys^{9}-Val^{10} (Figure 2-24). [132]

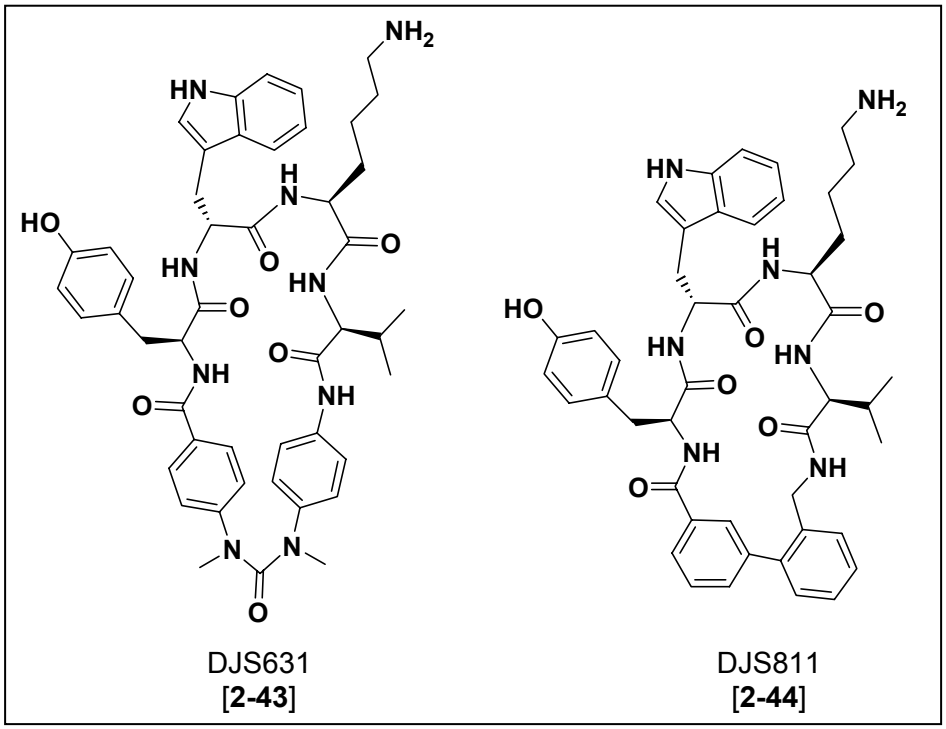

Figure 2-24: The *N*,*N*′-diphenylurea and biphenyl containing analogs of MK678 which were designed, synthesized, and evaluated in the DeGrado laboratories.

The *N,N'*-diphenylurea and biphenyl scaffolds were synthesized in solution, then attached to Wang resin via the carboxylic acid handle. The tetrapeptides were built onto the amine handle. The linear peptides were cleaved from the resin and cyclized in solution. Somatostatin receptor binding affinities were measured at either human (hsst) or mouse (msst) cloned receptor subtypes and are reported in Table 2-7. Both compounds were selective for sst2 and sst5. The 10-fold preference for sst5 that DJS811 [**2-44**] exhibits over DJS631 [**2-43**] was attributed to the flexibility of DJS811 [**2-44**].[132] Subsequent structural characterization by NMR analysis and molecular modeling showed that the compounds exist in type V' β-turn.[133]

Table 2-7: Sst receptor subtype binding affinities of DeGrado's compounds (IC_{50}, nM) were measured in human (hsst) and mouse (msst) cloned receptors.

Compound	hsst1	msst2	msst3	hsst4	hsst5
SRIF-14 [**2-1**]	0.1	0.6	0.1	1.2	0.2
MK678 [**2-5**]	>1000	0.1	268	>1000	23
DJS631 [**2-43**]	>1000	7	~1000	>1000	220
DJS811 [**2-44**]	>1000	1	>1000	n.d.	15

n.d. – not determined

Other scaffolded somatostatin analogs based on "sugar amino acids" were developed in the Kessler laboratories. The pyranoid ring structure featured in analog [**2-45**] (Figure 2-25) contains amino and carboxylic acid handles. All of the ring substituents lie in the equatorial position, making the chair conformation very stable

and rigid. The pyranoid scaffold was synthesized in solution, followed by the attachment of the two dipeptides, and subsequent ring closure. Conformational analysis confirmed the presence of the two β-turns, with a type II' β-turn about the tetrapeptide pharmacophore. Compound [**2-45**] had an IC_{50} 0.15 μM in a competitive binding assay in AtT20 cell membranes from mice.[134] Sugar-containing [**2-45**] was only 75 times less potent than L-363,301, which was considered remarkable since it does not contain the lipophilic residues on both sides of the pharmacophore that are considered to be important for high somatostatin activity.[7,74]

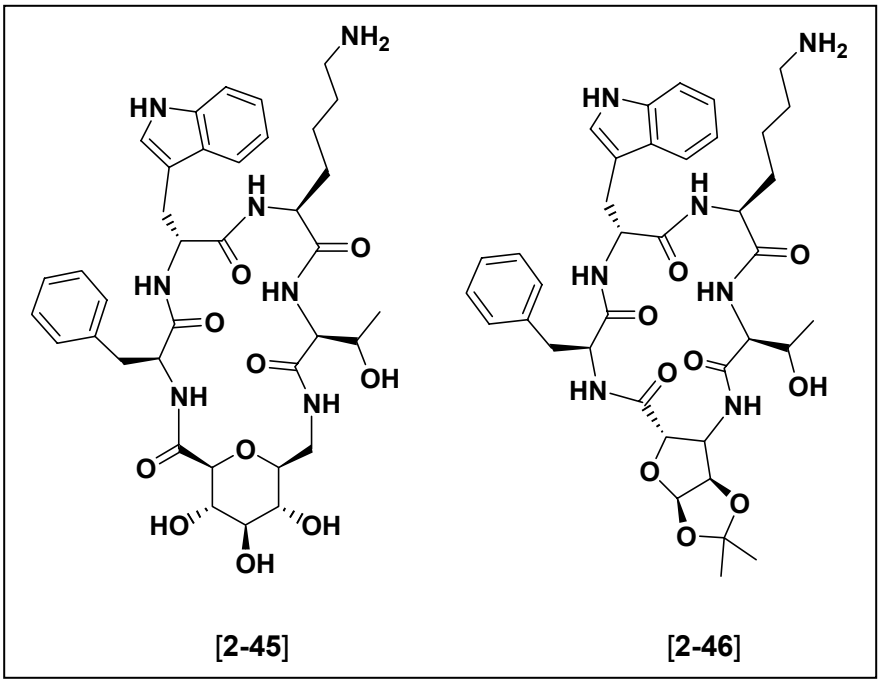

Figure 2-25: The sugar amino acid scaffolded somatostatin analogs designed and synthesized by Kessler and coworkers.

The Kessler laboratories synthesized a second sugar amino acid-based scaffold to constrain the somatostatin tetrapeptide pharmacophore.[135] Furanoid sugar [**2-46**] (Figure 2-25) was synthesized as part of a small library of somatostatin analogs, some of which possessed antiproliferative and apoptotic activity against both multi drug-resistant and drug-sensitive hepatoma carcinoma cells in the low μM range.

The results of DeGrado and Kessler inspired us to search for additional scaffolds which would further constrain the tetrapeptide pharmacophore of somatostatin in a rigid type II' β-turn conformation, thereby increasing the potency. We also chose to focus on hydrophobic moieties because a correlation between greater hydrophobicity and higher potency for cyclic hexapeptide somatostatin analogs has been observed.[76]

2.3.2 Somatostatin analogs containing a dibenzofuran scaffold

2.3.2.1 Design of the compounds

The focus of our research was on turn scaffolds which were hydrophobic, capable of readily joining two ends of a tetrapeptide, and arraying the D-Trp^{8}-Lys^{9} dipeptide in the *i*+2 and *i*+3 positions of a β-turn. Another requirement was that the molecule contained adequate conformational constraint to hold the ends of the tetrapeptide sequence in the appropriate orientation without significantly changing its own conformation.

S. Jiang of the Goodman laboratories utilized the distance geometry (DG) program, DGII, to model the somatostatin tetrapeptide pharmacophore cyclized with an array of known aromatic scaffolds (pictured in Figure 2-23). Minimum energy conformations of the highest populated clusters obtained from free molecular dynamics simulations were superimposed onto the known geometry of L,363-301 [**2-4**] (Figure 2-5) to find the closest conformational match. A dibenzofuran (DBF) based scaffold's core structure and side chains (yellow) adopted a conformation closest to that of L-363,301 (magenta), as shown in Figure 2-26.

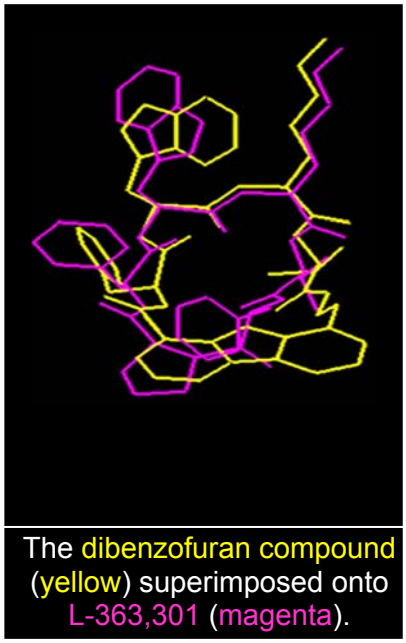

Figure 2-26: The lowest energy conformation of the dibenzofuran-based compound is the closest topological match to that of L-363,301 [**2-4**].

Kelly and coworkers designed the DBF scaffold to array peptide chains in β-sheet structures,[136,137] Figure 2-27. The DBF scaffold was chosen for our modeling studies because it had been thoroughly characterized and successfully incorporated into peptides. The preliminary modeling studies by S. Jiang of the Phe-D-Trp-Lys-Thr peptide cyclized onto Kelly's scaffold indicated that the amino acid side chains were arrayed in a spatial orientation similar to that of L-363,301 [**2-4**].

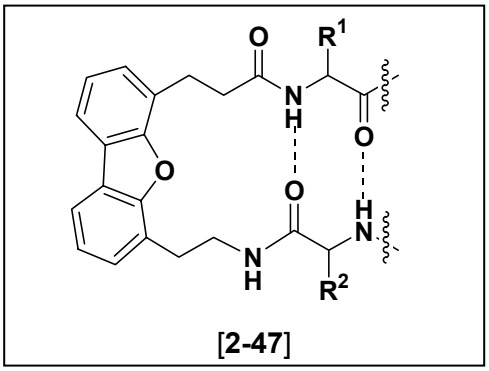

[**2-47**]

Figure 2-27: Kelly's dibenzofuran based scaffold was designed to array β-sheet structures.

Based on the results of the modeling studies, we decided to synthesize two dibenzofuran-scaffolded somatostatin analogs, shown in Figure 2-28. Analog [**2-48**] is based on L-363,301 [**2-4**], and contains the tetrapeptide sequence Phe-D-Trp-Lys-Thr, while analog [**2-49**] is based on MK678 [**2-5**] and contains the tetrapeptide sequence Tyr-D-Trp-Lys-Val. The following section describes our synthesis of the dibenzofuran scaffold. We viewed the original published synthesis of the dibenzofuran scaffold[137] as

a starting template for developmental work which would refine aspects of the published synthesis and maximize yields.

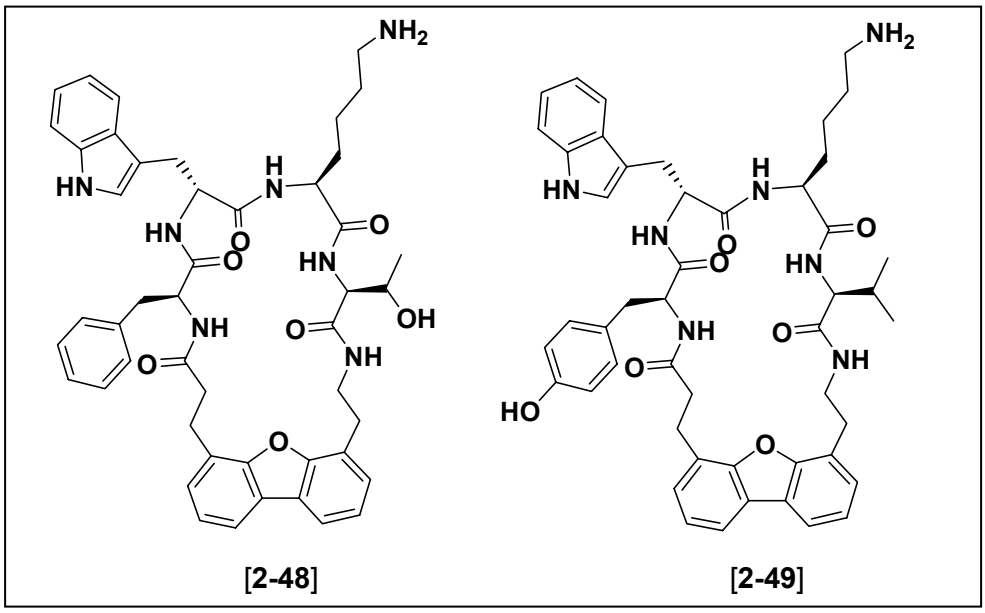

[**2-48**] [**2-49**]

Figure 2-28: Two dibenzofuran constrained somatostatin analogs based on the classical somatostatin hexapeptides, L-363,301 [**2-4**] and MK678 [**2-5**].

2.3.2.2 Synthesis of the dibenzofuran scaffold

Scheme 2-1 depicts the synthesis of the DBF scaffold which commences with lithiation of the 4-position of the DBF ring system [**2-50**] using n-butyl lithium. The addition of trimethylsilyl chloride (TMS-Cl) silylates the 4-position, which can be transformed to an iodide later in the synthesis. 4-TMS-dibenzofuran [**2-51**] was obtained in 85% yield after recrystalization from cold ACN which greatly enhanced

the purity by removing trace amounts of di- and tri-substituted material; the presence of which was found to complicate later steps of the synthesis.

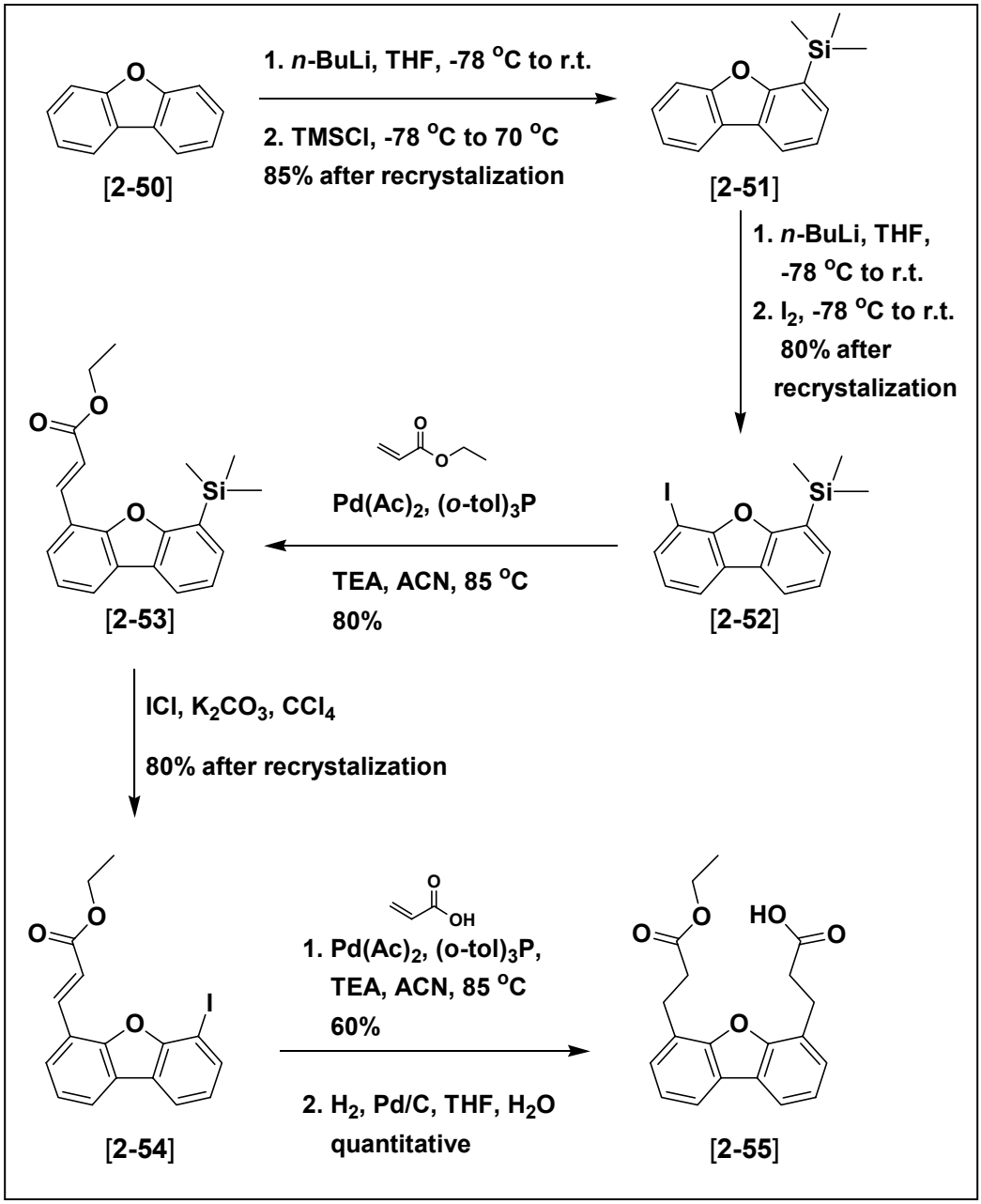

Scheme 2-1: Synthesis of the dibenzofuran-based scaffold includes two Heck cross-coupling reactions.

Lithiation of position 6 followed by iodination provided the Heck precursor [**2-52**] in 80% yield after recrystalization from cold ACN; another important purification step. Palladium acetate catalyzed Heck cross-coupling conditions with triorthotolylphosphine and ethyl acrylate required 4 eq. of TEA in order to attach the unsaturated ester handle to 4-TMS-6-iododibenzofuran [**2-52**] in 80% yield.

Ipso substitution of the TMS group of compound [**2-53**] with iodochloride (ICl) provided the 4-iodinated species [**2-54**] in 80% yield. Iodinated compound [**2-54**] was found to be sensitive to light and silica gel chromatography. Light exposure had to be limited, and purification was achieved by recrystalization from cold ACN. The purified material was quickly subjected to the second Heck cross-coupling reaction with acrylic acid and provided the differentiated, di-substituted dibenzofuran compound in 60% yield. Both double bonds were reduced using palladium-mediated catalytic hydrogenation. Numerous anhydrous conditions were explored for the hydrogenation reaction. The addition of MeOH or EtOH to the reaction mixture aided in the reduction of the double bonds, but also esterified the free acid side-chain through substrate-assisted acid catalysis. A catalytic amount of water to an EtOAc/ THF solvent system was essential for the catalytic reduction to proceed. Using this solvent mixture, intermediate [**2-55**] was obtained in quantitative yield.

In the published synthesis of the DBF scaffold, transformation of the acid functionality of compound [**2-55**] to a urethane protected amine was reported to be achieved directly through a Schmidt rearrangement in 70%-75% yield.[136,138] In our

hands, yields for this reaction were significantly lower which forced us to explore other routes. We chose to utilize Hoffman conditions, as described in Scheme 2-2.

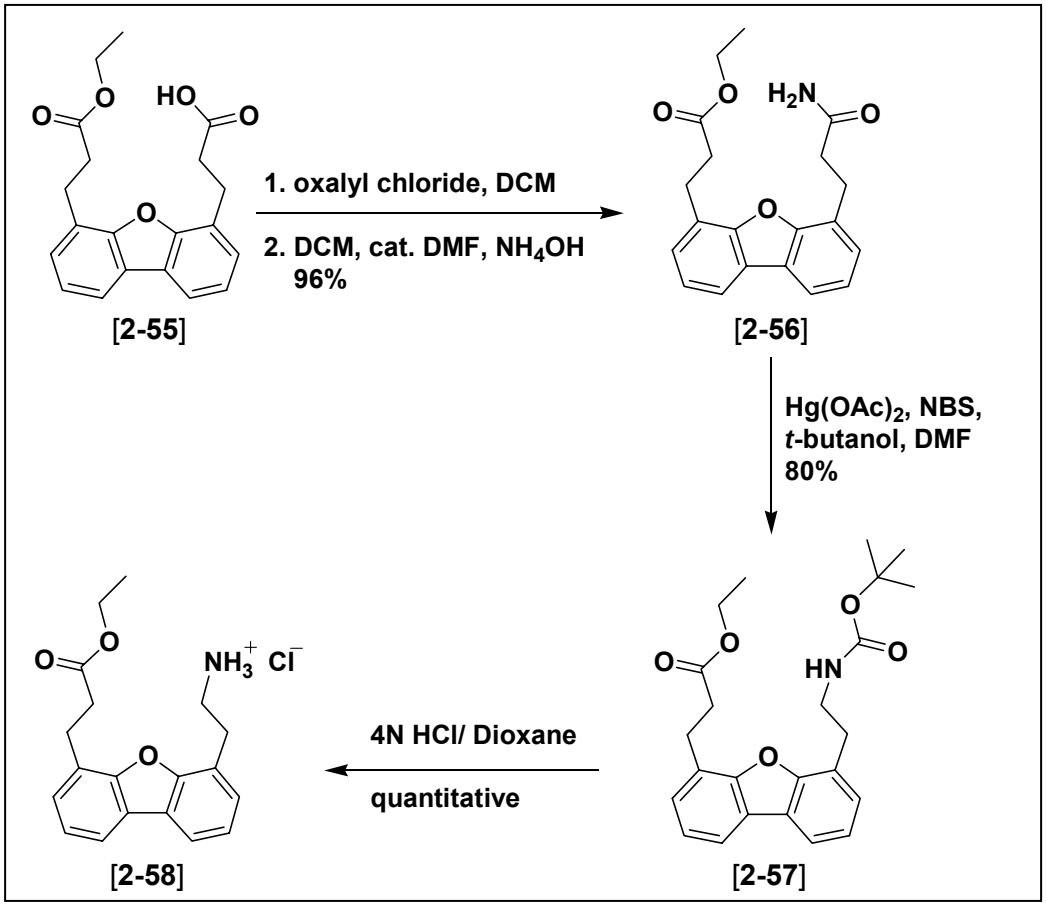

Scheme 2-2: The continued synthesis of the dibenzofuran-based scaffold which highlights the use of a Hoffman rearrangement to provide the Boc-protected amino acid.

Carboxylic acid [**2-55**] was dissolved in DCM and treated with oxalyl chloride at 0 ^{o}C. The solvents were removed under reduced pressure and the residue redissolved in DCM. The solution was cooled to 0 ^{o}C and a catalytic amount of DMF

was added followed by drop-wise addition of ammonium hydroxide. The terminal amide [**2-56**] was obtained in 96% yield. Exposure of amide [**2-56**] to Hoffman conditions using mercury acetate and *N*-bromosuccinimide in the presence of *t*-butanol provided the Boc-protected amine in 80% yield. The fully protected amino acid [**2-57**] could be stored at room temperature for long periods of time without degrading. When required, the Boc protecting group could be easily removed under standard acidc conditions to provide the free amino compound [**2-58**], ready for coupling to the desired peptides.

2.3.2.3 Synthesis of the dipeptides and coupling to the scaffold

Initially, we synthesized the tetrapeptides, Boc-Phe-D-Trp(For)-Lys(Z)-Thr(Bzl)-COOH and Boc-Tyr(Bzl)-D-Trp(For)-Lys(Z)-Val-COOH in solution and coupled them to the free amine handle of dibenzofuran scaffold [**2-58**]. The ethyl ester was saponified from the scaffold handles and the Boc-group was removed from the *N*-terminus of each of the peptides. However, the compounds would not cyclize in appreciable yields, though numerous reagents and conditions were explored. We presumed that the ring system was too constrained to allow the peptides to cyclize down onto the scaffolds. To circumvent this problem, we synthesized the comparable sets of dipeptides, Z-Lys(Boc)-Thr(*t*-But)-COOH [**2-61**] and H-Phe-D-Trp(Boc)-OMe [**2-68**], Z-Lys(Boc)-Val-COOH [**2-63**] and H-Tyr(*t*-But)-D-Trp(Boc)-OMe [**2-70**], attached each pair to the scaffold, and cyclized each of the peptides in solution in good yields.

The syntheses of the two lysine-containing dipeptides are depicted in Scheme 2-3. Z-Lys(Boc)-OH [**2-59**] was coupled to H-Thr(*t*-But)-OMe [**2-60**] using EDC and HOBt, and to H-Val-OMe [**2-66**] using DEPBT and TEA to provide the desired peptides in 73% and 85% yields, respectively. Saponification of the methyl esters of both peptides was achieved quantitatively with LiOH in a MeOH/ water mixture.

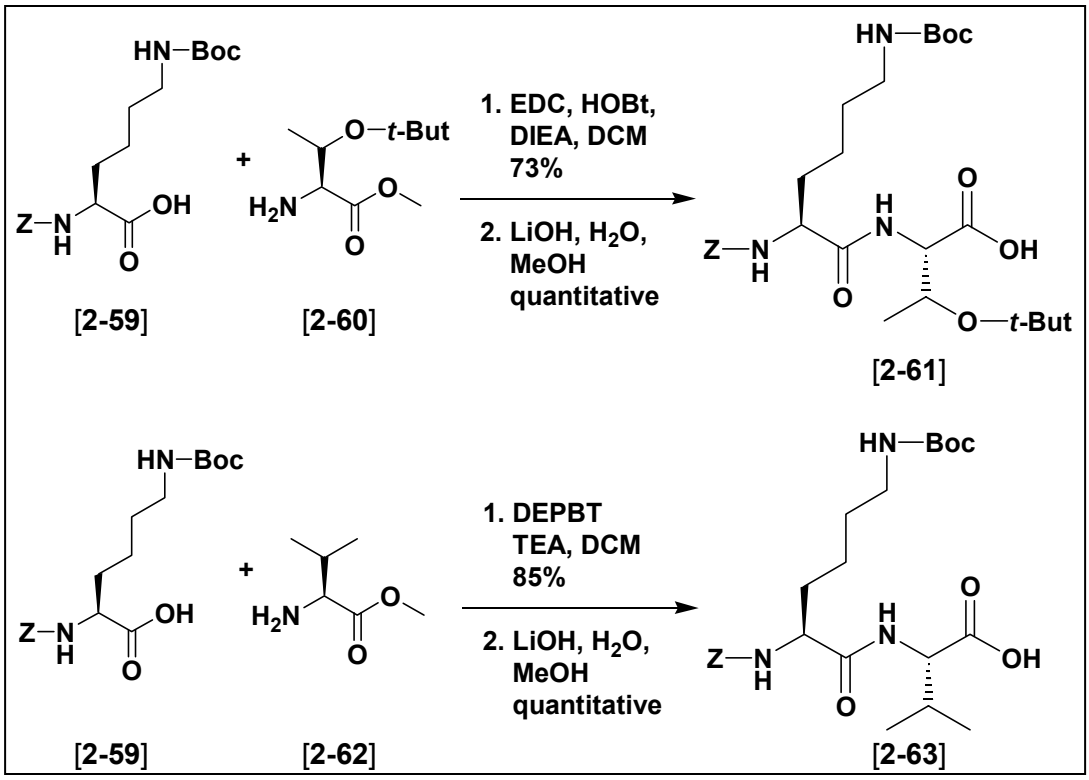

Scheme 2-3: Syntheses of the two Lysine-containing dipeptides.

Suitably protected D-Trp analogs were not commercially available. Scheme 2-4 describes the protection strategy that we employed to synthesize the desired orthogonally protected D-Trp compounds. Z-D-Trp-OH [**2-64**] was esterified with

thionyl chloride in methanol in quantitative yield. The nitrogen of the indole ring of the tryptophan was then Boc-protected with Boc-anhydride and a catalytic amount of dimethylaminopyridine (DMAP) in ACN to provide the fully protected amino acid in 72% yield. Removal of the Z-protecting group was achieved with palladium catalyzed hydrogenation and provided H-D-Trp(Boc)-OMe [**2-66**] in quantitative yield.

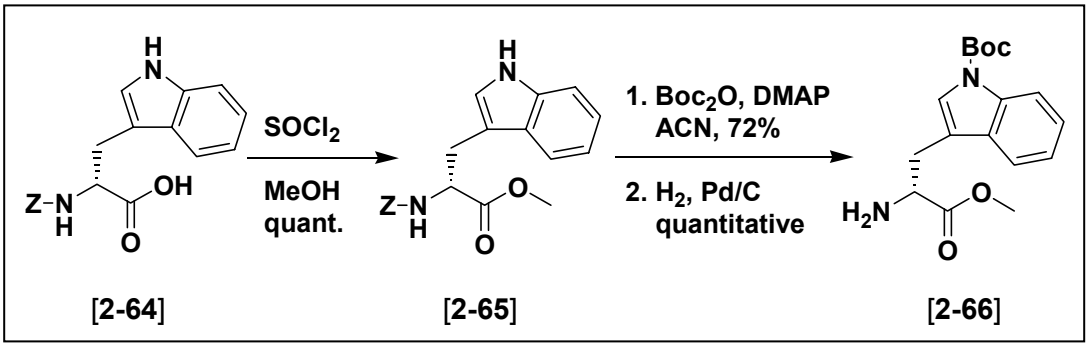

Scheme 2-4: Synthesis of an orthogonally protected D-Trp analog which was not commercially available.

Z-Phe-OH [**2-67**] and Z-Tyr(*t*-But)-OH [**2-69**] were each coupled to the synthesized D-Trp analog [**2-66**] using DEPBT to provide the fully protected dipeptides in 80% and 60% yields, respectively (Scheme 2-5). Removal of the Z-protecting group was achieved on both molecules using catalytic hydrogenation to give the desired free amines of both dipeptides in quantitative yields. The possibility of diketopiperazine formation was a concern when freeing the amine of the dipeptides. However, the formation of diketopiperazines was not observed with either dipeptide.

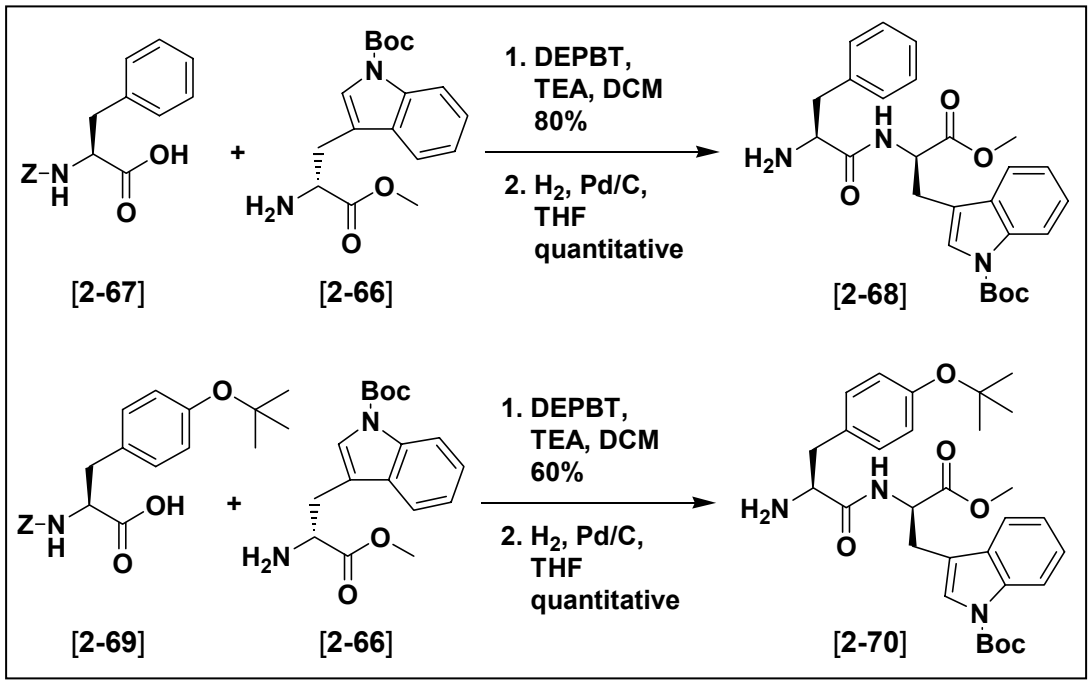

Scheme 2-5: Syntheses of the two D-Tryptophan-containing dipeptides.

The synthesized L-363,301 [**2-4**] analogous dipeptides were attached to the dibenzofuran scaffold [**2-58**] as shown in Scheme 2-6. The free amine of scaffold [**2-58**] was coupled to the carboxylic acid of Z-Lys(Boc)-Thr(*t*-But)-OH [**2-61**] with DEPBT in 70% yield. The ethyl ester of the scaffold was then saponified quantitatively with LiOH. The free carboxylic acid [**2-71**] was coupled to H-Phe-D-Trp(Boc)-OMe [**2-68**] using DEPBT in 70% yield. Deprotection of the amine function using hydrogenation and saponification of the methyl ester with LiOH were both achieved in quantitative yields to provide the cyclization precursor [**2-72**].

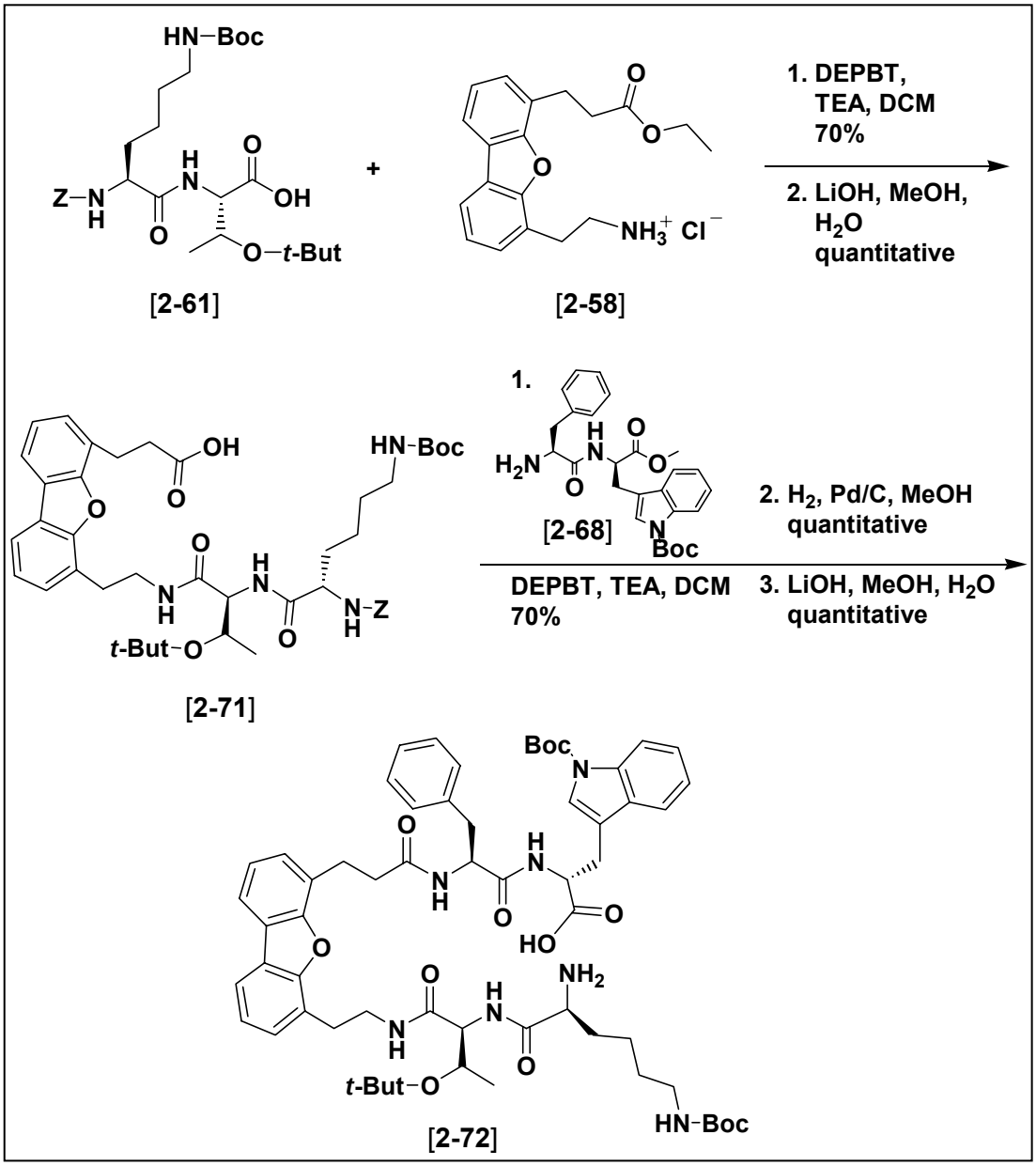

Scheme 2-6: Coupling of the L-363,301 [**2-4**]-analogous dipeptides to the dibenzofuran scaffold.

Treatment of analog [**2-72**] with DEPBT and TEA for two days in dilute DCM closed the ring in 40% yield. The side-chain protecting groups were removed by

treatment with TFA in the presence of anisole. The final analog [**2-48**] was isolated in 44% yield after preparative RP-HPLC purification.

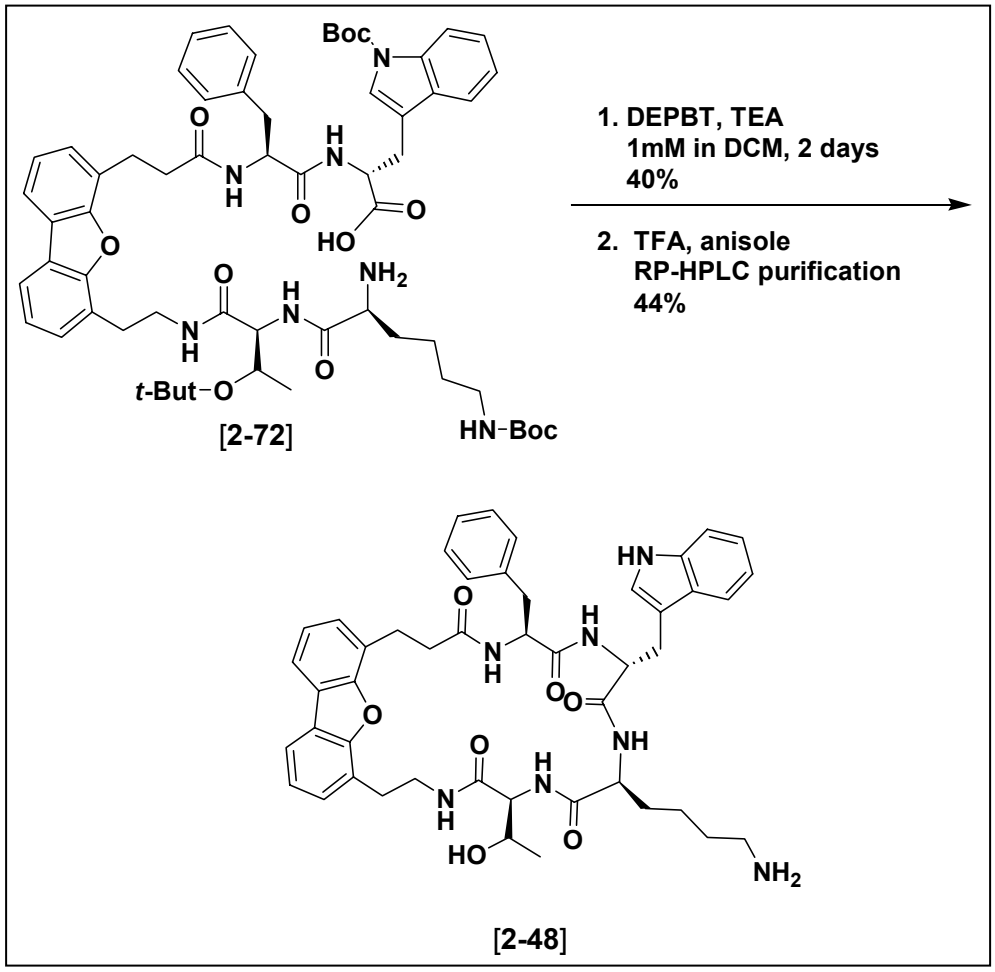

Scheme 2-7: Cyclization and final deprotection of Phe-D-Trp-Lys-Thr-dibenzofuran analog [**2-48**].

The second analog, Tyr-D-Trp-Lys-Val [**2-49**], based on MK678 [**2-5**], was synthesized in a similar manner. The coupling of Z-Lys(Boc)-Val-OH [**2-63**] and

H-Tyr(*t*-But)-D-Trp(Boc)-OMe [**2-70**] to the dibenzofuran scaffold [**2-58**] are shown in Scheme 2-8 while the cyclization and deprotection are shown in Scheme 2-9.

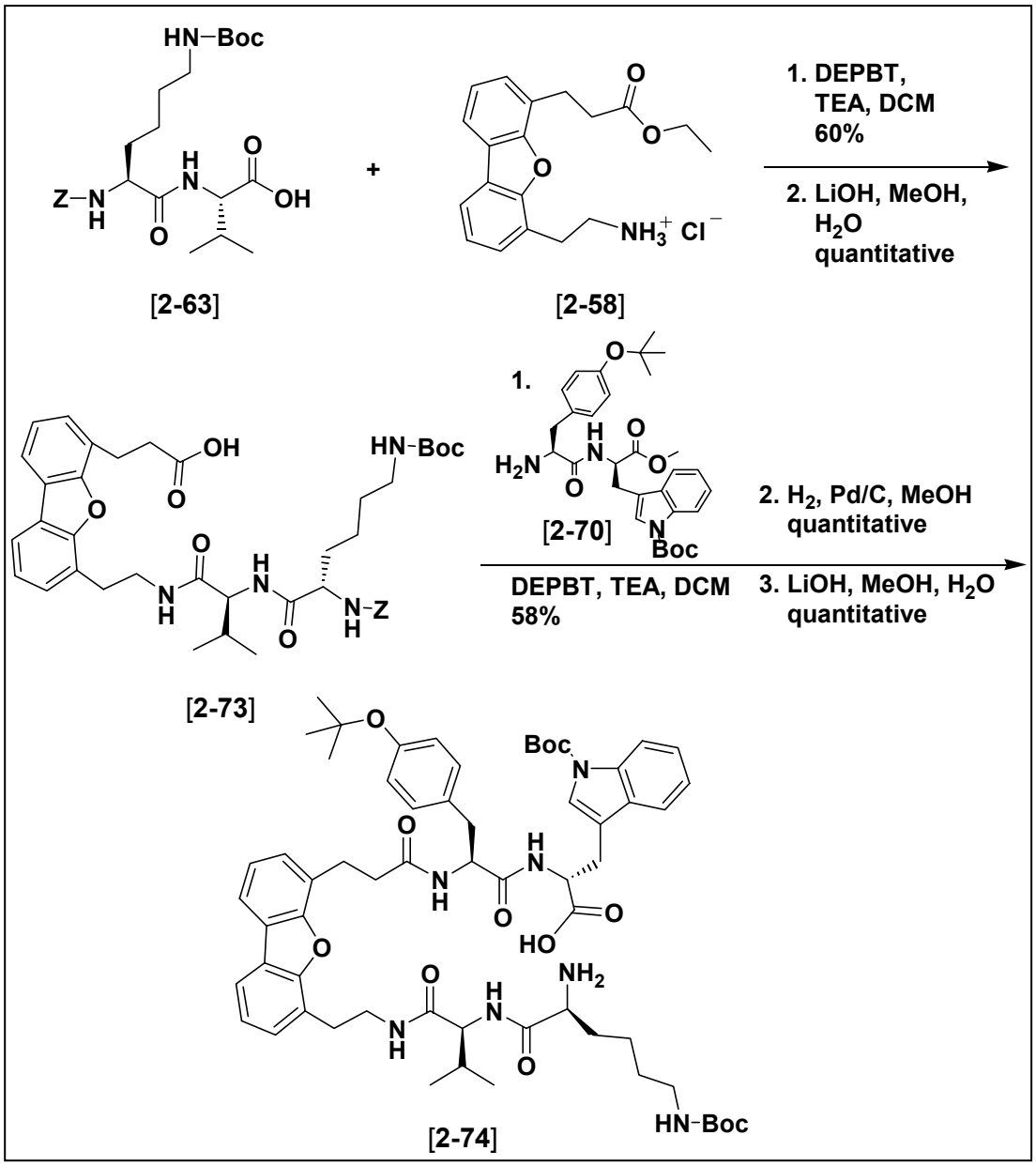

Scheme 2-8: Coupling of the MK678 [**2-5**]-analogous dipeptides to the dibenzofuran scaffold.

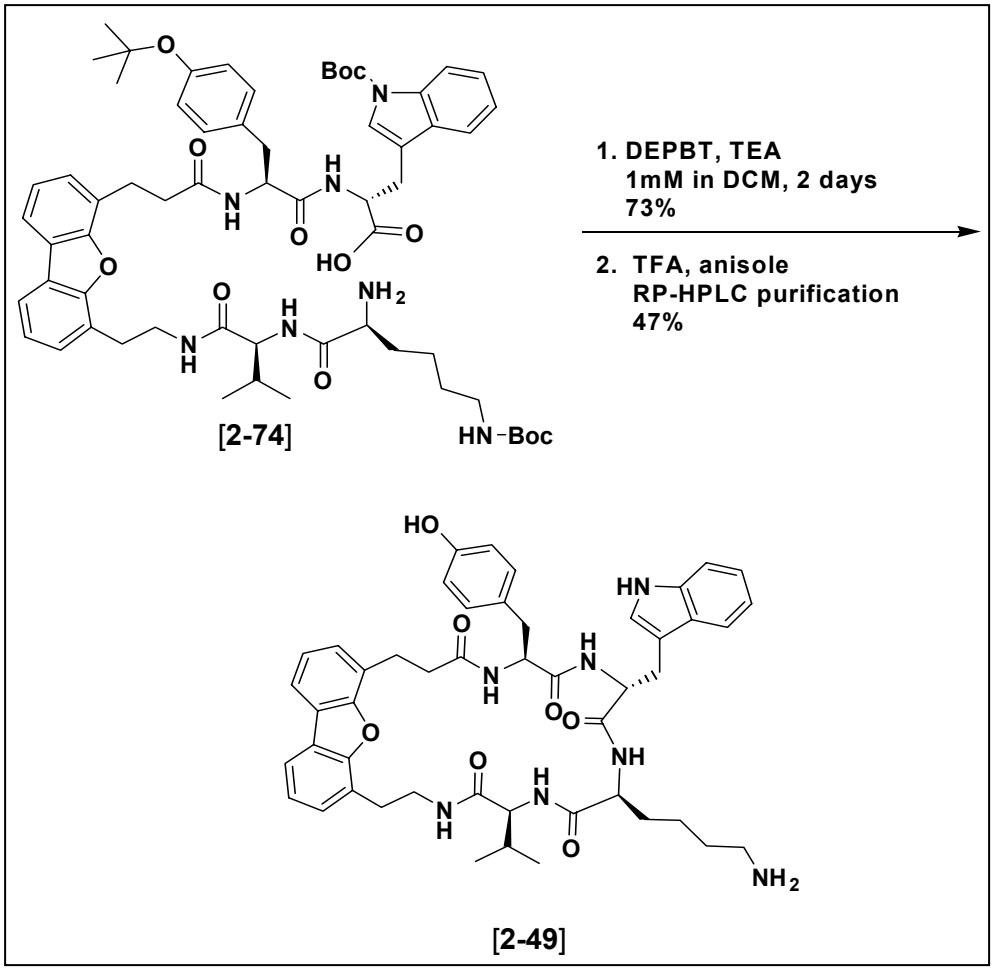

Scheme 2-9: Cyclization and final deprotection of Tyr-D-Trp-Val-Thr-dibenzofuran analog [**2-49**].

Both of the final compounds [**2-48**] and [**2-49**] were purified by preparative RP-HPLC and were characterized by gradient and isocratic analytical RP-HPLC, ^{1}H NMR, mass spectrometry (ESI) and high resolution time-of-flight mass spectrometry and elemental analysis.

2.3.2.4 NMR analysis

The 2D-NMR TOCSY and ROESY spectra of compounds [**2-48**] and [**2-49**] were recorded on a 700 MHz spectrometer in DMSO-d_6 and sequentially assigned by collaborators in the Melacini laboratory at McMaster University. Both analogs displayed strong D-Trp α-H-Lys NH ROEs, indicating a distance of ≤ 2.5 Å between those protons.

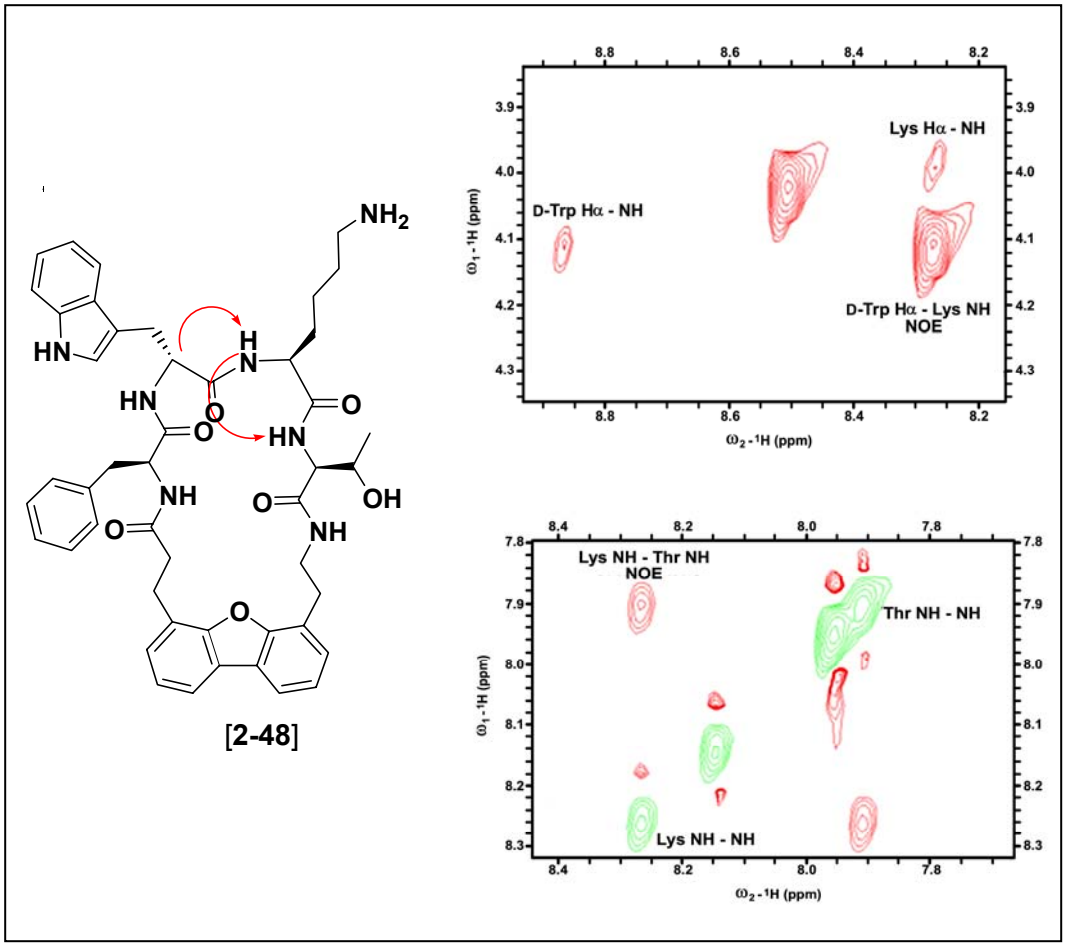

Figure 2-29: ROE data for the Phe-D-Trp-Lys-Thr analog [**2-48**] demonstrates the strong D-Trp α-H-Lys NH ROE and the medium Lys NH-Thr NH ROE, both of which support the presence of a type II' β-turn.

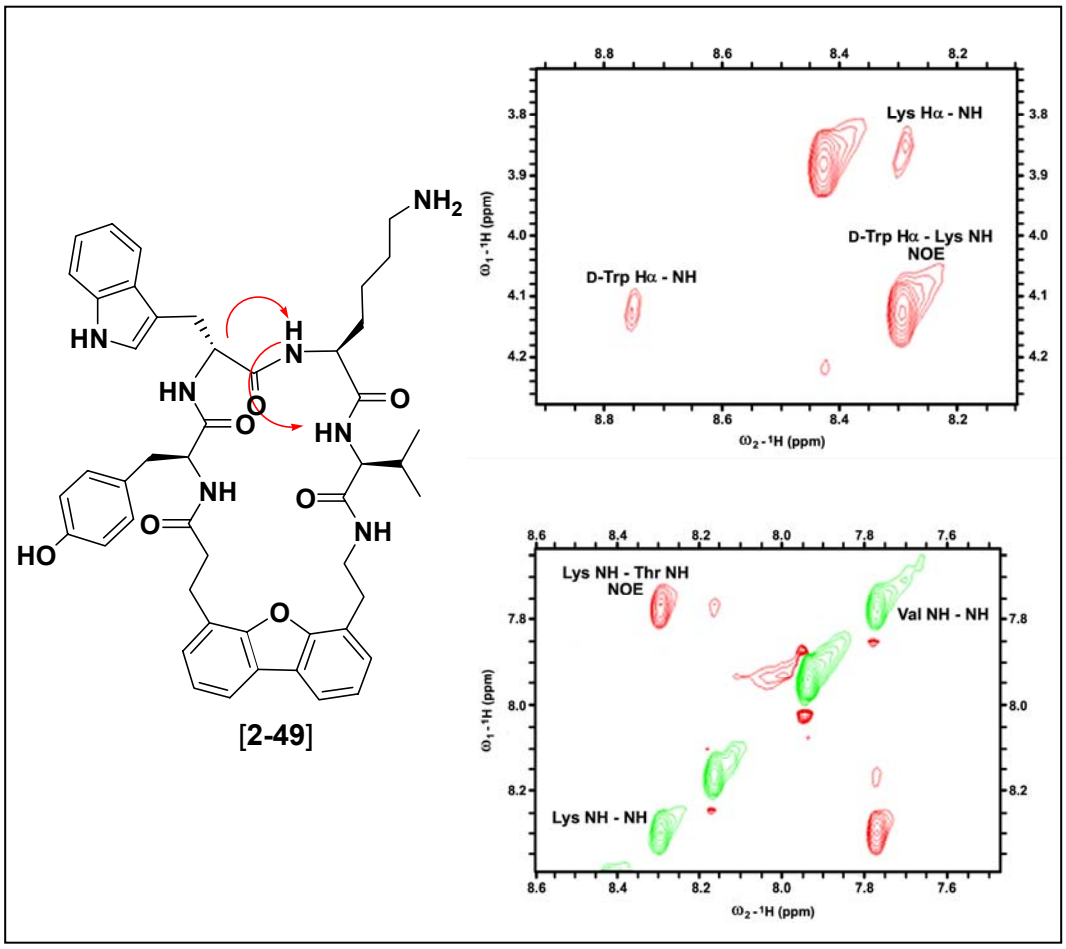

Figure 2-30: ROE data for the Tyr-D-Trp-Lys-Val analog [**2-49**] demonstrates the strong D-Trp α-H-Lys NH ROE and the medium Lys NH-Val NH ROE, both of which support the presence of a type II' β-turn.

A medium Lys NH-Thr NH or Lys NH-Val NH ROE was also identified in each respective compound which indicated a distance of > 2.5 ≤ 3.5 Å between those protons. These ROEs are indicative of the type II' β-turn spanning the D-Trp-Lys residues, as well as the Thr NH-Phe C=O or Val NH-Phe C=O hydrogen bond, as previously established in our laboratories.[139] The ROE data for the

Phe-D-Trp-Lys-Thr analog [**2-48**] are provided in Figure 2-29, while the ROE data for the Tyr-D-Trp-Lys-Val analog [**2-49**] are provided in Figure 2-30.

2.3.2.5 Results of the binding assays

The binding affinities of somatostatin and compounds [**2-48**] and [**2-48**] were evaluated by collaborators in the Kumar laboratories at McGill University. Each subtype of the hsst receptors was individually expressed in CHO-K1 cells. Competitive binding assays were then performed using radio-iodinated SRIF as the standard. The results of the assays measured by our collaborators are listed in Table 2-8, as well as the literature reported binding affinities of somatostatin [**2-1**], L-363,301 [**2-4**], and MK678 [**2-5**].

Table 2-8: Binding affinities (K_i in nM) of synthesized somatostatin analogs for the five human somatostatin receptor subtypes hsst1-5.

Compound	hsst1	hsst2	hsst3	hsst4	hsst5	Ref.
Somatostatin[a] [**2-1**]	0.38	0.04	0.66	1.78	2.32	[68]
L-363,301[a] [**2-4**]	>1000	5.1	129	>1000	25	[81]
MK678[a] [**2-5**]	>1000	1.5	27	127	2	[82]
Somatostatin[b] [**2-1**]	0.17	1.2	0.11	0.14	0.53	[140]
Analog [**2-48**]	>1000	199	421	>1000	351	[140]
Analog [**2-49**]	>1000	215	553	>10000	>1000	[140]

[a] Previously published results. [b] Results from this set of assays.

The synthesized compounds [**2-48**] and [**2-49**] bound to the receptor subtypes in the low μM range. Just like L-363,301 [**2-4**], neither compound showed any affinity for hsst1 or hsst4. The Phe-D-Trp-Lys-Thr compound [**2-48**] was slightly selective for hsst2 by about a factor of two over hsst3 and hsst5 and its selectivity was comparable to its parent compound, L-363,301. Unlike its parent compound MK678 [**2-5**], the Tyr-D-Trp-Lys-Val analog [**2-49**] displayed no affinity for hsst5. Compound [**2-49**] was selective for hsst2 over hsst3 by about a factor of two. While we had hoped that constraining the somatostatin tetrapeptide pharmacophores would improve hsst2 selectivity, but in these cases, we did not achieve that goal. These results indicate that conformational restriction is not the only factor which contributes to hsst2 selectivity.

2.4 Conclusions

A variety of aromatic scaffolds were virtually incorporated into the somatostatin tetrapeptide pharmacophore and modeled using molecular dynamics simulations to find a scaffold whose topography was closest to that of L-263,301 [**2-4**]. This search provided us with a lead scaffold based on dibenzofuran, [**2-57**], which we planned to incorporate into the somatostatin tetrapeptide sequences, Phe-D-Trp-Lys-Thr, based on L-363,301 [**2-4**], and Tyr-D-Trp-Lys-Val, based on MK678 [**2-5**].

We synthesized the dibenzofuran-based scaffold [**2-57**] in solution in good yield by modifying a published synthesis.[137] Lack of commercial availability required us to synthesize appropriately protected H-D-Trp(Boc)-OMe [**2-66**]. All four

dipeptides, Z-Lys(Boc)-Thr(*t*-but)-OH [**2-61**], Z-Lys(Boc)-Val-OH [**2-63**], H-Phe-D-Trp(Boc)-OMe [**2-68**], and H-Tyr(*t*-but)-D-Trp(Boc)-OMe [**2-70**] were also synthesized in solution in good yields, without the formation of diketopiperazine side products. The dipeptides were coupled to the scaffold in solution, and both fully deprotected final compounds were purified by preparative RP-HPLC and characterized by ^{1}H-NMR spectroscopy and mass spectrometry.

TOCSY and ROESY 2D-NMR spectroscopy of both compounds provided ROEs which supported the presence of a type II' β-turn spanning the D-Trp-Lys residues, as well as the Thr NH-Phe C=O or Val NH-Phe C=O hydrogen bond, as previously suggested in our laboratories.[139]

The binding affinities of somatostatin and compounds [**2-48**] and [**2-49**] were evaluated for potency selectivity for each subtype of the hsst receptors in competitive binding assays. Neither compound showed any affinity for hsst1 or hsst4. The Phe-D-Trp-Lys-Thr compound [**2-48**] was slightly selective for hsst2 (2 μM) by about a factor of two over hsst3 (4.2 μM) and hsst5 (3.5 μM). Unlike its parent compound MK678 [**2-5**], the Tyr-D-Trp-Lys-Val analog [**2-49**] did not display any affinity for hsst5. Compound [**2-49**] was selective for hsst2 (2.2 μM) over hsst3 (5.5 μM) by about a factor of two. While we had hoped that constraining the somatostatin tetrapeptide pharmacophores would improve hsst2 potency and selectivity over the parent compound L-363,301 [**2-4**], in these cases, we did not achieve that goal. These results indicate that conformational restriction is not the only factor which contributes to hsst2 selectivity.

Both dibenzofuran-scaffolded compounds, [**2-48**] and [**2-49**], were one to two orders of magnitude less potent in binding to the hsst receptors when compared to parent compound L-363,301 [**2-4**]. The loss of potency could be attributed to the lack of water solubility of both compounds, or to the inability of the dibenzofuran to fit into or interact with the receptors. Perhaps the scaffold was too rigid or planar to elicit strong binding to the receptors. Future scaffolds could be designed which incorporate polar, solubilizing groups to alleviate solubility problems. While initial molecular studies showed that the dibenzofuran compounds exhibited a conformation similar to that of L-363,301, a scaffold with slightly more flexibility could provide further insight into the conformational requirements for somatostatin receptor binding potency and subtype selectivity.

2.5 Experimental

2.5.1 General

The reagents were purchased from Sigma-Aldrich or Acros Organics and used without further purification. *n*-Butyl lithium was standardized prior to each use by titration using diphenylacetic acid as an indicator. All standard amino acids were donated by Senn Chemicals, U.S.A. THF was dried by refluxing over sodium/ benzophenone. DCM and TEA were dried by refluxing over calcium hydride. ACN and DMF were dried by storing over activated molecular sieves for 2 days. Silica gel 60 (230 – 400 mesh) was purchased from EM Scientific was used for column chromatography.

Reactions in solution were monitored by thin-layer chromatography (TLC) using 0.25 mm E. Merck silica gel plates (60F-254) and UV light as the visualizing agent. The NH-containing compounds were visualized by exposing the TLC plate to chlorine gas (generated by dissolving potassium permanganate in concentrated HCl) for 30-60 seconds. The TLC plate was then dipped into a solution of KI and *o*-tolidine (500 mg KI in 50 ml water combined with a solution of *o*-tolidine in 45 ml water and 8 ml glacial acetic acid). To confirm the presence of a free amine, TLC plates were dipped into a 2% ninhydrin/ ethanol solution and then heated. The following solvent systems were used to elute the TLCs: (A) 2% EtOAc/ hex, (B) 5% EtOAc/ hex, (C) 10% EtOAc/ hex, (D) 20% EtOAc/ hex, (E) 1:1 EtOAc:hex, (F) 3:2 EtOAc:hex, (G) 2:1 EtOAc:hex, (H) EtOAc, (I) 10% MeOH/ DCM.

The NMR spectra were obtained on a Varian HG-400 (400 MHz) spectrometer. Chemical shifts (δ) are reported in parts per million (ppm) relative to residual undeuterated solvent as an internal standard. The following abbreviations were used to explain the multiplicities: s = singlet, d = doublet, t = triplet, q = quartet, m = multiplet, bs = broad singlet, bm = broad multiplet, dd = doublet of doublets, dt = doublet of triplets, dm = doublet of multiplets, dbm = doublet of broad mutiplets.

Mass spectra were obtained from The Scripps Research Institute (TSRI), La Jolla, CA mass spectrometry facility using electrospray (ESI) and MALDI-FTMS techniques.

Analytical RP-HPLC was carried out on a Millenium 2010 system consisting of a Waters 715 Ultra WISP sample processor, a Waters TM 996 photodiode array detector, two Waters 510 pumps, and a NEC Power Mate 485/33I computer. The column was an Akzo Nobel KR100-5C18 kromasil column (250 mm x 4.6 mm). A 1 mg/ ml solution of each compound was made and 10 µl were injected at a flow rate of 1 ml/ min. Spectra were recorded at a wave length of λ = 220 nm. The solvents used were as follows: solvent A = 0.1% TFA in water, solvent B = 0.1% TFA in ACN.

Preparative RP-HPLC was carried out using a Waters 600 E system controller, a Waters 484 tunable absorbance detector, two Waters 510 pumps, and a C-18 preparative column (I.D. = 22 mm x 550 mm long, 10 microns, 100Å). Spectra were recorded at a wave length of λ = 220 nm. The solvents used were as follows: solvent A = 0.1% TFA in water, solvent B = 0.1% TFA in ACN, at a flow rate of 20 ml/ min.

2.5.2 Synthesis of the dibenzofuran scaffold

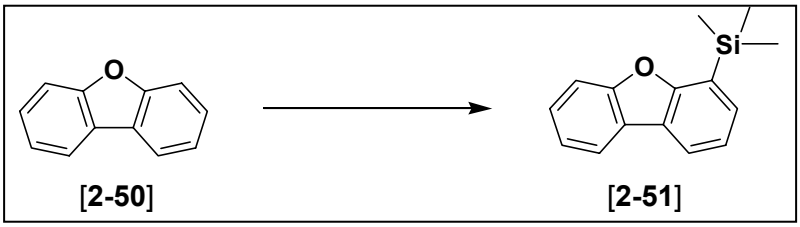

4-Trimethylsilyldibenzofuran [2-51]: A flame dried flask, fitted with a jacketed condenser and addition funnel under Ar atmosphere, was charged with dibenzofuran [**2-50**] (20.0 g, 118.92 mmol) and flushed several times with Ar. Distilled THF was added (200 ml), and the solution cooled to -78 °C in a dry ice/ isopropanol bath. The addition funnel was charged with *n*-butyl lithium (52.3 ml, 2.18 M in hexanes, 130.82 mmol) and flushed with Ar. The butyl lithium solution was added, drop-wise, over 1 h. The reaction was then allowed to warm to r.t. and stir under Ar for 3 h over which time the reaction became dark orange in color. The reaction was again cooled to -78 °C. The addition funnel was washed with 25 ml distilled THF and then charged with trimethylsilyl chloride (16.6 ml, 130.82 mmol) in distilled THF (150 ml). The solution was added, drop-wise, over 1 h. The reaction was then warmed to r.t. and placed into an oil bath. It was heated to 70 °C and left to reflux under Ar for 12 h. The reaction became pale yellow. The reaction was cooled to r.t. and poured into 0 °C water (200 ml) and stirred vigorously. The organic solvents were then removed under reduced pressure. The resulting aqueous mixture was extracted with DCM (5 x 100 ml). The organic washes were combined and dried over $MgSO_4$. The drying agent was filtered off and the filtrate concentrated to a yellow oil. The white solid product was

recrystallized from the oil with cold ACN to give 24.30 g (85% yield). R_f = 0.47 in solvent system (A); ^{1}H NMR (400 MHz, $CDCl_3$) δ 7.95 (overlapping d, 2 H, *J* = 7.6, 5.2 Hz, arom H1, H9), 7.56 (d, 1 H, *J* = 8.4 Hz, arom H3), 7.51 (dd, 1 H, *J* = 7.6, 6.8 Hz, arom H7), 7.43 (t, 1 H, *J* = 7.2, 8.4 Hz, arom H4), 7.32 (m, 2 H, arom H2, H8), 0.45 (s, 9 H, TMS); MS (GCMS) 240 $[M]^+$.

[**2-51**] [**2-52**]

6-Iodo-4-trimethylsilyldibenzofuran [2-52]: A flame dried flask, fitted with an addition funnel, was charged with 4-trimethylsilyldibenzofuran [**2-51**] (24.0 g, 99.8 mmol) and flushed several times with Ar. Freshly distilled THF (400 ml) was added and the solution cooled to -78 °C in a dry ice/ isopropanol bath. *n*-Butyl lithium (59.5 ml, 2.18 M in hexanes, 129.74 mmol) was added to the addition funnel, and then added to the reaction, drop-wise, over 30 min. The reaction was then warmed to r.t. and left to stir for 4 h under Ar during which it changed from bright yellow to blood red in color. The reaction was again cooled to -78 °C. A second oven dried flask was charged with iodine (50.7 g, 199.6 mmol) in distilled THF (200 ml) and flushed with Ar. The iodine solution was then transferred to the cooled reaction vessel via a cannula. The flask was washed with two additional 100 ml portions of THF which were added to the reaction. The reaction was then left to warm to r.t. and stir under Ar

over night. The reaction became dark red-brown in color. It was poured into a 20% solution of $NaHSO_3$ (400 ml) and stirred until the color changed to yellow. The organic solvents were then removed under reduced pressure. The resulting aqueous mixture was extracted with DCM (5 x 200 ml). The organic washes were combined and dried over $MgSO_4$. The drying agent was filtered off and the filtrate concentrated to a dark orange, viscous, oil. The product was crystallized from cold ACN to provide the product as an off-white solid (29.24 g, 80% yield). R_f = 0.36 in solvent system (A), R_f = 0.47 in solvent system (B); ^{1}H NMR (400 MHz, $CDCl_3$) δ 7.90 (dd, 2 H, *J* = 7.2, 7.2 Hz, arom H1, H9), 7.78 (d, 1 H, *J* = 7.6 Hz, arom H3), 7.54 (d, 1 H, *J* = 7.2 Hz, arom H7), 7.35 (t, 1 H, *J* = 7.2, 7.6 Hz, arom H8), 7.08 (t, 1 H, *J* = 8, 7.6 Hz, arom H2), 0.49 (s, 9 H, TMS); MS (GCMS) 366 $[M]^+$.

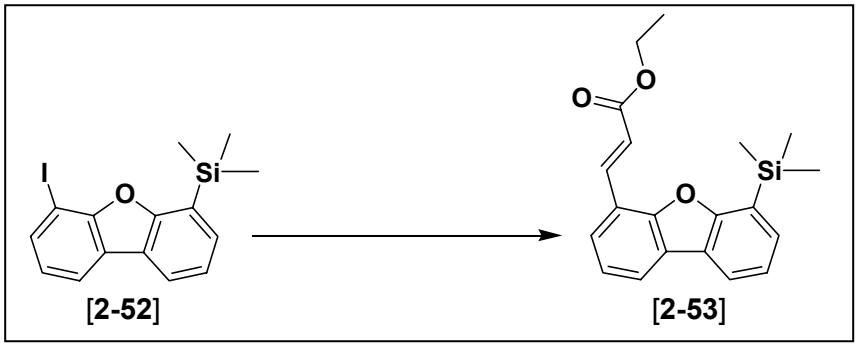

6-(2-Ethoxycarbonyl-vinyl)-4-trimethylsilyldibenzofuran [2-53]: A flame dried flask fitted with a jacketed water condenser was charged with 6-iodo-4-trimethylsilyldibenzofuran [**2-52**] (14.00 g, 38.22 mmol), palladium acetate (0.180 g, 2.1 mol%), triorthotolylphosphine (0.594 g, 5.1 mol%), and flushed several times with

Ar. Dry ACN (300 ml) was then added, followed by ethyl acrylate (16.57 ml, 152.88 mmol) and TEA (15.93 ml, 114.60 mmol). The reaction was heated to 85 °C in an oil bath and left to reflux over night under Ar. The dark brown reaction was cooled to r.t. and filtered to remove the black precipitate. The filtrate was then concentrated to a dark brown solid which was dissolved onto silica gel using DCM. It was purified by column chromatography in 5% EtOAc:hex to afford 10.35 g of a beige solid (80% yield). R_f = 0.18 in solvent system (B); ^{1}H NMR (400 MHz, $CDCl_3$) δ 7.95 (m, 2 H, arom H1, H9), 7.92 (d, 1 H, *J* = 16.4 Hz, α-vinylic H), 7.55 (t, 2 H, *J* = 10, 8.4 Hz, arom H3, H7), 7.35 (dt, 2 H, *J* = 7.6, 6.8 Hz, arom H2, H8), 7.15 (d, 1 H, *J* = 16.4 Hz, β-vinylic H), 4.30 (q, 2 H, *J* = 7.2, 6.8 Hz, CH_2), 1.37 (t, 3 H, *J* = 7.2 Hz, CH_3), 0.52 (s, 9 H, TMS); MS (ESI) 339 $[M+H]^+$, 361 $[M+Na]^+$.

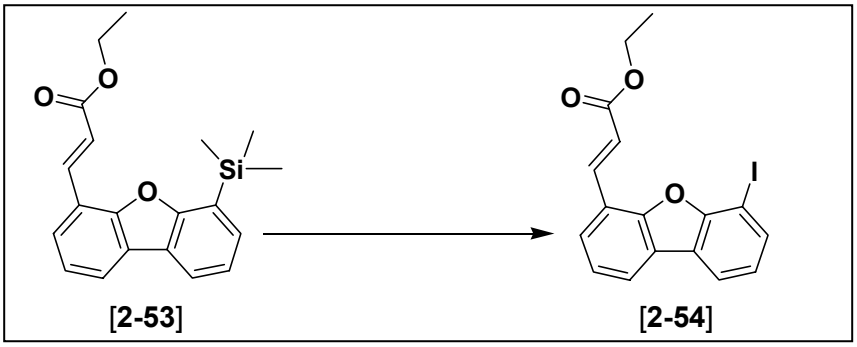

6-(2-Ethoxycarbonylvinyl)-4-iododibenzofuran [2-54]: A flame dried flask was charged with 6-(2-ethoxycarbonyl-vinyl)-4-trimethylsilyldibenzofuran [**2-53**] (8.55 g, 25.26 mmol), K_2CO_3 (10.47 g, 75.78 mmol), carbon tetrachloride (100 ml), and flushed several times with Ar. It was cooled to –20 °C in a dry ice/ isopropanol bath.

A second flame dried flask was charged with iodochloride (12.30 g, 75.78 mmol) and carbon tetrachloride (25 ml) and flushed with Ar. The iodochloride solution was then added to the cooled solution via a cannula. The flask was rinsed with carbon tetrachloride (3 x 25 ml) and the rises added to the reaction mixture. The reaction was wrapped in aluminum foil and left to warm to r.t. while stirring under Ar over night. The purple solution was poured into a 20% solution of sodium thiosulfate (200 ml) and stirred vigorously until the solution became colorless. The layers were then separated and the aqueous layer extracted with DCM (5 x 50 ml). The combined organic washes were washed with 20% sodium thiosulfate (1 x 25 ml), 1N HCl (1 x 25 ml), 1N NaOH (1 x 25 ml), brine (1 x 25 ml), and dried over Na_2SO_4. The drying agent was filtered off and the filtrate concentrated to a beige gel. The gel was crystallized with cold ACN to give 7.93 g of a powdery white solid (80% yield). R_f = 0.23 in solvent system (C), R_f = 0.57 in solvent system (F); ^{1}H NMR (400 MHz, $CDCl_3$) δ 7.85 (m, 3 H, arom H1, H3, H9), 7.40 (m, 2 H, arom H2, H7), 7.12 (t, 1 H, *J* = 7.8 Hz, arom H8), 5.86 (d, 1 H, *J* = 11.7 Hz, α-vinylic H), 5.47 (d, 1 H, *J* = 11.4 Hz, β-vinylic H), 4.38 (q, 2 H, *J* = 6.9, 7.2 Hz, CH_2), 1.38 (t, 3 H, *J* = 7.2 Hz, CH_3); MS (GCMS) 392 $[M]^+$.

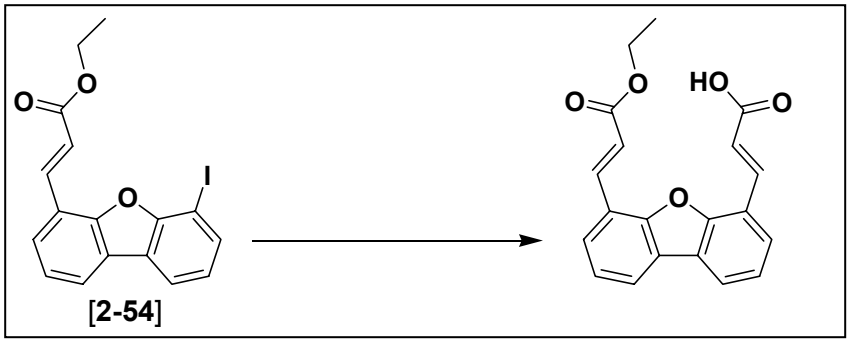

4-(2-Carboxyvinyl)-6-(2-ethoxycarbonylvinyl)-dibenzofuran: A flame dried flask fitted with a jacketed water condenser was charged with 6-(2-ethoxycarbonylvinyl)-4-iododibenzofuran [**2-54**] (7.50 g, 19.12 mmol), palladium acetate (0. 09 g, 2.2 mol%), and triorthotolylphosphine (0.29 g, 5.0 mol%), and flushed several times with Ar. Dry ACN (45 ml) was then added, followed by acrylic acid (3.9 ml, 57.36 mmol) and TEA (10.6 ml, 76.48 mmol). The reaction was heated to 85 °C in an oil bath and left to reflux over night under Ar. The dark brown reaction was cooled to r.t. and filtered to remove the black precipitate. The filtrate was then concentrated under reduced pressure to a dark brown solid which was then taken up in DCM and dissolved onto silica gel. The crude material was purified by column chromatography in 3:2 EtOAc:hex to afford 3.86 g of a beige solid (60% yield). R_f = 0.25 in solvent system (F); ^{1}H NMR (400 MHz, $CDCl_3$) δ 8.07 (d, 1 H, *J* = 16 Hz, α-vinylic H), 7.98 (d, 1 H, *J* = 16 Hz, α-vinylic H), 7.94 (t, 2 H, *J* = 7.6, 6.8 Hz, arom H1, H9), 7.58 (dd, 2 H, *J* = 7.6, 6.8 Hz, arom H3, H7), 7.38 (dt, 2 H, *J* = 7.6 Hz, arom H2, H8), 7.07 (d, 1 H, *J* = 16, β-vinylic H), 7.01 (d, 1 H, *J* = 16 Hz, β-vinylic H), 4.34 (q, 2 H, *J* = 6.8 7.2 Hz, CH_2), 1.42 (t, 3 H, *J* = 6.8, 7.2 Hz, CH_3); MS (ESI) 337 $[M+H]^+$, 359 $[M+Na]^+$, 335 $[M-H]^-$, 371 $[M+Cl]^-$.

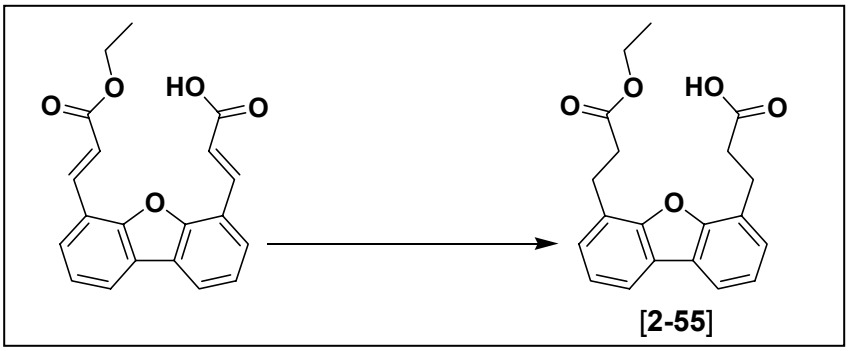

[**2-55**]

4-(2-Carboxyethyl)-6-(2-ethoxycarbonylethyl)-dibenzofuran [2-55]:

4-(2-Carboxyvinyl)-6-(2-ethoxycarbonylvinyl)-dibenzofuran (3.75 g, 11.15 mmol) was dissolved in a mixture of THF (150 ml) and EtOAc (37.5 ml) in a Parr hydrogenation flask. Three drops of water were added, followed by 10% palladium on carbon (0.750 g). The flask was placed onto the Parr hydrogenator and shaken under 63 psi of H_2 for 4 h. The reaction was then filtered over celite to remove the catalyst and the filter agent washed with DCM. The filtrate was concentrated under reduced pressure to afford 3.80 g of a white solid in quantitative yield. R_f = 0.34 in solvent system (F), R_f = 0.31 in solvent system (G); ^{1}H NMR (400 MHz, $CDCl_3$) δ 7.80 (dt, 2 H, *J* = 6.8, 7.6 Hz, arom H1, H9), 7.30 (m, 4 H, arom H2, H3, H7, H8), 4.15 (q, 2 H, *J* = 7.2 Hz, OCH_2), 3.34 (dt, 4 H, *J* = 7.2, 7.6, 8.4 Hz, α-CH_2), 2.85 (dt, 4 H, *J* = 7.2, 7.6, 8.0 Hz, β-CH_2), 1.23 (t, 3 H, *J* = 7.2 Hz, CH_3); MS (ESI) 341 $[M+H]^+$, 363 $[M+Na]^+$, 339 $[M-H]^-$, 375 $[M+Cl]^-$.

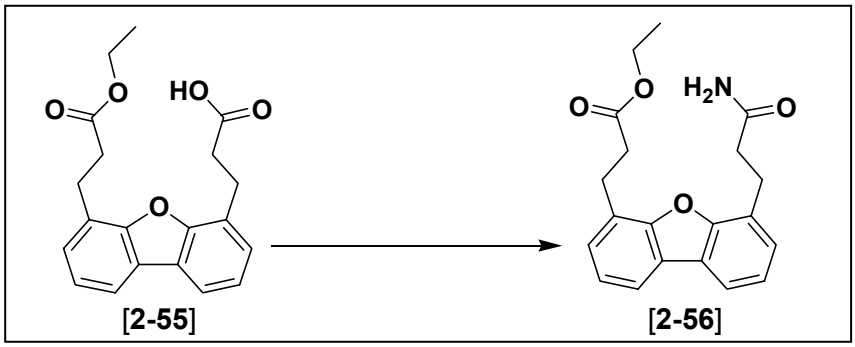

[**2-55**] [**2-56**]

4-(2-Amidoethyl)-6-(2-ethoxycarbonylethyl)-dibenzofuran [2-56]: A flame dried flask was charged with 4-(2-carboxyethyl)-6-(2-ethoxycarbonylethyl)-dibenzofuran [**2-55**] (3.75 g, 11.02 mmol), DCM (200 ml), DMF (3 drops), and flushed with Ar. The solution was cooled to 0 °C in an ice bath, and oxalyl chloride (1.93 ml, 22.04 mmol) was added, drop-wise, over 15 min. The reaction was allowed to slowly warm to r.t. It was then concentrated under reduced pressure to dryness and the residue taken up in DCM (200 ml). The reaction was again cooled to 0 °C in an ice bath and ammonium hydroxide (~50 ml) was added, drop-wise, over 15 min. with vigorous stirring. The reaction was allowed to warm to r.t. The solution was then acidified to pH=2 with 1N HCl, which caused a precipitate to form. The mixture was extracted with DCM (5 x 10 ml). The combined organic washes were dried over $MgSO_4$. The drying agent was filtered off and the filtrate concentrated to 3.80 g of a beige solid in quantitative yield. R_f = 0.11 in solvent system (G), R_f = 0.33 in solvent system (H); ^{1}H NMR (400 MHz, $CDCl_3$) δ 7.78 (d, 2 H, *J* = 7.2 Hz, arom H1, H9), 7.26 (m, 4 H, arom H2, H3, H7, H8), 5.88, 5.34 (bs, 2 H, NH_2), 4.07 (q, 2 H, *J* = 6.8, 7.6 Hz, OCH_2), 3.32 (dt, 4 H, *J* = 6.8, 7.6 Hz, α-CH_2), 2.81 (m, 4 H, β-CH_2), 1.17 (t, 3 H,

J = 6.8, 7.6 Hz, CH_3); MS (ESI) 340 $[M+H]^+$, 362 $[M+Na]^+$, 338 $[M-H]^-$, 374 $[M+Cl]^-$; HRMS (MALDI) 340.154 $[M+H]^+$, 362.133 $[M+Na]^+$.

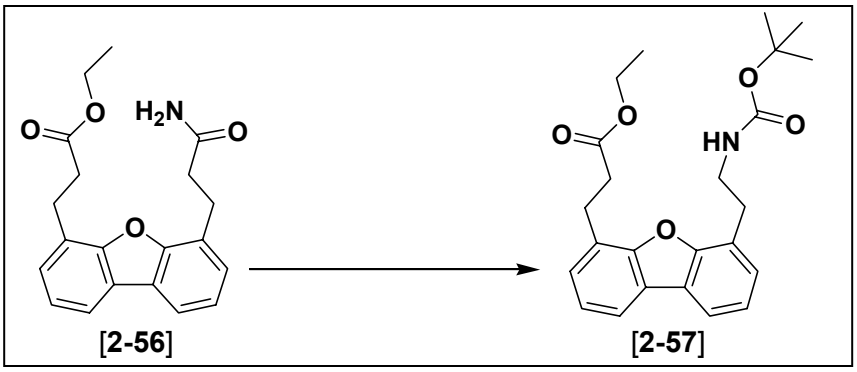

4-(2-*t*-Butyloxycarbonylaminoethyl)-6-(2-ethoxycarbonylethyl)-dibenzofuran [2-57]: An oven dried flask fitted with a jacketed water condenser was charged with mercury(II)acetate (6.57 g, 20.62 mmol) and flushed with Ar. 4-(2-Amidoethyl)-6-(2-ethoxycarbonylethyl)-dibenzofuran [**2-56**] (3.50 g, 10.31 mmol) was dissolved in dry DMF (30 ml) and added to the reaction flask with a syringe. *t*-Butanol (24.5 ml, 257.75 mmol) was added, followed by a solution of *N*-bromosuccinimide (3.60 g, 20.62 mmol) in dry DMF (35 ml). The reaction was stirred at r.t. for 30 min., then heated to 75 °C in an oil bath (solution became yellow) and was left to stir at that temperature over night under Ar. The reaction became orange with a white solid dispersed in it. The reaction was cooled to r.t. and concentrated under reduced pressure to dryness. The residue was then suspended in DCM and filtered to remove the white solid. The filtrate was concentrated under reduced pressure to an orange gel which was dissolved in 20% EtOAc:hex and purified by column chromatography in

20% EtOAc:hex. A slightly yellow solid was obtained (3.40 g, 80%). R_f = 0.26 in solvent system (D), R_f = 0.58 in solvent system (H); ^{1}H NMR (400 MHz, $CDCl_3$) δ 7.78 (d, 2 H, *J* = 7.2 Hz, arom H1, H9), 7.26 (m, 4 H, arom H2, H3, H7, H8), 4.70 (bs, 1 H, NH), 4.12 (q, 2 H, *J* = 7.2 Hz, OCH_2), 3.56 (m, 2 H, β-CH_2, amine arm), 3.31 (t, 2 H, *J* = 7.6, 8 Hz, β-CH_2 ester arm), 3.17 (t, 2 H, *J* = 6.4, 6.8 Hz, α-CH_2 amine arm), 2.81 (t, 2 H, *J* = 7.6, 8 Hz, β-CH_2 ester arm), 1.37 (s, 9 H, *t*-But), 1.22 (t, 3 H, *J* = 6.8, 7.2 Hz, CH_3); ^{13}C NMR (400 MHz, $CDCl_3$) δ 172.6 (1 C, COO of ester), 155.6 (1 C, COO of Boc), 154.3 (1 C, arom C4a), 154.0 (1 C, arom C6a), 127.5 (1 C, arom C1a), 126.9 (2 C, arom C3, C7), 124.2 (1 C, arom C4), 123.9 (1 C, arom C6), 122.7 (2 C, arom C2, C9), 118.8 (1 C, arom C9a), 118.6 (2 C, arom C1, C9), 60.4 (2 C, OCH_2), 40.5 (1 C, *t*-but C), 34.2 (1 C, N-CH_2), 30.5 (1 C, ester β-CH_2), 28.4 (3 C, *t*-but CH_3), 25.4 (2 C, α-CH_2 of both arms), 14.2 (1 C, ester CH_3); HRMS (MALDI-FTMS) 434.193 $[M+Na]^+$.

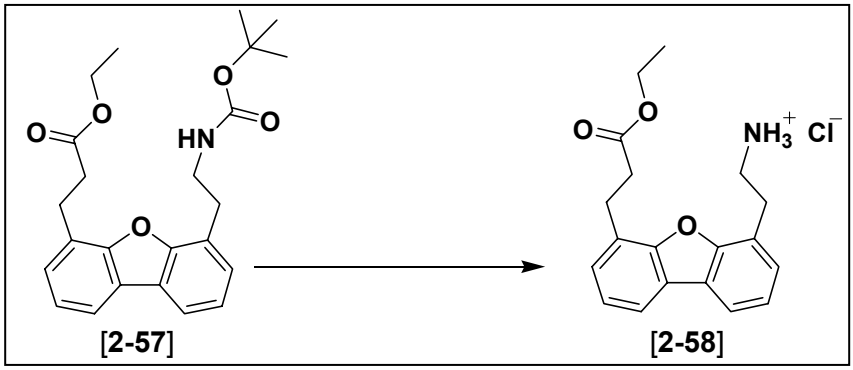

4-(2-Aminoethyl)-6-(2-ethoxycarbonylethyl)-dibenzofuran [2-58]:

4-(2-*t*-Butyloxycarbonylaminoethyl)-6-(2-ethoxycarbonylethyl)-dibenzofuran [**2-57**] (0.400 g, 0.98 mmol) was dissolved in 4N HCl/dioxane (30 ml) and stirred for 1 h.

The solvents were then removed under reduced pressure to afford the free amino compound as a white solid (0.340 g, quantitative). R_f = 0.08 in solvent system (D), R_f = 0.23 in solvent system (I); ^{1}H NMR (400 MHz, $CDCl_3$) δ 7.76 (d, 2 H, *J* = 6.8 Hz, arom H1, H9), 7.25 (m, 4 H, arom H2, H3, H7, H8), 4.10 (q, 2 H, *J* = 7.2 Hz, OCH_2), 3.28 (t, 2 H, *J* = 7.6, 8 Hz, β-CH_2, amine arm), 3.16 (m, 4 H, β-CH_2 ester arm, α-CH_2 amine arm), 2.79 (t, 2 H, *J* = 7.6, 8 Hz, β-CH_2 ester arm), 2.14 (s, 2 H, NH_2), 1.20 (t, 3 H, *J* = 7.2 Hz, CH_3); MS (ESI) 312 $[M+H]^+$.

2.5.3 Syntheses of the dipeptides

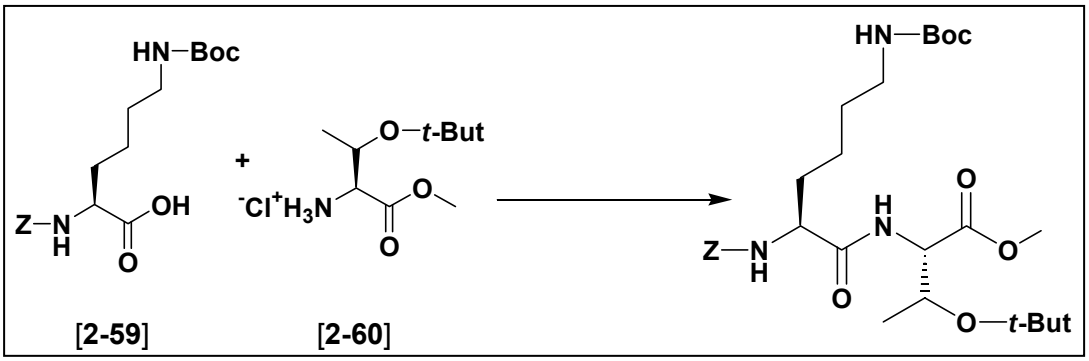

Z-Lys(Boc)-Thr(*t*-But)-OMe: Z-Lys(Boc)-OH [**2-59**] (5.0 g, 13.14 mmol), EDC (3.02 g, 15.77 mmol), HOBt (2.13 g, 15.77 mmol), and DIEA (9.38 ml, 52.56 mmol) were dissolved in DCM (75 ml) and stirred for 10 min. H-Thr(*t*-But)-OH · HCl [**2-60**] (2.74 g, 14.46 mmol) was then added and the colorless solution left to stir over night. The solution became pale yellow. It was concentrated under reduced pressure and the

residue dissolved in EtOAc (50 ml). It was then washed with 1N HCl (3 x 25 ml), conc. $NaHCO_3$ (3 x 25 ml), brine (1 x 25 ml), and dried over $MgSO_4$. The drying agent was filtered off and the filtrate concentrated to a gold foam. The crude material was dissolved in warm 1:1 EtOAc:hex and purified by column chromatography in the same solvent system to give a 5.30 g white solid (73% yield). R_f = 0.30 in solvent system (E), R_f = 0.56 in solvent system (H), R_f = 0.63 in solvent system (I); ^{1}H NMR (400 MHz, $CDCl_3$) δ 7.32 (m, 5 H, arom), 6.49 (d, 1 H, *J* = 10 Hz, Lys α-NH), 5.52 (d, 1 H, *J* = 7.2 Hz, Thr NH), 5.09 (s, 2 H, bzl CH_2), 4.74 (bs, 1 H, Lys ζ-NH), 4.45 (dd, 1 H, *J* = 9.2, 8.8 Hz, Thr α-H), 4.24 (m, 2 H, Lys α-H, Thr β-H), 3.69 (s, 3 H, OCH_3), 3.09 (bm, 2 H, Lys ε-CH_2), 1.90, 1.70 (dbm, 2 H, Lys β-CH_2), 1.81 (m, 2 H, Lys δ-CH_2), 1.46 (bm, 2 H, Lys γ-CH_2), 1.40 (s, 9 H, Boc), 1.13 (d, 3 H, Thr CH_3), 1.09 (s, 9 H, O-*t*-But).

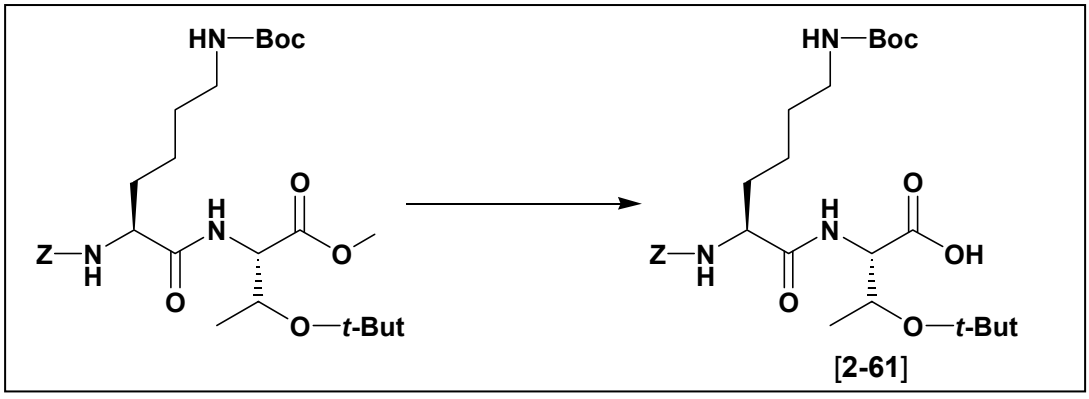

[2-61]

Z-Lys(Boc)-Thr(*t*-But)-OH [2-61]: Z-Lys(Boc)-Thr(*t*-But)-OMe (0.761 g, 1.38 mmol) was dissolved in MeOH (30 ml). Separately, $LiOH \cdot H_2O$ (0.232 g, 5.53 mmol) was dissolved in H_2O (15 ml), and then added to the MeOH solution. The reaction was

left to stir for 3 h. The organic solvents were then removed under reduced pressure and the remaining aqueous mixture acidified to pH = 2 with 1N HCl. It was then extracted with DCM (5 x 20 ml) and dried over $MgSO_4$. The drying agent was filtered off and the filtrate concentrated to afford 0.74 g of a white foam in quantitative yield. ^{1}H NMR (400 MHz, $CDCl_3$) δ 7.32 (m, 5 H, arom), 6.83 (d, 1 H, *J* = 7.2 Hz, Lys α-NH), 5.64 (d, 1 H, *J* = 10 Hz, Thr NH), 5.10 (s, 2 H, bzl CH_2), 4.67 (bs, 1 H, Lys ζ-NH), 4.45 (m, 1 H, Thr α-H), 4.31 (m, 1 H, Lys α-H), 4.22 (m, 1 H, Thr β-H), 3.08 (bm, 2 H, Lys ε-CH_2), 1.90, 1.70 (bm, 2 H, Lys β-CH_2), 1.41 (m, 13 H, Lys γ-CH_2, Lys δ-CH_2, Boc), 1.26 (s, 9 H, O-*t*-But), 1.09 (d, 3 H, *J* = 5.6 Hz, Thr CH_3).

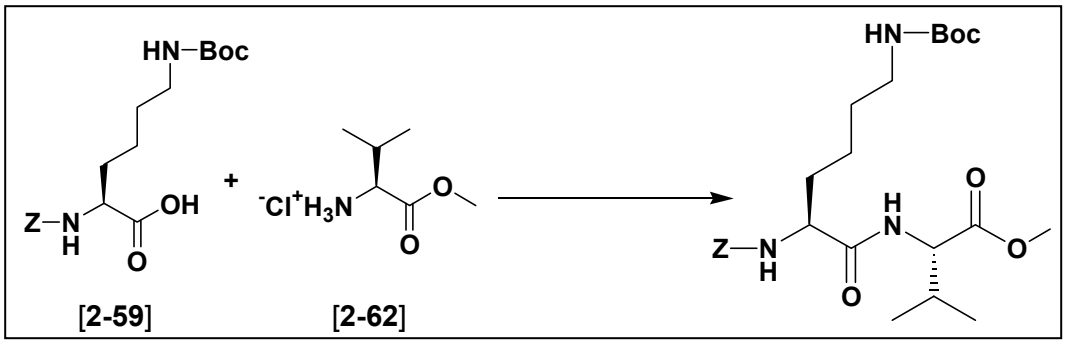

Z-Lys(Boc)-Val-OMe: Z-Lys(Boc)-OH [**2-59**] (3.0 g, 7.89 mmol) and DEPBT (2.83 g, 9.47 mmol) were dissolved in DCM (50 ml). TEA (3.95 ml, 28.40 mmol) was added (turned bright yellow) and stirred for 10 min. Val-OMe · HCl [**2-60**] (1.59 g, 9.47 mmol) was then added and the reaction left to stir over night. The solvents were removed under reduced pressure and the residue was dissolved onto silica gel using DCM. The crude material was purified by column chromatography in 1:1 EtOAc:hex

to afford 3.32 g of a white solid (85% yield). R_f = 0.32 in solvent system (E), R_f = 0.59 in solvent system (H); ^{1}H NMR (400 MHz, $CDCl_3$) δ 7.30 (m, 5 H, arom), 6.53 (bd, 1 H, *J* = 7.2 Hz, Lys α-NH), 5.49 (bd, 1 H, *J* = 6 Hz, Val NH), 5.08 (s, 2 H, bzl CH_2), 4.65 (bs, 1 H, Lys ζ-NH), 4.48 (dd, 1 H, *J* = 4.8, 5.2 Hz, Lys α-H), 4.27 (m, 1 H, Val α-H), 3.71 (s, 3 H, OCH_3), 3.06 (bm, 2 H, Lys ε-CH_2), 2.13 (m, 1 H, Val β-H), 1.82, 1.63 (bm, 2 H, Lys β-CH_2), 1.42 (m, 2 H, Lys δ-CH_2), 1.37 (bm, 2 H, Lys γ-CH_2), 1.39 (s, 9 H, Boc), 0.86 (dd, 6 H, *J* = 6.4, 7.2 Hz, Val CH_3).

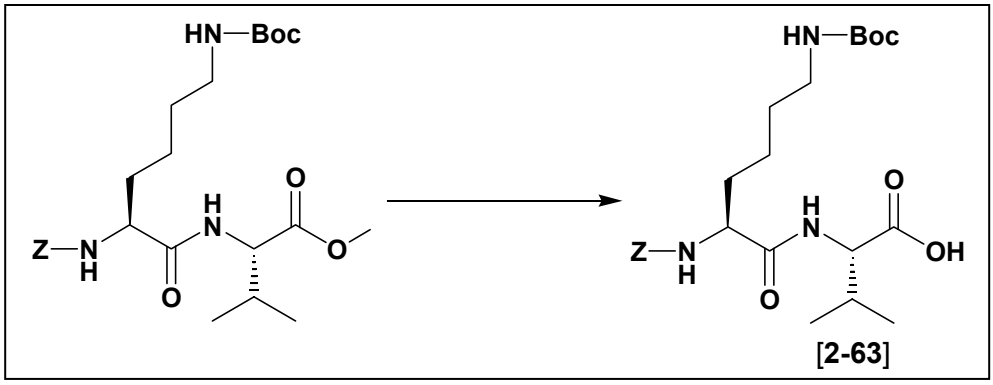

Z-Lys(Boc)-Val-OH [2-63]: Z-Lys(Boc)-Val-OMe (0.51 g, 1.04 mmol) was dissolved in MeOH (10 ml). Separately, LiOH · H_2O (0.18 g, 2.08 mmol) was dissolved in H_2O (5 ml), and then added to the MeOH solution. It was left to stir for 1½ h. The organic solvents were then removed under reduced pressure and the remaining aqueous mixture acidified to pH = 2 with 1N HCl. It was then extracted with DCM (5 x 10 ml) and dried over $MgSO_4$. The drying agent was filtered off and the filtrate concentrated to afford 0.50 g of a white solid in quantitative yield. R_f = 0.15 in solvent system (H); ^{1}H NMR (400 MHz, $CDCl_3$) δ 9.67 (bs, 1 H, OH) 7.29 (m,

5 H, arom), 7.04 (bd, 1 H, *J* = 8.4 Hz, Val NH), 5.97 (d, 1 H, *J* = 8 Hz, Lys α-NH), 5.06 (s, 2 H, bzl CH_2), 4.86 (bs, 1 H, Lys ζ-NH), 4.49 (bm, 1 H, Lys α-H), 4.28 (bs, 1 H, Val α-H), 3.02 (bs, 2 H, Lys ε-CH_2), 2.18 (m, 1 H, Val β-H), 1.75, 1.62 (bm, 2 H, Lys β-CH_2), 1.39 (m, 13 H, Lys δ-CH_2, Lys γ-CH_2, Boc), 0.89 (overlap d, 6 H, Val CH_3).

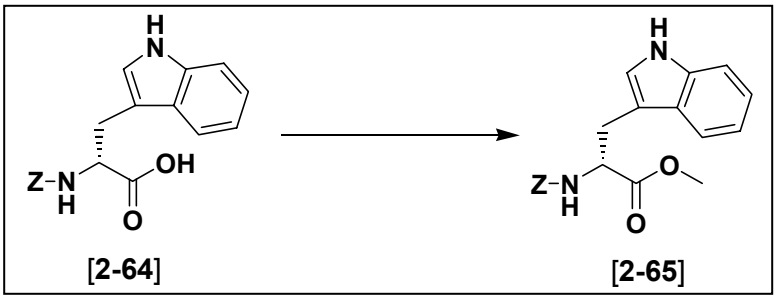

Z-D-Trp-OMe [2-65]: Z-D-Trp-OH [**2-64**] (5.0 g, 14.78 mmol) was dissolved in MeOH (250 ml). $SOCl_2$ (2.15 ml, 29.55 mmol) was added, drop-wise, over 30 min. The reaction was left to stir over night. It was then concentrated under reduced pressure to give 5.75 g of a purple foam in quantitative yield. R_f = 0.34 in solvent system (E), R_f = 0.79 in solvent system (I); ^{1}H NMR (400 MHz, $CDCl_3$) δ 8.20 (bs, 1 H, indole H4), 7.50 (d, 1 H, *J*= 8 Hz, indole H7), 7.31 (m, 6 H, arom Z, indole H2), 7.17 (t, 1 H, *J* = 8.0, 6.8 Hz, indole H6), 7.07 (t, 1 H, *J* = 8.0, 6.8 Hz, indole H5), 6.94 (d, 1 H, *J* = 2.0 Hz, indole H1), 5.29 (d, 1 H, *J* = 8.0 Hz, α-NH), 5.09 (s, 2 H, Z CH_2), 4.70 (dt, 1 H, *J* = 5.6, 4.8 Hz, α-H), 3.66 (s, 3 H, OCH_3), 3.30 (d, 2 H, *J* = 5.2 Hz, β-CH_2).

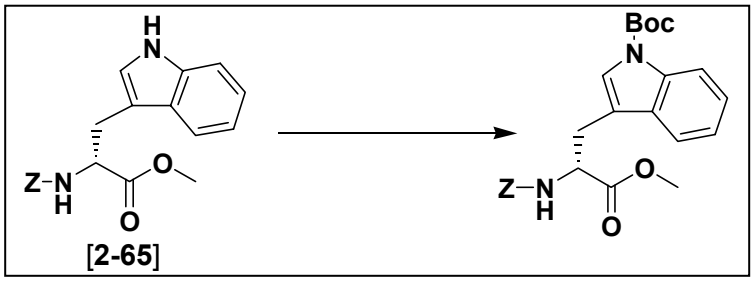

Z-D-Trp(Boc)-OMe: Z-D-Trp-OMe [**2-65**] (2.75 g, 7.09 mmol) was dissolved in ACN (35ml). Boc_2O (2.32 g, 10.64 mmol) and DMAP (0.087 g, 0.709 mmol) were added and the reaction was left to stir over night. The reaction was then concentrated under reduced pressure and the residue dissolved in 30% EtOAc:hex. The crude material was purified by column chromatography in 30% EtOAc:hex to give a beige solid (2.31 g, 72% yield). R_f = 0.20 in solvent system (D), R_f = 0.52 in solvent system (E); ^{1}H NMR (400 MHz, $CDCl_3$) δ 8.10 (bd, 1 H, *J* = 6.0 Hz, indole H4), 7.46 (d, 1 H, *J* = 7.6 Hz, indole H7), 7.40 (s, 1 H, indole H2), 7.31 (m, 6 H, arom Z, indole H6), 7.19 (t, 1 H, *J* = 8.0, 6.8 Hz, indole H5), 5.43 (d, 1 H, *J* = 8.0 Hz, α-NH), 5.11 (s, 2 H, Z CH_2), 4.73 (dt, 1 H, *J* = 6.0, 5.2 Hz, α-H), 3.68 (s, 3 H, OCH_3), 3.23 (dd, 2 H, *J* = 5.2, 5.6 Hz, β-CH_2), 1.65 (s, 9 H, Boc).

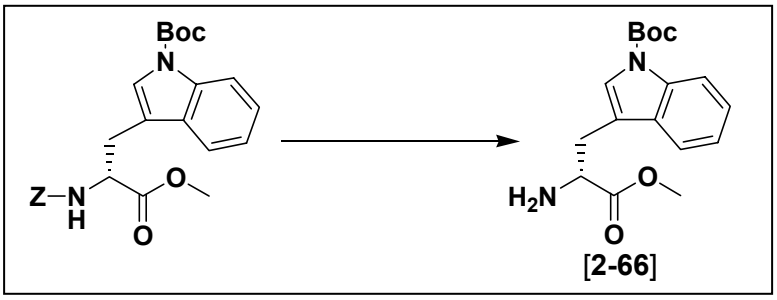

H-D-Trp(Boc)-OMe [2-66]: Z-D-Trp(Boc)-OMe (2.25 g, 4.97 mmol) was dissolved in THF (40 ml). 10% Pd/C (0.35 g) was then added and the reaction placed under H_2 atmosphere to stir over night. The reaction was filtered over celite to remove the catalyst. The filtrate was concentrated under reduced pressure to afford a colorless gel (1.58 g, quantitative yield). R_f = 0.09 in solvent system (E), R_f = 0.18 in solvent system (H); ^{1}H NMR (400 MHz, $CDCl_3$) δ 8.11 (bs, 1 H, indole H4), 7.51 (d, 1 H, *J* = 8.0 Hz, indole H7), 7.44 (s, 1 H, indole H2), 7.29 (t, 1 H, *J* = 8.0, 6.8 Hz, indole H6), 7.21 (t, 1 H, *J* = 8.0, 6.8 Hz, indole H5), 3.81 (dd, 1 H, *J* = 5.2, 4.8 Hz, αH), 3.69 (s, 3 H, OCH_3), 3.18 (m, 2 H, β-CH_2), 1.64 (s, 9 H, Boc).

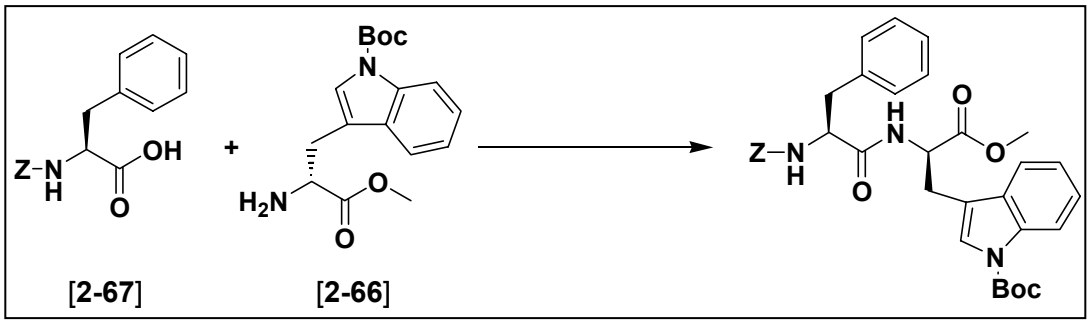

Z-Phe-D-Trp(Boc)-OMe: Z-Phe-OH [**2-67**] (0.34 g, 1.14 mmol) and DEPBT (0.27 g, 0.91 mmol) were dissolved in DCM (10 ml). TEA (0.21 ml, 1.52 mmol) was added and the reaction became bright yellow. It was stirred for 10 min. H-D-Trp(Boc)-OMe [**2-66**] (0.240 g, 0.76 mmol) was then added and the reaction left to stir over night. The reaction was concentrated under reduced pressure and the residue dissolved in EtOAc. It was then washed with 1N HCl (3 x 10 ml), conc. $NaHCO_3$ (3 x 10 ml), brine (1 x 15 ml), and dried over $MgSO_4$. The drying agent was filtered off and the filtrate concentrated under reduced pressure to a gold foam. The crude material was dissolved in 3:2 hex:EtOAc and purified by column chromatography in the same solvent system to afford a white foam (0.36 g, 80% yield). R_f = 0.37 in solvent system (E), R_f = 0.41 in solvent system (I); ^{1}H NMR (400 MHz, $CDCl_3$) δ 8.07 (bd, 1 H, *J* = 6.8 Hz, indole H4), 7.40 (d, 1 H, *J* = 8.0 Hz, indole H7), 7.28 (m, 13 H, arom Z, Phe, indole H6, H5, H2), 6.40 (bs, 1 H, Phe NH), 5.27 (bs, 1 H, D-Trp NH), 4.98 (s, 2 H, Z CH_2), 4.85 (q, 1 H, *J* = 6.0, 7.6 Hz, Phe α-H), 4.43 (d, 1 H, *J* = 6.0 Hz, D-Trp α-H), 3.60 (s, 3H, OCH_3), 3.04 (m, 4 H, Phe β-CH_2, D-Trp β-CH_2), 1.63 (s, 9 H, Boc).

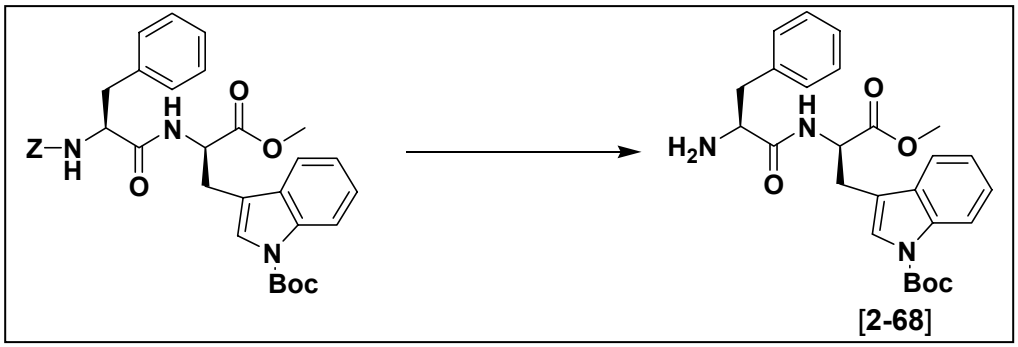

[**2-68**]

H-Phe-D-Trp(Boc)-OMe [2-68]: Z-Phe-D-Trp(Boc)-OMe (0.35 g, 0.58 mmol) was dissolved in MeOH (10 ml). 10% Pd/C (0.05 g) was then added and the reaction placed under H_2 atmosphere to stir over night. The reaction was filtered to remove the catalyst. The filtrate was concentrated under reduced pressure to afford a white solid (0.27 g, quantitative yield). R_f = 0.08 in solvent system (E), R_f = 0.14 in solvent system (I); ^{1}H NMR (400 MHz, $CDCl_3$) δ 8.06 (bd, 1 H, indole H4), 7.80 (d, 1 H, *J* = 8.0 Hz, Trp NH), 7.48 (d, 1 H, *J* = 7.6 Hz, indole H7), 7.39 (s, 1 H, indole H2), 7.26 (m, 8 H, arom Phe, indole H6, H5), 4.90 (m, 1 H, Phe α-H), 3.68 (s, 3H, OCH_3), 3.55 (bdd, 1 H, *J* = 3.6, 9.6 Hz, D-Trp α-H), 3.24 (m, 4 H, Phe β-CH_2, D-Trp β-CH_2), 1.63 (s, 9 H, Boc).

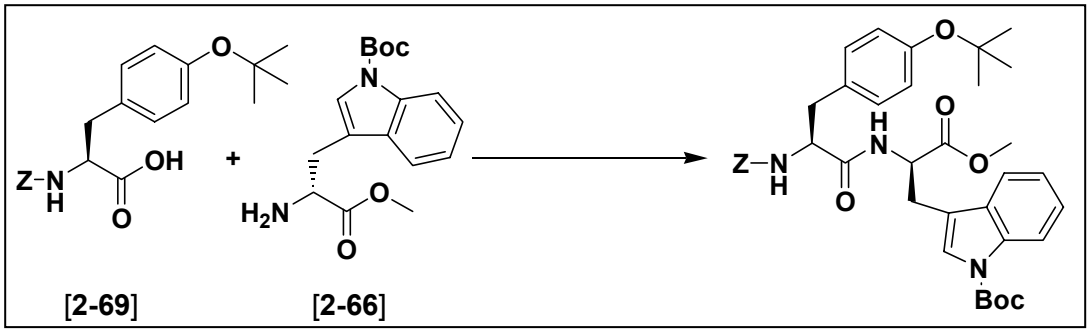

Z-Tyr(*t*-But)-D-Trp(Boc)-OMe: Z-Tyr(*t*-But)-OH · DCHA (2.20 g, 3.97 mmol) was dissolved in EtOAc, washed with 1N HCl to liberate the carboxylic acid, and dried over $MgSO_4$. The drying agent was filtered off and the filtrate concentrated to afford free carboxylic acid [**2-69**]. Z-Tyr(*t*-But)-OH [**2-69**] was dissolved in DCM (15 ml) and DEPBT (1.19 g, 3.97 mmol) and TEA (0.92 ml, 6.62 mmol) were added and stirred for 10 min. H-D-Trp(Boc)-OMe [**2-66**] (1.05 g, 3.31 mmol) was dissolved in DCM (15 ml) and added to the reaction. It was left to stir over night. The reaction was concentrated under reduced pressure and the residue dissolved in EtOAc. It was then washed with 1N HCl (3 x 30 ml), conc. $NaHCO_3$ (3 x 30 ml), brine (1 x 30 ml), and dried over $MgSO_4$, The drying agent was filtered off and the filtrate concentrated under reduced pressure to a gold foam. The crude material was dissolved in 1:1 EtOAc:hex and purified by column chromatography in the same solvent mixture to afford a white foam (1.33 g, 60% yield). R_f = 0.43 in solvent system (E); ^{1}H NMR (400 MHz, $CDCl_3$) δ 8.07 (d, 1 H, *J* = 8.0 Hz, indole H4), 7.42 (d, 1 H, *J* = 8.0 Hz, indole H7), 7.35 (s, 1 H, indole H2), 7.26 (m, 7 H, arom Z, indole H6, H5), 6.96 (d, 2 H, *J* = 8.0 Hz, Tyr arom), 6.81 (d, 2 H, *J* = 8.4 Hz, Tyr arom), 6.61 (bs, 1 H, Tyr NH), 5.37 (bs, 1 H, D-Trp NH), 4.98 (s, 2 H, Z CH_2), 4.85 (q, 1 H, *J* = 6.8, 7.6, 6.0 Hz, Tyr

α-H), 4.43 (d, 1 H, *J* = 6.0 Hz, D-Trp α-H), 3.58 (s, 3H, OCH_3), 3.07 (m, 2 H, Tyr β-CH_2), 2.97 (m, 2 H, D-Trp β-CH_2), 1.62 (s, 9 H, Boc), 1.27 (s, 9 H, *t*-But).

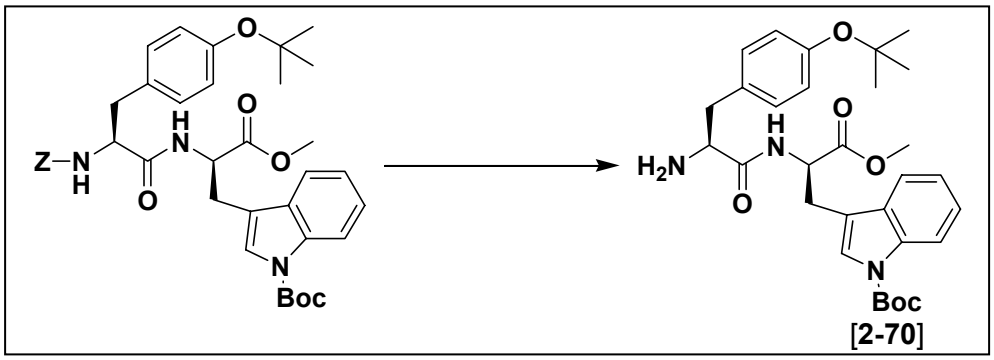

[2-70]

H-Tyr(*t*-But)-D-Trp(Boc)-OMe [2-70]: Z-Tyr(*t*-But)-D-Trp(Boc)-OMe (0.44 g, 0.65 mmol) was dissolved in MeOH (250 ml). 10% Pd/C (0.07 g) was then added and the reaction placed under H_2 atmosphere to stir over night. The reaction was filtered to remove the catalyst. The filtrate was concentrated under reduced pressure to afford a white solid (0.35 g, quantitative yield). R_f = 0.08 in solvent system (E); ^{1}H NMR (400 MHz, $CDCl_3$) δ 8.04 (bd, 1 H, *J* = 6.4 Hz, indole H4), 7.89 (d, 1 H, *J* = 8.0 Hz, D-Trp NH), 7.45 (d, 1 H, *J* = 7.6 Hz, indole H7), 7.38 (s, 1 H, indole H2), 7.26 (m, 1 H, indole H6), 7.19 (m, 1 H, indole H5), 7.01 (d, 2 H, *J* = 8.4 Hz, Tyr arom), 6.85 (d, 2 H, *J* = 8.4 Hz, Tyr arom), 4.85 (m, 2 H, Tyr α-H, D-Trp α-H), 3.64 (s, 3H, OCH_3), 3.16 (m, 4 H, Tyr β-CH_2, D-Trp β-CH_2), 1.59 (s, 9 H, Boc), 1.27 (s, 9 H, *t*-But).

2.5.4 Preparation of final compounds

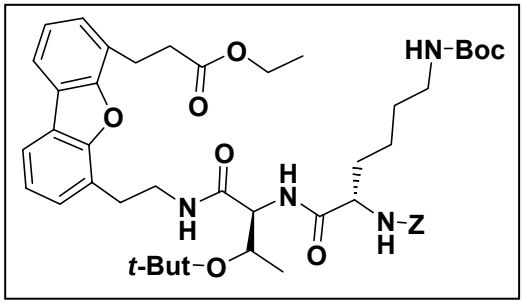

6-(2-Ethoxycarbonylethyl)-4-(Z-Lys(Boc)-Thr(*t*-But)-(2-aminoethyl))-dibenzofuran: Z-Lys(Boc)-Thr(*t*-But)-OH [**2-61**] (0.42 g, 0.78 mmol), DEPBT (0.23 g, 0.78 mmol), and TEA (0.22 ml, 1.56 mmol) were dissolved in DCM (15 ml) and stirred for 10 min. 4-(2-Aminoethyl)-6-(2-ethoxycarbonylethyl)-dibenzofuran [**2-58**] (0.20 g, 0.65 mmol) was dissolved in DCM (7 ml) and added to the reaction. It was left to stir over night. The solvents were removed under reduced pressure and the residue dissolved in 1:1 EtOAc:hex. The crude material was purified by column chromatography in the same solvent system to afford 0.38 g of a white solid (70% yield). R_f = 0.20 in solvent system (E), R_f = 0.25 in solvent system (G), R_f = 0.57 in solvent system (H); ^{1}H NMR (400 MHz, $CDCl_3$) δ 7.80 (m, 2 H, DBF H1, H9), 7.28 (m, 9 H, arom Z, DBF H2, H3, H8, H7), 7.71, 7.03, 5.64, 4.65 (bs, 4 H, NHs), 5.07 (s, 2 H, Z CH_2), 4.12 (m, 5 H, α-Hs, Thr β-H, OCH_2), 3.81 (m, 2 H, β-CH_2 amine arm), 3.32 (t, 2 H, β-CH_2 ester arm), 3.25 (m, α-CH_2 amine arm), 3.12 (bm, 2 H, Lys ε-CH_2), 2.82 (t, 2 H, α-CH_2 ester arm), 1.85, 1.69 (bm, 2 H, Lys β-CH_2), 1.45 (m, 13 H, Lys

γ-CH_2, Lys δ-CH_2, Boc), 1.23 (t, 3 H, ester CH_3), 1.01 (s, 9 H, O-*t*-But), 0.91 (d, 3 H, Thr CH_3).

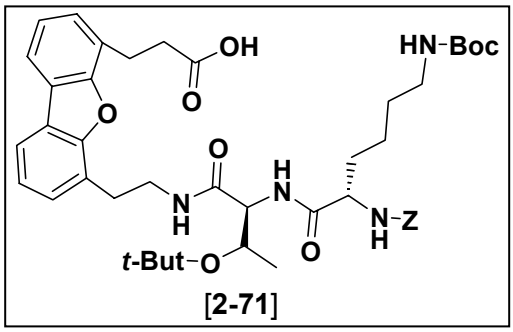

[2-71]

6-(2-Carboxyethyl)-4-(Z-Lys(Boc)-Thr(*t*-But)-(2-aminoethyl))-dibenzofuran [2-71]: 6-(2-Ethoxycarbonylethyl)-4-(Z-Lys(Boc)-Thr(*t*-But)-(2-aminoethyl))-dibenzofuran [**2-71**] (0.38 g, 0.46 mmol) was dissolved in a mixture of EtOH (5 ml) and THF (2 ml). Separately, LiOH · H_2O (0.16 g, 0.92 mmol) was dissolved in H_2O (4 ml), and then added to the reaction. It was left to stir for 1½ h. The organic solvents were then removed under reduced pressure and the remaining aqueous solution acidified to pH = 2 with 1N HCl. It was then extracted with DCM (5 x 15 ml) and dried over $MgSO_4$. The drying agent was filtered off and the filtrate concentrated under reduced pressure to afford a white foam (0.37 g, quantitative yield). R_f = 0.40 in solvent system (H), R_f = 0.39 in solvent system (I); ^{1}H NMR (400 MHz, $CDCl_3$) δ 7.80 (m, 2 H, DBF H1, H9), 7.28 (m, 9 H, arom Z, DBF H2, H3, H8, H7), 7.71, 7.03, 5.64, 4.65 (bs, 4 H, NHs), 5.07 (s, 2 H, Z CH_2), 4.12 (m, 3 H, α-Hs, Thr β-H), 3.81 (m, 2 H, β-CH_2 amine arm), 3.32 (t, 2 H, β-CH_2 acid arm), 3.25 (m, α-CH_2 amine arm), 3.12 (bm, 2 H, Lys ε-CH_2), 2.82 (t, 2 H, α-CH_2 acid arm), 1.85, 1.69 (bm, 2 H, Lys

β-CH_2), 1.45 (m, 13 H, Lys γ-CH_2, Lys δ-CH_2, Boc), 1.01 (s, 9 H, O-*t*-But), 0.91 (d, 3 H, Thr CH_3).

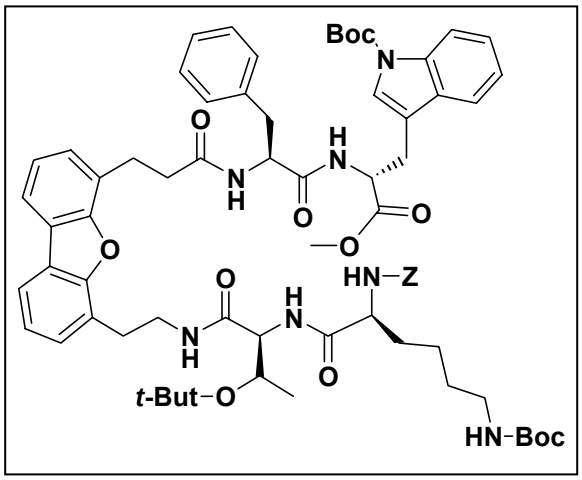

6-((2-Carbonylethyl)-Phe-D-Trp(Boc)-OMe)-4-(Z-Lys(Boc)-Thr(*t*-But)-(2-aminoethyl))-dibenzofuran: 6-(2-Carboxyethyl)-4-(Z-Lys(Boc)-Thr(*t*-But)-(2-aminoethyl))-dibenzofuran [**2-71**] (0.37 g, 0.46 mmol), DEPBT (0.16 g, 0.55 mmol), and TEA (0.13 ml, 0.92 mmol) were dissolved in DCM (8 ml) and stirred for 10 min. H-Phe-D-Trp(Boc)-OMe [**2-68**] (0.21 g, 0.46 mmol) was dissolved in DCM (8 ml) and added to the reaction. It was left to stir over night. The solvents were removed under reduced pressure and the residue dissolved in EtOAc (50 ml). It was washed with 1N HCl (3 x 15 ml), conc. $NaHCO_3$ (3 x 15 ml), brine (1 x 25 ml), and dried over $MgSO_4$. The drying agent was filtered off and the filtrate concentrated to a white solid. The crude material was dissolved onto silica gel with DCM and purified by column chromatography in 2:1 EtOAc:hex to afford a white solid (0.40 g, 70% yield). R_f = 0.17 in solvent system (G), R_f = 0.53 in solvent system (H), R_f = 0.68 in solvent

system (I); ^{1}H NMR (400 MHz, $CDCl_3$) complicated, but can see new dipeptide signals; MS (ESI) 1250 $[M+H]^+$, 1272 $[M+Na]^+$.

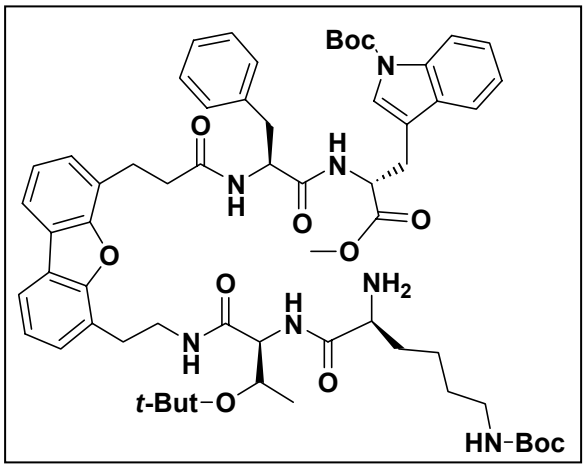

6-((2-Carbonylethyl)-Phe-D-Trp(Boc)-OMe)-4-(H-Lys(Boc)-Thr(*t*-But)-(2-aminoethyl))-dibenzofuran: 6-((2-Carbonylethyl)-Phe-D-Trp(Boc)-OMe)-4-(Z-Lys(Boc)-Thr(*t*-But)-(2-aminoethyl))-dibenzofuran (0.40 g, 0.32 mmol) was dissolved in a mixture of MeOH (20 ml) and THF (6 ml). 10% Pd/C (0.04 g) was then added and the reaction placed under H_2 atmosphere to stir over night. The reaction was filtered over celite to remove the catalyst. The filter cake was washed with THF. The filtrate was concentrated under reduced pressure to afford 0.36 g of a beige solid in quantitative yield. R_f = 0.54 in solvent system (I); ^{1}H NMR (400 MHz, $CDCl_3$) complicated, but Z group is gone; MS (ESI) 1116 $[M+H]^+$, 1138 $[M+Na]^+$.

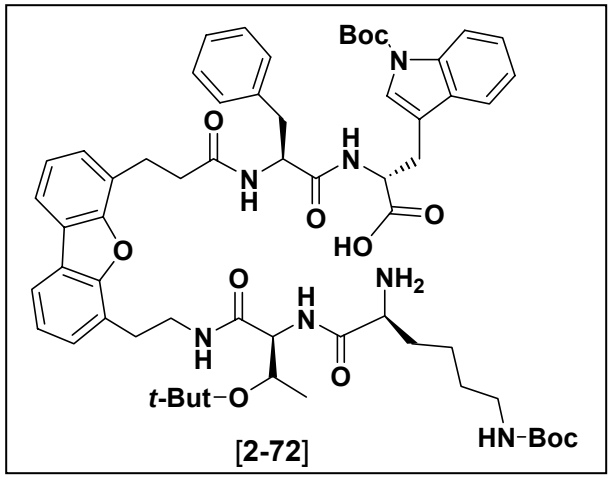

[2-72]

6-((2-Carbonylethyl)-Phe-D-Trp(Boc)-OH)-4-(H-Lys(Boc)-Thr(*t*-But)-(2-aminoethyl))-dibenzofuran [2-72]: 6-((2-Carbonylethyl)-Phe-D-Trp(Boc)-OMe)-4-(H-Lys(Boc)-Thr(*t*-But)-(2-aminoethyl))-dibenzofuran (0.36 g, 0.32 mmol) was dissolved in a mixture of MeOH (8 ml) and THF (2 ml). Separately, $LiOH \cdot H_2O$ (0.06 g, 1.28 mmol) was dissolved in H_2O (6 ml), and then added to the reaction. It was left to stir for 3 h. The organic solvents were then removed under reduced pressure and the remaining aqueous solution acidified to pH = 2 with 1N HCl. It was then extracted with EtOAc (5 x 20 ml). The combined organic washers were dried over $MgSO_4$. The drying agent was filtered off and the filtrate concentrated to a beige foam (0.36 g, quantitative yield). R_f = 0.09 in solvent system (I); ^1H NMR (400 MHz, $CDCl_3$) complicated, but OME is gone; MS (ESI) 1102 $[M+H]^+$, 1124 $[M+Na]^+$.

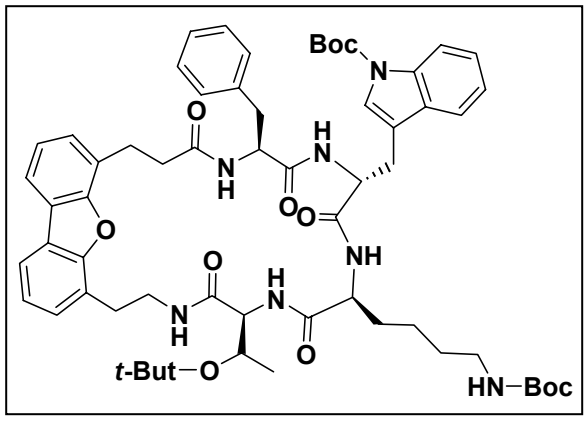

c[6-((2-Carbonylethyl)-Phe-D-Trp(Boc)-Lys(Boc)-Thr(*t*-But)-4-(2-aminoethyl))-dibenzofuran]: 6-((2-Carbonylethyl)-Phe-D-Trp(Boc)-OH)-4-(H-Lys(Boc)-Thr (*t*-But)-(2-aminoethyl))-dibenzofuran [**2-72**] (0.36 g, 0.32 mmol) was dissolved in distilled DCM (320 ml). DEPBT (0.28 g, 0.96 mmol) and TEA (0.18 ml, 1.28 mmol) were added and the colorless reaction left to stir under Ar for 2 days. It became yellow in color. The reaction was concentrated under reduced pressure and the residue dissolved in EtOAc (50 ml). It was washed with 1N HCl (3 x 20 ml), conc. $NaHCO_3$ (3 x 20 ml), brine (1 x 30 ml), and dried over $MgSO_4$. The drying agent was filtered off and the filtrate concentrated under reduced pressure to a gold gel. The crude was dissolved in 4% MeOH/ DCM and purified by column chromatography in the same solvent system to afford 0.14 g of a white solid (40% yield). R_f = 0.67 in solvent system (I); MS (ESI) 1084 $[M+H]^+$, 1106 $[M+Na]^+$.

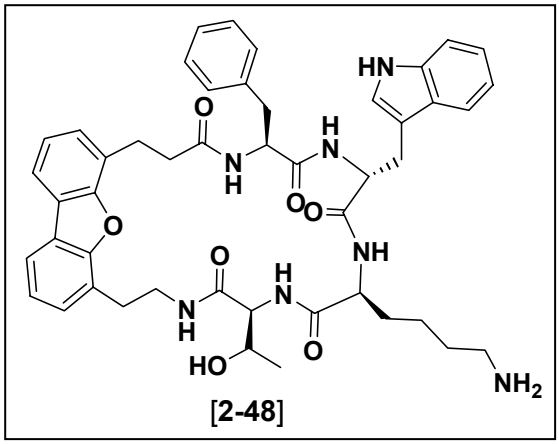

[**2-48**]

c[6-((2-Carbonylethyl)-Phe-D-Trp-Lys-Thr-4-(2-aminoethyl))-dibenzofuran] [2-48]: c[6-((2-Carbonylethyl)-Phe-D-Trp(Boc)-Lys(Boc)-Thr(*t*-But)-4-(2-aminoethyl))-dibenzofuran] (0.140 g, 0.13 mmol) was mixed with anisole (4 ml), followed by addition of anhydrous TFA (20 ml). The solution was stirred for 1 h. It was then concentrated under reduced pressure to a gel. The crude material was evaporated from toluene three times to remove residual TFA. The resulting gel was then precipitated with diethylether which provided a pale gold solid (0.1254 g). The crude material was dissolved in 55A:45B (80 ml, The compound had to be dissolved in B first because it would not dissolve in A.) and purified via preparative RP-HPLC using an isocratic solution of 55A:45B. Four injections of 20 ml of solution were made. The product eluted at about 27 min. The purest fractions of each injection were pooled, frozen, and lyophilized. A fluffy white solid was obtained (0.048 g, 44% yield). Analytical RP-HPLC: 70A:30B → 10A:90B / 30 min. r_t = 18.49 min, as a single peak; isocratic 57A:43B / 30 min. r_t = 20.77 min, as a single peak. ^{1}H NMR (400 MHz, CD_3OD) δ 7.88 (m, 2 H, DBF H1, H9), 7.44 (d, 1 H, *J* = 8.0 Hz, indole

H4), 7.26 – 6.96 (m, 13 H, arom), 4.65 (q, 1 H, *J* = 5.2, 3.6 Hz, Phe α-H), 4.54 (m, 1 H, D-Trp α-H), 4.14 (q, 1 H, *J* = 5.2, 5.6 Hz, Lys α-H), 4.04 (dd, 1 H, *J* = 10.8, 3.2, Thr α-H), 3.72 (m, 1 H, Thr β-H), 3.91-2.4 (many overlapping m, 14 H, Phe β-CH_2, D-Trp β-CH_2, 4 arm CH_2, Lys ε-CH_2), 1.70 (m, 2 H, Lys β-CH_2), 1.25 (m, 2 H, Lys δ-CH_2), 1.11 (m, 2 H, Lys γ-CH_2), 0.54 (d, 3 H, *J* = 6.4 Hz, Thr CH_3); MS (ESI) 828 $[M+H]^+$, 850 $[M+Na]^+$; HRMS (TOF MS ES) (*m/z*): $[M+H]^+$ calcd for $C_{47}H_{54}N_7O_7$ 828.4085 found 828.4081.

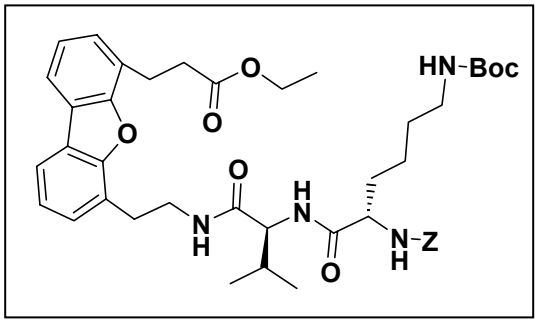

6-(2-Ethoxycarbonylethyl)-4-(Z-Lys(Boc)-Val-(2-aminoethyl))-dibenzofuran:

Z-Lys(Boc)-Val-OH [**2-63**] (0.48 g, 1.0 mmol) and DEPBT (0.30 g, 1.0 mmol) were dissolved in DCM (9 ml). TEA (0.23 ml, 1.66 mmol) was added and the reaction stirred for 10 min. 4-(2-Aminoethyl)-6-(2-ethoxycarbonylethyl)-dibenzofuran [**2-58**] (0.26 g, 0.83 mmol) was dissolved in DCM (9 ml) and added to the reaction. It was left to stir over night. The reaction was then concentrated under reduced pressure and the residue dissolved in EtOAc (100 ml). It was then washed with 1N HCl (3 x 50 ml), conc. $NaHCO_3$ (3 x 50 ml), brine (1 x 50 ml), and dried over $MgSO_4$. The drying

agent was filtered off and the filtrate concentrated under reduced pressure to a gold foam. The crude material was dissolved onto silica gel using DCM and purified by column chromatography in 2:1 EtOAc:hex to afford a white solid (0.37 g, 60% yield). R_f = 0.30 in solvent system (G), R_f = 0.55 in solvent system (I); ^{1}H NMR (400 MHz, $CDCl_3$) δ 7.78 (m, 2 H, DBF H1, H9), 7.30 (m, 9 H, arom Z, DBF H2, H3, H8, H7), 6.48, 6.39, 5.68, 4.69 (bs, 4 H, NHs), 5.06 (m, 2 H, Z CH_2), 4.12 (m, 4 H, α-Hs, OCH_2), 3.71 (m, 2 H, β-CH_2 amine arm), 3.33 (t, 2 H, β-CH_2 ester arm), 3.25 (m, α-CH_2 amine arm), 3.06 (bm, 2 H, Lys ε-CH_2), 2.81 (t, 2 H, α-CH_2 ester arm), 1.85, 1.69 (bm, 2 H, Lys β-CH_2), 1.68 (m, 1 H, Val β-H), 1.42 (m, 13 H, Lys γ-CH_2, Lys δ-CH_2, Boc), 1.21 (t, 3 H, ester CH_3), 0.80, 0.73 (dd, 6 H, Val CH_3).

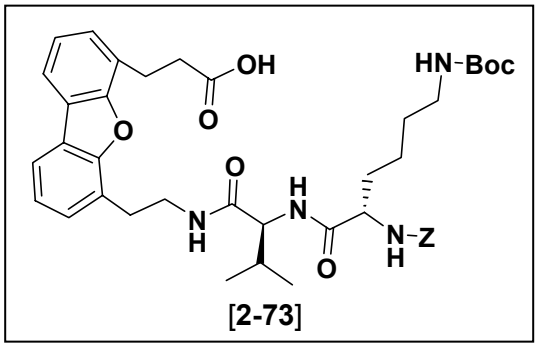

[2-73]

6-(2-Carboxyethyl)-4-(Z-Lys(Boc)-Val-(2-aminoethyl))-dibenzofuran [2-73]:

6-(2-Ethoxycarbonylethyl)-4-(Z-Lys(Boc)-Val-(2-aminoethyl))-dibenzofuran (0.37 g, 0.48 mmol) was dissolved in a mixture of MeOH (10 ml) and THF (2 ml). Separately, $LiOH \cdot H_2O$ (0.09 g, 1.92 mmol) was dissolved in H_2O (6 ml), and then added to the reaction. It was left to stir for 3 h. The organic solvents were then removed under

reduced pressure and the remaining aqueous solution acidified to pH = 2 with 1N HCl. It was then extracted with EtOAc (5 x 20 ml) and dried over $MgSO_4$. The drying agent was filtered off and the filtrate concentrated to 0.36 g of a beige solid in quantitative yield. R_f = 0.35 in solvent system (I); ^{1}H NMR (400 MHz, $CDCl_3$) δ 7.78 (m, 2 H, DBF H1, H9), 7.30 (m, 9 H, arom Z, DBF H2, H3, H8, H7), 7.04, 7.12, 5.61, 4.70 (bs, 4 H, NHs), 5.06 (m, 2 H, Z CH_2), 4.25, 4.13 (t, 2 H, α-Hs), 3.84 (t, 2 H, β-CH_2 acid arm), 3.60 (m, 2 H, β-CH_2 amine arm), 3.40 (t, 2 H, α-CH_2 acid arm), 3.25 (m, α-CH_2 amine arm), 3.06 (bm, 2 H, Lys ε-CH_2), 2.91 (dbm, 2 H, Lys β-CH_2), 1.68 (m, 1 H, Val β-H), 1.42 (m, 13 H, Lys γ-CH_2, Lys δ-CH_2, Boc), 0.50, 0.21 (dd, 6 H, Val CH_3).

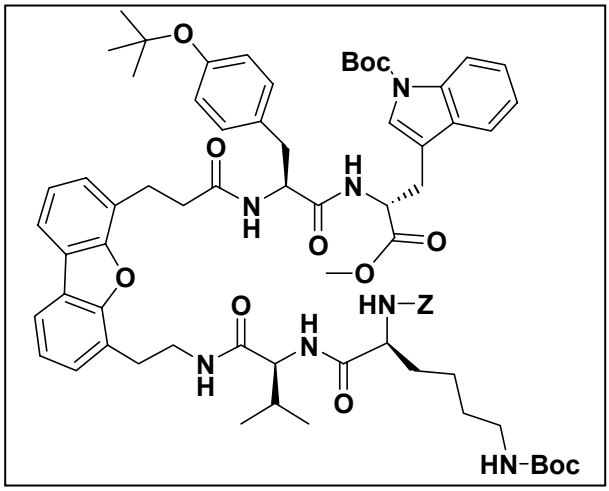

6-((2-Carbonylethyl)-Tyr(*t*-But)-D-Trp(Boc)-OMe)-4-(Z-Lys(Boc)-Val-(2-aminoethyl))-dibenzofuran: H-Tyr(*t*-But)-D-Trp(Boc)-OMe [**2-70**] (0.31 g, 0.58 mmol) and DEPBT (0.17 g, 0.58 mmol) were dissolved in DCM (10 ml). TEA (0.20 ml, 1.44 mmol) was added and stirred for 10 min. 6-(2-Carboxyethyl)-4-(Z-Lys(Boc)-Val-(2-aminoethyl))-dibenzofuran [**2-73**] (0.36 g, 0.48 mmol) was dissolved in DCM

(10 ml) and added to the reaction. It was left to stir over night. The reaction was then concentrated under reduced pressure and the residue dissolved in EtOAc (50 ml). It was washed with 1N HCl (3 x 20 ml), conc. $NaHCO_3$ (3 x 20 ml), brine (1 x 20 ml), and dried over $MgSO_4$. The drying agent was filtered off and the filtrate concentrated under reduced pressure to a white solid. The crude material was then dissolved onto silica gel using DCM and purified by column chromatography in 2:1 EtOAc:hex to afford a white solid (0.21 g, 58% yield). R_f = 0.60 in solvent system (I); ^{1}H NMR (400 MHz, $CDCl_3$) δ complicated, but can see new dipeptide signals; MS (ESI) 1264 $[M+H]^+$, 1286 $[M+Na]^+$.

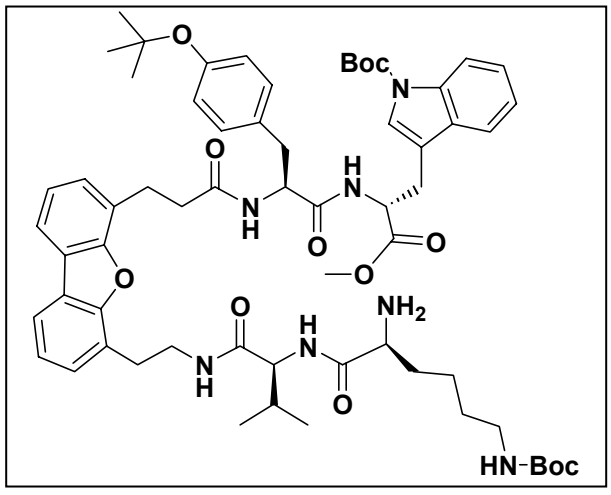

6-((2-Carbonylethyl)-Tyr(*t*-But)-D-Trp(Boc)-OMe)-4-(H-Lys(Boc)-Val-(2-aminoethyl))-dibenzofuran: 6-((2-Carbonylethyl)-Tyr(*t*-But)-D-Trp(Boc)-OMe)-4-(Z-Lys(Boc)-Val-(2-aminoethyl))-dibenzofuran (0.21 g, 0.17 mmol) was dissolved in a mixture of MeOH (15 ml) and THF (7 ml). 10% Pd/C (0.03 g) was then added and the reaction placed under H_2 atmosphere to stir over night. The reaction was filtered to

remove the catalyst. The filtrate was concentrated under reduced pressure to afford a white solid (0.19 g, quantitative yield). R_f = 0.34 in solvent system (I); ^{1}H NMR (400 MHz, $CDCl_3$) δ complicated, but Z group is gone; MS (ESI) 1130 $[M+H]^+$, 1152 $[M+Na]^+$.

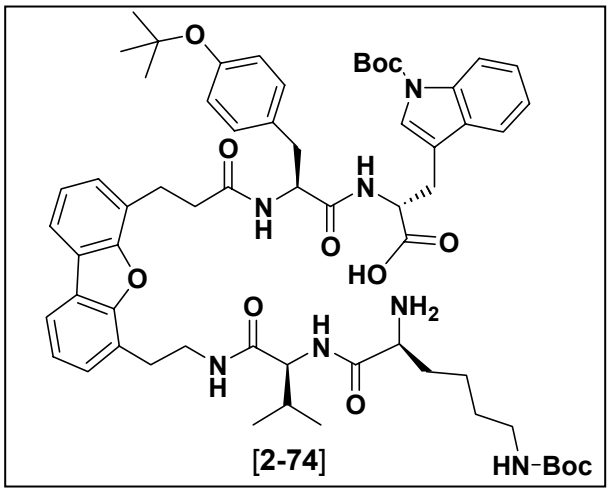

6-((2-Carbonylethyl)-Tyr(*t*-But)-D-Trp(Boc)-OH)-4-(H-Lys(Boc)-Val-(2-aminoethyl))-dibenzofuran [2-74]: 6-((2-Carbonylethyl)-Tyr(*t*-But)-D-Trp(Boc)-OMe)-4-(H-Lys(Boc)-Val-(2-aminoethyl))-dibenzofuran (0.19 g, 0.17 mmol) was dissolved in MeOH (20 ml). Separately, LiOH · H_2O (0.03 g, 0.68 mmol) was dissolved in H_2O (12 ml), and then added to the reaction. It was left to stir for 3 h. The organic solvents were then removed under reduced pressure and the remaining aqueous solution acidified to pH = 2 with 1N HCl. It was then extracted with EtOAc (5 x 15 ml) and dried over $MgSO_4$. The drying agent was filtered off and the filtrate and concentrated to 0.19 g of a white solid in quantitative yield. R_f = 0.02 in solvent

system (I); ^{1}H NMR (400 MHz, $CDCl_3$) δ complicated, but OME is gone; MS (ESI) 1116 $[M+H]^+$, 1138 $[M+Na]^+$.

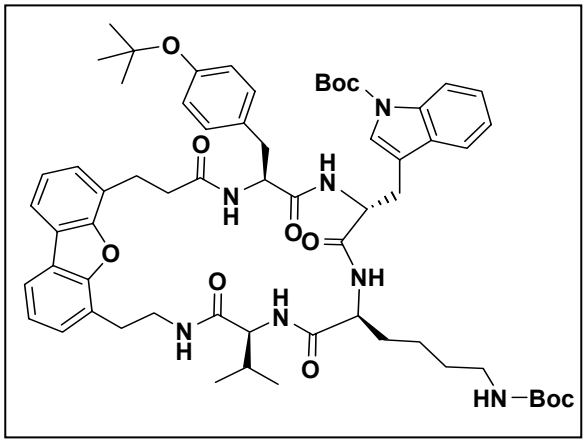

c[6-((2-Carbonylethyl)-Tyr(*t*-But)-D-Trp(Boc)-Lys(Boc)-Val-4-(2-aminoethyl))-dibenzofuran]: 6-((2-Carbonylethyl)-Tyr(*t*-But)-D-Trp(Boc)-OH)-4-(H-Lys(Boc)-Val-(2-aminoethyl))-dibenzofuran [**2-74**] (0.19 g, 0.17 mmol) was dissolved in distilled DCM (165 ml). DEPBT (0.15 g, 0.51 mmol) and TEA (0.09 ml, 0.68 mmol) were added and the colorless reaction left to stir under Ar for 2 days. It became yellow in color. The reaction was concentrated under reduced pressure and the residue dissolved in EtOAc (50 ml). It was washed with 1N HCl (3 x 15 ml), conc. $NaHCO_3$ (3 x 15 ml), brine (1 x 25 ml), and dried over $MgSO_4$. The drying agent was filtered off and the filtrate concentrated under reduced pressure to a gold gel. The crude material was dissolved in 2% MeOH/ DCM and purified by column chromatography in the same solvent system to afford 0.138 g of a white solid (73% yield). R_f = 0.63 in solvent system (I); MS (ESI) 1098 $[M+H]^+$, 1120$[M+Na]^+$.

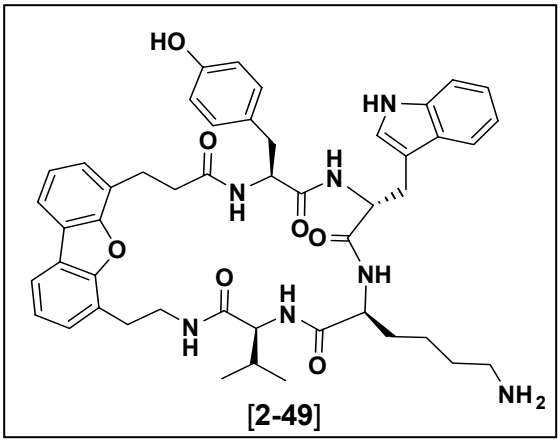

[**2-49**]

c[6-((2-Carbonylethyl)-Tyr-D-Trp-Lys-Val-4-(2-aminoethyl))-dibenzofuran] [2-49]: c[6-((2-Carbonylethyl)-Tyr(*t*-But)-D-Trp(Boc)-Lys(Boc)-Val-4-(2-aminoethyl))-dibenzofuran] (0.138 g, 0.13 mmol) was mixed with anisole (4 ml), followed by addition of anhydrous TFA (20 ml). The solution was stirred for 1 h. It was then concentrated under reduced pressure to a gel. The crude material was evaporated from toluene three times to remove residual TFA. The resulting gel was then precipitated with diethylether which provided a beige solid (0.1196 g). The crude material was dissolved in 58A:42B (80 ml, The compound had to be dissolved in B first because it would not dissolve in A.) and purified via preparative RP-HPLC using an isocratic solution of 58A:42B. Four injections of 20 ml of solution were made. The product eluted at about 17 min. The purest fractions of each injection were pooled, frozen, and lyophilized. A fluffy white solid was obtained (0.051 g, 47 % yield). Analytical RP-HPLC: 70A:30B → 10A:90B / 30 min. r_t = 18.47 min, as a single peak; isocratic 57A:43B / 30 min. r_t = 17.48 min, as a single peak. ^{1}H NMR (400 MHz, CD_3OD) δ 7.86 (m, 2 H, DBF H1, H9), 7.46 (d, 1 H, *J* = 8.0 Hz, indole H4), 7.26 –

7.00 (m, 8 H, arom D-Trp, DBF), 6.81, 6.59 (d, 4 H, J = 8.4, 8.4 Hz, Try arom), 4.59 (m, 2 H, Phe α-H, D-Trp α-H), 4.16 (m, 1 H, Lys α-H), 3.94 (m, 1 H, Val α-H), 3.40-2.20 (many overlapping m, 16 H, Tyr β-CH_2, D-Trp β-CH_2, 4 arm CH_2, Lys ε-CH_2, Val β-H), 1.90, 1.73 (m, 2 H, Lys β-CH_2), 1.21 (m, 4 H, Lys δ-CH_2, Lys γ-CH_2), 0.72, 0.33 (d, 6 H, J = 6.4, 6.4 Hz, Val CH_3); MS (ESI) 842 $[M+H]^+$, 864 $[M+Na]^+$; HRMS (TOF MS ES) (*m/z*): $[M+H]^+$ calcd for $C_{48}H_{56}N_7O_7$ 842.4241 found 828.4224.

2.6 References

1. Brazeau, P.; Vale, W.; Burgus, R.; Ling, N.; Butcher, M.; Rivier, J.; Guillemin, R. *Science*, **1973**, *179*, 77-79.

2. Reisine, T. *Am. J. Physiol. (Gastrointest. Liver Physiol.)*, **1995**, *269*, G813-G820.

3. Pradayrol, L.; Joernvall, H.; Mutt, V.; Ribert, A. *FEBS Lett.*, **1980**, *109*, 55-58.

4. Benoit, R.; Esch, F.; Bennett, H. P. J. *Metabolism*, **1990**, *39 (Suppl. 2)*, 22-25.

5. Bersani, M.; Thim, L.; Baldissera, F. G. A.; Holst, J. J. *J. Biol. Chem.*, **1989**, *264*, 10633-10636.

6. Sevarino, K.; Felix, R.; Banks, C.; Low, M.; Montminy, M.; Mandel, G.; Goodman, R. *J. Biol. Chem.*, **1987**, *262*, 4987-4993.

7. Veber, D. F. In *Peptides: Chemistry, Structure, and Biology. Proceedings of the 12th American Peptide Symposium*; Smith, J. A., Rivier, J. E., Eds.; ESCOM: Leiden: 1992, p 3-14.

8. Veber, D. F. In *Peptides: Synthesis, Structure, and Function. Proceedings of the 7th American Peptide Symposium*; Rich, D. H., Gross, V. J., Eds.; Pierce Chemical, Co.: Rockford, IL: 1981, p 685-694.

9. Weil, C.; Muller, E. E.; Thorner, M. O. *Somatostatin*; Springer-Verlag Berlin: Heidelberg, 1992.

10. Reichlin, S. *N. Engl. J. Med.*, **1983**, *309*, 1495-1501.

11. Reichlin, S. *N. Engl. J. Med.*, **1983**, *309*, 1556-1563.

12. Epelbaum, J. *Prog. Neurobiol.*, **1986**, *27*, 63-100.

13. Schettini, G. *Pharmacol. Res.*, **1991**, *23*, 203-215.

14. Mandarino, L.; Stenner, D.; Blanchard, W.; Nissen, S.; Gerich, J.; Ling, N.; Brazeau, P.; Bohlen, P.; Esch, F.; Guillemin, R. *Nature*, **1981**, *291*, 76-77.

15. Bloom, S. R.; Mortimer, C. H.; Thorner, M. O.; Besser, G. M.; Hall, R.; Gomez-Pan, A.; Roy, V. M.; Russell, R. C.; Coy, D. H.; Kastin, A. J.; Schally, A. V. *Lancet*, **1974**, *2*, 1106-1109.

16. Da Cunha, A.; Reusch, D. M.; Leiden, L. E. *Proc. Natl. Acad. Sci. USA*, **1995**, *92*, 1371-1375.

17. Lamberts, S. W. J.; Van Der Ley, A. J.; de Herder, W. W.; Hofland, L. J. *Metab. Clin. Exp.*, **1996**, *45*, 104-106.

18. Robbins, R. J. *Metab. Clin. Exp.*, **1996**, *45*, 98-100.

19. Vale, W.; Brazeau, P.; Rivier, C.; Brown, M.; Boss, B.; Rivier, J.; Burgus, R.; Ling, N.; Guillemin, R. *Recent Progr. Horm. Res.*, **1975**, *31*, 365-397.

20. Rivier, J.; Brown, M.; Vale, W. *Biochem. Biophys. Res. Commun.*, **1975**, *65*, 746-751.

21. Brown, M.; Rivier, J.; Vale, W. *Metab. Clin. Exp.*, **1976**, *25*, 1501-1503.

22. Veber, D. F.; Holly, F. W.; Nutt, R. F.; Bergstrand, S. J.; Brady, S. F.; Hirschmann, R.; Glitzer, M. S.; Saperstein, R. *Nature*, **1979**, *280*, 512-514.

23. Reubi, J. C. *Neurosci. Lett.*, **1984**, *49*, 259-263.

24. Srikant, C. B.; Patel, Y. C. In *Proceedings of the International Conference on Somatostatin.*; Reichlin, S., Ed. Plenum, NY, 1987, p 89-102.

25. Patel, Y. C.; Murthy, K. K.; Escher, E.; Banville, D.; Spleiss, J.; Srikant, C. B. *Metabolism (suppl. 2)*, **1990**, *39*, 63-69.

26. Tran, V. T.; Beal, M. F.; Martin, J. B. *Science*, **1985**, *228*, 492-495.

27. Reubi, J. C.; Maurer, R. *Regul. Pept.*, **1986**, *14*, 301-311.

28. Hoyer, D.; Lubbert, H.; Bruns, C. *Naunyn-Schmiedebergs Archives of Pharmacology*, **1994**, *350*, 441-453.

29. Patel, Y. C.; Greenwood, M. T.; Warszynska, A.; Panetta, R.; Srikant, C. B. *Biochem. Biophys. Res. Commun.*, **1994**, *198*, 605-612.

30. Jakobs, K.; Aktories, K.; Schultz, G. *Nature*, **1983**, *303*, 17885-17897.

31. Law, S. F.; Manning, D.; Reisine, T. *J. Biol. Chem.*, **1991**, *266*, 17885-17897.

32. Koch, B.; Schonbrunn, A. *Endocrinology*, **1984**, *114*, 1784-1790.

33. Palczewski, K.; Kumasaka, T.; Hori, T.; Behnke, C. A.; Motoshima, H.; Fox, B. A.; Le Trong, I.; Teller, D. C.; Okada, T.; Stenkamp, R. E.; Yamamoto, M.; Miyano, M. *Science*, **2000**, *289*, 739-745.

34. Baldwin, J. M. *Curr. Opin. Cell Biol.*, **1994**, *6*, 180-190.

35. Reisine, T.; Bell, G. I. *Endocr. Rev.*, **1995**, *16*, 427-442.

36. Kluxen, F.-W.; Bruns, C.; Lubbert, H. *Proc. Natl. Acad. Sci. USA*, **1992**, *89*, 4618-4622.

37. O'Dowd, B. F.; Hnatowich, M.; Caron, M. G.; Lefkowitz, R. J.; Bouvier, M. *J. Biol. Chem.*, **1989**, *264*, 7564-7569.

38. Yamada, Y.; Post, S. R.; Wang, K.; Tager, H. S.; Bell, G. I.; Seiono, S. *Proc. Natl. Acad. Sci. USA*, **1992**, *89*, 251-255.

39. Raynor, K.; O'Caroll, A. M.; Kong, H.; Yasuda, K.; Mahan, L. C.; Bell, G. I.; Reisine, T. *Mol. Pharmacol.*, **1993**, *44*, 385-392.

40. Corness, J. D.; Demchyshyn, L. L.; Seeman, P.; Vantol, H. H. M.; Srikant, C. B.; Kent, G.; Patel, Y. C.; Niznik, H. B. *FEBS Lett.*, **1993**, *321*, 279-284.

41. O'Caroll, A. M.; Raynor, K.; Lolait, S. J.; Reisine, T. *Mol. Pharmacol.*, **1994**, *46*, 291-298.

42. Srikant, C. B.; Patel, Y. C. *Endocrinology*, **1982**, *110*, 2138-2144.

43. Meyerhof, W.; Paust, H. J.; Schoenrock, C.; Richter, D. *DNA Cell Biol.*, **1991**, *10*, 689-694.

44. Bruno, J. F.; Xu, Y.; Song, J.; Berelowitz, M. *Proc. Natl. Acad. Sci. USA*, **1992**, *89*, 11151-11155.

45. O'Caroll, A. M.; Lolait, S. J.; Konig, M.; Mahan, L. C. *Mol. Pharmacol.*, **1992**, *42*, 939-946.

46. Yasuda, K.; Rens-Domiano, S.; Breder, C. D.; Law, S. F.; Saper, C. B.; Reisine, T.; Bell, G. I. *J. Biol. Chem.*, **1992**, *267*, 20422-20428.

47. Schwabe, W.; Brennan, M. B.; Hochgeschwender, U. *Gene*, **1996**, *168*, 233-235.

48. Patel, Y. C.; Greenwood, M. T.; Panetta, R.; Demchyshyn, L. L.; Niznik, H. B.; Srikant, C. B. *Life Sci.*, **1995**, *57*, 1249-1265.

49. Reisine, T.; Kong, H.; Raynor, K.; Yano, H.; Takeda, J.; Yasuda, K.; Bell, G. I. *Mol. Pharmacol.*, **1994**, *44*, 1008-1015.

50. Wilkinson, G. F.; Feniuk, W.; Humphrey, P. P. A. *British J. Pharmacol.*, **1997**, *121*, 91-96.

51. Carruthers, A. M.; Warner, A. J.; Michel, A. D.; Feniuk, W.; Humphrey, P. P. A. *British J. Pharmacol.*, **1999**, *126*, 1221-1229.

52. Siehler, S.; Seuwen, K.; Hoyer, D. *Naunyn-Schmiedebergs Archives of Pharmacology*, **1999**, *360*, 488-499.

53. Castro, S. W.; Buell, G.; Feniuk, W.; Humphrey, P. P. A. *British J. Pharmacol.*, **1996**, *117*, 639-646.

54. Bruns, C.; Raulf, F.; Hoyer, D.; Schloos, J.; Lubbert, H.; Weckbecker, G. *Metab. Clin. Exp.*, **1996**, *45*, 17-20.

55. Rossowski, W. J.; Coy, D. H. *Biochem. Biophys. Res. Commun.*, **1994**, *205*, 341-346.

56. Rossowski, W. J.; Gu, Z. F.; Akarca, U. S.; Jensen, R. T.; Coy, D. H. *Peptides*, **1994**, *15*, 1421-1424.

57. Buchan, A. M. J.; Lin, C. Y.; Choi, J.; Barber, D. L. *J. Biol. Chem.*, **2002**, *277*, 28431-28438.

58. Raynor, K.; Murphy, W. A.; Coy, D. H.; Taylor, J. E.; Moreau, J. P.; Yasuda, K.; Bell, G. I.; Reisine, T. *Mol. Pharmacol.*, **1993**, *43*, 838-844.

59. Rohrer, S. P.; Schaeffer, J. M. *J. Physiol.*, **2000**, *94*, 211-215.

60. Lloyd, K. C.; Amirmozzami, S.; Friedik, F.; Chew, P.; Walsh, J. H. *Am. J. Physiol. (Gastrointest. Liver Physiol.)*, **1997**, *272*, G1481-G1488.

61. Sharma, K.; Patel, Y. C.; Srikant, C. B. *Mol. Endocrin.*, **1996**, *10*, 1688-1696.

62. Gu, Z. F.; Corleto, V. D.; Mantey, S. A.; Coy, D. H.; Maton, P. N.; Jensen, R. T. *Am. J. Physiol. (Gastrointest. Liver Physiol.)*, **1995**, *268*, G739-G748.

63. Mori, M.; Aihara, M.; Shimizu, T. *Neuroscience Lett.*, **1997**, *223*, 185-188.

64. Coy, D. H.; Taylor, J. E. *Metab. Clin. Exp.*, **1996**, *45*, 21-23.

65. Raynor, K.; Reisine, T. *Neurobiol.*, **1992**, *16*, 273-289.

66. Florio, T.; Schettini, G. *J. Mol. Endocrin.*, **1996**, *17*, 89-100.

67. Patel, Y. C.; Srikant, C. B. *Trends Endocrin. Metab.*, **1997**, *8*, 398-405.

68. Janecka, A.; Zubrycka, M.; Janecki, T. *J. Peptide Res.*, **2001**, *58*, 91-107.

69. Vale, W.; Rivier, J.; Ling, N.; Brown, M. *Metabolism*, **1978**, *27*, 1391-1401.

70. Nutt, R. F.; Veber, D. F.; Curley, P.; Saperstein, R.; Hirschmann, R. *Int. J. Pept. Protein Res.*, **1983**, *21*, 66-73.

71. Brown, M.; Rivier, J.; Vale, W. *Science*, **1977**, *196*, 1467-1469.

72. Guillemin, R.; Gerich, J. *Annu. Rev. Med.*, **1976**, *27*, 379-388.

73. Schally, A. V.; Coy, D. H.; Meyers, C. A. *Annu. Rev. Biochem.*, **1978**, *47*, 89-128.

74. Veber, D. F.; Friedinger, R. M.; Schwenk Perlow, D.; Paleveda, W. J.; Holly, F. W.; Strachan, R. G.; Nutt, R. F.; Arison, B. H.; Homnick, C.; Randall, W. C.; Glitzer, M. S.; Saperstein, R.; Hirschmann, R. *Nature*, **1981**, *292*, 55-58.

75. Hutchinson, E. G.; Thornton, J. M. *Protein Sci.*, **1994**, *3*, 2207-2216.

76. Veber, D. F.; Saperstein, R.; Nutt, R. F.; Friedinger, R. M.; Brady, S. F.; Curley, P.; Perlow, D. S.; Paleveda, W. J.; Colton, C. D.; Zacchei, A. G.; Tocco, D. J.; Hoff, D. R.; Vandlen, R.; Gerich, J.; Hall, R.; Mandarino, L.; Cordes, E. H.; Anderson, P. S.; Hirschmann, R. *Life Sci.*, **1984**, *34*, 1371-1378.

77. Bauer, W.; Briner, U.; Doepfner, W.; Haller, R.; Huguenin, R.; Marbach, P.; Petcher, T. J.; Pless, J. *Life Sci.*, **1982**, *31*, 1133-1140.

78. Cai, R.-Z.; Szoke, B.; Lu, R.; Fu, D.; Redding, T. W.; Schally, A. V. *Proc. Natl. Acad. Sci. USA*, **1986**, *83*, 1896-1900.

79. Murphy, W. A.; Lance, V. A.; Moreau, J. P.; Coy, D. H. *Life Sci.*, **1987**, *40*, 2515-2522.

80. Taylor, J. E.; Bogden, A. E.; Moreau, J. P.; Coy, D. H. *Biochem. Biophys. Res. Commun.*, **1988**, *153*, 81-86.

81. Tran, T.-A.; Mattern, R.-H.; Afargan, M.; Amitay, O.; Ziv, O.; Morgan, B. A.; Taylor, J. E.; Hoyer, D.; Goodman, M. *J. Med. Chem.*, **1998**, *41*, 2679-2685.

82. Patel, Y. C.; Srikant, C. B. *Endocrinology*, **1994**, *135*, 2814-2817.

83. Rueter, J. K.; Mattern, R.-H.; Zhang, L.; Taylor, J. E.; Morgan, B. A.; Hoyer, D.; Goodman, M. *Biopolymers*, **2000**, *53*, 497-505.

84. Goodman, M.; Jiang, X.; Igarashi, J.; Li, H.; Tran, T.-A.; Mattern, R.-H. In *Peptide Science: Present and Future, Proceedings of the International Peptide Symposium*; Shimonishi, Y., Ed.; Kluwer: Dordrecht, Neth.: 1997, p 342-345.

85. Danoff, A.; Kleinberg, D. *Endocrine*, **2003**, *20*, 291-297.

86. Colao, A.; Filippella, M.; Di Somma, C.; Manzi, S.; Rota, F.; Pivonello, R.; Gaccione, M.; DeRosa, M.; Lombardi, G. *Endocrine*, **2003**, *20*, 279-283.

87. de Herder, W. W.; Lamberts, S. W. J. *Endocrine*, **2003**, *20*, 283-290.

88. Panel, A. T. C. D. *Am. J. Med.*, **1994**, *97*, 468-473.

89. Van Der Ley, A. J.; de Herder, W. W. *Endocrine*, **2003**, *20*, 307-311.

90. Schally, A. V.; Nagy, A. *Eur. J. Endocrinol.*, **1999**, *141*, 1-14.

91. Capello, A.; Krenning, E. P.; Breeman, W. A. P.; Bernard, B. F.; Konijnenberg, M. W.; de Jong, M. *Cancer. Biother. Radiopharm.*, **2003**, *18*, 761-768.

92. Marks, N.; Stern, F. *FEBS Lett.*, **1975**, *55*, 220-224.

93. Marks, N.; Stern, F.; Benuck, M. *Nature (London)*, **1976**, *261*, 511-512.

94. Pallai, P. V.; Struthers, R. S.; Goodman, M.; Moroder, L.; Wunsch, E.; Vale, W. *Biochemistry*, **1985**, *24*, 1933-1941.

95. Mierke, D. F.; Pattaroni, C.; Delaet, N.; Toy, A.; Goodman, M.; Tancredi, T.; Motta, A.; Temussi, P. A.; Moroder, L.; Bovermann, G.; Wunsch, E. *Int. J. Pept. Protein Res.*, **1990**, *36*, 418-432.

96. Huang, Z. W.; He, Y. B.; Raynor, K.; Tallent, M.; Reisine, T.; Goodman, M. *J. Am. Chem. Soc.*, **1992**, *114*, 9390-9401.

97. Moore, S. B.; Grant, M.; Rew, Y.; Bosa, E.; Fabbri, M.; Kumar, U.; Goodman, M. *J. Peptide Res.*, **2005**, *66*, 404-422.

98. He, Y. B.; Huang, Z. W.; Raynor, K.; Reisine, T.; Goodman, M. *J. Am. Chem. Soc.*, **1993**, *115*, 8066-8072.

99. Melacini, G.; Zhu, Q.; Osapay, G.; Goodman, M. *J. Med. Chem*, **1997**, *40*, 2252-2258.

100. Osapay, G.; Prokai, L.; Kim, H. S.; Medzihradszky, K. F.; Coy, D. H.; Liapakis, G.; Reisine, T.; Melacini, G.; Zhu, Q.; Wang, S. H. H.; Mattern, R.-H.; Goodman, M. *J. Med. Chem.*, **1997**, *40*, 2241-2251.

101. Miller, S. M.; Sinar, R. J.; Ng, S.; Zuckermann, R. N.; Kern, J.; Moos, W. H. *Drug Dev. Res.*, **1995**, *35*, 20-32.

102. Simon, R. J.; Kania, R. S.; Zuckermann, R. N.; Heubner, V. D.; Jewell, D. A.; Banville, S.; Ng, S.; Wang, L.; Rosenberg, S.; Marlowe, C. K.; Spellmeyer, D. C.; Tan, R. Y.; Frankel, A. D.; Santi, D. V.; Cohen, F. E.; Bartlett, P. A. *Proc. Natl. Acad. Sci. USA*, **1992**, *89*, 9367-9371.

103. Mouna, A. M.; Nguyen, C.; Rage, I.; Xie, J.; Nee, G.; Mazaleyrat, J. P.; Wakselman, M. *Synth. Commun.*, **1994**, *24*, 2429-2435.

104. Mattern, R.-H.; Tran, T.-A.; Goodman, M. *J. Med. Chem.*, **1998**, *41*, 2686-2692.

105. Tran, T.-A.; Mattern, R.-H.; Morgan, B. A.; Taylor, J. E.; Goodman, M. *J. Peptide Res.*, **1999**, *53*, 134-145.

106. Bruns, C.; Lewis, I.; Briner, U.; Meno-Tetang, G.; Weckbecker, G. *Eur. J. Endocrinol.*, **2002**, *146*, 707-716.

107. Hirschmann, R.; Nicolaou, K. C.; Pietranico, S.; Salvino, J.; Leahy, E. M.; Sprengeler, P. A.; Furst, G.; Smith III, A. B.; Strader, C. D.; Cascieri, M. A.; Candelore, M. R.; Donaldson, C.; Vale, W.; Maechler, L. *J. Am. Chem. Soc.*, **1992**, *114*, 9217-9218.

108. Hirschmann, R.; Nicolaou, K. C.; Pietranico, S.; Leahy, E. M.; Salvino, J.; Arison, B. H.; Cichy, M. A.; Spoors, P. G.; Shakespeare, W. C.; Sprengeler, P. A.; Hamley, P.; Smith III, A. B.; Reisine, T.; Raynor, K.; Maechler, L.; Donaldson, C.; Vale, W.; Freidinger, R. M.; Cascieri, M. A.; Strader, C. D. *J. Am. Chem. Soc.*, **1993**, *115*, 12550-12568.

109. Papageorgiou, C.; Haltiner, R.; Bruns, C.; Petcher, T. J. *Bioorg. Med. Chem. Lett.*, **1992**, *2*, 135-140.

110. Papageorgiou, C.; Borer, X. *Bioorg. Med. Chem. Lett.*, **1996**, *6*, 267-272.

111. Damour, D.; Barreau, M.; Blanchard, J.-C.; Burgevin, M. C.; Doble, A.; Herman, F.; Pantel, G.; James-Surcouf, E.; Vuilhorgne, M.; Mignani, S.; Poitout, L.; Le Merrer, Y.; Depezay, J.-C. *Bioorg. Med. Chem. Lett.*, **1996**, *6*, 1667-1672.

112. Souers, A. J.; Rosenquist, A.; Jarvie, E. M.; Ladlow, M.; Feniuk, W.; Ellman, J. A. *Bioorg. Med. Chem. Lett.*, **2000**, *10*, 2731-2733.

113. Liu, S.; Tang, C.; Ho, B.; Ankersen, M.; Stidsen, C. E.; Crider, A. M. *J. Med. Chem.*, **1998**, *41*, 4693-4705.

114. Ankersen, M.; Crider, A. M.; Liu, S.; Ho, B.; Andersen, H. S.; Stidsen, C. E. *J. Am. Chem. Soc.*, **1998**, *120*.

115. Poitout, L.; Roubert, P.; Contour-Galera, M. O.; Moinet, C.; Lannoy, J.; Pommier, J.; Plas, P.; Bigg, D.; Thurieau, C. *J. Med. Chem*, **2001**, *44*, 2990-3000.

116. Berk, S. C.; Rohrer, S. P.; Degrado, S. J.; Birzin, E. T.; Mosley, R. T.; Hutchins, S. M.; Pasternak, A.; Schaeffer, J. M.; Underwood, D. J.; Chapman, K. T. *J. Comb. Chem.*, **1999**, *1*, 388-396.

117. Parmar, R. M.; Chan, W. W.-S.; Dashkevicz, M.; Hayes, S. P.; Rohrer, S. P.; Smith, R. G.; Schaeffer, J. M.; Blake, A. D. *Biochem. Biophys. Res. Commun.*, **1999**, *263*, 276-280.

118. Veber, D. F. In *Peptides: Prodeedings of the 6th American Peptide Symposium*; Gross, E., Meienhofer, J., Eds.; Pierce Chemical Co.: Rockford, IL: 1979, p 409-419.

119. Veber, D. F.; Holly, F. W.; Paleveda, W. J.; Nutt, R. F.; Bergstrand, S. J.; Torchiana, M.; Glitzer, M. S.; Saperstein, R.; Hirschmann, R. *Proc. Natl. Acad. Sci. USA*, **1978**, *75*, 2636-2640.

120. Jiang, S.; Gazal, S.; Gelerman, G.; Ziv, O.; Karpov, O.; Litman, P.; Bracha, M.; Afargan, M.; Gilon, C.; Goodman, M. *J. Peptide Sci.*, **2001**, *7*, 521-528.

121. Pohl, E.; Heine, A.; Sheldrick, G. *Acta. Cryst.*, **1995**, *D51*, 48-59.

122. Kessler, H.; Bernd, M.; Kogler, H.; Zarbock, J.; Sorenson, O. W.; Bodenhausen, G.; Ernst, R. R. *J. Am. Chem. Soc.*, **1983**, *105*, 6944-6952.

123. Elseviers, M.; Jaspers, H.; Delaet, N.; DeVadder, S.; Pepermans, H.; Tourwe, D.; Van Binst, G. In *Peptides, Chemistry, Structure, and Biology. Proceedings of the 11th American Peptide Symposium*; Rivier, J. E., Marshall, G. R., Eds.; ESCOM: Leiden: 1989, p 198-200.

124. MacDonald, M.; Aube, J. *Curr. Org. Chem.*, **2001**, *5*, 417-438.

125. Feigel, M. *J. Am. Chem. Soc.*, **1986**, *108*, 181-182.

126. Boger, D. L.; Meyers, J., J. B. *J. Org. Chem.*, **1991**, *56*, 5385-5390.

127. Sarabu, R.; Lovey, K.; Madison, V. S.; Fry, D. C.; Greeley, D. N.; Cook, C. M.; Olson, G. L. *Tetrahedron*, **1993**, *49*, 3629-3640.

128. Brandmeier, V.; Feigel, M. *Tetrahedron*, **1989**, *45*, 1365-1376.

129. Jackson, S.; DeGrado, W. F.; Dwivedi, A.; Parthasasthy, A.; Higley, A.; Krywko, J.; Rockwell, A.; Markwalder, J.; Wells, G.; Wexler, R.; Mousa, S. A.; Harlow, R. *J. Am. Chem. Soc.*, **1994**, *116*, 3220-3230.

130. Ernest, I.; Kalvoda, J.; Rihs, G.; Mutter, M. *Tetrahedron Lett.*, **1990**, *31*, 4011-4014.

131. Tran, T.-A.; Mattern, R.-H.; Zhu, Q.; Goodman, M. *Bioorg. Med. Chem. Lett.*, **1997**, *7*, 997-1002.

132. Suich, D. J.; Mousa, S. A.; Singh, G.; Liapakis, G.; Reisine, T.; DeGrado, W. F. *Bioorg. Med. Chem.*, **2000**, *8*, 2229-2241.

133. Cheng, R. P.; Suich, D. J.; Cheng, H.; Roder, H.; DeGrado, W. F. *J. Am. Chem. Soc.*, **2001**, *123*, 12710-12711.

134. Graf von Roedern, E.; Lohof, E.; Hessler, G.; Hoffmann, M.; Kessler, H. *J. Am. Chem. Soc.*, **1996**, *118*, 10156-10167.

135. Gruner, S. A. W.; Keri, G.; Schwab, R.; Venetianer, A.; Kessler, H. *Org. Lett.*, **2001**, *3*, 3723-3725.

136. Diaz, H.; Kelly, J. W. *Tetrahedron Lett.*, **1991**, *32*, 5725-5728.

137. Kelly, J. W.; PCT/US97/09512., WO 9746547: USA, 1997.

138. Tsang, K. Y.; Diaz, H.; Graciani, N.; Kelly, J. W. *J. Am. Chem. Soc.*, **1994**, *116*, 3988-4005.

139. Melacini, G.; Zhu, Q.; Goodman, M. *Biochemistry*, **1997**, *36*, 1233-1241.

140. Kumar, U., personal communication.

CHAPTER 3

3. NONNATURALLY OCCURRING, NITROGEN-CONTAINING, FUSED 5,6-HETEROCYCLIC, AROMATIC ALPHA AMINO ACIDS

3.1 Introduction

3.1.1 The use of nonnatural amino acids in peptides

Nonnaturally occurring α-amino acids have become important tools in the synthesis of biologically active peptides, peptidomimetics, and small molecule analogs. Synthetic building blocks can be particularly useful as conformational probes. Their inclusion can provide insight into the bioactive conformations of parent peptides as well as the topological and chemical requirements of the recognition sites of cell-surface receptors. Furthermore, the inclusion of unnatural residues can protect the entire ligand from enzymatic degradation and aids in identifying the required pharmacophoric groups for the development of potent and receptor subtype-specific ligands. The Goodman laboratory has synthesized numerous nonnatural amino acids and incorporated them into ligands for somatostatin, opioid, and integrin receptors.

The importance of tryptophan for the biological function of many peptides is well recognized. Specifically, tryptophan in position 8 of somatostatin has been shown to be a major contributor to both receptor binding and the biological activity elicited by somatostatin. The incorporation of side chain-modified tryptophan residues into somatostatin analogs could provide more detailed information about the requirements for receptor binding, subtype specificity, and potency. In keeping with our efforts to develop novel building blocks as well as biologically active somatostatin derivatives, we chose to examine the role of the indole ring of tryptophan by replacing it with a focused group of nitrogen-containing 5-6-fused ring aromatic heterocyclic amino acid residues. We envisioned incorporating these analogs into the D-Trp^{8} position of

c[Pro^6-Phe^7-D-Trp^8-Lys^9-Thr^{10}-Phe^{11}] or L-363,301 [**2-4**] (Chapter 2, Figure 2-5). These nonnatural analogs would incorporate small, subtle changes into a well characterized system, thus allowing us to examine and correlate even modest changes in biological activity and conformation.

3.1.2 Known modifications to the Trp^8 residue of somatostatin analogs

While somatostatin research has been conducted for 35 years, a limited amount has focused on the modification of the Trp^8 residue and the effects of those modifications on receptor binding and biological activity. The early structure-activity relationship (SAR) studies of somatostatin highlighted the importance of the Trp^8 residue for biological activity. Replacement of Trp^8 in somatostatin by L-alanine,[1,2] D-alanine,[3] and tyrosine,[4] resulted in the complete loss of inhibitory activity against growth hormone (GH), insulin and glucagon by each analog. The incorporation of D-Tyr^8 into SRIF-14 [**2-1**] resulted in a slight retention of inhibition of GH, insulin, glucagon release. It was originally believed that the indole of Trp^8 was simply involved in the buildup of the aromatic hydrophobic nucleus (along with residues Phe^6, Phe^7, and Phe^{11}). However, the low potency of the D-Tyr^8 analog highlights the unique properties of the indole ring, which seems to be recognized to some extent by somatostatin receptors.[5]

Early circular dichroic studies of somatostatin suggested the tetrapeptide pharmacophore, Phe^7-Trp^8-Lys^9-Thr^{10}, forms a β-turn with Trp^8 in the *i*+1 position.[6] Knowing that the D-configuration of the amino acid in the *i*+1 position will stabilize a

β-turn, Rivier et al replaced the Trp^8 residue with its enantiomer, D-tryptophan.[7] The new analog was eight times more potent than SRIF-14 in inhibiting growth hormone secretion *in vitro* in isolated rat pituitary cells. The D-Trp^8 compound was also six times more potent in inhibiting glucagon release and eight times more potent in the inhibition of insulin release in *in vivo* assays in cats. The majority of subsequent analogs of somatostatin included the D-enantiomer of tryptophan in position 8. Table 3-1 summarizes the relative inhibitory potencies of SRIF-14 and the D-Trp^8 and D-Tyr^8 analogs against insulin, glucagon, and GH.

Table 3-1: The relative inhibitory potencies of SRIF-14, D-Trp^8-SRIF-14 and D-Tyr^8-SRIF-14 against insulin, glucagon, and GH.[5]

Compound	Insulin	Glucagon	GH
SRIF-14 [**2-1**]	1	1	1
D-Tyr^8-SRIF-14	0.28	<0.10	0.10
D-Trp^8-SRIF-14	8.43	6.39	80.21

Shortly thereafter, the D-Trp^8-SRIF-14 analog was shown to be equipotent to SRIF-14 in inhibiting gastric acid[8,9] and pancreatic[9,10] secretions. In order to probe the effects of indole ring substituents of D-Trp^8 on the inhibition of gastric acid, glucagon, and insulin secretion, the L- and D-enantiomers of 5-F-, 5-Br-, 6-F-, 5-Me-, and 5-OMe-Trp were incorporated into position 8 of SRIF-14, Figure 3-1.[11]

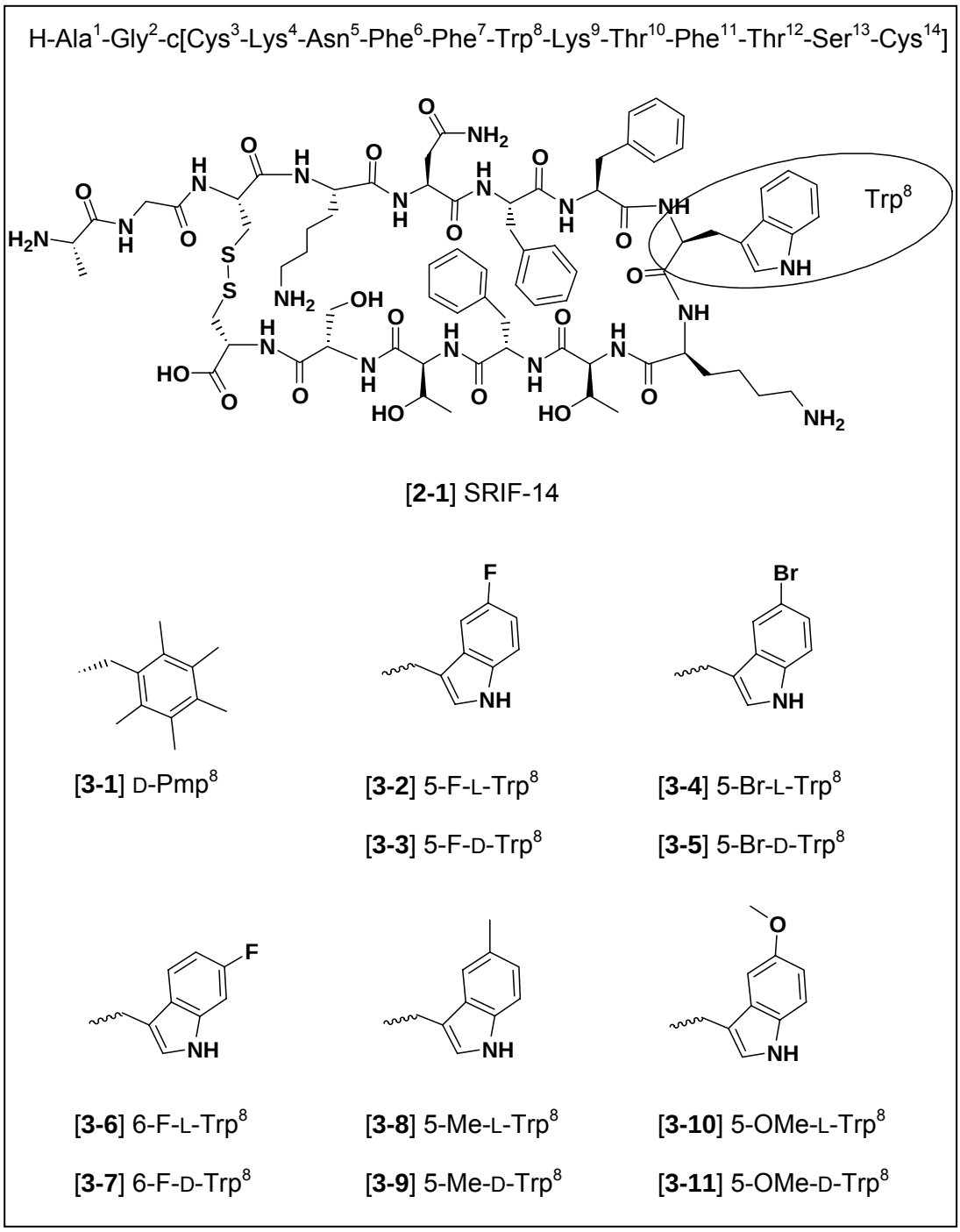

Figure 3-1: The structure of SRIF-14 and the substituted tryptophan analogs which were incorporated into the peptide in place of Trp^8.

The 5-F-D-Trp^8 [**3-3**] and 6-F-D-Trp^8 [**3-7**] analogs were significantly more potent than SRIF-14 in inhibiting gastric acid secretion while the rest of the substituted indole compounds were just slightly more or less potent than SRIF-14.[11] All of the halogenated Trp^8 analogs were more potent that SRIF-14 in inhibiting GH secretion. The 5-F-D-Trp^8 [**3-3**] and 5-Br-D-Trp^8 [**3-5**] compounds were the most potent and inhibited GH release 25 and 30 times more potently than SRIF-14, respectively; the most active somatostatin analogs reported at the time. The 6-F-D-Trp^8 analog [**3-7**] was equipotent to the D-Trp^8 analog in inhibiting GH release.[12] All of these substitutions were designed to investigate the electronic factors important for receptor recognition of the Trp^8 residue. Replacement of the 5- or 6-H by F, Br, Me, or OMe, might be expected to affect the electron density of the aromatic nucleus of the indole ring. The incorporation of fluoro, and to a lesser extent bromo and methoxy groups, would be predicted to have electron-withdrawing activity, whilst methyl would be predicted to be an electron-donating group. The researchers suggested that the similarity of activities of the analogs with these substitutions implied that that the electron density of the aromatic nucleus of Trp^8 is relatively unimportant in determining the gastric acid inhibitory activity of somatostatin. [11]

The same group of researchers also incorporated D-pentamethylphenylalanine (D-Pmp^8 [**3-1**]) into position 8. The resulting peptide showed only 10% of the inhibitory activity of SRIF-14. The incorporation of 1-Nal^8 and 2-Nal^8 (1- and 2-naphthylalanine) provided compounds that were completely inactive. All of the synthesized analogs' relative potencies are listed in Table 3-2.

Table 3-2: Comparison of gastric acid,[11] glucagon,[11] insulin,[11] and GH[12] inhibitory potencies of somatostatin analogs containing Trp^8 modified residues relative to SRIF-14 [**2-1**].

Compound	Gastric Acid	Glucagon	Insulin	GH
SRIF-14 [**2-1**]	1	1	1	1
D-Trp^8	1.65	6.39	80.21	8.43
D-Pmp^8 [**3-1**]	0.07	0.29	0.20	0.03
5-F-L-Trp^8 [**3-2**]	1.39	0.77	n.d.	4.76
5-F-D-Trp^8 [**3-3**]	3.69	1.27	0.32	24.99
5-Br-L-Trp^8 [**3-4**]	1.11	n.d.	n.d.	5.48
5-Br-D-Trp^8 [**3-5**]	1.15	0.35	n.d.	30.02
6-F-L-Trp^8 [**3-6**]	1.45	n.d.	n.d.	1.18
6-F-D-Trp^8 [**3-7**]	2.80	n.d.	n.d.	8.46
5-Me-L-Trp^8 [**3-8**]	1.17	n.d.	n.d.	n.d.
5-Me-D-Trp^8 [**3-9**]	0.84	n.d.	n.d.	n.d.
5-OMe-L-Trp^8 [**3-10**]	0.87	n.d.	n.d.	n.d.
5-OMe-D-Trp^8 [**3-11**]	0.63	n.d.	n.d.	n.d.

n.d. – not determined.

Researchers at Merck incorporated the L- and D-enantiomers of 5-F-, 6-F-, 5-OMe, and 1-Me-Trp into the cyclic hexapeptide somatostatin analog L-363,301

[**2-4**] (Chapter 2, Figure 2-5). All four fluoro-substituted compounds showed potencies similar to that of L-363,301 [**2-4**].

Table 3-3: Comparison of insulin, glucagon, and GH inhibitory potencies L-363,301 [**2-4**] and Trp^8 modified analogs of L-363,301 relative to SRIF-14 [**2-1**].[13]

Compound	Insulin	Glucagon	GH
SRIF-14 [**2-1**]	1	1	1
L-363,301 [**2-4**]	5.2	8.0	1.7
L-Trp^8-L-363,301	7.9	9.1	1.6
5-F-D-Trp^8	8.1	5.8	2.4
5-F-L-Trp^8	4.9	5.0	2.5
6-F-D-Trp^8	3.7	1.5	1.0
6-F-L-Trp^8	2.9	4.2	0.63
5-OMe-D-Trp^8	0.2	0.5	0.02
5-OMe-L-Trp^8	1.9	1.5	0.15
1-Me-D-Trp^8	2.4	5.2	0.26
1-Me-L-Trp^8	<0.07	<0.07	0.007

The researchers hypothesized that since fluorine substitutions represented electronic modifications with negligible effects on the steric environment, the high relative potencies of those four compounds indicated that receptor interaction was not

affected by the electron distribution of the indole ring.[13] Both enantiomers of the 1-Me- and 5-OMe-Trp analogs were less active than L-363,301. A summary of the binding potencies of the L-363,301 analogs are listed in Table 3-3.

Other laboratories have also reported somatostatin analogs with nonnatural amino acids substituted for the Trp[8] residue as a part of their SAR studies. Unfortunately, the reported analogs were not noteworthy in their potencies. Studies of RC-121 [**2-7**] included the substitution of D-Pal (3-(3-Pyridyl)-D-Alanine) into the Trp[8] position. The resulting octapeptide [**3-12**] (Figure 3-2) did not inhibit GH secretion.[14]

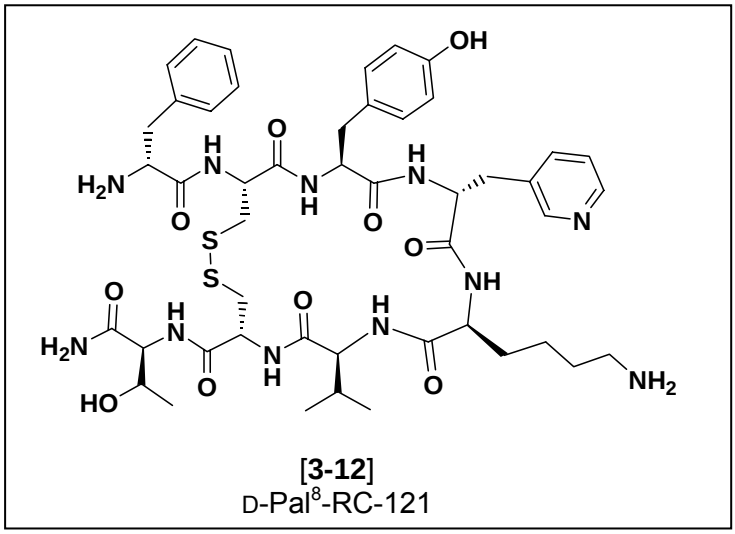

Figure 3-2: An analog of RC-121 [**2-7**] which contains 3-(3-Pyridyl)-D-Alanine (D-Pal[8]) in place of the Trp[8] residue.

Rivier and coworkers synthesized a series of disulfide bridged Des-AA [1,2,5]-somatostatin peptides which contained IAmp[9] (4-(*N*-isopropyl)-

aminomethylphenlyalanine) [**3-13**] in place of the Lys[9] residue (Figure 3-3). The analog which contained D-Trp[8] [**3-14**] bound to hsst1 and hsst3 with an IC_{50} of 33 and 345 nM, respectively, and displayed no affinity for the other receptors. Incorporation of D-Nal[8] yielded analog [**3-15**] which bound exclusively to hsst1 with an IC_{50} of 248 nM.[15]

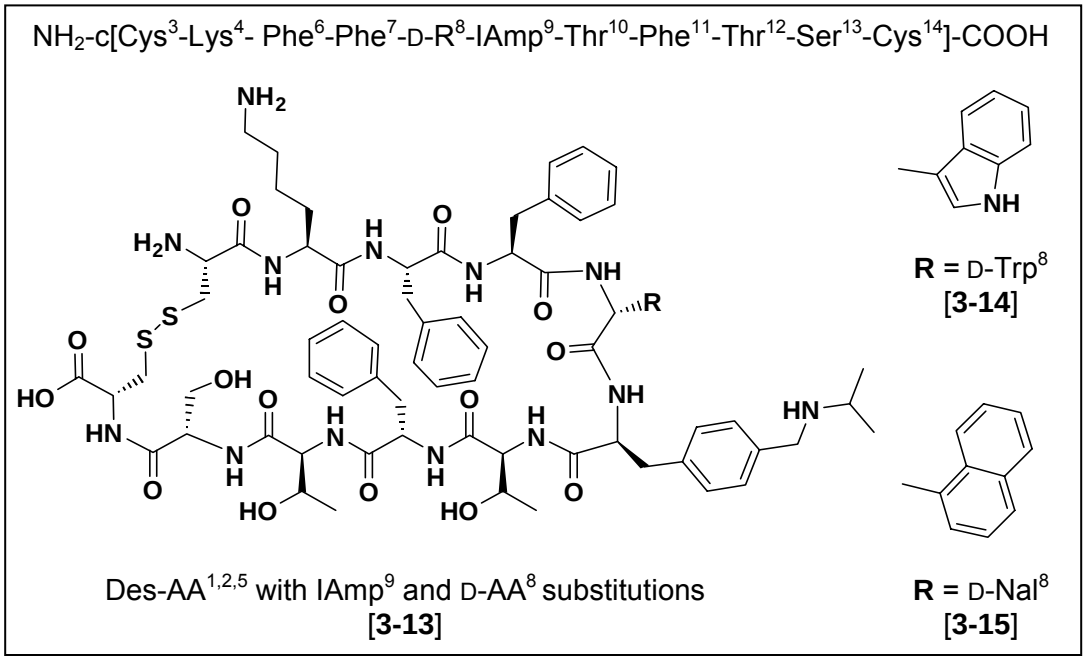

Figure 3-3: Des-AA [1,2,5]-somatostatin analogs with IAmp[9] and additional substitutions of Trp[8].

The same laboratory designed and synthesized 'betidamino' acids; *N'*-monoacylated (or optionally, *N'*-monoacylated and *N*-mono- or *N*,*N'*-dialkylated) amino glycine derivatives where each *N'*-acyl/ alkyl group mimicked naturally

occurring amino acid side chains or introduced novel functionalities. The betidamino acids were then incorporated into the disulfide bridged octapeptide NH_2-c[Cys^3-Phe^6-Phe^7-D-Trp^8-Lys^9-Thr^{10}-Phe^{11}-Cys^{14}]-COOH [**3-16**] also known as ODT-8.[16] The substitutions of Trp^8 included D-2-Nal^8 (which provided peptide ODN-8, [**3-17**]), D-Agl-$(2\text{-naphtholyl})^8$ (or (2-naphtholyl)-aminoglycine, also called betidennaphthylalanine) which provided peptide [**3-18**], and D-Agl-((Me, 2-naphtholyl)-aminoglycine)[8] which provided peptide [**3-19**]. Figure 3-4 depicts the three peptide analogs.

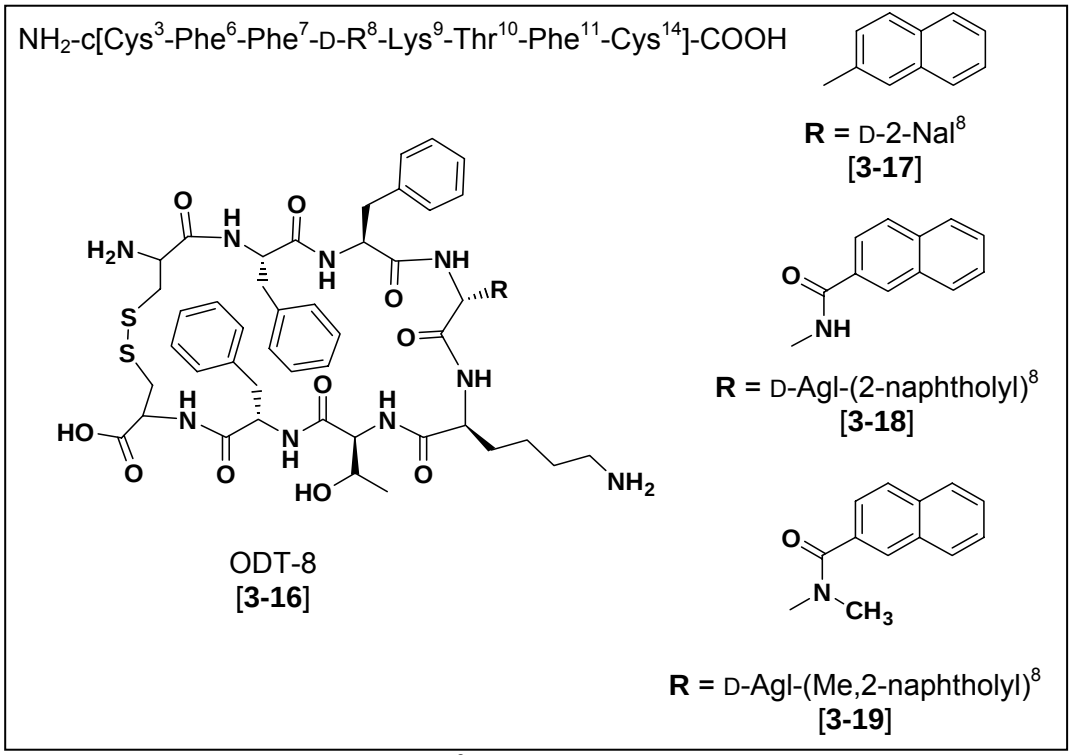

Figure 3-4: Substitution of the Trp^8 position of the cyclic octapeptide ODT-8 with D-2-Nal and betidamino acids.

D-2-Nal[8] substituted [**3-17**] lost affinity for receptor subtypes hsst1, hsst2, and hsst4 compared to ODT-8 [**3-16**]. The introduction of betidennaphthylalanine[8] to provide peptide [**3-18**] resulted in loss of binding at all but sst4 with an IC_{50} = 165 nM. Methylation of the side chain (compound [**3-19**]) restored binding to hsst3 and increased selectivity by >100-fold.[16] A summary of the binding data is presented in Table 3-4.

Table 3-4: Binding affinities of ODT-8 and analogs containing D-2-Nal[8] and betidamino acids and for the somatostatin receptor subtypes (IC_{50}, nM).

Compound	hsst1	hsst2	hsst3	hsst4	hsst5
Somatostatin-28 [**2-2**]	3.9	3.3	7.1	3.8	3.9
ODT-8 [**3-16**]	28	44	13	1.3	45
D-2Nal[8] (ODN-8) [**3-17**]	607	173	6.7	56	28
D-Agl[8](2-naptholyl) [**3-18**]	>10000	>10000	>1000	165	>10000
D-Agl[8](Me, 2-naptholyl) [**3-19**]	>10000	>10000	70	>10000	>10000

As discussed in section 2.2.3 of Chapter 2, researchers in the Goodman laboratories prepared all four diastereomers of β-methyl tryptophan and incorporated them into L-363,301. Substitution of D-Trp with (2*R*,3*S*)-β-methyl tryptophan produced compound [**3-20**] (Figure 3-5) which was the only compound of the group with binging affinity greater than that of the parent hexapeptide L-363,301 when

assayed for binding at a mixture of all five receptor subtypes (which did not allow for the determination of subtype selectivity).[17]

The (2*R*,3*S*)-β-methyl tryptophan compound [**3-20**] was recently resynthesized and tested for binding to all five hsst receptor subtypes. Its binding affinity profile mirrored that of L-363,301.[18]

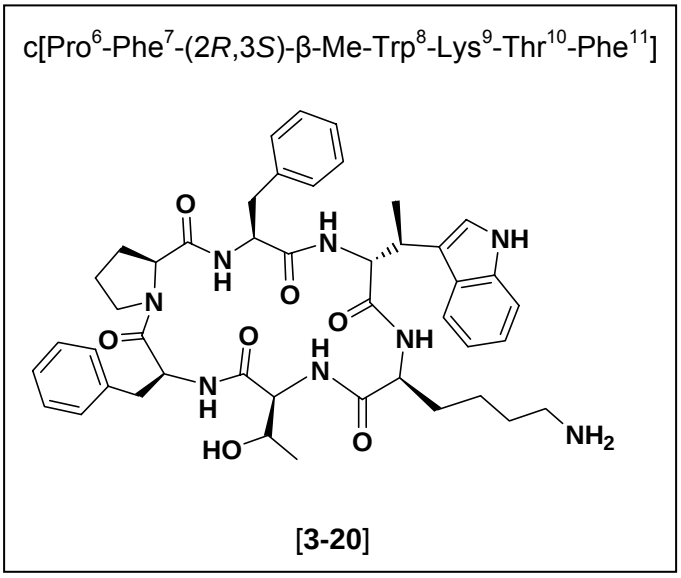

Figure 3-5: An analog of L-363,301 which contains (2*R*,3*S*)-β-methyl Tryptophan[8].

The Trp[8] residue of somatostatin and its analogs is known to be particularly important for cellular receptor binding and secretion inhibitory activity. However, the substitution of this residue and the tolerance of the receptors for substitution of this residue have not been extensively reported on in the literature. From the small amount of research presented, it is difficult to correlate definitive structure-activity

relationships about the residue in question. The known substitutions were made into various different parent compounds, which in some cases included additional modifications to other residues, making it difficult to quantify or compare the results. The substituted compounds were biologically evaluated using two different methods which are unrelatable; some of the compounds were evaluated in functional assays for secretion inhibition, while others were evaluated in competitive binding assays for receptor subtype binding affinity and selectivity. Even with these difficulties, two general trends can be elucidated. The incorporation of the D-enantiomer of the tryptophan analogs into position 8 resulted in compounds which retained the activity of the parent compound or produced an increase in the measured activity. A fused ring system in the side chain of residue 8 provided compounds with better biological profiles than those containing a single ring. Compounds with naphthylene analogs and substituted indoles in the side chain retained some activity, were equipotent, and in some cases displayed an increase in activity when compared to parent compounds, while those which included Phe analogs such as D-Tyr, D-Pmp, and D-Pal, all displayed a substantial loss in activity.

Perhaps the lack of somatostatin analogs with modifications to the Trp^8 residue which display increased binding affinity or potency has turned researchers away from further efforts. However, novel, unnatural amino acids with fused 5,6-ring systems could be incorporated into somatostatin analogs. A focused library of analogs could probe the topospace of the receptor subtypes and provide additional SARs as well as compounds with novel biological profiles.

3.2 The design and syntheses of nitrogen-containing heterocyclic α-amino acids

In our effort to develop unnatural amino acids for employment in our research programs, particularly in the area of somatostatin, we designed a number of nitrogen-containing, fused 5,6-heterocyclic, aromatic α-amino acids.

The amino acids pictured in Figure 3-6 are shown in the D-configuration and are based on benzimidazole [**3-21**], benzotriazole [**3-22**] and [**3-23**], 4-azabenzimidazole [**3-24**] and [**3-25**], indazole [**3-26**], and purine [**3-27**] and [**3-28**]. These compounds were designed to be analogs of naturally occurring tryptophan. Of the eight structures pictured, only two are known compounds; the benzimidazole [**3-21**] and indazole [**3-26**] analogs. Searches of the literature and commercial sources found that the Aldrich Fine Chemicals Catalog has <50 mg of the benzimidazole compound [**3-21**] available for purchase, though a synthesis has not been published. Indazole analog [**3-26**] is known and has been synthesized in small quantities using a tryptophan synthase obtained from *E. coli*.[19] Our research represents the first reported chemical synthesis of all eight of the heterocyclic amino acids presented in Figure 3-6.

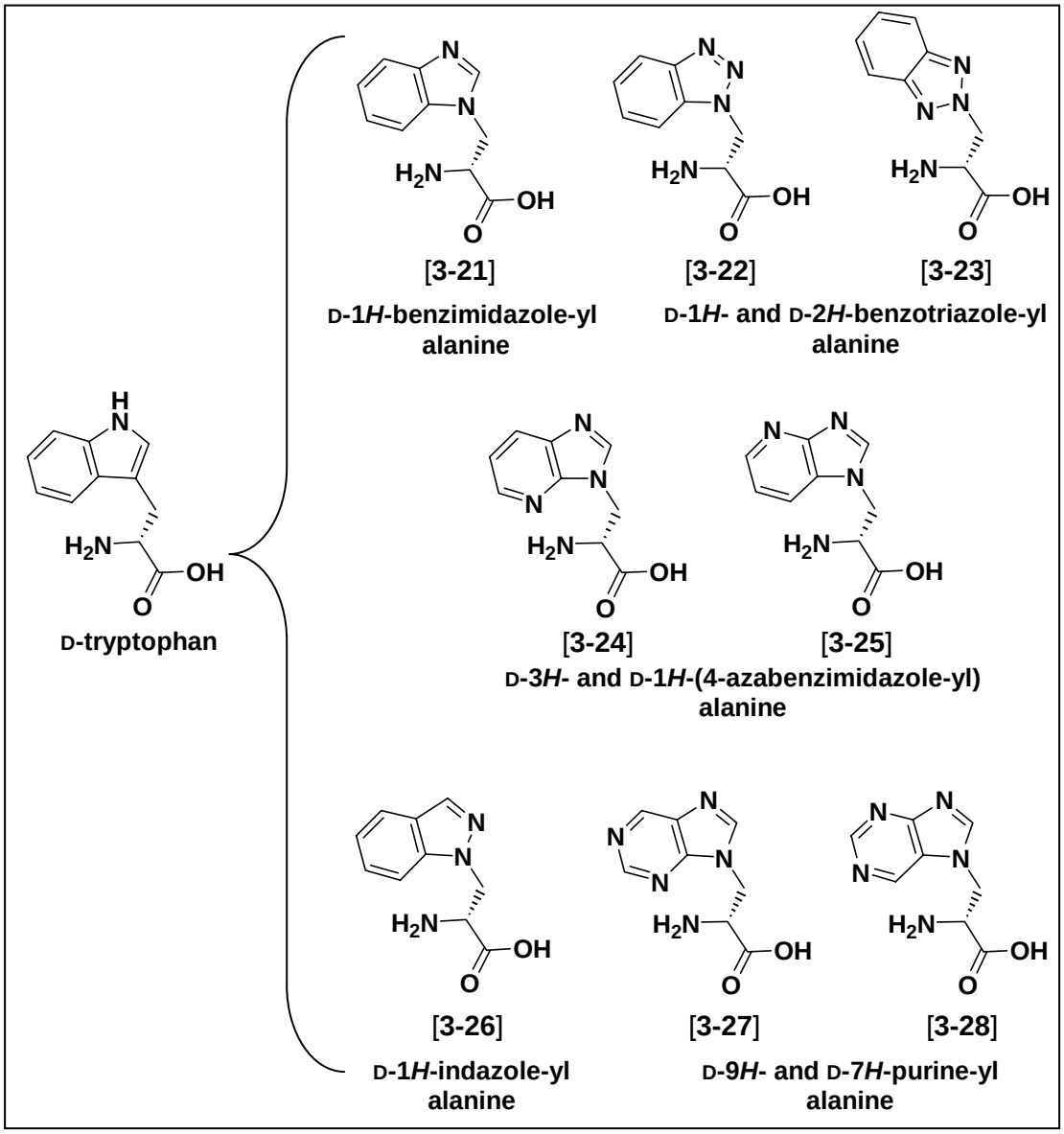

Figure 3-6: Nitrogen-containing, fused 5,6-heterocyclic, aromatic α-amino acids.

When designing a synthetic route, we envisioned a serine-derived common intermediate whose synthesis was stereoselective, scalable, and which could be derivatized with each heterocycle to provide all of the desired compounds. Our

initial efforts focused on a method utilized in our laboratories to create orthogonally protected lanthionine derivatives in solution.[20] With suitable, bulky protecting groups, the iodide of 3-iodoalanine was displaced by the sulfur of cysteine derivatives without forming dehydroalanine [**3-31**] as a side product. Unfortunately, when we reacted deprotonated benzimidazole [**3-30**] with the same 3-iododalanine derivative, trityl-3-iodoalanine benzyl ester [**3-29**], the deprotonated amine was more basic than it was nucleophilic and we obtained dehydroalanine [**3-31**] as the exclusive product (Scheme 3-1).

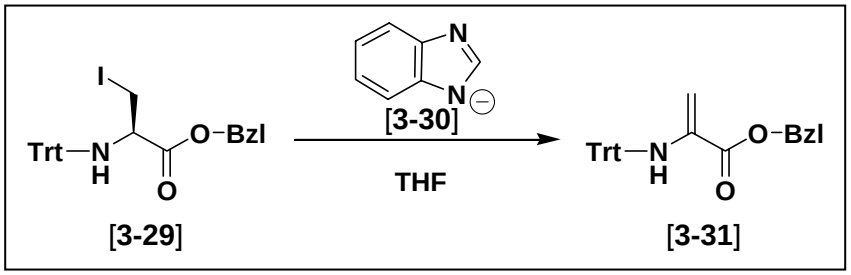

Scheme 3-1: Reaction of deprotonated benzimidazole with Trt-3-iodoalanine-OBzl provided hydroalanine as the exclusive product.

These results encouraged us to look for ways to further decrease the acidity of the α-proton of the 3-iodoalanine aduct, while also maintaining steric bulk. The ortho ester (2,6,7-trioxobicyclo[2.2.2]octyl ester) has been shown to signifigantly decrease the acidity of the α-proton of amino acids.[21,22] We attempted to synthesize this protecting group from Z-Ser-oxetane [**3-22**], which we then planned to convert to the complementary 3-iodoalanine derivative for use in our synthetic program.

Unfortunately, the ortho ester of Z-serine [**3-33**] was found to be very unstable, and decomposed within one to two days, even when stored at cold temperatures and under an inert atmosphere. The introduction of the ester was also not amenable to synthesis on multigram scale (Scheme 3-2).

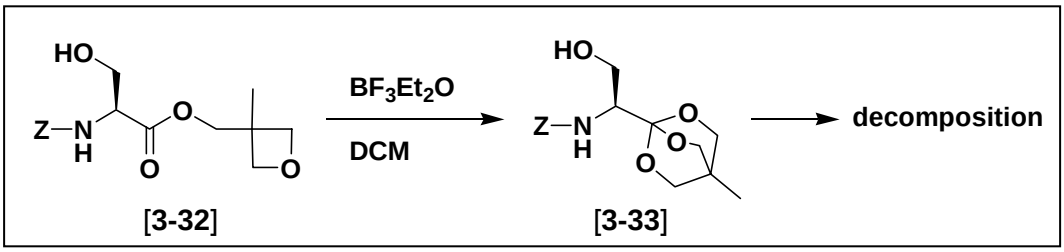

Scheme 3-2: The ortho ester of Z-Serine was unstable and decomposed within one to two days.

We shifted our focus to the Mitsunobu reaction in which hydroxyl groups are converted to leaving groups *in situ* in the presence of triphenyl phosphine and diisopropyl azodicaboxylate (DIAD). A nucleophile with an acidic proton of p*K*a < 13 can then displace the activated alcohol to provide the desired amino compound.[23] The application of the Mitsunobu reaction to benzimidazole with various protected serine derivatives provided no product presumably because the N-H of benzimidazole (pKa = 12.75)[24] is at the upper limit of the reaction requirements (Scheme 3-3).

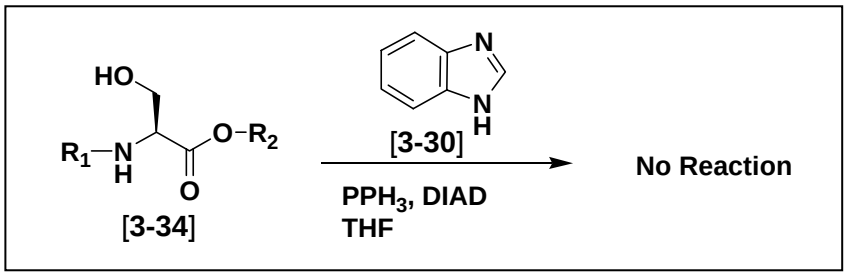

Scheme 3-3: The reaction of various protected serine derivatives with benzimidazole under Mitsunobu conditions did not provide any product.

During our search for alternative synthetic strategies, we considered employing Garner's aldehyde[25] as a common intermediate for derivatization by the desired heterocycles. Garner's aldehyde has been used extensively as a chiral building block in asymmetric synthesis. Introduction of the heterocycles could be achieved by reductive amination of the aldehyde with the various heterocyclic amines. Unfortunately, a test reaction with propionaldehyde and benzimidazole did not provide any product. Only starting material was recovered, so we did not pursue the aldehyde route (Scheme 3-4).

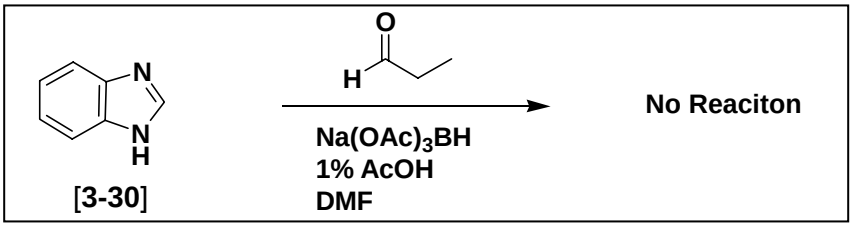

Scheme 3-4: Reductive amination of benzimidazole with propionaldehyde provided no product. Only starting material was recovered.

However, the alcohol intermediate [**3-38**] (Scheme 3-5) of the Garner's aldehyde synthesis intrigued us because it could be converted to a leaving group which could be displaced by the heterocyclic amines. This concept was supported by the known displacement of tosylates by deprotonated benzimidazole.[26] Additionally, the α-proton of the oxazolidine-bound tosylate intermediate [**3-39**] was not acidic, so competing elimination reactions could be avoided (Scheme 3-5).

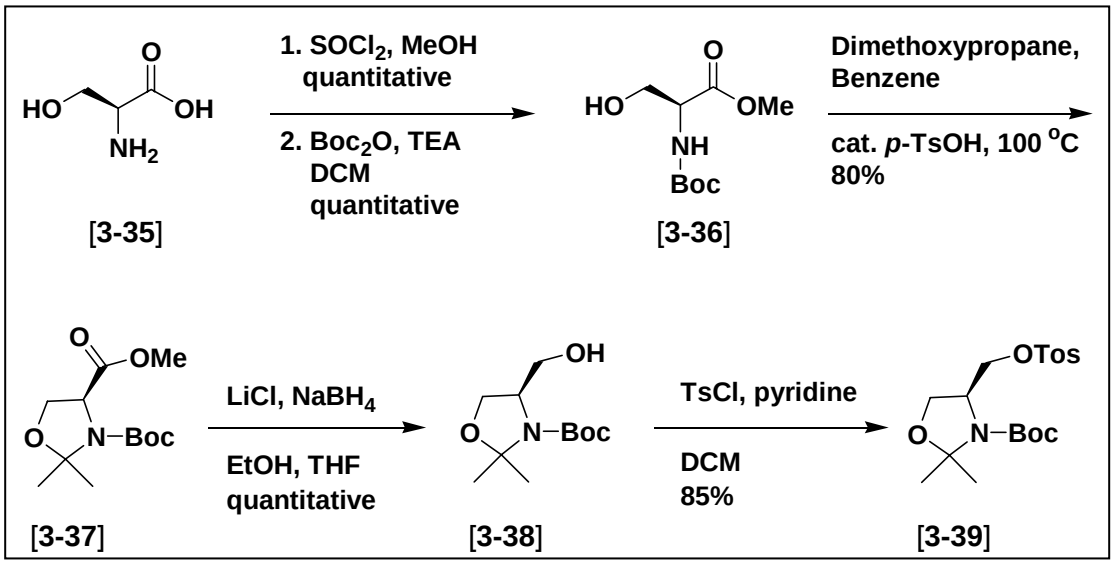

Scheme 3-5: Synthesis of the Boc-protected tosyl-oxazolidine intermediate [**3-39**] from L-serine.

As shown in Scheme 3-5, the synthesis of Garner's alcohol commenced with the esterification of L-serine [**3-35**] with thionyl chloride in methanol. The amine was urethane-protected with Boc_2O and triethylamine which provided Boc-Ser-OMe [**3-36**] in quantitative yield for both protection steps. Compound [**3-36**] was then

treated with dimethoxypropane and catalytic *p*-toluenesulfonic acid in refluxing benzene which cyclized the side chain alcohol to the Boc-protected nitrogen and provided oxazolidine ester [**3-37**] in 80% yield. Reduction of ester [**3-37**] to alcohol [**3-38**] was achieved quantitatively with sodium borohydride in the presence of lithium chloride. Alcohol [**3-38**] was treated with tosyl chloride and pyridine to provide key intermediate [**3-39**] in 85% yield.

The displacement of the tosylate of compound [**3-39**] by deprotonated benzimidazole gave poor yields of only 25% (Scheme 3-6). With the product in hand, we subjected intermediate [**3-40**] to Jones oxidation conditions using chromium trioxide and sulfuric acid. The acidity opened the ring of oxazolidine [**3-40**]. The alcohol, which was the original amino acid side chain, was oxidized to become the α-carboxylic acid; inverting the stereochemistry from the L-configuration to the D-configuration. The Boc-protected benzimidazole amino acid [**3-41**] was isolated in 50% yield. Loss of the Boc-group contributed to the low yield of the final product, and the free amino acid was detected in the crude reaction mixture.

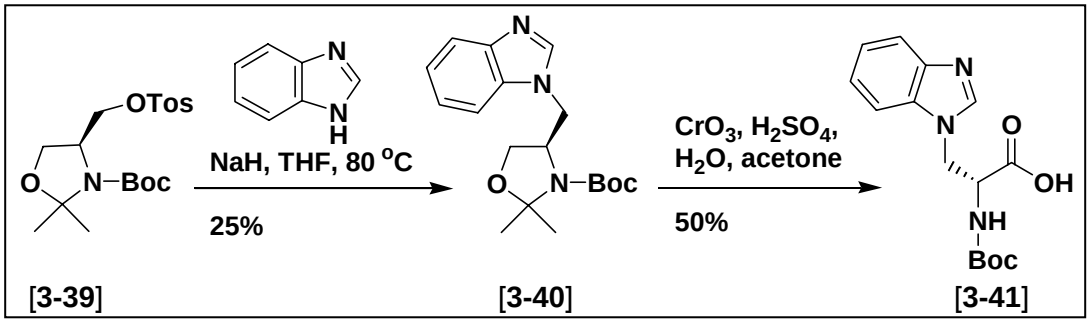

Scheme 3-6: Displacement of the tosylate with benzimidazole, followed by ring opening and oxidation to the Boc-protected amino acid.

We theorized that the low yield of the tosyl displacement reaction by benzimidazole was a result of steric hindrance caused by the bulky *t*-butyl of the nitrogen-protecting Boc group. To test our hypothesis, we synthesized the Cbz-protected, tosylated oxazolidine [**3-45**], as shown in Scheme 3-7.

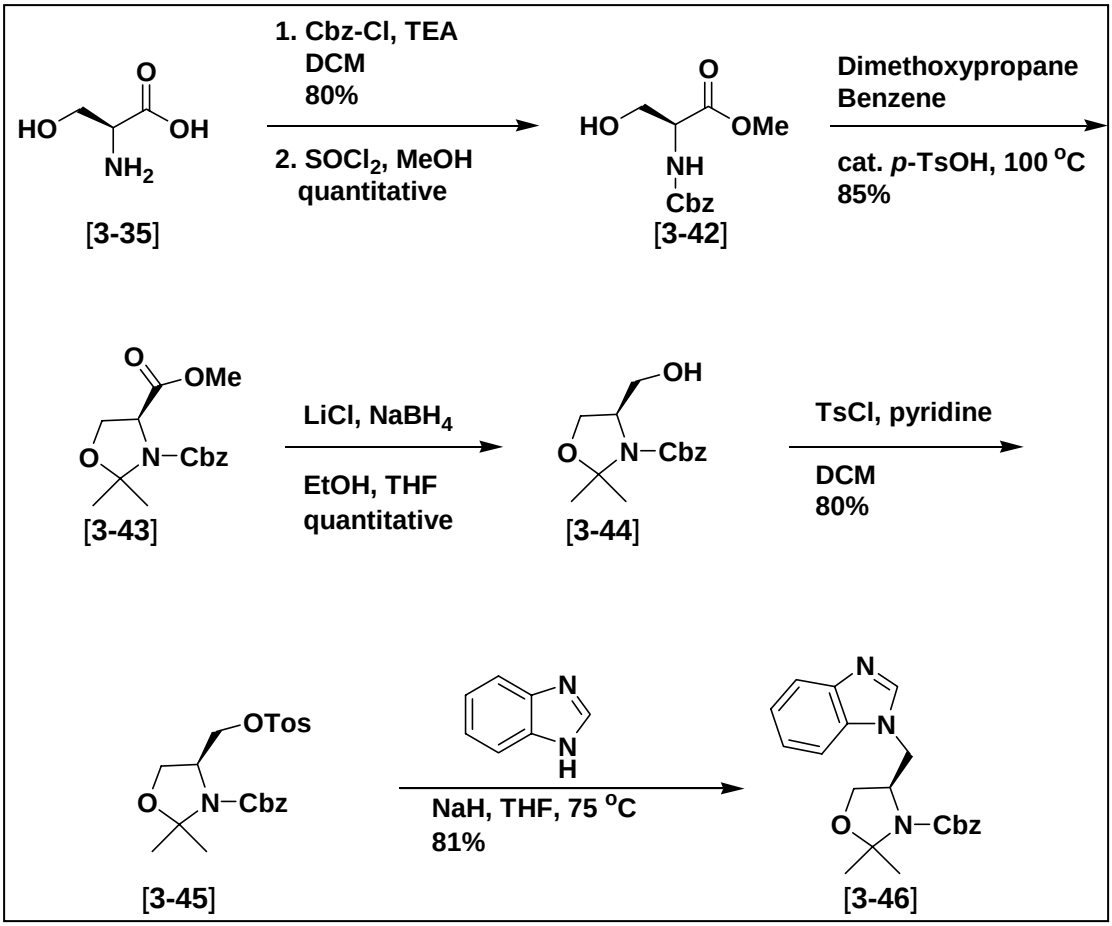

Scheme 3-7: Synthesis of Cbz-protected tosylate oxazolidine intermediate.

The synthesis of key intermediate [**3-45**] followed a similar protocol as that described for the Boc-protected analog, with similar yields for each step. It is

important to note that tosylate [**3-45**] was found to be unstable, even when stored at -20 ^{o}C, under inert atmosphere. Therefore, alcohol [**3-44**] was prepared in multigram quantity and stored for future use. The tosylate was freshly prepared for all subsequent synthetic applications.

Nucleophilic displacement of the tosylate of Cbz-protected oxazolidine [**3-45**] with deprotonated benzimidazole was achieved in 81% yield; a significant improvement over the analogous step of the synthesis of the Boc-protected analog. Treatment of the Cbz-protected benzimidazole oxazolidine [**3-46**] with Jones oxidation conditions produced a bluish-green, insoluble metal complex, which was not encountered in the Boc-protected analog synthesis (Scheme 3-8).

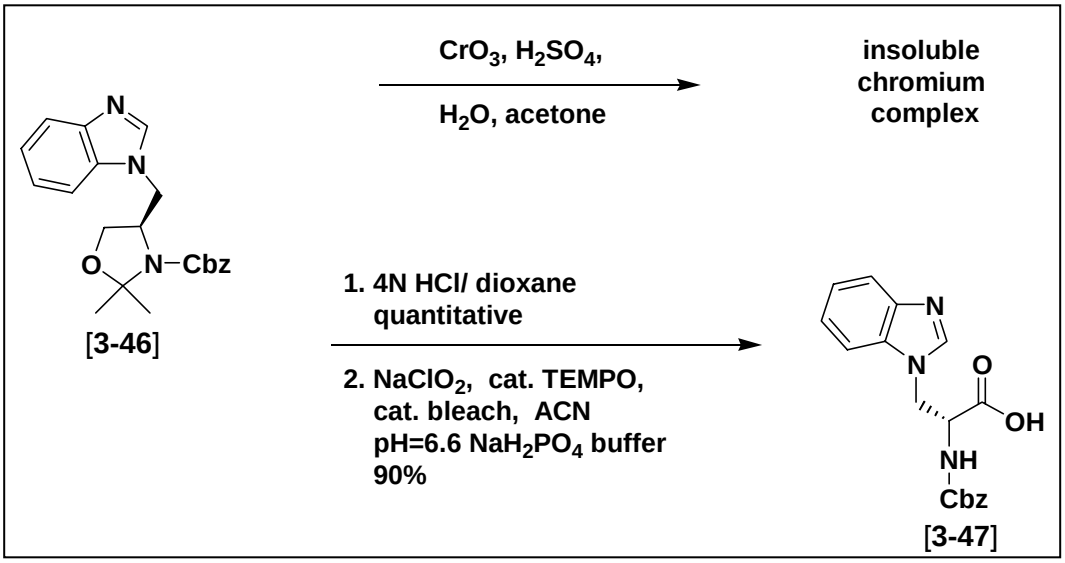

Scheme 3-8: Opening of the oxazolidine ring and the final oxidation of the alcohol to the carboxylic acid provided the Cbz-protected benzimidazole amino acid.

To circumvent the Jones oxidation problem, compound [**3-46**] was first treated with 4N HCl in dioxane which opened the oxazolidine ring and provided the free primary alcohol in quantitative yield. The alcohol was then oxidized directly to the carboxylic acid under mild conditions[27] using sodium hypochlorite (NaOCl, or bleach), sodium chlorite ($NaClO_2$), and a catalytic amount of TEMPO (2,2,6,6-tetramethylpiperidinyl-1-oxy) in a pH=6.6 phosphate buffer to provide the desired benzimidazole amino acid [**3-47**] in 90% yield. The benzimidazole amino acid [**3-47**] was synthesized in an overall yield of 40% from L-serine.

The displacement of the tosylate of key intermediate [**3-45**] with benzotriazole proceeded in an overall yield of 80% with 2:1 regioselectivity in favor of the 1-substituted analog [**3-48**] over the 2-substituted analog [**3-49**] (Scheme 3-9). The ring opening of both analogs proceeded in quantitative yield. Oxidation of the 1-sudstituted benzotriazole alcohol was quantitative, while the 2-substituted benzotriazole amino acid was isolated in 85% yield after oxidation.

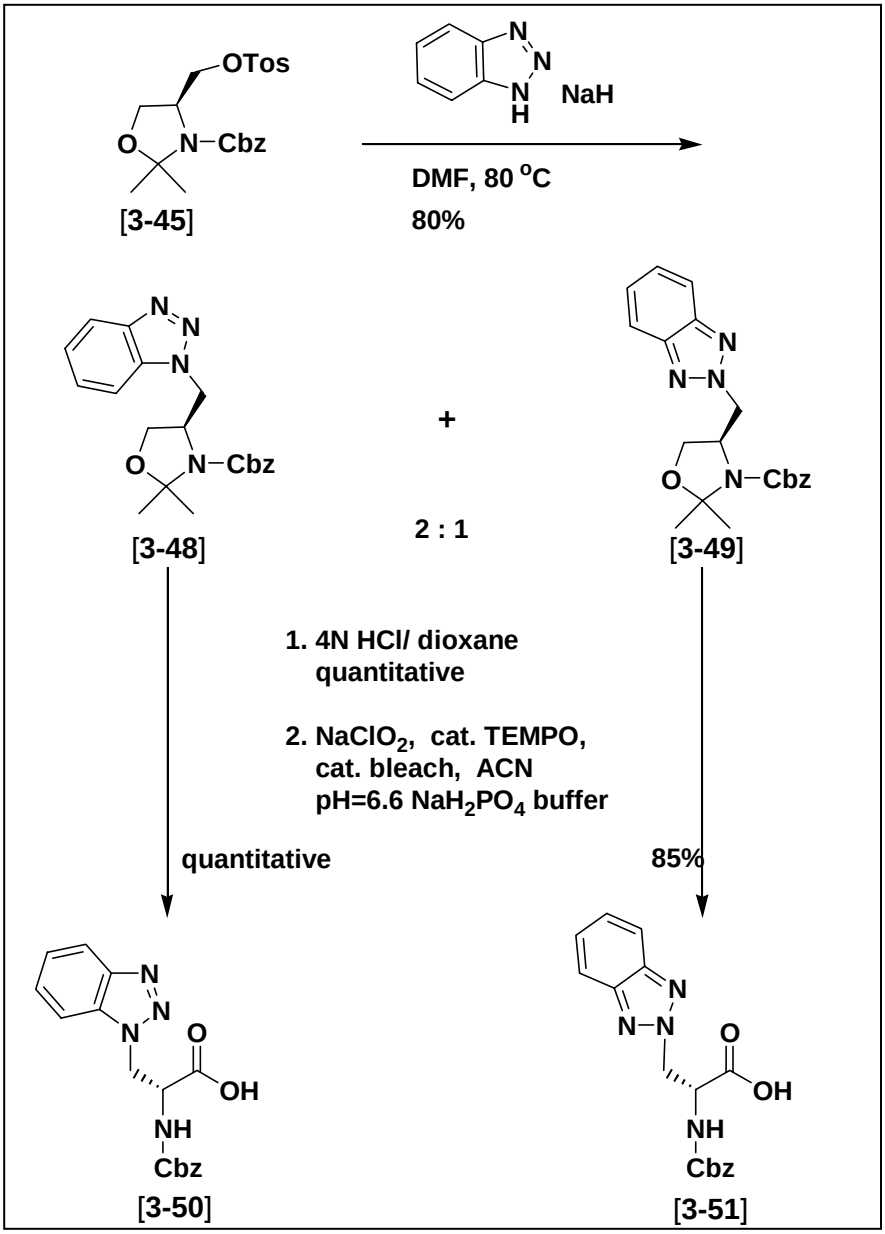

Scheme 3-9: The displacement of the tosylate by benzotriazole provided two regioisomers which are isolated and oxidized separately to the corresponding Cbz-protected amino acids.

It has been well documented that *N*-substituted benzotriazoles are typically prepared as a mixture of the 1- and 2-substituted isomers when reacted with alkylating agents in the presence of base. The reported regioselectivity for 1-alkylated benzotriazoles is poor, and usually in the range of 1:1 to 3:1.[28-30] The two alkylated benzotriazole analogs, [**3-48**] and [**3-49**] were easily separated by column chromatography. As shown in Figures 3-7 and 3-8, the 1- and 2-benzotriazole oxazolidine structures were assigned by comparing the aromatic region of the ^{1}H NMR spectrum of each of the compounds. The aromatic ring system of 2-substituted benzotriazole analog [**3-51**] is symmetrical with only two chemical environments for the ring hydrogens to experience. Therefore there are only two signals exhibited by the four aromatic protons on the benzotriazole ring in the ^{1}H NMR spectrum (Figure 3-7). The ring of the 1-substituted benzotriazole analog [**3-50**] is unsymmetrical, placing each of the four benzotriazole ring protons in slightly different environments, which results in multiple signals in the ^{1}H NMR spectrum (Figure 3-8).

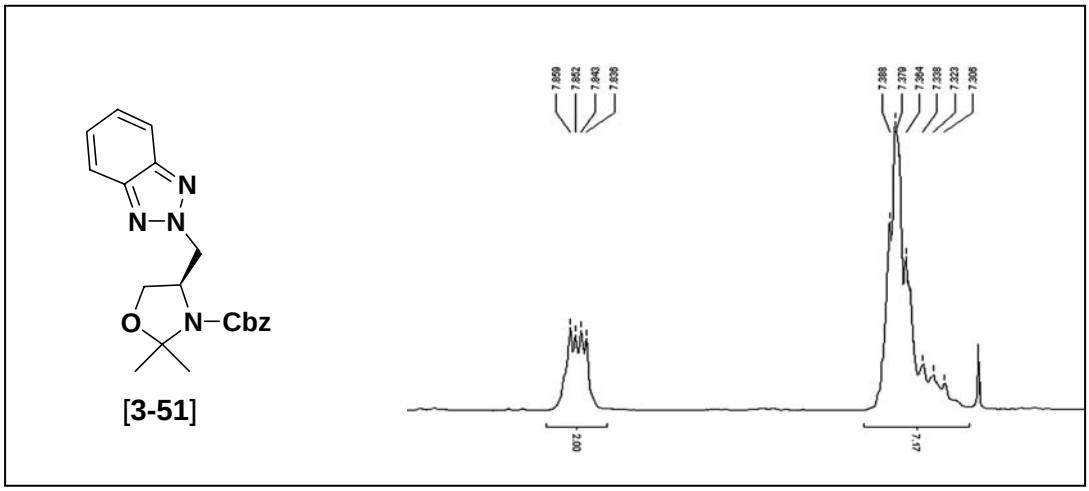

Figure 3-7: The aromatic ring of the 2-substituted benzotriazole analog has only two signals in the aromatic region of the ^{1}H NMR spectrum.

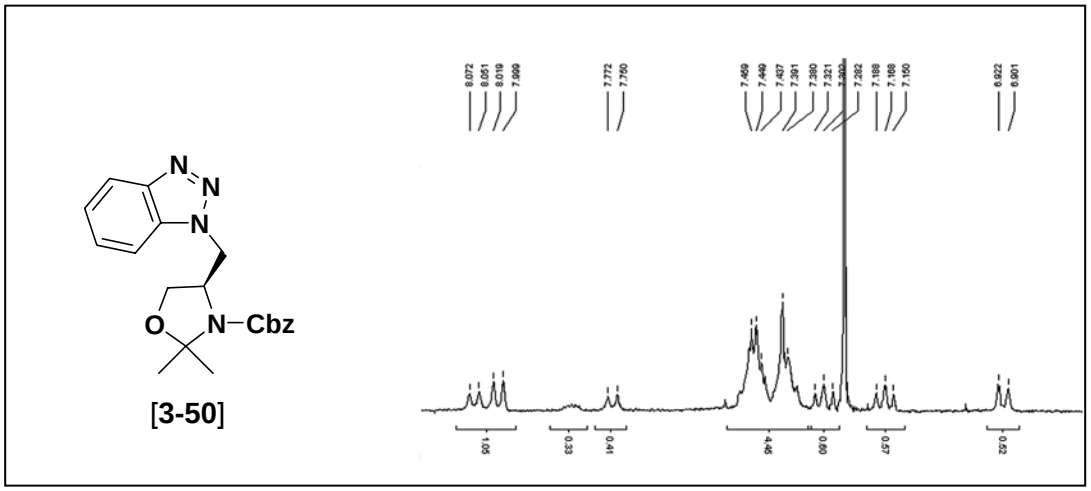

Figure 3-8: The aromatic ring of the 1-substituted benzotriazole analog has many signals in the aromatic region of the ^{1}H NMR spectrum.

Tosylate [**3-45**] was reacted with deprotonated indazole which provided oxazolidine [**3-52**] in 60% yield. Opening of the oxazolidine ring and oxidation of the alcohol to indazole amino acid [**3-53**] both proceeded in quantitative yield.

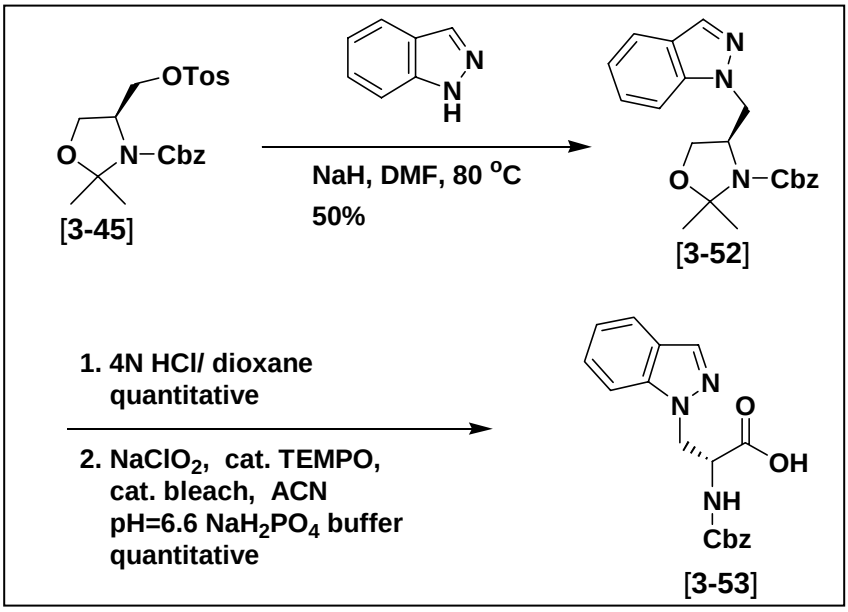

Scheme 3-10: The synthesis of the indazole amino acid from the tosyl-oxazolidine intermediate.

Substitution of the tosylate of compound [**3-45**] by purine provided both the N9- and N7-substituted regioisomers, [**3-54**] and [**3-55**], in 2:1 regioselectivity, respectively (Scheme 3-11). The regioisomers were easily separated by column chromatography. Both purine oxazolidines were opened to the corresponding alcohol and oxidized to the N9- and N7-substituted purine amino acids [**3-56**] and [**3-57**].

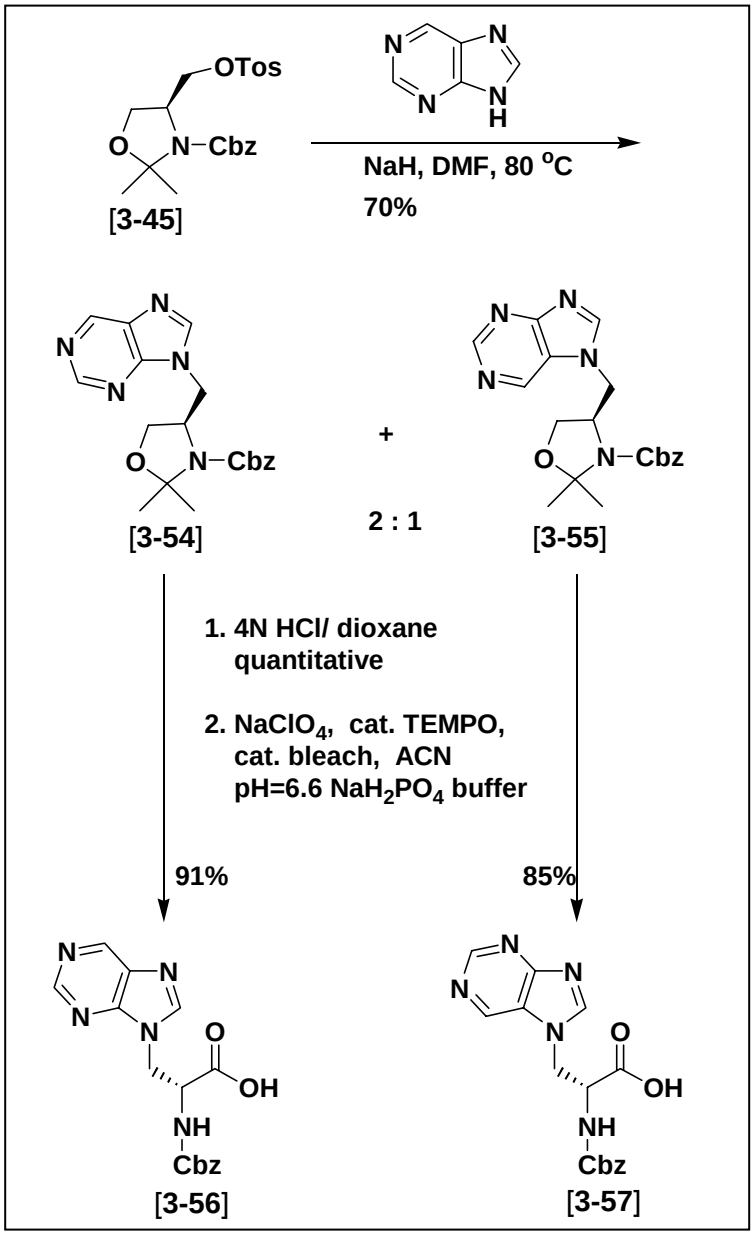

Scheme 3-11: The syntheses of N9- and N7-substituted purine amino acids from a common tosyl-oxazolidine intermediate.

To validate the structural assignment of each regioisomer, two dimensional NMR NOESY experiments were performed on a Bruker 600 MHZ spectrometer. As shown in Figure 3-9, the N9-substituted analog [**3-54**] should not exhibit a hydrogen-hydrogen NOE between the β-hydrogens and the purine N3 because there is no hydrogen on that nitrogen. An NOE also does not exist between the β-hydrogens and the purine H6 because they are too far from each other. An NOE was expected and confirmed to exist between the β-hydrogens and the hydrogen on carbon 6 of the purine in the N7-substituted analog [**3-55**] (Figure 3-10). The NOE data are consistent with the structural assignments.

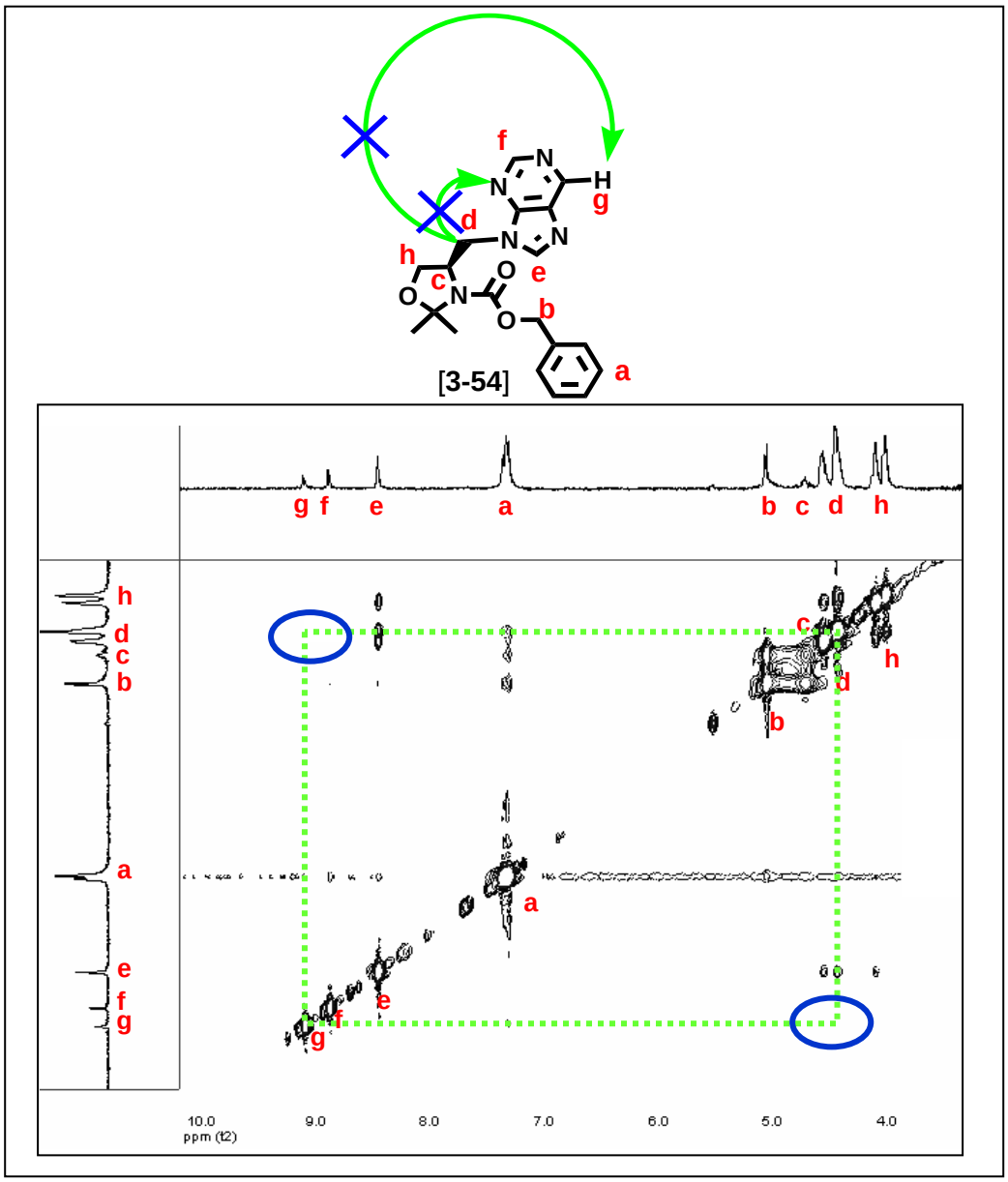

Figure 3-9: 2D-NOESY NMR spectra of N9-substituted purine analog [**3-54**] do not have an NOE between the β-hydrogens (**d**) and N3 because there are no protons on the nitrogen. There are also no NOEs between the β-hydrogens (**d**) and the purine H6 (**g**) because they are too far away from each other.

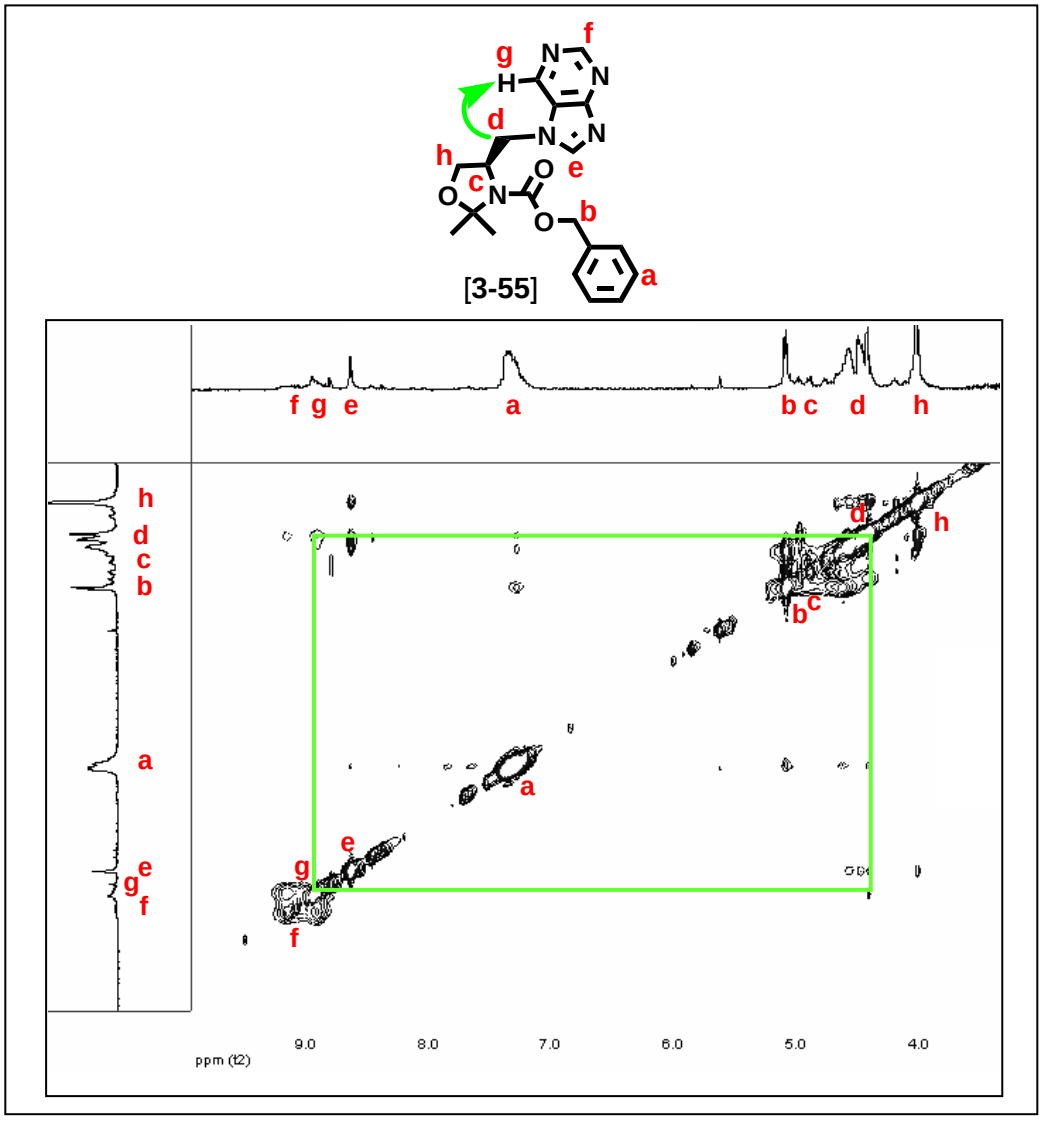

Figure 3-10: 2D-NOESY NMR spectra of N7-substituted purine analog [**3-55**] shows an NOE between the β-hydrogens (**d**) and the purine H6 (**g**).

The structural assignment of the purine regioisomers was further supported by ^{1}H NMR data. The signal of H8 for an N9-substituted purine is known to be shifted upfield in the ^{1}H NMR spectrum, relative to the corresponding signal of H8 for the

N7-substituted isomer.[31] This upfield shift was observed in the ^{1}H NMR spectra of the N9-substituted oxazolidine [**3-54**], alcohol [**3-58**], and acid [**3-56**] when compared to the spectra of the corresponding N7-substituted analogs. The aromatic regions of the ^{1}H NMR spectra of purine intermediates N9-substutited alcohol [**3-58**] and N7-substituted alcohol [**3-59**] are compared in Figure 3-11.

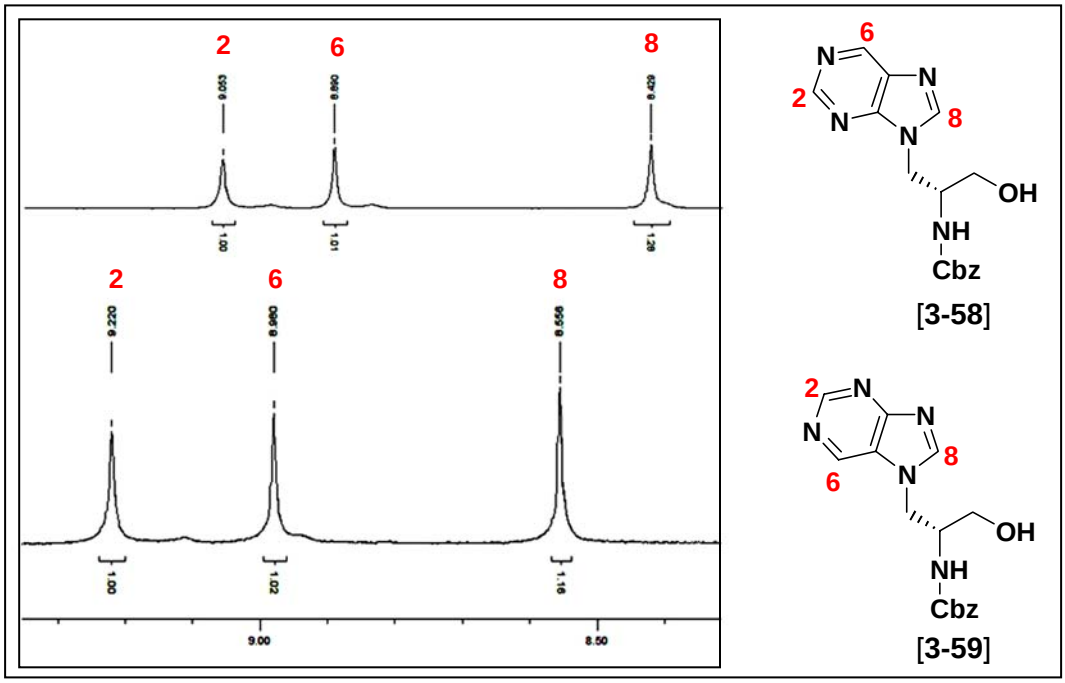

Figure 3-11: The aromatic regions of the ^{1}H NMR spectra of the N9-substituted purine alcohol [**3-58**] and N7-substituted purine alcohol [**3-59**]. The signal of H8 for compound [**3-58**] (8.429 ppm) is shifted upfield relative to the corresponding signal of H8 for compound [**3-59**] (8.556 ppm). This upfield shift supports the structural assignments of the regioisomers.[31]

Scheme 3-12 depicts the substitution of the tosylate of compound [**3-45**] by 4-azabenzimidazole which provided both the N3- and N1-substituted regioisomers, [**3-60**] and [**3-61**], in 1.5:1 regioselectivity, respectively.

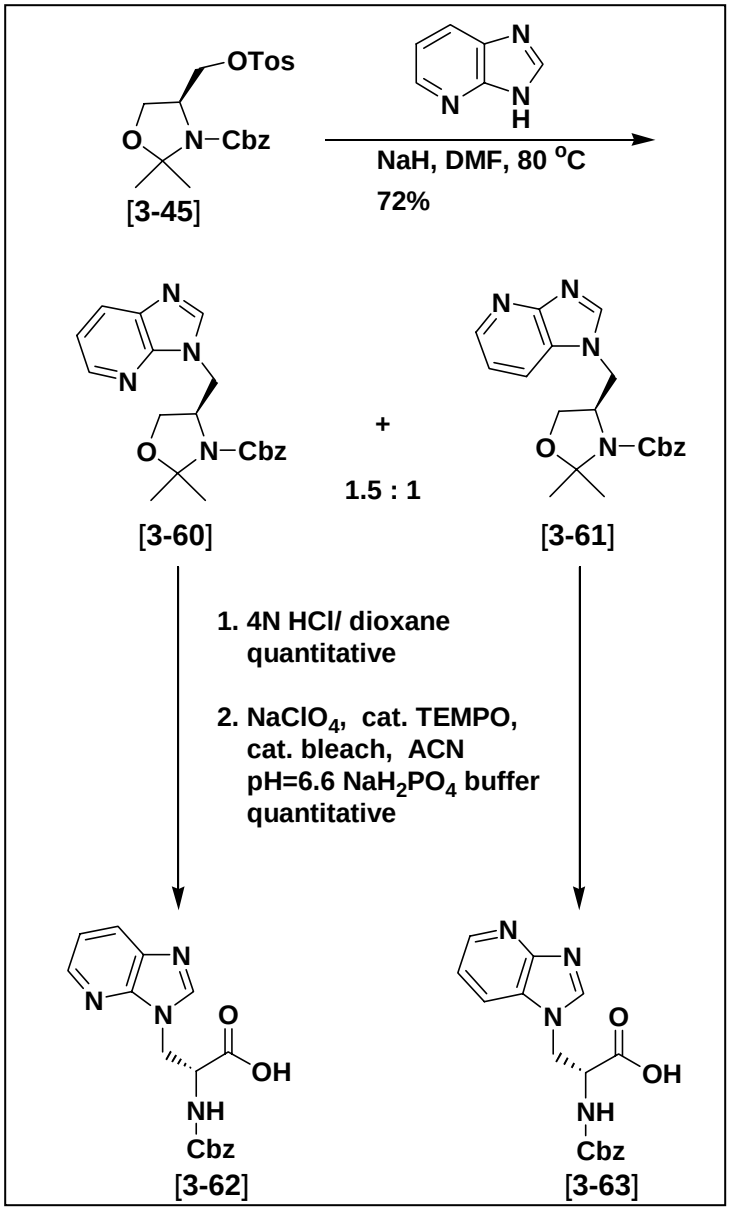

Scheme 3-12: The syntheses of N3- and N1-substituted 4-azabenzimidazole amino acids from a common tosyl-oxazolidine intermediate.

The regioisomers [**3-60**] and [**3-61**] were easily separated by column chromatography. Both 4-azabenzimidazole oxazolidines were opened and oxidized to provide the N3- and N1-substituted 4-azabenzimidazole amino acids [**3-62**] and [**3-63**] in quantitative yields.

To establish the structural assignment of each regioisomer, two dimensional NMR NOESY experiments were performed on a Bruker 600 MHZ spectrometer. As shown in Figure 3-12, the N3-substituted analog [**3-60**] should not exhibit a hydrogen-hydrogen NOE between the β-hydrogens and the 4-azabenzimidazole N4 because there is no hydrogen at that position. An NOE also does not exist between the β-hydrogens and the 4-azabenzimidazole H7. An NOE can be expected to exist between the β-hydrogens and the hydrogen on carbon 7 of the 4-azabenzimidazole in the N1-substituted analog [**3-61**] (Figure 3-13). The NOE data are consistent with the structural assignment.

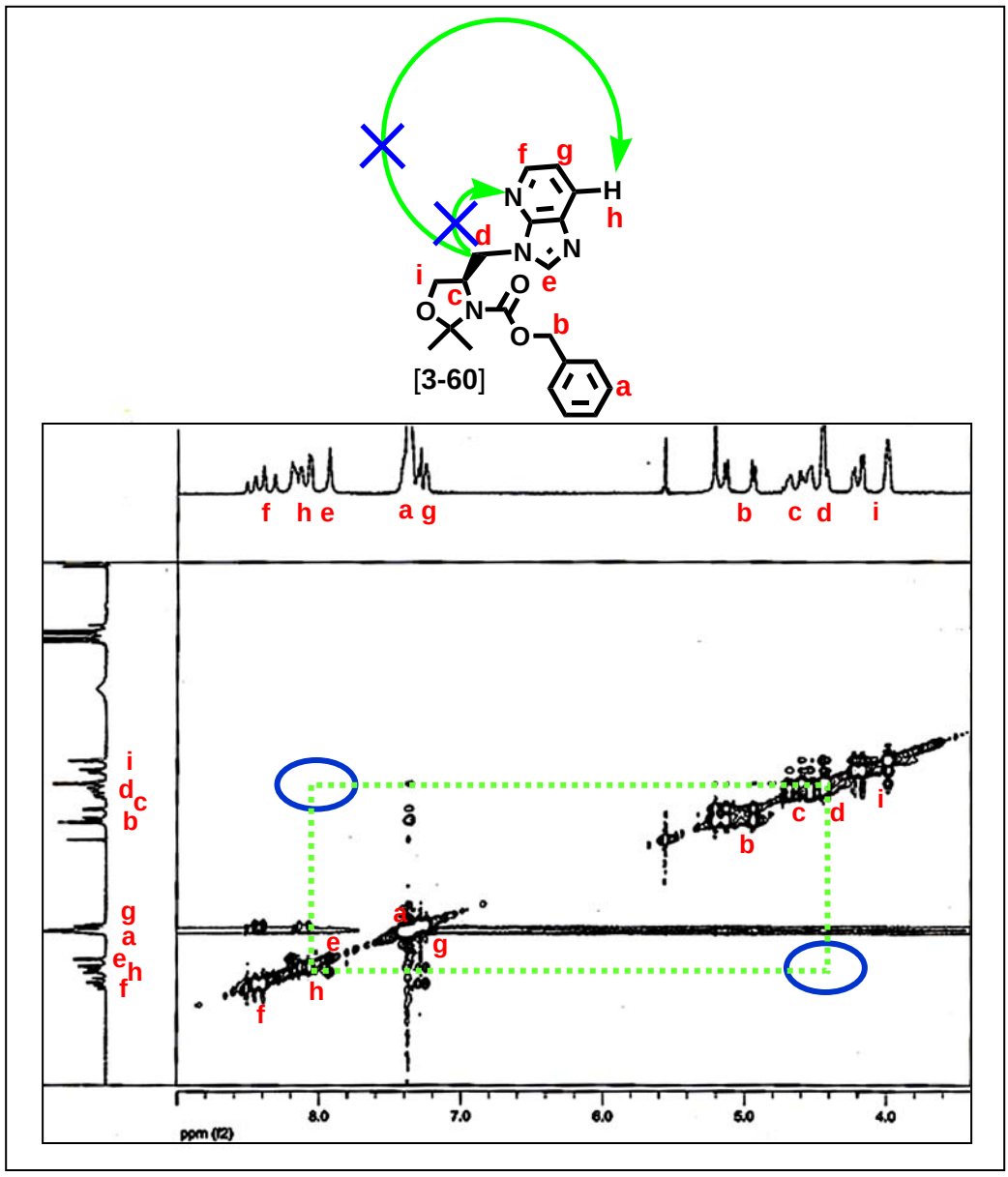

Figure 3-12: 2D-NOESY NMR spectra of N3-substituted 4-azabenzimidazole analog [**3-60**] do not have an NOE between the β-hydrogens (**d**) and N4 because there are no protons on the nitrogen. There are also no NOEs between the β-hydrogens (**d**) and the 4-azabenzimidazole H7 (**h**) because they are too far away from each other.

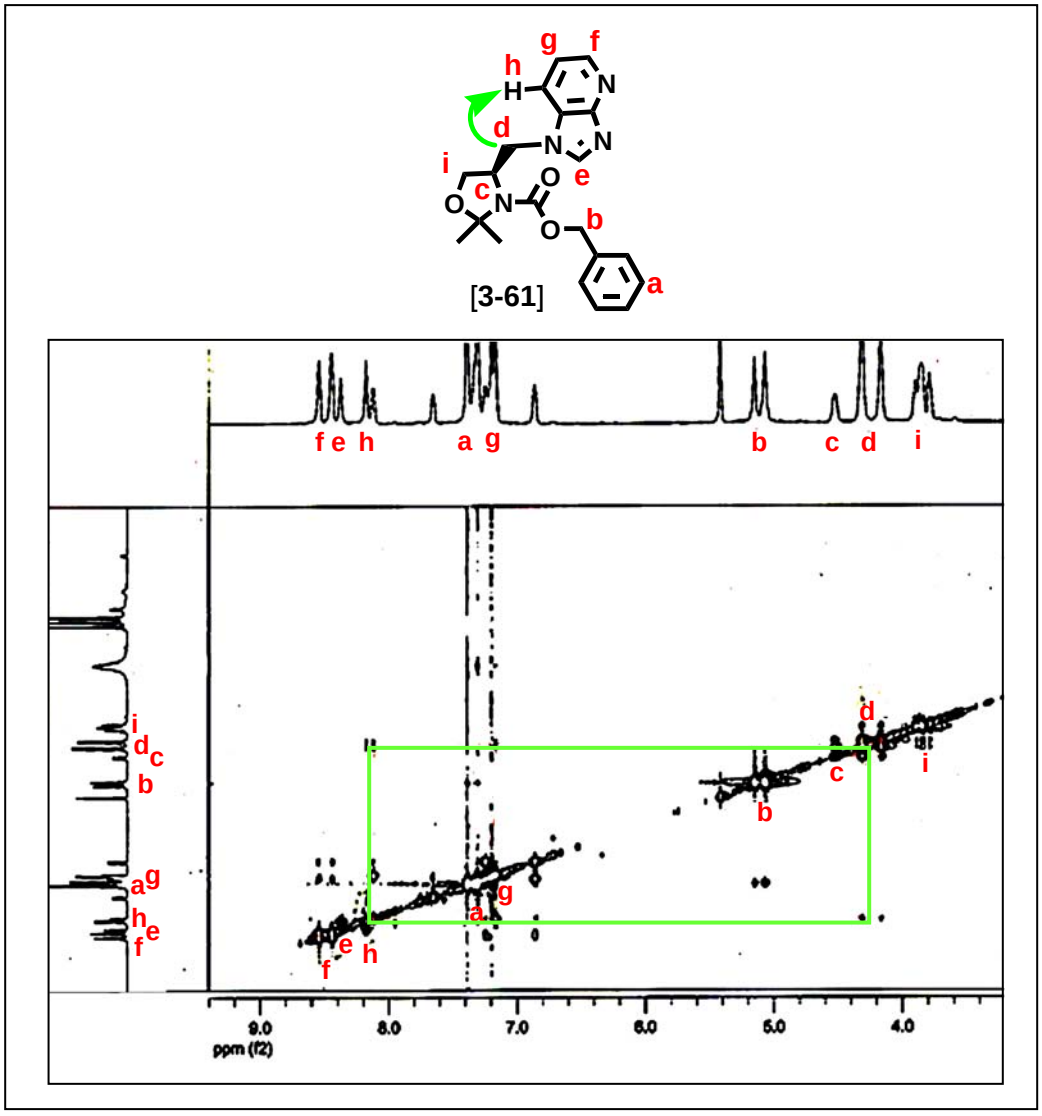

Figure 3-13: 2D-NOESY NMR spectra of N1-substituted 4-azabenzimidazole analog [**3-61**] shows an NOE between the β-hydrogens (**d**) and 4-azabenzimidazole H7 (**h**).

The structural assignment of the 4-azabenzimidazole regioisomers was further supported by ^{1}H NMR data. Similar to the previously described purine analogs, the signal of H2 for the N3-substituted 4-azabenzimidazole amino acid [**3-62**] was shifted

upfield (8.966 ppm) in the ^{1}H NMR spectrum, relative to the corresponding signal of H2 for the N1-substituted isomer [**3.63**] (9.182 ppm). The aromatic regions of the ^{1}H NMR spectra of 4-azabenzimidazole amino acids, N3-substutited alcohol [**3-62**] and N1-substituted [**3-63**] are compared in Figure 3-14.

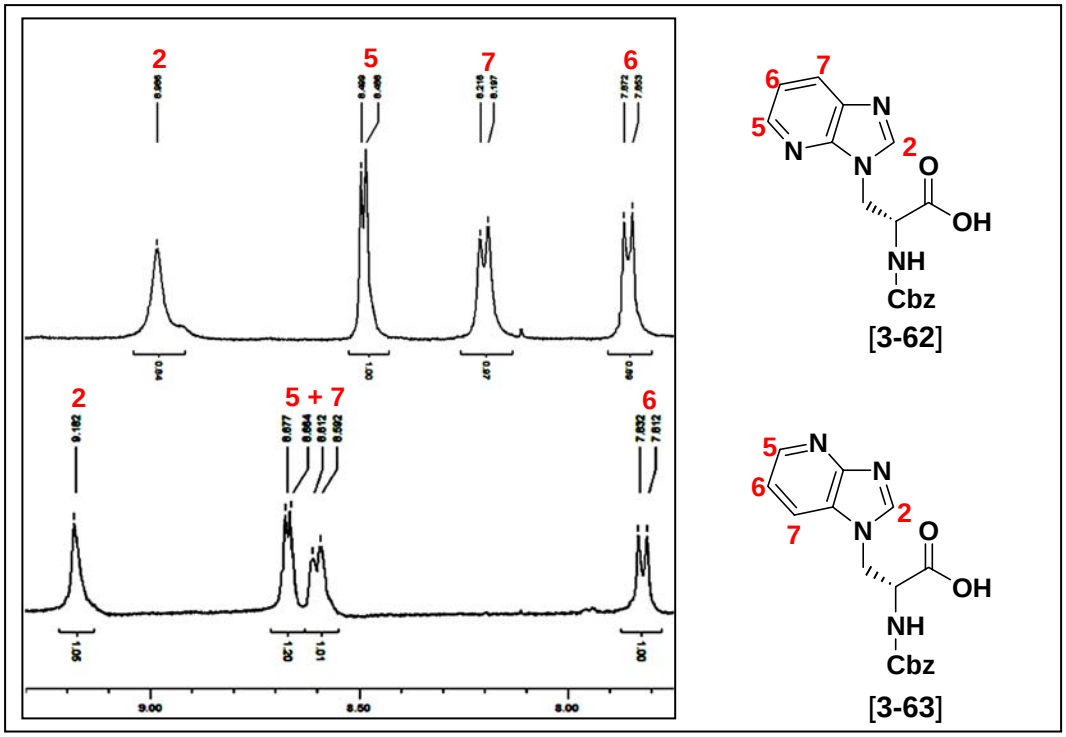

Figure 3-14: The aromatic regions of the ^{1}H NMR spectra of the N3-substituted 4-azabenzimidazole amino acid [**3-62**] and N1-substituted 4-azabenzimidazole amino acid [**3-63**]. The signal of H2 for compound [**3-62**] (8.966 ppm) is shifted upfield relative to the corresponding signal of H2 for compound [**3-63**] (9.182 ppm). This upfield shift supports the structural assignments of the regioisomers.

3.3 Incorporation of synthesized amino acids into peptides

With the amino acid derivatives in hand, we wanted to incorporate them into the structure of L-363,301 [**2-4**]. We chose three of the analogs as our initial targets, including the heterocyclic amino acids based on benzimidazole [**3-47**], 1-benzotriazole [**3-50**], and indazole [**3-53**]. We planned to synthesize the peptides on solid support and then cleave them from the resin and cyclize in solution.

Fmoc-Phe-OH was loaded onto chlorotrityl resin using TEA under inert, dry conditions. After loading and washing, the resin was dried and weighed. The Fmoc-protecting group was then removed with piperidine. The resin was again washed, dried and weighed. The change in mass of the dry resin before and after Fmoc-deprotection enabled us to calculate a loading of 1.01 mmol/ g. Additionally, a known mass of resin was treated with 1% TFA/ DCM to remove the amino acid from the resin. The resulting residue was dried and weighed to determine how much amino acid was present. This enabled us to calculate a loading of 0.98 mmol/ g.

The peptides were elongated by stepwise coupling of Fmoc-amino acid derivatives using DIC/ HOBt under standard coupling procedures. As demonstrated in Scheme 3-13 with the dibenzofuran amino acid [**3-47**], the three Cbz-protected unnatural amino acids were coupled to the resin bound pentapeptide, H-Lys(Boc)-Thr(*t*-But)-Phe-Pro-Phe-Trt resin [**3-64**]. The peptide was cleaved from the resin using 1% TFA in DCM in the presence of anisole to provide the linear hexapeptide [**3-65**] in 88% yield based on the calculated loading of the first Phe residue.

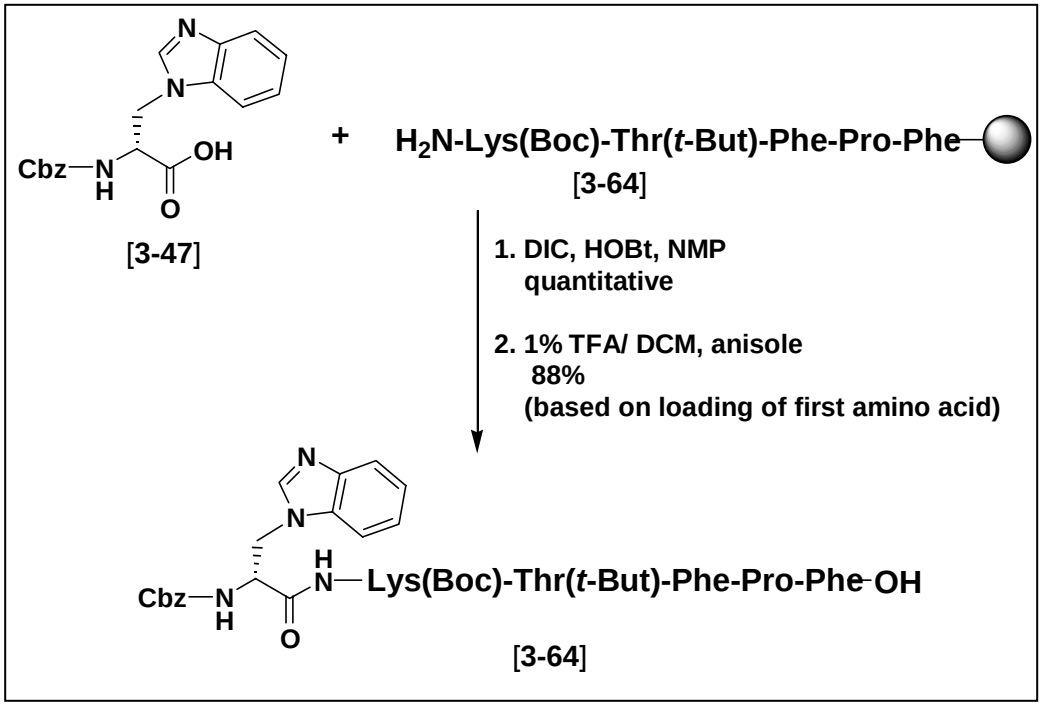

Scheme 3-13: The coupling of the building blocks to the resin bound pentapeptide and subsequent cleavage from the resin, using the benzimidazole amino acid [**3-47**] as a representative example.

The analytical RP-HPLC trace in Figure 3-15 demonstrates the high purity of the crude linear hexapeptide [**3-65**] after cleavage from the resin.

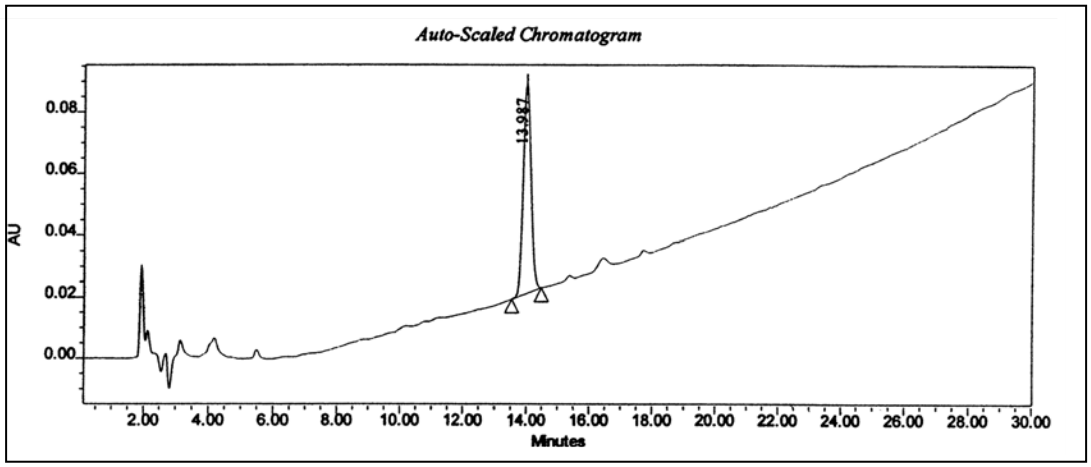

Figure 3-15: An analytical RP-HPLC trace of the crude linear hexapeptide [**3-63**] after cleavage from the resin.

The Cbz protecting group was removed from the peptide with palladium mediated catalytic hydrogenation in trifluoroethanol to provide free amine [**3-64**] (Scheme 3-13) in 80% yield. The peptide was then cyclized in solution using EDC, HOBt, and DIEA in a dilute mixture of 2:1 DCM:DMF over night. After washing with diethyl ether, the cyclic peptide was obtained in 60% yield and was >99% pure as measured by analytical RP-HPLC. The protecting groups were quantitatively removed by treatment with TFA in presence of anisole to provide the deprotected cyclic peptide [**3-67**] in quantitative yield. Figure 3-16 depicts the three cyclic hexapeptide analogs of L-363,301 which incorporate the unnatural amino acids in place of the D-Trp residue. Peptide [**3-67**] incorporates the benzimidazole analog, peptide [**3-68**] contains the 1-benzotriazole analog, and peptide [**3-69**] contains the indazole analog. The syntheses of analogs [**3-68**] and [**3-69**] are analogous to the synthesis of compound [**3-67**].

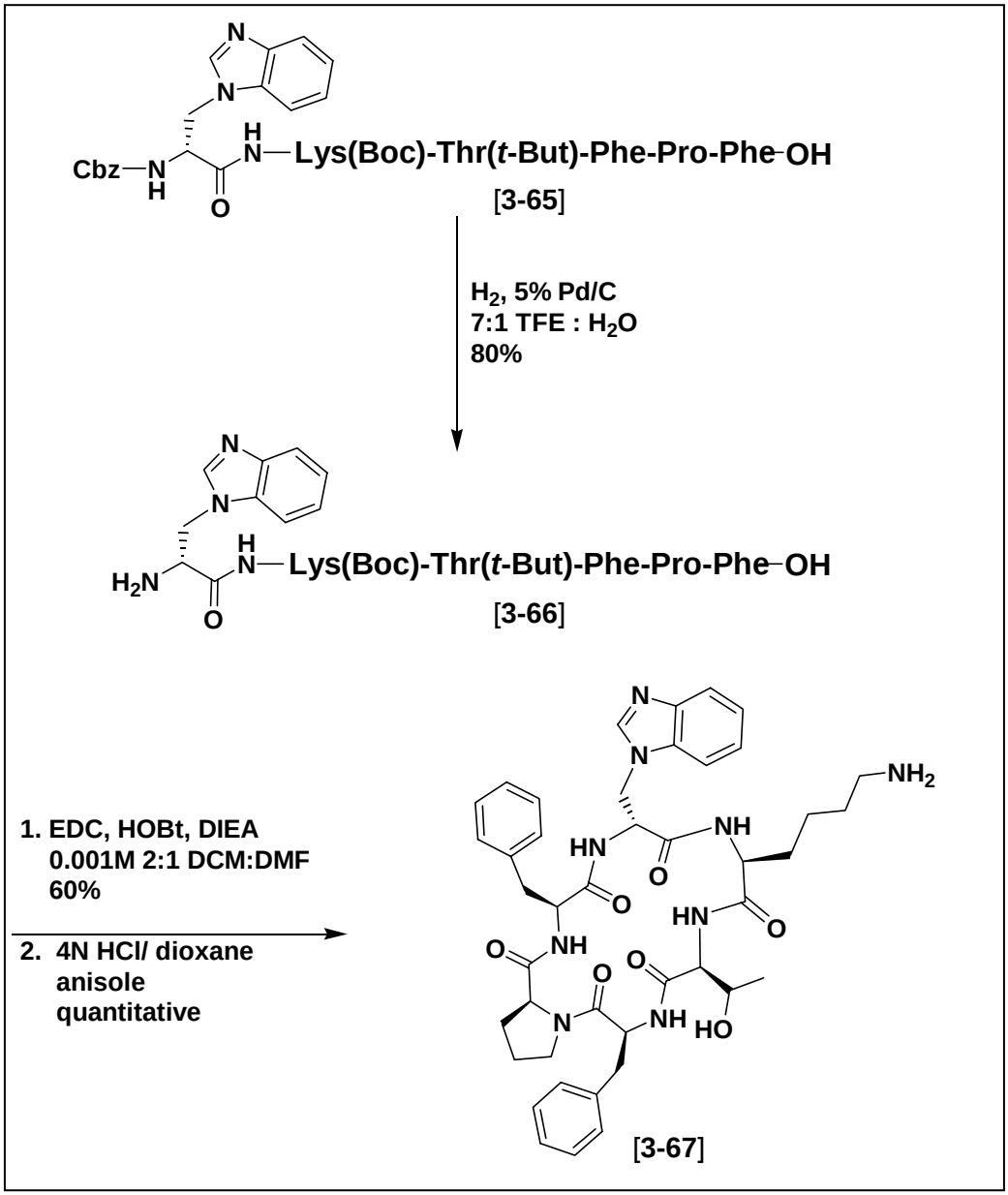

Scheme 3-14: Cbz-deprotection of the amine terminus, macrocyclization, and final deprotection with TFA provided cyclic hexapeptide [**3-67**].

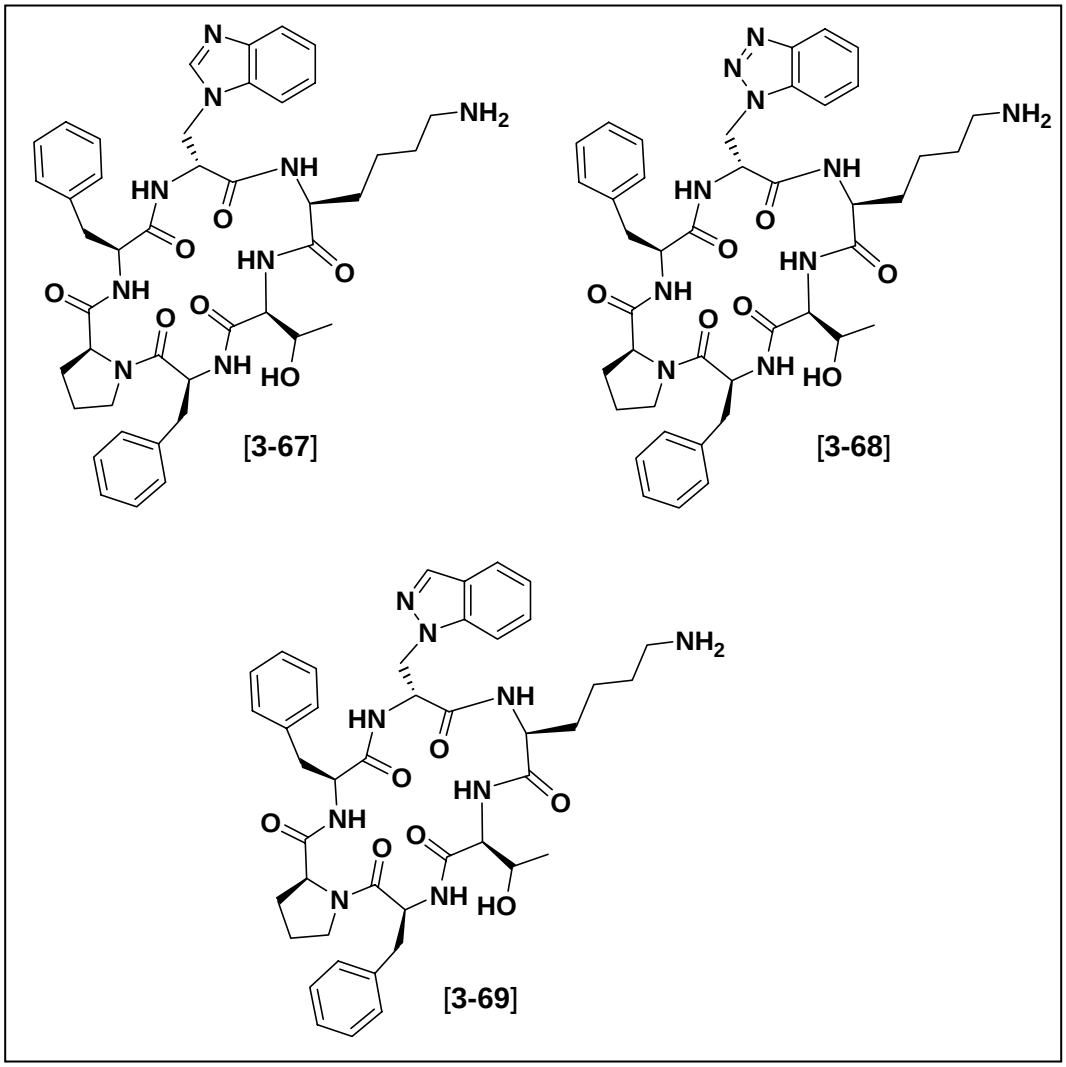

Figure 3-16: The cyclic hexapeptide analogs of L-363,301 which contain the synthesized unnatural amino acids in place of the D-Trp residue: benzimidazole-containing [**3-67**], 1-benzotriazole-containing [**3-68**], and indazole-containing [**3-69**].

3.4 Conclusions

We designed and synthesized unnatural nitrogen-containing, fused 5,6-heterocyclic, aromatic α-amino acids for use in our research programs. The syntheses of all the compounds involved the nucleophilic displacement of a tosyl group on Garner's alcohol, a common intermediate. The synthetic route of the common intermediate was completed on multigram scale. The route allowed us to begin with L-serine and, through an inversion of configuration, provided the desired D-amino acids in good yields.

The target compounds were designed to be analogs of naturally occurring tryptophan for incorporation into our somatostatin program. The amino acids are based on benzimidazole [**3-47**], 1-benzotriazole [**3-50**], 2-benzotriazole [**3-51**], indazole [**3-53**], N9-purine [**3-54**], N7-purine [**3-55**], N3-4-azabenzimidazole [**3-62**], and N1-4-azabenzimidazole [**3-63**]. The benzotriazole, purine, and 4-azabenzimidazole analog syntheses each produced two regioisomers. In each case, the regioisomers were easily separated by column chromatography and structure assignments were made using ^{1}H-NMR and 2D-NMR techniques.

Three of the amino acids, *Z*-D-1*H*-benzimidazole-yl alanine [**3-47**], *Z*-D-1*H*-benzotriazole-yl alanine [**3-50**], and *Z*-D-1*H*-indazole-yl alanine [**3-53**], were incorporated into the pentapeptide, H-Lys(Boc)-Thr(*t*-But)-Phe-Pro-Phe [**3-64**] on solid supports in an effort to synthesize compounds comparable to somatostatin analog L-363,301 [**2-4**]. The three linear hexapeptides were cleaved from the resin, the

N-terminal Cbz-group removed, cyclized in solution, and deprotected to provide cyclic hexapeptides [**3-67**], [**3-68**], and [**3-69**] cleanly and in good yields.

To carry this research program forward, the remaining synthesized unnatural amino acids, *Z*-D-2*H*-benzotriazole-yl alanine [**3-51**], *Z*-D-9*H*-purine-yl alanine [**3-54**], *Z*-D-7*H*-purine-yl alanine [**3-55**], *Z*-D-3*H*-(4-azabenzimidazole-yl) alanine [**3-62**], and *Z*-D-1*H*-(4-azabenzimidazole-yl) alanine [**3-63**], would be incorporated into the peptide sequence. The peptides could then be assayed for binding affinity, potency, and selectivity at all five human somatostatin receptors, hsst1-5, in radiolabeled competitive binding assays. The results of the assays could help to establish structure-activity relationships for the aromatic ring system of the residues in the D-Trp position. The varied nitrogen placements among the designed amino acids could provide insight into the nature of the binding pocket of the receptors. Compounds which exhibited potent and selective binding could provide additional information if evaluated in functional assays for inhibition of GH, insulin, and glucagon secretion.

3.5 Experimental

3.5.1 General

The reagents were purchased from Sigma-Aldrich or Acros Organics and used without further purification. All standard amino acids were donated by Senn Chemicals, U.S.A. Chlorotrityl resin was donated by Rohm Haas. THF was dried by refluxing over sodium/ benzophenone. DCM and TEA were dried by refluxing over calcium hydride. DMF, DIEA, and ACN were dried by storing over activated molecular sieves for 2 days. Silica gel 60 (230 – 400 mesh) purchased from EM Scientific was used for column chromatography.

Reactions in solution were monitored by thin-layer chromatography (TLC) which was carried out on 0.25 mm E. Merck silica gel plates (60F-254) using UV light as the visualizing agent. The N-H containing compounds were visualized by exposing the TLC plate to chlorine gas (generated by dissolving potassium permanganate in concentrated HCl) for 30-60 seconds. The TLC plate was then dipped into a solution of KI and *o*-tolidine (500 mg KI in 50 mL water combined with a solution of *o*-tolidine in 45 mL water and 8 mL glacial acetic acid). To confirm the presence of a free amine, TLC plates were dipped into a 2% ninhydrin/ ethanol solution and then heated. The following solvent systems were used: (A) 20% EtOAc/ hex, (B) 1:1 EtOAc:hex, (C) 2:1 EtOAc:hex, (D) 2% acetone/ DCM, (E) 5% MeOH/ DCM, (F) 10% MeOH/ DCM, (G) 9:1:1 DCM:MeOH:AcOH, (H) 9:1:0.3 DCM:MeOH:AcOH.

Optical rotation ($[\alpha]_D^{20}$) was measured on a Perkin Elmer 241 polarimeter.

The 1D-NMR spectra were obtained on a Varian HG-400 (400 MHz) spectrometer. Chemical shifts (δ) are reported in parts per million (ppm) relative to residual undeuterated solvent as an internal standard. The following abbreviations were used to explain the multiplicities: s = singlet, d = doublet, t = triplet, q = quartet, m = multiplet, bs = broad singlet, bm = broad multiplet, dd = doublet of doublets, dt = doublet of triplets, dm = doublet of multiplets, dbm = doublet of broad multiplets.

The 2-D NMR NOESY spectra were obtained on a Bruker 600 MHz spectrometer.

Mass spectra were obtained from The Scripps Research Institute (TSRI), La Jolla, CA mass spectrometry facility using electrospray (ESI) and MALDI-FTMS techniques.

Analytical RP-HPLC was carried out on a Millenium 2010 system consisting of a Waters 715 Ultra WISP sample processor, a Waters TM 996 photodiode array detector, two Waters 510 pumps, and a NEC Power Mate 485/33I computer. The column was an Akzo Nobel KR100-5C18 kromasil column (250 mm x 4.6 mm). A 1 mg/ mL solution of each compound was made and 10 µl were injected at a flow rate of 1 mL/ min. Spectra were recorded at a wave length of λ = 220 nm. The solvents used were as follows: solvent A = 0.1% TFA in water, solvent B = 0.1% TFA in ACN.

3.5.2 Syntheses of amino acids

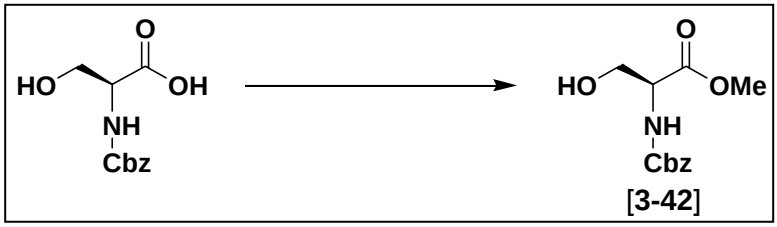

(2*S*)-2-Benzyloxycarbonylamino-3-hydroxypropionic acid methyl ester [3-42]: Cbz-L-Serine (15.0 g, 62.74 mmol) was dissolved in MeOH (450 mL) in a 1 L round bottom flask. $SOCl_2$ (9.11 mL, 125.48 mmol) was added, drop-wise, over 1 h. The reaction was left to stir for 4 h until complete as determined by TLC. The solution was concentrated under reduced pressure to provide 15.9 g of white, waxy crystals in quantitative yield. R_f = 0.36 in solvent system (A); $[\alpha]_D^{20}$ = -13.7° (*c* = 1.00, MeOH, 589 nm); ^{1}H NMR ($CDCl_3$, 400 MHz) δ 7.31 (m, 5 H, arom Z), 5.77 (d, 1 H, *J* = 6.8 Hz, NH), 5.12 (s, 2 H, Z CH_2), 4.44 (m, 1 H, α-H), 3.94 (dd, 2 H, β-CH_2), 3.76 (s, 3 H, OMe); MS (ESI) 276 M+Na]$^+$.

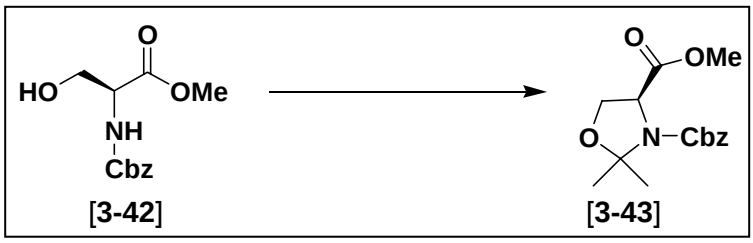

(4*S*)-*N*-Benzyloxycarbonyl-4-methoxycarbonyl-2,2-dimethyloxazolidine [3-43]: A 500 mL round bottom flask was charged with (2*S*)-2-benzyloxycarbonylamino-3-hydroxypropionic acid methyl ester [**3-42**] (17.18 g, 67.84 mmol), *p*-TsOH·H_2O

(0.19 g, 1.02 mmol), and 2, 2-dimethoxypropane (16.9 mL, 135.68 mmol) in benzene (310 mL). The reaction was heated at reflux for 45 min. The flask was then fitted with a Dean-Stark trap and 270 mL of distillate was collected. Additional benzene (134 mL) and 2,2-dimethoxypropane (5.1 mL, 40.70 mmol) were added and the reaction refluxed for 30 min. An additional 128 mL of distillate was collected. The cooled solution was diluted with DCM (200 mL) and washed with conc. $NaHCO_3$ (3 x 100 mL) and brine (1 x 150mL). The organic layer was dried over $MgSO_4$, filtered, and the filtrate concentrated under reduced pressure to a red-brown oil (21.0 g). The crude material was purified by column chromatography using 20% EtOAc/ hex as the eluent to yield a pale yellow oil (17.16 g, 84%). R_f = 0.23 in solvent system (A), R_f = 0.51 in solvent system (B), R_f = 0.60 in solvent system (C); $[\alpha]_D^{20}$ = -49.7° (*c* = 1.00, DCM, 589 nm); ^{1}H NMR ($CDCl_3$, 400 MHz) δ 7.32 (m, 5 H, arom Z), 5.18, 5.05 (rotamers, d, 1, 1 H, *J* = 12.2 Hz, Z CH_2), 4.54, 4.47 (rotamers, dd, 0.3, 0.7 H, *J* = 6.8, 2.8 Hz, α-H), 4.16, 4.09 (rotamers, m, 1, 1 H, CH_2), 3.77, 3.63 (rotamers, s, 1, 2 H, OMe), 1.70, 1.64 (rotamers, s, 2, 1 H, CH_3), 1.56, 1.49 (rotamers, s, 2, 1 H, CH_3); MS (ESI) 294 $[M+H]^+$, 316 $[M+Na]^+$.

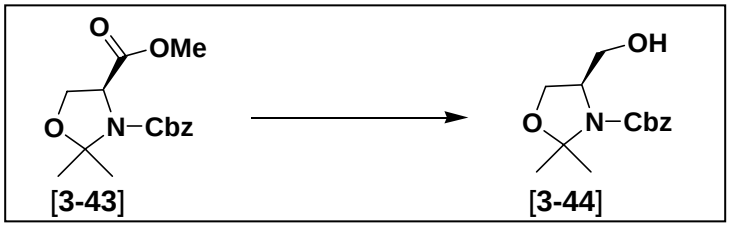

(4*R*)-*N*-Benzyloxycarbonyl-4-hydroxymethy-2,2-dimethyloxazolidine [3-44]: (4*S*)-*N*-Benzyloxycarbonyl-4-methoxycarbonyl-2,2-dimethyloxazolidine [**3-43**] (12.0 g, 40.91 mmol) was dissolved in dry THF (120 mL) in a 500 mL round bottom flask and cooled to 0 °C in an ice water bath. LiCl (3.46 g, 81.82 mmol) was added and the mixture stirred until most had dissolved. In a separate flask, $NaBH_4$ (3.10 g, 81.82 mmol) was suspended in dry EtOH and added to the reaction mixture at a rate which maintained the reaction temperature below 5 °C. When the addition was complete, the clear, colorless reaction was allowed to slowly warm to r.t. and stir over night. The reaction became cloudy with white precipitate. TLC confirmed the completion of the reaction. The solid was filtered from the solution and washed with EtOAc (200 mL). The filtrate was concentrated under reduced pressure to an oil. The oil was dissolved in EtOAc (300 mL) and washed with water (2 x 100 mL) and brine (1 x 150 mL). The organic layer was dried over $MgSO_4$, filtered, and the filtrate concentrated to a yellow oil (12.1 g). The crude material was purified by column chromatography using 2:1 hex: EtOAc as the eluent and switching to 1:1 hex: EtOAc after the yellow band eluted, to yield a pale yellow oil (10.31 g, 95%). R_f = 0.32 in solvent system (B); $[\alpha]_D^{20}$ = -19.4° (*c* = 1.00, DCM, 589 nm); ^{1}H NMR ($CDCl_3$, 400 MHz) δ 7.34 (m, 5 H, arom Z), 5.12 (d, 2 H, *J* = 14 Hz, Z CH_2), 4.09 (m, 1 H, α-H),

3.98, 3.84 (rotamers, m, 1, 1 H, CH_2), 3.76, 3.60 (rotamers, m, 1, 1 H, CH_2), 1.52 (m, 6 H, CH_3); MS (ESI) 288 $[M+Na]^+$.

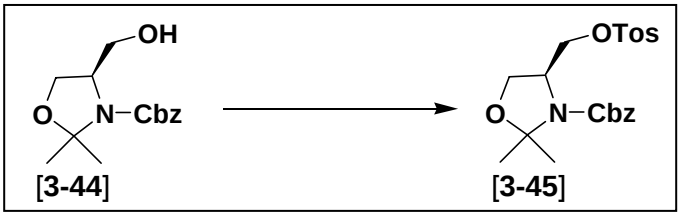

(4*S*)-*N*-Benzyloxycarbonyl-4-(*p*-toluenesulfonyloxymethyl)-2,2-dimethyl oxazolidine [3-45]: (4*R*)-*N*-Benzyloxycarbonyl-4-hydroxymethy-2,2-dimethyloxazolidine [**3-44**] (4.0 g, 14.74 mmol) was dissolved in freshly distilled DCM (35 mL) in 100 mL round bottom flask which was flushed with Ar. The flask was placed into an ice water bath and cooled to 0 °C. Pyridine (2.88 mL, 35.38 mmol) was added, followed by *p*-toluenesulfonyl chloride (3.37 g, 17.69 mmol). The reaction was allowed to slowly warm to r.t. and stir over night under Ar. Completion was confirmed by TLC. The solution was concentrated under reduced pressure. The resulting solid was dissolved in hot EtOAc and purified by column chromatography using 20% EtOAc/ hex as the eluent to yield a white, crystalline solid (4.64 g, 75%). (*Note: compound was not found to be stable for longer than 2 days, even when stored under high vacuum or under Ar at 0 °C.) R_f = 0.50 in solvent system (B), R_f = 0.43 in solvent system (D), R_f = 0.85 in solvent system (E); $[\alpha]_D^{20}$ = -44.1° (*c* = 1.00, DCM, 589 nm); ^{1}H NMR ($CDCl_3$, 400 MHz) δ 7.78, 7.67 (rotamers, d, 0.8, 1.2 H, *J* = 7.6 Hz, arom tos-H), 7.32 (m, 7 H, arom Z, tos-H), 5.09 (m, 2 H, Z CH_2), 4.17 (m, 2 H,

β-CH_2), 3.92 (m, 2 H, ring CH_2), 3.86 (t, 1 H, J = 10.4, 28.4 Hz, α-H), 2.43 (s, 3 H, tos CH_3), 1.48 (m, 6 H, CH_3); MS (ESI) 442 $[M+Na]^+$.

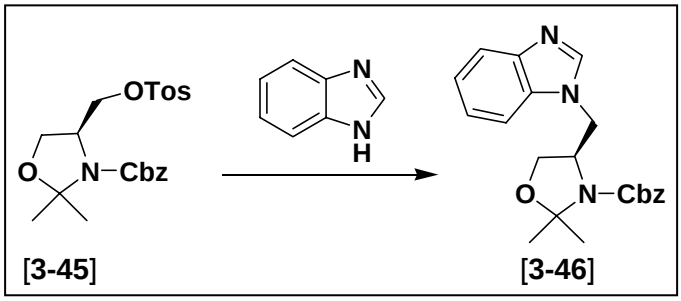

(4*S*)-*N*-Benzyloxycarbonyl-4-(1*H*-methyl-benzimidazole-yl)-2,2-dimethyloxazolidine [3-46]: (4*S*)-*N*-Benzyloxycarbonyl-4-(*p*-toluenesulfonyloxymethyl)-2,2-dimethyloxazolidine [**3-45**] (3.0 g, 7.15 mmol) was dissolved in freshly distilled THF (20 mL) under Ar atmosphere. Meanwhile, benzimidazole (1.01 g, 8.58 mmol) was dissolved in freshly distilled THF (20 mL) under Ar atmosphere. Solid 60% NaH (0.40 g, 10.01 mmol) was then slowly added. When gas evolution ceased, the slurry was added to the solution of tosylate and washed in with an additional portion of THF (12 mL). The reaction was then heated to 80 °C and left to stir over night under Ar. The reaction was cooled to r.t. and diluted with water (30 mL). It was washed with EtOAc (4 x 30 mL). The combined organic extracts were then washed with brine (1 x 50 mL), dried over $MgSO_4$, filtered, and the filtrate concentrated under reduced pressure to a gold solid (2.70 g). The solid was dissolved in DCM and purified by column chromatography using 3% MeOH/ DCM as the eluent to yield a white, crystalline foam (2.00 g, 77%). R_f = 0.06 in solvent system (B), R_f = 0.33 in solvent system (E), R_f = 0.68 in solvent system (F); $[\alpha]_D^{20}$ = +27.5°

(*c* = 1.00, DCM, 589 nm); ^{1}H NMR ($CDCl_3$, 400 MHz) δ 8.04, 7.99 (rotamers, s, 1 H, arom bi H2), 7.77 (m, 2 H, arom bi H4, H7), 7.33 (m, 7 H, arom Z, bi H5, H6), 5.20 (m, 2 H, Z CH_2), 4.53, 4.31 (rotamers, dm, 0.4, 0.6 H, α-H), 4.27, 4.15 (rotamers, dm, 2 H, β-CH_2), 3.82 (m, 2 H, ring CH_2), 1.55 (rotamers, dd, 6 H, CH_3); MS (ESI) 366 $[M+H]^+$.

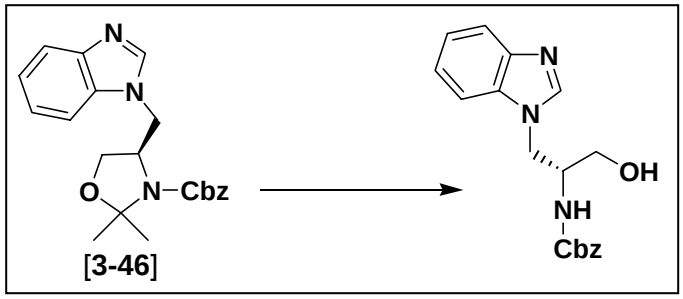

(2*S*)-3-(1*H*-Benzimidazole-yl)-2-benzyloxycarbonylamino-propanol: (4*S*)-*N*-Benzyloxycarbonyl-4-(1*H*-methyl-benzimidazole-yl)-2,2-dimethyloxazolidine [**3-46**] (0.66 g, 1.80 mmol) was dissolved in 4N HCl/ dioxane (10 mL) and allowed to stir for 1 h. A white solid precipitate formed. The solution was concentrated under reduced pressure to afford 0.56 g of a white solid in quantitative yield. R_f = 0.56 in solvent system (F); $[\alpha]_D^{20}$ = +35° (*c* = 1.00, MeOH, 589 nm); ^{1}H NMR ($CDCl_3$ and CD_3OD , 400 MHz) δ 9.55 (s, 1 H, arom bi H2), 7.88 (m, 1 H, arom bi H7), 7.73 (m, 1 H, arom bi H4), 7.54 (m, 2 H, arom bi H5, H6), 7.19 (m, 5 H, arom Z), 4.90 (s, 2 H, Z CH_2), 4.71, 4.51 (dd, 1,1 H, *J* = 8.0, 9.2 Hz, β-CH_2), 3.59 (m, 3 H, α-H, alc CH_2); MS (ESI) 326 $[M+H]^+$, 348 $[M+Na]^+$.

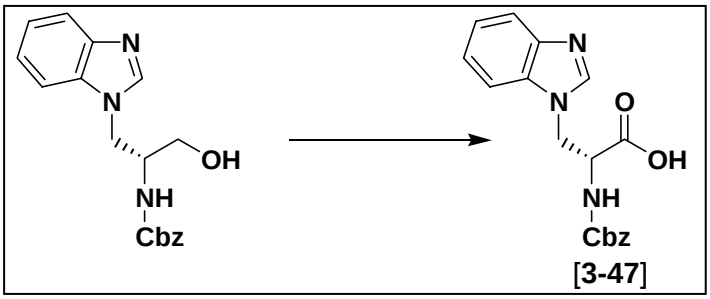

(2*S*)-3-(1*H*-Benzimidazole-yl)-2-benzyloxycarbonylamino-propanoic acid (or *Z*-D-1*H*-benzimidazole alanine) [3-47]: (2*S*)-3-(1*H*-Benzimidazole-yl)-2-benzyloxycarbonylamino-propanol (0.60 g, 1.66 mmol) was dissolved in ACN (9 mL), added to pH = 6.7 phosphate buffer (7 mL), and heated to 50 °C. A catalytic amount of TEMPO (0.026 g, 0.166 mmol) was added, followed by simultaneous addition of sodium chlorite solution (0.55 g of 80% $NaClO_2$ in 2.4 mL water) and bleach solution (0.12 mL of household bleach (~ 5% NaOCl) in 2.4 mL water) over 10 minutes. **Caution! Do NOT mix the sodium chlorite and bleach solutions prior to addition, as the mixture appears to be unstable.[27]** The brown solution was left to stir over night at 50 °C. By TLC the reaction was complete. The reaction was cooled to 0 °C in an ice water bath. Water was added (25 mL), followed by drop-wise addition of a saturated solution of Na_2SO_3 until the solution became colorless. The product precipitated, was filtered from the solution, and dried under reduced pressure afford 0.50 g of a white solid (90% yield). R_f = 0.21 in solvent system (G); $[\alpha]_D^{20}$ = +72.0° (*c* = 1.00, DMF, 589 nm), $[\alpha]_D^{20}$ = +36.3° (*c* = 1.00, 4.5:4.0:1.0 MeOH:ACN:water, 589 nm); Analytical RP-HPLC: 90A:10B → 10A:90B / 30 min. r_t = 17.18 min, as a single peak; ^{1}H NMR (CD_3CN and CD_3OD, 400 MHz) δ 8.06 (s, 1 H, arom bi H2), 7.68 (m,

1 H, arom bi H7), 7.58 (m, 1 H, arom bi H4), 7.30 (m, 7 H, arom Z, bi H6, H5), 5.00 (s, 2 H, Z CH_2), 4.73 (q, 1 H, J = 10.0 Hz, α-H), 4.61 (t, 2 H, J = 10.0 Hz, β-CH_2); ^{13}C NMR (400 MHz, DMSO-d_6) δ 171.7 (1 C, COOH), 156.5 (1 C, C=O of Z), 145.0 (1 C, Z C1), 143.8 (1 C, bi C2), 137.3, 134.5 (2 C, bi C7a, C3a), 128.9, 128.4, 128.1 (5 C, Z C2-C6), 123.1, 122.2 (2 C, bi C5, C6), 120.0, 110.9 (2 C, bi C4, C7), 66.3 (1 C, Z CH_2), 54.9 (1 C, α-C), 45.4 (1 C, β-C); MS (ESI) 340 $[M+H]^+$, 338 $[M-H]^-$.

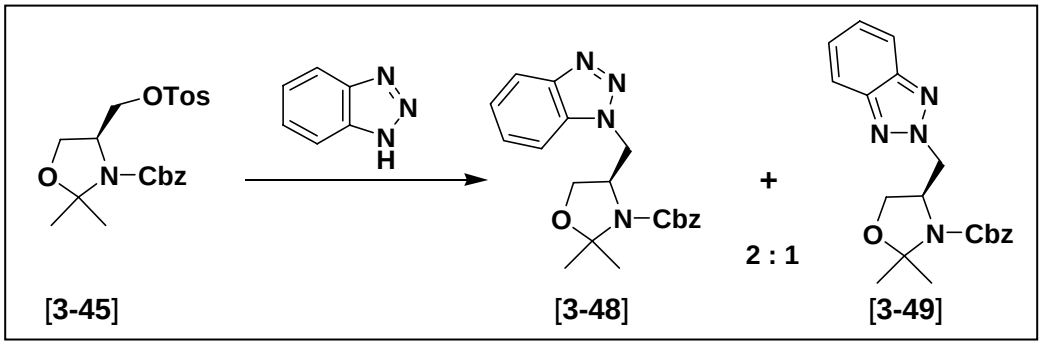

(4*S*)-*N*-Benzyloxycarbonyl-4-(1*H*-methyl-benzotriazole-yl)-2,2-dimethyloxazolidine [3-48] and **(4*S*)-*N*-Benzyloxycarbonyl-4-(2*H*-methyl-benzotriazole-yl)-2,2-dimethyloxazolidine [3-49]:** (4*S*)-*N*-Benzyloxycarbonyl-4-(*p*-toluenesulfonyloxymethyl)-2,2-dimethyloxazolidine [**3-45**] (2.0 g, 4.77 mmol) was dissolved in freshly distilled DMF (20 mL) under Ar atmosphere. Separately, benzotriazole (0.68 g, 5.72 mmol) was dissolved in freshly distilled DMF (15 mL) under Ar atmosphere. Solid 60% NaH (0.27 g, 6.68 mmol) was then slowly added. When gas evolution ceased, the slurry was added to the solution of tosylate and washed in with an additional portion of DMF (5 mL). The reaction was heated to 80 °C and left to stir over night under Ar. The yellow reaction was complete by TLC

and was concentrated under reduced pressure to a yellow residue. The residue was partitioned between DCM (40 mL) and water (40 mL). The layers were separated and the aqueous phase back-extracted with DCM (40 mL). The combined organic solution was washed with brine (1 x 50 mL), dried over $MgSO_4$, filtered, and the filtrate concentrated under reduced pressure to a gold solid (2.0 g). The solid was dissolved in 2% acetone/ DCM and purified by column chromatography in the same solvent system to yield two regioisomers in a 2:1 ratio with an overall yield of 80%.

(4*S*)-*N*-Benzyloxycarbonyl-4-(1*H*-methyl-benzotriazole-yl)-2,2-dimethyloxazolidine [3-48]: The more polar compound, (4*S*)-*N*-Benzyloxycarbonyl-4-(1*H*-methyl-benzotriazole-yl)-2,2-dimethyloxazolidine [**3-48**] was isolated as a white solid (0.93 g). R_f = 0.18 in solvent system (D), R_f = 0.73 in solvent system (E); $[\alpha]_D^{20}$ = +48.5° (*c* = 1.00, DCM, 589 nm); ^{1}H NMR ($CDCl_3$, 400 MHz) δ 8.06, 8.00 (rotamers, d, 1 H, *J* = 8.4, 8.0 Hz, arom bt H7), 7.85, 7.75 (rotamers, m, 1 H, arom bt H4), 7.39 (m, 5 H, arom Z), 7.32, 7.17 (t, 1 H, *J* = 7.6, 8.0 Hz, arom bt H6, H5), 5.23, 5.16 (rotamers, d, 2 H, *J* = 4.4 Hz, Z CH_2), 4.88, 4.68 (rotamers, m, 2 H, β-CH_2), 4.27, 4.22 (rotamers, m, 1 H, α-H), 4.16 (dd, 1 H, *J* = 9.2, 9.6 Hz, ring CH_2), 3.87 (dm, 1 H, ring CH_2), 1.59 (rotamers, m, 6 H, CH_3); MS (ESI) 367 $[M+H]^+$, 389 $[M+Na]^+$.

(4*S*)-*N*-Benzyloxycarbonyl-4-(2*H*-methyl-benzotriazole-yl)-2,2-dimethyloxazolidine [3-49]: The less polar compound, (4*S*)-*N*-Benzyloxycarbonyl-4-(2*H*-methyl-benzotriazole-yl)-2,2-dimethyloxazolidine [**3-49**] was isolated as a white

solid (0.47 g). R_f = 0.35 in solvent system (D), R_f = 0.74 in solvent system (E); $[\alpha]_D^{20}$ = +27.4° (*c* = 1.00, DCM, 589 nm); ^{1}H NMR ($CDCl_3$, 400 MHz) δ 7.85 (m, 2 H, arom bt H7, H4), 7.37 (m, 7 H, arom Z, bt H6, H5), 5.18 (m, 2 H, Z CH_2), 4.93, 4.78 (rotamers, m, 2 H, β-CH_2), 4.62 (m, 1 H, α-H), 4.10, 3.95 (rotamers, m, 2 H, ring CH_2), 1.54 (rotamers, m, 6 H, CH_3); MS (ESI) 389 $[M+Na]^+$.

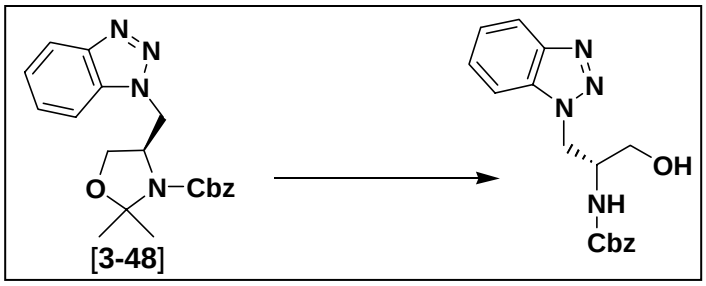

(2*S*)-3-(1*H*-Benzotriazole-yl)-2-benzyloxycarbonylamino-propanol: (4*S*)-*N*-Benzyloxycarbonyl-4-(1*H*-methyl-benzotriazole-yl)-2,2-dimethyloxazolidine [**3-48**] (0.61 g, 1.66 mmol) was dissolved in 4N HCl/ dioxane (12 mL) and allowed to stir for 1 h. The solution was concentrated under reduced pressure to afford 0.54 g of a white solid in quantitative yield. R_f = 0.38 in solvent system (E), R_f = 0.63 in solvent system (F), R_f = 0.78 in solvent system (G); $[\alpha]_D^{20}$ = +23.1° (*c* = 1.00, MeOH, 589 nm); ^{1}H NMR (CD_3OD, 400 MHz) δ 7.98 (d, 1 H, *J* = 8.4, Hz, arom bt H7), 7.85 (d, *J* = 8.4 Hz, 1 H, arom bt H4), 7.56 (t, 1 H, *J* = 7.2, 8.0 Hz, arom bt H6), 7.48 (t, 1 H, *J* = 7.2, 8.0 Hz, arom bt H5), 7.29 (m, 5 H, arom Z), 5.02 (m, 2 H, Z CH_2), 4.83 (m, 2 H, β-CH_2), 4.19 (m, 1 H, α-H), 3.66 (d, 2 H, *J* = 5.6 Hz, alc CH_2); MS (ESI) 327 $[M+H]^+$, 349 $[M+Na]^+$.

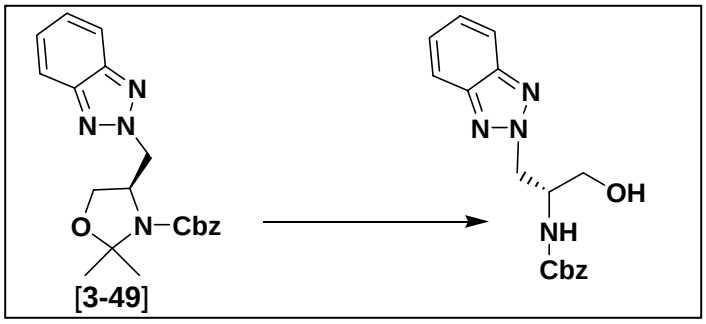

[**3-49**]

(2*S*)-3-(2*H*-Benzotriazole-yl)-2-benzyloxycarbonylamino-propanol: (4*S*)-*N*-Benzyloxycarbonyl-4-(2*H*-methyl-benzotriazole-yl)-2,2-dimethyloxazolidine [**3-49**] (0.40 g, 1.10 mmol) was dissolved in 4N HCl/ dioxane (8 mL) and allowed to stir for 1 h. The solution was concentrated under reduced pressure to afford 0.36 g of a white foam in quantitative yield. R_f = 0.27 in solvent system (E), R_f = 0.44 in solvent system (F), R_f = 0.63 in solvent system (G); $[\alpha]_D^{20}$ = +36.1° (*c* = 1.00, MeOH, 589 nm); ^{1}H NMR (CD_3OD, 400 MHz) δ 7.83 (m, 2 H, arom bt H7, H4), 7.41 (m, 2 H, arom bt H6, H5), 7.22 (m, 5 H, arom Z), 4.96 (m, 2 H, Z CH_2), 4.83 (m, 2 H, β-CH_2), 4.35 (m, 1 H, α-H), 3.65 (dd, 2 H, *J* = 1.6 Hz, alc CH_2); MS (ESI) 349 $[M+Na]^+$.

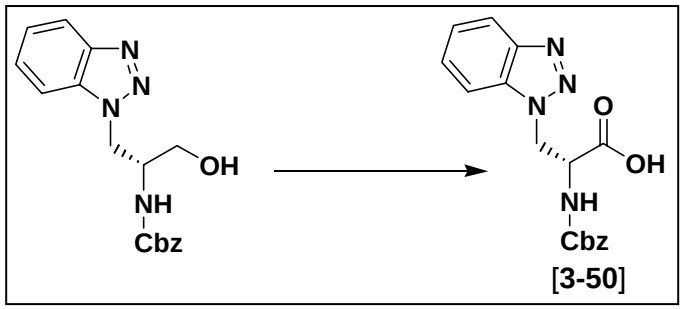

[**3-50**]

(2*S*)-3-(1*H*-Benzotriazole-yl)-2-benzyloxycarbonylamino-propanoic acid (or Z-D-1*H*-benzotriazole alanine) [3-50]: (2*S*)-3-(1*H*-Benzotriazole-yl)-2-

benzyloxycarbonylamino-propanol (0.56 g, 1.40 mmol) was dissolved in ACN (8 mL), added to pH = 6.7 phosphate buffer (6 mL), and heated to 50 °C. A catalytic amount of TEMPO (0.022 g, 0.140 mmol) was added, followed by simultaneous addition of sodium chlorite solution (0.46 g of 80% $NaClO_2$ in 2 mL water) and bleach solution (0.10 mL of household bleach (~ 5% NaOCl) in 2 mL water) over 10 minutes. **Caution! Do NOT mix the sodium chlorite and bleach solutions prior to addition, as the mixture appears to be unstable.[27]** The brown-orange solution was left to stir over night at 50 °C. By TLC the reaction was complete. The reaction was cooled to 0 °C in an ice water bath. Water was added (16 mL), followed by drop-wise addition of a saturated solution of Na_2SO_3 until the solution became colorless. The solution was basified to pH = 9 with 1 N NaOH (~ 20 mL). The aqueous solution was washed with Et_2O (4 x 20 mL) until the washes showed no uv activity on TLC plates. The aqueous solution was then acidified to pH = 6 with 1 N HCl (~ 25 mL) and saturated with NaCl. It was extracted with THF (6 x 25 mL) until no product remained in the aqueous layer by TLC. The organic washes were then dried over $MgSO_4$, filtered, and concentrated under reduced pressure to afford 0.47 g of a white foam in quantitative yield. R_f = 0.20 in solvent system (F), R_f = 0.58 in solvent system (G); $[\alpha]_D^{20}$ = -12.2° (*c* = 1.00, THF, 589 nm); Analytical RP-HPLC: 80A:20B → 10A:90B / 30 min. r_t = 18.75 min, 96% pure; ^{1}H NMR (DMSO-d_6, 400 MHz) δ 7.99 (d, 1 H, *J* = 8.4, Hz, arom bt H7), 7.82 (d, *J* = 8.4 Hz, 1 H, arom bt H4), 7.52 (t, 1 H, *J* = 7.2, 8.0 Hz, arom bt H6), 7.37 (t, 1 H, *J* = 7.2, 8.0 Hz, arom bt H5), 7.28 (m, 5 H, arom Z), 5.10 (dd, 1 H, *J* = 4.4 Hz, Z CH_2), 4.90 (m, 2 H, bzl CH_2, α-H) 4.45 (m, 2 H, β-CH_2); ^{13}C NMR

(400 MHz, DMSO-d_6) δ 171.4 (1 C, COOH), 156.3 (1 C, C=O of Z), 145.6 (1 C, Z C1), 137.4 (1 C, bt C7a), 134.0, (1 C, bt C4a), 128.9, 128.3, 128.0, (5 C, Z C2-C6), 127.8, 124.4 (2 C, bt C5, C6), 120.0, 111.4 (2 C, bt C4, C7), 66.1 (1 C, Z CH_2), 55.5 (1 C, β-C), 49.3 (1 C, α-C); MS (ESI) 339 $[M-H]^-$.

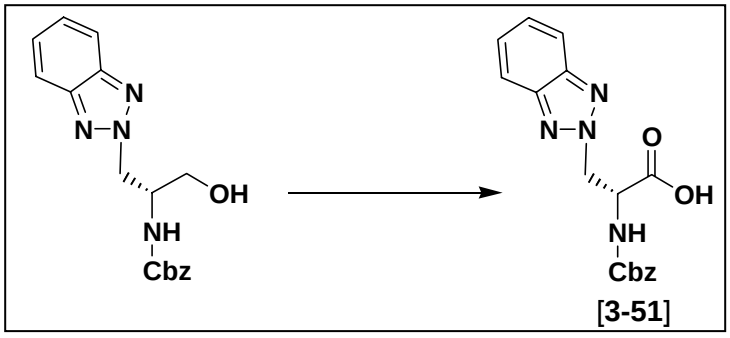

(2*S*)-3-(2*H*-Benzotriazole-yl)-2-benzyloxycarbonylamino-propanoic acid (or Z-D-2*H*-benzotriazole alanine) [3-51]: (2*S*)-3-(2*H*-Benzotriazole-yl)-2-benzyloxycarbonylamino-propanol (0.33 g, 1.01 mmol) was dissolved in ACN (5.5 mL), added to pH = 6.7 phosphate buffer (4 mL), and heated to 50 °C. A catalytic amount of TEMPO (0.016 g, 0.10 mmol) was added, followed by simultaneous addition of sodium chlorite solution (0.34 g of 80% $NaClO_2$ in 1.5 mL water) and bleach solution (0.08 mL of household bleach (~ 5% NaOCl) in 1.5 mL water) over 10 minutes. **Caution! Do NOT mix the sodium chlorite and bleach solutions prior to addition, as the mixture appears to be unstable.[27]** The brown-orange solution was left to stir over night at 50 °C. By TLC the reaction was complete. The reaction was cooled to 0 °C in an ice water bath. Water was added (15 mL), followed by drop-wise addition of a saturated solution of Na_2SO_3 until the solution became colorless. The

solution was basified to pH = 10 with 1 N NaOH (~ 6 mL). The aqueous solution was washed with Et_2O (3 x 30 mL) until the washes showed no uv activity on TLC plates. The aqueous solution was then acidified to pH = 2 with 1 N HCl (~ 10 mL) and became cloudy with white precipitate. It was extracted with EtOAc (4 x 40 mL) until no product remained in the aqueous layer by TLC. The organic washes were then dried over $MgSO_4$, filtered, and concentrated under reduced pressure to afford 0.29 g of a white solid (85% yield). R_f = 0.13 in solvent system (F), R_f = 0.50 in solvent system (G); $[\alpha]_D^{20}$ = -13.2° (*c* = 1.00, THF, 589 nm); Analytical RP-HPLC: 80A:20B → 10A:90B / 30 min. r_t = 18.09 min, 97.5% pure; ^{1}H NMR (DMSO-d_6, 400 MHz) δ 7.89 (m, 2 H, arom bt H7, H4), 7.77 (d. 1 H, *J* = 8.8 Hz, NH), 7.42 (m, 2 H, arom bt H6, H5), 7.22 (m, 5 H, arom Z), 5.13, 5.05 (dd, 1 H, *J* = 4.8, 9.2 Hz, bzl CH_2), 4.95 (m, 2 H, β-CH_2), 4.78 (m, 1 H, α-H); ^{13}C NMR (400 MHz, DMSO-d_6) δ 171.2 (1 C, COOH), 156.5 (1 C, C=O of Z), 145.6 (1 C, Z C1), 137.5 (2 C, bt C7a, C4a), 129.0, 128.4, 128.1, (5 C, Z C2-C6), 127.2, (2 C, bt C5, C6), 118.6 (2 C, bt C4, C7), 66.1 (1 C, Z CH_2), 56.8 (1 C, β-C), 54.7 (1 C, α-C); MS (ESI) 341 $[M+H]^+$, 363 $[M+Na]^+$, 385 $[M-H+2Na]^+$.

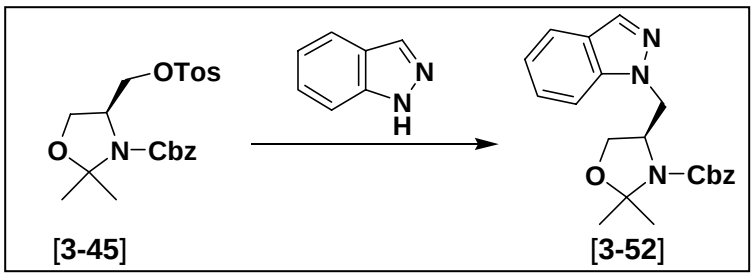

(4*S*)-*N*-Benzyloxycarbonyl-4-(1*H*-methyl-indazole-yl)-2,2-dimethyloxazolidine [3-52]: (4*S*)-*N*-Benzyloxycarbonyl-4-(*p*-toluenesulfonyloxymethyl)-2,2-dimethyloxazolidine [**3-45**] (0.50 g, 1.19 mmol) was dissolved in dry DMF (5 mL) under Ar atmosphere. Separately, indazole (0.17 g, 1.43 mmol) was dissolved in dry DMF (2 mL) under Ar atmosphere. Solid 60% NaH (0.07 g, 1.67 mmol) was then slowly added. When gas evolution ceased, the slurry was added to the solution of tosylate and washed in with an additional portion of DMF (3 mL). The reaction was then heated to 80 °C and left to stir over night under Ar. The cloudy, yellow reaction was cooled to r.t. and diluted with water (5 mL). It was concentrated to dryness under reduced pressure. The resulting residue was partitioned between water (15 mL) and DCM (20 mL). The layers were separated and the organic washed with brine (1 x 15 mL), dried over $MgSO_4$, filtered, and the filtrate concentrated under reduced pressure to a gold gel (0.49 g). The gel was dissolved in DCM and purified by column chromatography using 1% acetone/ DCM as the eluent to yield a white solid (0.22 g, 50%). R_f = 0.23 in solvent system (D), R_f = 0.71 in solvent system (E); $[\alpha]_D^{20}$ = +51.9° (*c* = 1.00, DCM, 589 nm); ^{1}H NMR ($CDCl_3$, 400 MHz) δ 7.98, 7.94 (rotamers, s, 1 H, arom ind H3), 7.69 (rotamers, 1 H, dd, *J* = 8.0, 8.8 Hz, arom ind H4), 7.42 (m, 6 H, arom Z, ind H7), 7.07 (m, 2 H, arom ind H6, H5), 5.18 (m, 2 H, Z CH_2), 4.40

(rotamers, m, 3 H, α-H, β-CH_2), 4.22, 3.83 (rotamers, dm, 2 H, ring CH_2), 1.66, 1.54, 1.43 (rotamers, s, s, d, 2, 2, 2 H, CH_3); MS (ESI) 366 $[M+H]^+$, 388 $[M+Na]^+$.

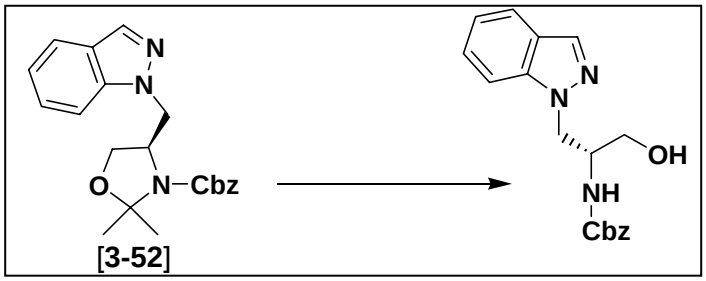

(2*S*)-3-(1*H*-Indazole-yl)-2-benzyloxycarbonylamino-propanol:

(4*S*)-*N*-Benzyloxycarbonyl-4-(1*H*-methyl-indazole-yl)-2,2-dimethyloxazolidine [**3-52**] (0.30 g, 0.82 mmol) was dissolved in 4N HCl/ dioxane (6 mL) and allowed to stir for 1 h. A white solid precipitate formed. The solution was concentrated under reduced pressure to afford 0.27 g of a white solid in quantitative yield. R_f = 0.42 in solvent system (E); $[\alpha]_D^{20}$ = +12.4° (*c* = 1.00, MeOH, 589 nm); ^{1}H NMR ($CDCl_3$, 400 MHz) δ 7.99 (s, 1 H, arom ind H3), 7.74 (d, 1 H, *J* = 8.0 Hz, arom ind H4), 7.60 (d, 1 H, *J* = 8.4 Hz, arom ind H7), 7.29 (m, 7 H, arom Z, ind H6, H5), 4.92 (s, 2 H, Z CH_2), 4.60, 4.50 (dd, 2 H, *J* = 5.6, 7.2 Hz, β-CH_2), 4.11 (m, 1 H, α-H), 3.56 (d, 2 H, *J* = 6.0 Hz, alc CH_2); MS (ESI) 326 $[M+H]^+$, 348 $[M+Na]^+$.

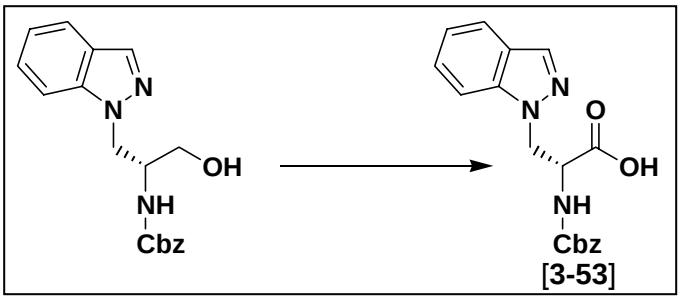

(2*S*)-3-(1*H*-Indazole-yl)-2-benzyloxycarbonylamino-propanoic acid (or *Z*-D-1*H*-Indazole alanine) [3-53]: (2*S*)-3-(1*H*-Indazole-yl)-2-benzyloxycarbonylamino-propanol (0.23 g, 0.63 mmol) was dissolved in ACN (4 mL), added to pH = 6.7 phosphate buffer (3 mL), and heated to 50 °C. A catalytic amount of TEMPO (0.010 g, 0.064 mmol) was added, followed by simultaneous addition of sodium chlorite solution (0.21 g of 80% $NaClO_2$ in 0.9 mL water) and bleach solution (0.05 mL of household bleach (~ 5% NaOCl) in 0.9 mL water) over 10 min. **Caution! Do NOT mix the sodium chlorite and bleach solutions prior to addition, as the mixture appears to be unstable.[27]** The brownish orange solution was left to stir over night at 50 °C. The reaction became colorless with white solid dispersed in it. By TLC the reaction was complete. It was cooled to 0 °C in an ice water bath. Water was added (7 mL), followed by drop-wise addition of a saturated solution of Na_2SO_3 (~ 3 mL). The solution was basified with 1 N NaOH (~ 6 mL) and washed with Et_2O (4 x 10 mL) until nothing was seen in the washes by TLC. The aqueous solution was acidified to pH = 4 with 1 N HCl (7 mL) and saturated with solid NaCl. It was extracted with 20 mL portions of EtOAc until no more product came out by TLC. The

organic washes were combined and dried over $MgSO_4$. The drying agent was removed by filtration and the filtrate concentrated under reduced pressure to afford 0.21 g of a white solid in quantitative yield. R_f = 0.17 in solvent system (F), R_f = 0.76 in solvent system (G); $[\alpha]_D^{20}$ = -21.6° (*c* = 1.00, THF, 589 nm); Analytical RP-HPLC: 80A:20B → 10A:90B / 30 min. r_t = 21.19 min, as a single peak; ^{1}H NMR (DMSO-d_6, 400 MHz) δ 8.07 (s, 1 H, arom ind H3), 7.72 (d, 1 H, *J* = 8.0 Hz, arom ind H4), 7.60 (m, 1 H, arom ind H7), 7.29, 7.14 (m, 7 H, arom Z, ind H6, H5), 4.89 (m, 2 H, Z CH_2), 4.70 (d, 2 H, *J* = 6.8 Hz, β-CH_2), 4.51 (m, 1 H, α-H); ^{13}C NMR (400 MHz, DMSO-d_6) δ 171.8 (1 C, COOH), 156.3 (1 C, C=O of Z), 140.5 (1 C, Z C1), 134.1 (2 C, ind C3, C7a), 128.9, 128.3, 128.0 (5 C, Z C2-C6), 126.7 (1 C, ind C6), 124.0 (1 C, ind C3a), 121.4, 121.0 (2 C, ind C4, C5), 110.3 (1 C, ind C7), 66.1 (1 C, Z CH_2), 55.2 (1 C, β-C), 49.5 (1 C, α-C); MS (ESI) 338 $[M-H]^-$.

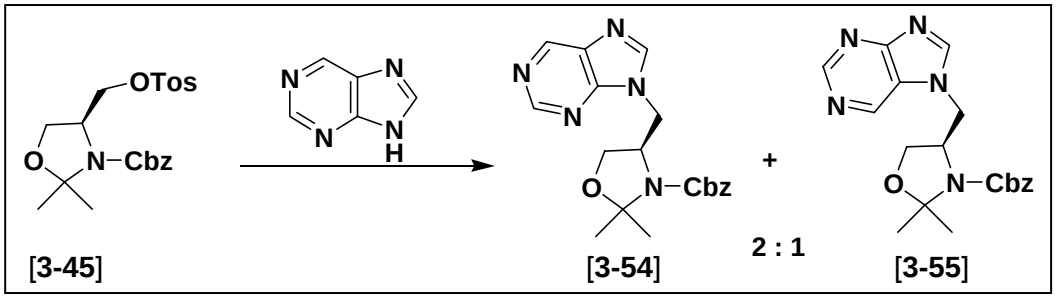

(4*S*)-*N*-Benzyloxycarbonyl-4-(9*H*-methyl-purine-yl)-2,2-dimethyloxazolidine [3-54] and **(4*S*)-*N*-Benzyloxycarbonyl-4-(7*H*-methyl-purine-yl)-2,2-dimethyloxazolidine [3-55]:** (4*S*)-*N*-Benzyloxycarbonyl-4-(*p*-toluenesulfonyloxymethyl)-2,2-dimethyloxazolidine [**3-45**] (1.46 g, 3.5 mmol) was

dissolved in freshly distilled DMF (10 mL) under Ar atmosphere. Separately, purine (0.50 g, 4.20 mmol) was dissolved in freshly distilled DMF (5 mL) under Ar atmosphere. Solid 60% NaH (0.20 g, 4.9 mmol) was then slowly added. When gas evolution ceased, the dark orange slurry was added to the solution of tosylate and washed in with an additional portion of DMF (5 mL). The reaction was heated to 80 °C and left to stir over night under Ar. The dark orange reaction was complete by TLC. Water (5 mL) was added, and the solution was concentrated under reduced pressure to an orange solid. The solid was dissolved in 5% MeOH/ DCM and purified by column chromatography in the same solvent system to yield two regioisomers in a 2:1 ratio with an overall yield of 70%.

(4*S*)-*N*-Benzyloxycarbonyl-4-(9*H*-methyl-purine-yl)-2,2-dimethyloxazolidine [3-54]: The less polar compound, (4*S*)-*N*-Benzyloxycarbonyl-4-(9*H*-methyl-purine-yl)-2,2-dimethyloxazolidine [**3-54**] was isolated as a pale yellow foam (0.61 g). R_f = 0.28 in solvent system (E), R_f = 0.63 in solvent system (F); $[\alpha]_D^{20}$ = +2.5° (*c* = 1.00, DCM, 589 nm); ^{1}H NMR ($CDCl_3$, 400 MHz) δ 9.07, 8.92 (rotamers, s, 2 H, arom pur H6, H2), 7.99, 7.76 (rotamers, s, 0.5, 0.5 H, arom pur H8), 7.33 (m, 5 H, arom Z), 5.17 (rotamers, s, 1 H, Z CH_2), 4.98 (rotamers, dd, 1 H, *J* = 12 Hz, Z CH_2), 4.50 (rotamers, m, 1 H, α-H), 4.39 (rotamers, m, 2 H, β-CH_2), 4.13, 4.00 (rotamers, dm, 2 H, ring CH_2), 1.52, 1.40, 1.32 (rotamers, d, s, s, 2, 2, 2 H, CH_3); MS (ESI) 368 $[M+H]^+$, 390 $[M+Na]^+$.

4*S*)-*N*-Benzyloxycarbonyl-4-(7*H*-methyl-purine-yl)-2,2-dimethyloxazolidine [3-55]: The more polar compound, (4*S*)-*N*-Benzyloxycarbonyl-4-(7*H*-methyl-purine-yl)-2,2-dimethyloxazolidine [**3-55**] was isolated as a pale yellow foam (0.30 g). R_f = 0.05 in solvent system (E), R_f = 0.60 in solvent system (F); $[\alpha]_D^{20}$ = +36.7° (*c* = 1.00, DCM, 589 nm); ^{1}H NMR ($CDCl_3$, 400 MHz) δ 9.23, 9.18, 9.11 (rotamers, s, 1.5 H, arom pur H6, H2), 8.58 (rotamers, s, 0.5 H, arom pur H6, H2), 8.21, 8.10 (rotamers, s, 0.5, 0.5 H, arom pur H8), 7.34 (m, 5 H, arom Z), 5.17 (rotamers, m, 2 H, Z CH_2), 4.39 (rotamers, m, 3 H, α-H, β-CH_2), 3.85, 3.80 (rotamers, dm, 2 H, ring CH_2), 1.66, 1.55, 1.43 (rotamers, s, s, s, 1.5, 1.5, 3 H, CH_3); MS (ESI) 368 $[M+H]^+$, 390 $[M+Na]^+$, 757 $[M_2+Na]^+$.

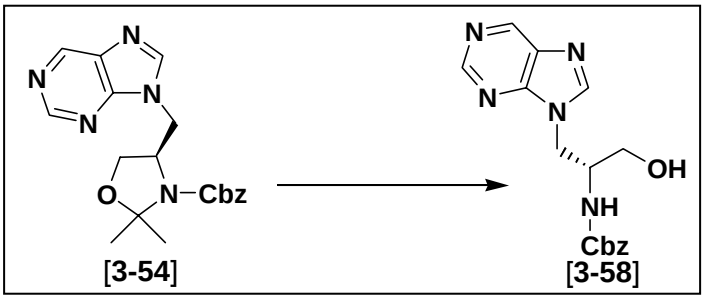

(2*S*)-3-(9*H*-Purine-yl)-2-benzyloxycarbonylamino-propanol [3-58]: (4*S*)-*N*-Benzyloxycarbonyl-4-(9*H*-methyl-purine-yl)-2,2-dimethyloxazolidine [**3-54**] (0.47 g, 1.28 mmol) was dissolved in 4N HCl/ dioxane (9 mL) and allowed to stir for 1 h. A white solid precipitate formed. The solution was concentrated under reduced pressure to afford 0.42 g of a white solid in quantitative yield. R_f = 0.13 in solvent system (F); $[\alpha]_D^{20}$ = +36.2° (*c* = 1.00, MeOH, 589 nm); ^{1}H NMR (CD_3OD, 400 MHz) δ

9.05 (s, 1 H, arom pur H2), 8.89 (s, 1 H, arom pur H6), 8.43 (s, 1 H, arom pur H8), 7.24 (m, 5 H, arom Z), 4.89 (m, 2 H, Z CH_2), 4.64, 4.41 (dd, 2 H, J = 4.0, 8.8 Hz, β-CH_2), 4.19 (m, 1 H, α-H), 3.31 (m, 2 H, alc CH_2); MS (ESI) 328 $[M+H]^+$, 350 $[M+Na]^+$.

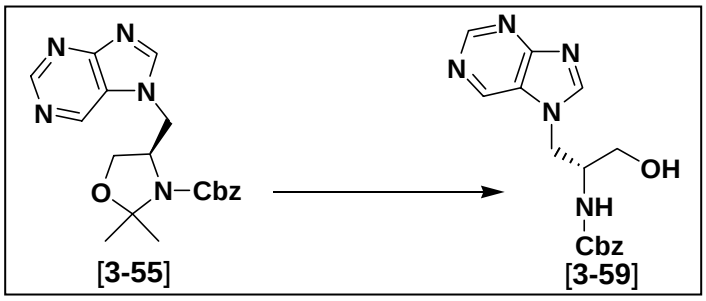

(2*S*)-3-(7*H*-Purine-yl)-2-benzyloxycarbonylamino-propanol [3-59]: (4*S*)-*N*-Benzyloxycarbonyl-4-(7*H*-methyl-purine-yl)-2,2-dimethyloxazolidine [**3-55**] (0.17 g, 0.46 mmol) was dissolved in 4N HCl/ dioxane (3 mL) and allowed to stir for 1 h. A white solid precipitate formed. The solution was concentrated under reduced pressure to afford 0.15 g of a white solid in quantitative yield. R_f = 0.08 in solvent system (F); $[\alpha]_D^{20}$ = +38.7° (*c* = 1.00, MeOH, 589 nm); ^{1}H NMR (CD_3OD, 400 MHz) δ 9.22 (s, 1 H, arom pur H2), 8.98 (s, 1 H, arom pur H6), 8.56 (s, 1 H, arom pur H8), 7.27 (m, 5 H, arom Z), 4.88 (m, 2 H, Z CH_2), 4.66, 4.41 (dd, 2 H, J = 4.4, 8.8 Hz, β-CH_2), 4.13 (m, 1 H, α-H), 3.31 (m, 2 H, alc CH_2); MS (ESI) 328 $[M+H]^+$, 350 $[M+Na]^+$.

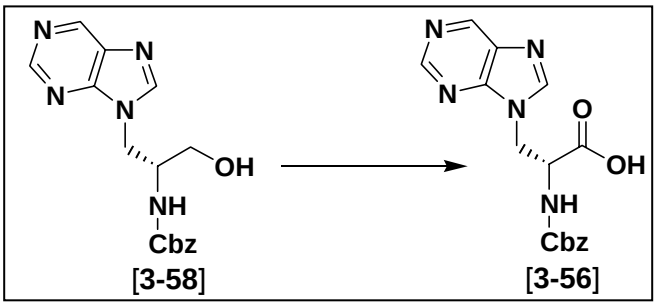

(2*S*)-3-(9*H*-Purine-yl)-2-benzyloxycarbonylamino-propanoic acid (or *Z*-D-7*H*-Purine alanine) [3-56]: (2*S*)-3-(9*H*-Purine-yl)-2-benzyloxycarbonylamino-propanol [**3-58**] (0.42 g, 1.28 mmol) was dissolved in ACN (7 mL), added to pH = 6.7 phosphate buffer (5 mL), and heated to 50 °C. A catalytic amount of TEMPO (0.020 g, 0.13 mmol) was added, followed by simultaneous addition of sodium chlorite solution (0.44 g of 80% $NaClO_2$ in 1.9 mL water) and bleach solution (0.10 mL of household bleach (~ 5% NaOCl) in 1.9 mL water) over 10 min. **Caution! Do NOT mix the sodium chlorite and bleach solutions prior to addition, as the mixture appears to be unstable.[27]** The brownish orange solution was left to stir over night at 50 °C. The reaction became pale yellow. By TLC the reaction was complete. It was cooled to 0 °C in an ice water bath. Water was added (15 mL), followed by drop-wise addition of a saturated solution of Na_2SO_3 (~ 3 mL). The solution was basified to pH = 10 with 1 N NaOH (~ 8 mL) and washed with Et_2O (3 x 30 mL) until nothing was seen in the washes by TLC. The aqueous solution was acidified to pH = 2 with 1 N HCl (12 mL) and saturated with solid NaCl. It was extracted with THF (3 x 50 mL) until no more product came out by TLC. The organic washes were combined and dried over $MgSO_4$. The drying agent was removed by

filtration and the filtrate concentrated under reduced pressure to afford 0.40 g of a beige solid (91% yield). R_f = 0.16 in solvent system (G); $[\alpha]_D^{20}$ = +41.8° (*c* = 1.00, 1:1 MeOH: water, 589 nm); Analytical RP-HPLC: 90A:10B → 20A:80B / 30 min. r_t = 12.01 min, 95% pure; ^{1}H NMR (DMSO-d_6, 400 MHz) δ 9.20 (s, 1 H, arom pur H2), 8.97 (s, 1 H, arom pur H6), 8.54 (s, 1 H, arom pur H8), 7.83 (d, 1 H, *J* = 8.0 Hz, NH), 7.26, 7.18 (m, 5 H, arom Z), 4.91 (m, 2 H, Z CH_2), 4.71 (m, 1 H, α-H), 4.57 (m, 2 H, β-CH_2); ^{13}C NMR (400 MHz, DMSO-d_6) δ 171.6 (1 C, COOH), 156.6 (1 C, C=O of Z), 152.2, 152.1 (2 C, pur C2, C4), 148.6 (1 C, pur C8), 147.6 (1 C, pur C6), 137.4 (1 C, Z C1), 134.1 (1 C, pur C5), 128.9, 128.5, 128.2 (5 C, Z C2-C6), 66.1 (1 C, Z CH_2), 60.4 (1 C, α-C), 53.8 (1 C, β-C); MS (ESI) 342 $[M+H]^+$.

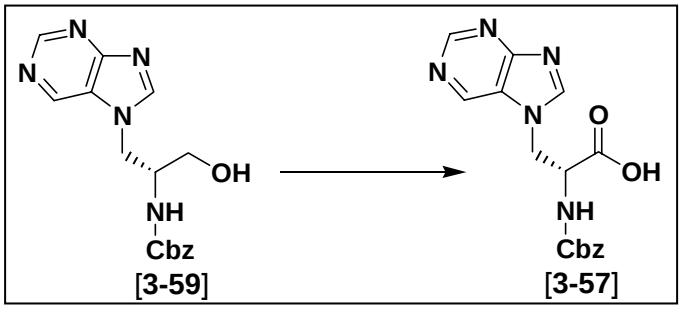

(2*S*)-3-(7*H*-Purine-yl)-2-benzyloxycarbonylamino-propanoic acid (or *Z*-D-9*H*-Purine alanine) [3-57]: (2*S*)-3-(7*H*-Purine-yl)-2-benzyloxycarbonylamino-propanol [**3-59**] (0.15 g, 0.46 mmol) was dissolved in ACN (2.5 mL), added to pH = 6.7 phosphate buffer (2 mL), and heated to 50 °C. A catalytic amount of TEMPO (0.007 g, 0.046 mmol) was added, followed by simultaneous addition of sodium chlorite solution (0.14 g of 80% $NaClO_2$ in 0.6 mL water) and bleach solution (0.03 mL of household bleach (~ 5% NaOCl) in 0.6 mL water) over 10 minutes.

Caution! Do NOT mix the sodium chlorite and bleach solutions prior to addition, as the mixture appears to be unstable.[27] The brownish orange solution was left to stir over night at 50 °C. The reaction became pale yellow. By TLC the reaction was complete. It was cooled to 0 °C in an ice water bath. Water was added (10 mL), followed by drop-wise addition of a saturated solution of Na_2SO_3 (~ 2 mL). The solution was basified to pH = 10 with 1 N NaOH (~ 5 mL) and washed with Et_2O (3 x 30 mL) until nothing was seen in the washes by TLC. The aqueous solution was acidified to pH = 2 with 1 N HCl (8 mL) and saturated with solid NaCl. It was then extracted with THF (3 x 50 mL) until no more product came out by TLC. The organic washes were combined and dried over $MgSO_4$. The drying agent was removed by filtration and the filtrate concentrated under reduced pressure to afford 0.14 g of a beige solid (85% yield). R_f = 0.16 in solvent system (G); $[\alpha]_D^{20}$ = +14.8° (*c* = 1.00, 1:1 MeOH: water, 589 nm); Analytical RP-HPLC: 90A:10B → 20A:80B / 30 min. r_t = 10.47 min. (76%), 11.41 min. (25%); ^{1}H NMR (DMSO-d_6, 400 MHz) δ 9.28 (s, 1 H, arom pur H2), 8.98 (s, 1 H, arom pur H6), 8.65 (s, 1 H, arom pur H8), 7.80 (d, 1 H, *J* = 8.0 Hz, NH), 7.24, 7.08 (m, 5 H, arom Z), 4.82 (m, 2 H, Z CH_2), 4.03 (m, 1 H, α-H), 3.67 (m, 2 H, β-CH_2); ^{13}C NMR (400 MHz, DMSO-d_6) δ 171.5 (1 C, COOH), 156.5 (1 C, C=O of Z), 152.4, 150.9 (2 C, pur C2, C4), 141.4 (1 C, pur C8), 140.1 (1 C, pur C6), 137.3 (1 C, Z C1), 129.5, 129.0, 128.4, 127.9 (6 C, Z C2-C6, pur C5), 67.7 (1 C, Z CH_2), 67.0 (1 C, α-C), 54.4 (1 C, β-C); MS (ESI) 342 $[M+H]^+$.

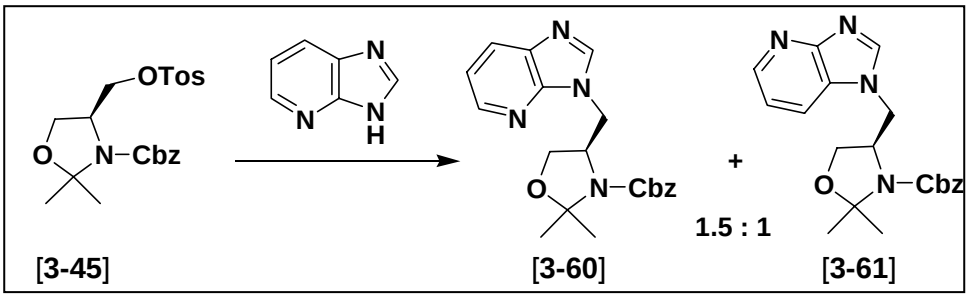

(4*S*)-*N*-Benzyloxycarbonyl-4-(3*H*-methyl-(4-azabenzimidazole)-yl)-2,2-dimethyloxazolidine [3-60] and **(4*S*)-*N*-Benzyloxycarbonyl-4-(1*H*-methyl-(4-azabenzimidazole)-yl)-2,2-dimethyloxazolidine [3-61]:** (4*S*)-*N*-Benzyloxycarbonyl-4-(*p*-toluenesulfonyloxymethyl)-2,2-dimethyloxazolidine [**3-45**] (0.59 g, 1.40 mmol) was dissolved in freshly distilled DMF (2 mL) under Ar atmosphere. Separately, 4-azabenzimidazole (0.20 g, 1.68 mmol) was dissolved in freshly distilled DMF (2 mL) under Ar atmosphere. Solid 60% NaH (0.078 g, 1.96 mmol) was then slowly added. When gas evolution ceased, the purple-pink slurry was added to the solution of tosylate and washed in with an additional portion of DMF (4 mL). The reaction became yellow in color. It was heated to 80 °C and left to stir over night under Ar. The dark yellow reaction was complete by TLC. Water was added (4 mL) and the solution was concentrated under reduced pressure to an orange solid. The solid was dissolved in 5% MeOH/ DCM and purified by column chromatography in the same solvent system to yield two regioisomers in a 2:1 ratio with an overall yield of 72%.

(4*S*)-*N*-Benzyloxycarbonyl-4-(3*H*-methyl-(4-azabenzimidazole)-yl)-2,2-dimethyloxazolidine [3-60]: The less polar compound, (4*S*)-*N*-Benzyloxycarbonyl-4-

(3*H*-methyl-(4-azabenzimidazole)-yl)-2,2-dimethyloxazolidine [**3-60**] was isolated as a white solid (0.22 g). R_f = 0.28 in solvent system (E); $[\alpha]_D^{20}$ = +16.2° (*c* = 1.00, DCM, 589 nm); ^{1}H NMR ($CDCl_3$, 400 MHz) δ 8.40, 8.35 (rotamers, s, 1 H, arom abi H5), 8.04 (rotamers, m, 1 H, arom abi H7), 7.80 (s, 1 H, arom abi H2), 7.35 (m, 5 H, arom Z), 7.22 (m, 1 H, arom abi H6), 5.18 (rotamers, s, 1 H, Z CH_2), 5.10 (rotamers, dd, 0.5, 0.5 H, *J* = 12.0 Hz, Z CH_2), 4.42 (rotamers, m, 3 H, α-H, β-CH_2), 4.13, 3.95 (rotamers, dm, 2 H, ring CH_2), 1.57, 1.50, 1.40, 1.35 (rotamers, s, s, s, s, 2, 2, 1, 1 H, CH_3); MS (ESI) 367 $[M+H]^+$.

(4*S*)-*N*-Benzyloxycarbonyl-4-(1*H*-methyl-(4-azabenzimidazole)-yl)-2,2-dimethyloxazolidine [3-61]: The more polar compound, (4*S*)-*N*-Benzyloxycarbonyl-4-(1*H*-methyl-(4-azabenzimidazole)-yl)-2,2-dimethyloxazolidine [**3-61**] was isolated as a white solid (0.15 g). R_f = 0.17 in solvent system (E), $[\alpha]_D^{20}$ = +61.0° (*c* = 1.00, DCM, 589 nm); ^{1}H NMR ($CDCl_3$, 400 MHz) δ 8.57, 8.48 (rotamers, s, 1 H, arom abi H5), 8.15 (s, 1 H, arom abi H2), 8.06 (rotamers, m, 1 H, arom abi H7), 7.37 (m, 5 H, arom Z), 7.17 (m, 1 H, arom abi H6), 5.22 (rotamers, s, 1 H, Z CH_2), 5.12 (rotamers, q, 2 H, *J* = 8.8 Hz, Z CH_2), 4.16 (rotamers, m, 3 H, α-H, β-CH_2), 3.83, 3.76 (rotamers, dm, 2 H, ring CH_2), 1.68, 1.54, 1.49, 1.45 (rotamers, s, s, s, s, 2, 2, 1, 1 H, CH_3); MS (ESI) 367 $[M+H]^+$, 389 $[M+Na]^+$, 755 $[M_2+Na]^+$.

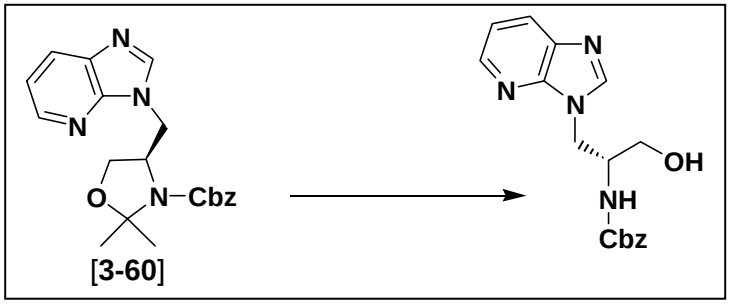

(2*S*)-3-(3*H*-(4-Azabenzimidazole)-yl)-2-benzyloxycarbonylamino-propanol: (4*S*)-*N*-Benzyloxycarbonyl-4-(3*H*-methyl-(4-azabenzimidazole)-yl)-2,2-dimethyloxazolidine [**3-60**] (0.21 g, 0.58 mmol) was dissolved in 4N HCl/ dioxane (9 mL) and allowed to stir for 1 h. A white precipitate formed. The solution was concentrated under reduced pressure to afford 0.19 g of a white solid in quantitative yield. R_f = 0.31 in solvent system (F); $[\alpha]_D^{20}$ = +10.0° (*c* = 1.00, MeOH, 589 nm); ^{1}H NMR (CD_3OD, 400 MHz) δ 9.64 (s, 1 H, arom abi H2), 8.71 (d, 1 H, *J* = 4.0 Hz, arom abi H5), 8.29 (d, 1 H, *J* = 8.0 Hz, arom abi H7), 7.70 (m, 1 H, arom abi H6), 7.27 (m, 5 H, arom Z), 4.72 (m, 2 H, Z CH_2), 4.65 (m, 2 H, β-CH_2), 4.30 (m, 1 H, α-H), 3.72 (m, 2 H, alc CH_2); MS (ESI) 327 $[M+H]^+$, 349 $[M+Na]^+$.

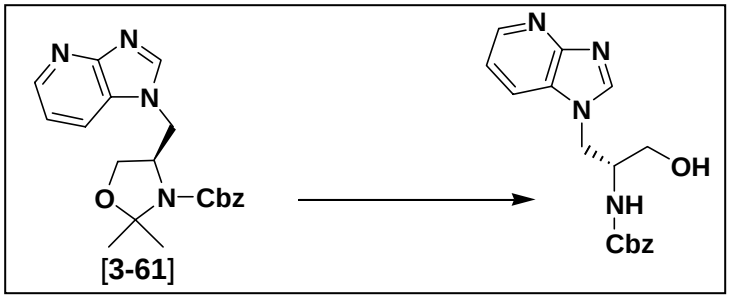

(2*S*)-3-(1*H*-(4-Azabenzimidazole)-yl)-2-benzyloxycarbonylamino-propanol: (4*S*)-*N*-Benzyloxycarbonyl-4-(1*H*-methyl-(4-azabenzimidazole)-yl)-2,2-

dimethyloxazolidine [**3-61**] (0.11 g, 0.31 mmol) was dissolved in 4N HCl/ dioxane (6 mL) and allowed to stir for 1 h. A white precipitate formed. The solution was concentrated under reduced pressure to afford 0.10 g of a white solid in quantitative yield. R_f = 0.28 in solvent system (F); $[\alpha]_D^{20}$ = +44.7° (*c* = 1.00, MeOH, 589 nm); ^{1}H NMR (CD_3OD, 400 MHz) δ 9.11 (s, 1 H, arom abi H2), 8.72 (m, 2 H, arom abi H5, H7), 7.71 (m, 1 H, arom abi H6), 7.29, 7.16 (m, 5 H, arom Z), 4.78 (m, 2 H, Z CH_2), 4.54 (m, 2 H, β-CH_2), 4.15 (m, 1 H, α-H), 3.66 (dm, 2 H, alc CH_2); MS (ESI) 327 $[M+H]^+$.

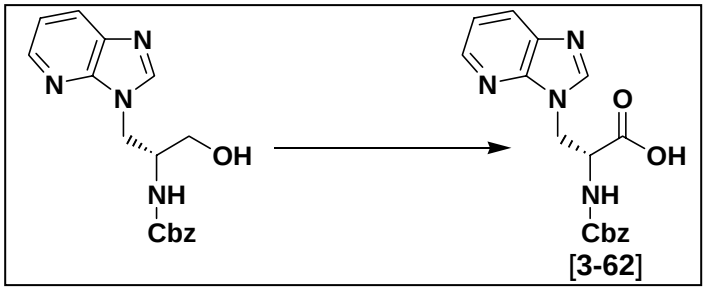

(2*S*)-3-(3*H*-(4-Azabenzimidazole)-yl)-2-benzyloxycarbonylamino-propanoic acid (or *Z*-D-3*H*-(4-Azabenzimidazole)-alanine) [3-62]: (2*S*)-3-(3*H*-(4-Azabenzimidazole)-yl)-2-benzyloxycarbonylamino-propanol (0.19 g, 0.58 mmol) was dissolved in ACN (3 mL), added to pH = 6.7 phosphate buffer (2.5 mL), and heated to 50 °C. A catalytic amount of TEMPO (0.009 g, 0.058 mmol) was added, followed by simultaneous addition of sodium chlorite solution (0.18 g of 80% $NaClO_2$ in 0.8 mL water) and bleach solution (0.04 mL of household bleach (~ 5% NaOCl) in 0.8 mL water) over 10 minutes. **Caution! Do NOT mix the sodium chlorite and bleach solutions prior to addition, as the mixture appears to be unstable.[27]** The brownish

orange solution was left to stir over night at 50 °C. The reaction became pale yellow. By TLC the reaction was complete. It was cooled to 0 °C in an ice water bath. Water was added (10 mL), followed by drop-wise addition of a saturated solution of Na_2SO_3 (~ 2 mL). The solution was basified to pH = 10 with 1 N NaOH (~ 5 mL) and washed with Et_2O (3 x 30 mL) until nothing was seen in the washes by TLC. The aqueous solution was acidified to pH = 2 with 1 N HCl (8 mL) and saturated with solid NaCl. It was then extracted with THF (3 x 50 mL) until no more product came out by TLC. The organic washes were combined and dried over $MgSO_4$. The drying agent was removed by filtration and the filtrate concentrated under reduced pressure to afford 0.20 g of a beige solid in quantitative yield. R_f = 0.27 in solvent system (G); $[\alpha]_D^{20}$ = +28.8° (*c* = 1.00, 1:1 MeOH: water, 589 nm); Analytical RP-HPLC: 90A:10B → 20A:80B / 30 min. r_t = 17.16 min, as a single peak; ^{1}H NMR (DMSO-d_6, 400 MHz) δ 8.99 (s, 1 H, arom abi H2), 8.49 (d, 1 H, *J* = 4.8 Hz, arom abi H5), 8.20 (d, 1 H, *J* = 8.0 Hz, arom abi H7), 7.79 (d, 1 H, *J* = 8.0 Hz, arom abi H6), 7.46 (m, 1 H, NH), 7.28 (m, 5 H, arom Z), 4.90 (m, 2 H, Z CH_2), 4.80 (m, 1 H, α-H), 4.61 (m, 2 H, β-CH_2); ^{13}C NMR (400 MHz, DMSO-d_6) δ 171.5 (1 C, COOH), 156.6 (1 C, C=O of Z), 146.2 (1 C, abi C5), 142.7 (1 C, Z C1), 137.3 (1 C, abi C2), 129.0, 128.5, 128.2 (5 C, Z C2-C6), 126.9, 120.6 (2 C, abi C6, C7), 95.5 (1 C, abi C9), 94.5 (1 C, abi C8), 66.2 (1 C, Z CH_2), 53.7 (1 C, β-C), 44.9 (1 C, α-C); MS (ESI) 341 $[M+H]^+$, 363 $[M+Na]^+$.

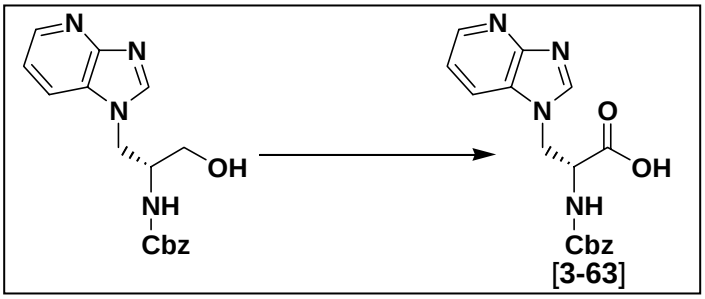

(2*S*)-3-(1*H*-(4-Azabenzimidazole)-yl)-2-benzyloxycarbonylamino-propanoic acid (or *Z*-D-1*H*-(4-Azabenzimidazole)-alanine) [3-63]: (2*S*)-3-(1*H*-(4-Azabenzimidazole)-yl)-2-benzyloxycarbonylamino-propanol (0.10 g, 0.31 mmol) was dissolved in ACN (1.5 mL), added to pH = 6.7 phosphate buffer (1.25 mL), and heated to 50 °C. A catalytic amount of TEMPO (0.005 g, 0.031 mmol) was added, followed by simultaneous addition of sodium chlorite solution (0.09 g of 80% $NaClO_2$ in 0.4 mL water) and bleach solution (0.02 mL of household bleach (~ 5% NaOCl) in 0.4 mL water) over 10 minutes. **Caution! Do NOT mix the sodium chlorite and bleach solutions prior to addition, as the mixture appears to be unstable.[27]** The brownish orange solution was left to stir over night at 50 °C. The reaction became pale yellow. By TLC the reaction was complete. It was cooled to 0 °C in an ice water bath. Water was added (8 mL), followed by drop-wise addition of a saturated solution of Na_2SO_3 (~ 1 mL). The solution was basified to pH = 10 with 1 N NaOH (~ 3 mL) and washed with Et_2O (3 x 10 mL) until nothing was seen in the washes by TLC. The aqueous solution was acidified to pH = 2 with 1 N HCl (4 mL) and saturated with solid NaCl. It was then extracted with THF (3 x 30 mL) until no more product came out by TLC. The organic washes were combined and dried over $MgSO_4$. The drying agent was

removed by filtration and the filtrate concentrated under reduced pressure to afford 0.11 g of a beige solid in quantitative yield. R_f = 0.21 in solvent system (G); $[\alpha]_D^{20}$ = +23.4° (*c* = 1.00, THF, 589 nm); Analytical RP-HPLC: 90A:10B → 20A:80B / 30 min. r_t = 9.08 min, 95% pure; ^{1}H NMR (DMSO-d_6, 400 MHz) δ 9.18 (s, 1 H, arom abi H2), 8.67 (d, 1 H, *J* = 5.2 Hz, arom abi H5), 8.60 (d, 1 H, *J* = 8.0 Hz, arom abi H7), 7.81 (d, 1 H, *J* = 8.0 Hz, arom abi H6), 7.64 (m, 1 H, NH), 7.27, 7.11 (m, 5 H, arom Z), 4.80 (m, 3 H, Z CH_2, α-H), 4.66 (m, 2 H, β-CH_2); ^{13}C NMR (400 MHz, DMSO-d_6) δ 171.2 (1 C, COOH), 156.5 (1 C, C=O of Z), 148.7 (1 C, abi C5), 142.6 (1 C, Z C1), 139.8 (1 C, abi C2), 137.2 (1 C, abi C7), 129.0, 128.5, 128.1 (5 C, Z C2-C6), 125.8, 125.5 (2 C, abi C6, C8), 120.3 (1 C, abi C9), 94.5 (1 C, abi C8), 67.7 (1 C, α-C), 66.3 (1 C, Z CH_2), 54.1 (1 C, β-C); MS (ESI) 341 $[M+H]^+$.

3.5.3 Syntheses of peptides

An oven dried flask was flushed with Ar and charged with 2-chlorotrityl resin (7.00 g, 10.5 mmol, theoretical loading = 1.5 mmol/ g, which had been stored in a dessicator in the presence of KOH). The resin was swelled with dry DCM (70 mL) for 15 min. which was then removed. In a separate oven dried flask, Fmoc-Phe-OH (4.88 g, 12.6 mmol, which had been stored in a dessicator in the presence of KOH for a minimum of 3 days) was dissolved in dry DCM (70 mL) and dry TEA (7.0 mL, 50.4 mmol). The Fmoc-Phe-OH solution was then added to the swelled resin via cannula. The mixture was left to stir for 4 h under Ar. The resin was then washed 3 x 10% MeOH/ DCM, 3 x alternating MeOH and DCM, and 3 x DCM. The resin was

dried under reduced pressure over night (9.5091 g dry resin). The resin was swelled in DMF and treated with 20% piperidine in DMF for 20 min. to remove the Fmoc-protecting group. The resin was then washed 3 x DMF, 2 x DCM, 2 x alternating MeOH and DCM, and 3 x DCM. The resin was then dried over night under reduced pressure (7.9483 g, a loss of 1.5608 g, 7.05 mmol of Fmoc residue). The calculated loading of H-Phe-OH on the resin was 1.01 mmol/ g. A sample of resin was removed (0.1044 g) and treated with 1.0% TFA in DCM for 1 h. The resin was filtered off and the filtrate concentrated under reduced pressure. A white solid was obtained (TFA^- ^+H_3N-Phe-OH, 28.57 g, 0.1023 mmol/ 0.1044 g). The loading was calculated to be 0.98 mmol/ g.

The peptides were elongated by stepwise coupling of Fmoc-amino acid derivatives (Fmoc-Pro-OH, Fmoc-Phe-OH, Fmoc-Thr(*t*-But)-OH, and Fmoc-Lys(Boc)-OH) using standard coupling procedures. Specifically, DIC (3 eq.) and HOBt (3 eq.) in NMP were used as activation reagents for peptide bond formation using 3 eq. of each amino acid (in relation to the theoretical loading of the resin). Removal of the Fmoc-protecting groups was achieved by treatment with 20% piperidine in DMF for 20 minutes.

The synthesized building blocks, Z-D-1*H*-benzimidazole alanine [**3-47**], Z-D-1*H*-benzotriazole alanine [**3-50**], and Z-D-1*H*-indazole alanine [**3-53**] were each coupled to 300 mg of the resin bound peptide [**3-64**] in a similar manner, using 2 eq. of each amino acid, DIC, and HOBt. The three linear hexapeptides were cleaved from the resin by treatment with anisole (1 mL) and 1% TFA/ DCM (10 mL) for 3 h. The

resin was filtered off and again treated with the cleavage solution. This process was repeated 6 times. The resin was then washed with MeOH (5 x 15 mL). The combined filtrates were concentrated under reduced pressure to a solid, washed with Et_2O (3 x 20 mL), and dried under reduced pressure.

The Cbz protecting groups were removed by catalytic hydrogenation using 5% Pd/C (50% of the weight of the peptide) in a mixture of trifluoroethanol (6 mL) and water (1 mL) over a period of 12 h. The reaction was diluted with DMF (5 mL) and MeOH (10 mL) and filtered over celite to remove the catalyst. The filtrate was concentrated under reduced pressure. The resulting residue was triturated with Et_2O to provide beige solids.

Each of the peptides were cyclized using 3 eq. of EDC·HCl, 3 eq. HOBt, and 5 eq. DIEA in a mixture of DCM:DMF (2:1, 0.001M) over 2 days. The solutions were then concentrated under reduced pressure and the residues dissolved in EtOAc (10 mL). They were washed with 1 N HCl (2 x 3 mL), conc. $NaHCO_3$ (2 x 3 mL), and brine. The organic phases were then concentrated under reduced pressure. The resulting residues were triturated with Et_2O to provide white solids.

H_2N-Lys(Boc)-Thr(*t*-But)-Phe-Pro-Phe-OH

[3-64]

H-Lys(Boc)-Thr(*t*-But)-Phe-Pro-Phe-OH [3-64]: Analytical RP-HPLC: 60A:40B → 10A:90B / 30 min. r_t = 11.80 min (95%); MS (ESI) 795 $[M+H]^+$, 817 $[M+Na]^+$, 839 $[M-H+2Na]^+$.

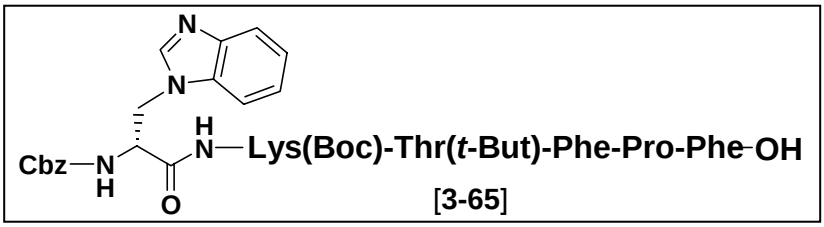

[3-65]

(Z-D-1*H*-Benzimidazole-Ala)-Lys(Boc)-Thr(*t*-But)-Phe-Pro-Phe-OH [3-65]: 297 mg (88% based on the calculated loading of the first amino acid onto the resin). R_f = 0.18 in solvent system (F), R_f = 0.73 in solvent system (H); Analytical RP-HPLC: 60A:40B → 10A:90B / 30 min. r_t = 19.21 min (85%); MS (ESI) 1116 $[M+H]^+$, 1138 $[M+Na]^+$, 1160 $[M-H+2Na]^+$.

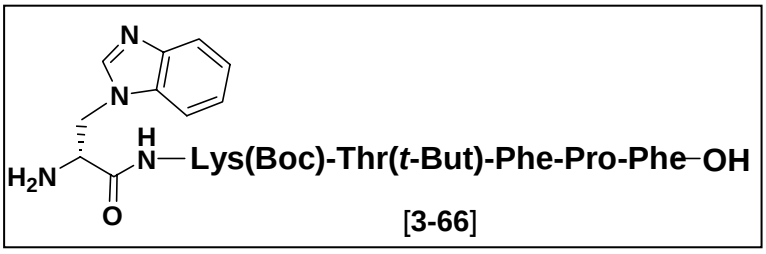

[3-66]

(H-D-1*H*-Benzimidazole-Ala)-Lys(Boc)-Thr(*t*-But)-Phe-Pro-Phe-OH [3-66]: 212 mg (80% yield). R_f = 0.10 in solvent system (F), R_f = 0.27 in solvent system (H); Analytical RP-HPLC: isocratic 60A:40B / 30 min. r_t = 14.91 min (98.5%); MS (ESI) 982 $[M+H]^+$, 1004 $[M+Na]^+$, 1026 $[M-H+2Na]^+$.

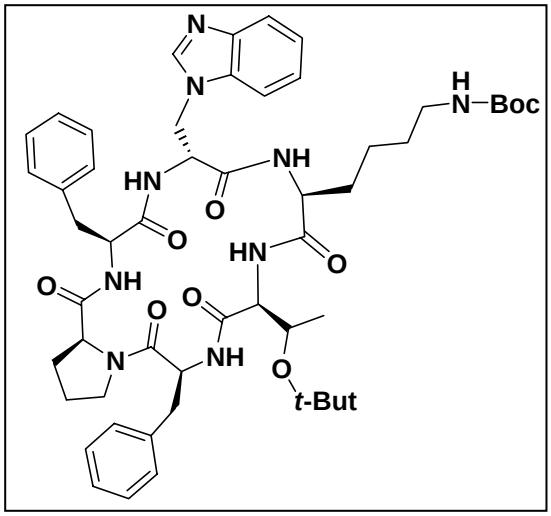

c[(D-1*H*-Benzimidazole-Ala)-Lys(Boc)-Thr(*t*-But)-Phe-Pro-Phe]: 127 mg (60% yield). R_f = 0.71 in solvent system (F); Analytical RP-HPLC: 60A:40B → 10A:90B / 30 min. r_t = 14.19 min (99.9%), 90A:10B → 10A:90B / 30 min. r_t = 24.16 min (99.9%); MS (ESI) 964 $[M+H]^+$, 986 $[M+Na]^+$.

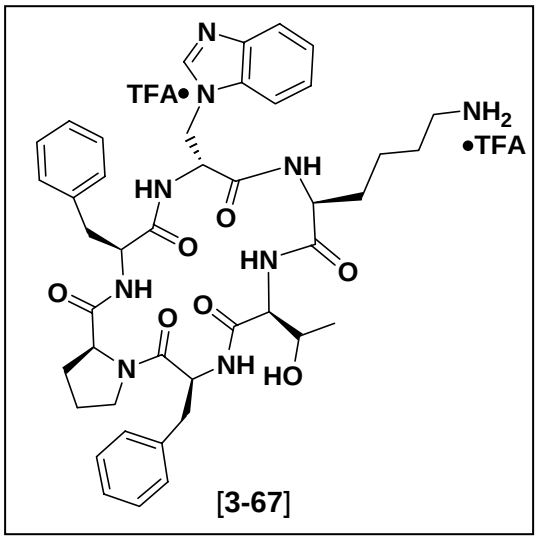

c[(D-1*H*-Benzimidazole-Ala)-Lys-Thr-Phe-Pro-Phe] [3-67]: 134 mg (quantitative yield). Analytical RP-HPLC: 90A:10B → 10A:90B / 30 min. r_t = 15.30 min (85%); MS (ESI) 807 $[M+H]^+$, 830 $[M+Na]^+$.

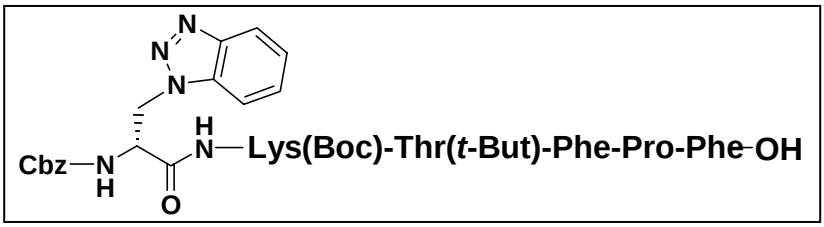

(Z-D-1*H*-Benzotriazole-Ala)-Lys(Boc)-Thr(*t*-But)-Phe-Pro-Phe-OH: 288 mg (85% based on the calculated loading of the first amino acid onto the resin). R_f = 0.21 in solvent system (F), R_f = 0.87 in solvent system (H); Analytical RP-HPLC: 60A:40B → 10A:90B / 30 min. r_t = 23.00 min (90%); MS (ESI) 1115 $[M-H]^-$.

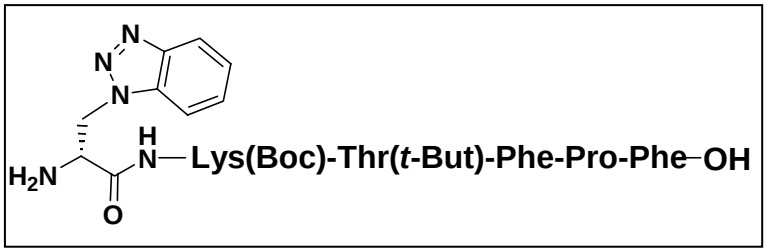

(H-D-1*H*-Benzotriazole-Ala)-Lys(Boc)-Thr(*t*-But)-Phe-Pro-Phe-OH: 209 mg (82% yield). R_f = 0.18 in solvent system (F), R_f = 0.37 in solvent system (H); Analytical RP-HPLC: 60A:40B → 10A:90B / 30 min. r_t = 14.14 min (70%), 14.62 min (30%); MS (ESI) 981 $[M-H]^-$.

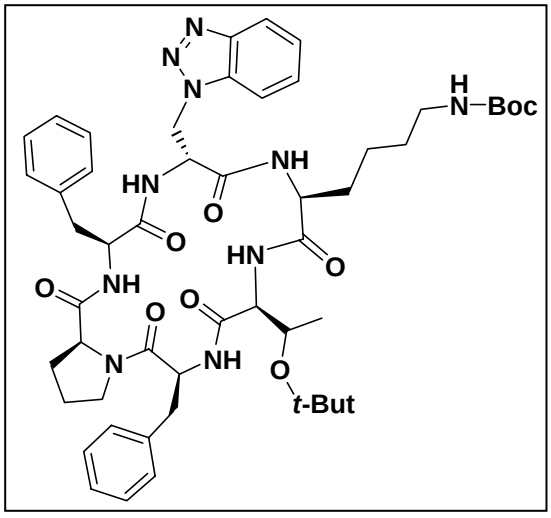

c[(D-1*H*-Benzotriazole-Ala)-Lys(Boc)-Thr(*t*-But)-Phe-Pro-Phe]: 112 mg (55% yield). R_f = 0.50 in solvent system (F); Analytical RP-HPLC: 60A:40B → 10A:90B / 30 min. r_t = 21.89 min (99.9%), 90A:10B → 10A:90B / 30 min. r_t = 26.94 min (99.9%); MS (ESI) 987 $[M+Na]^+$.

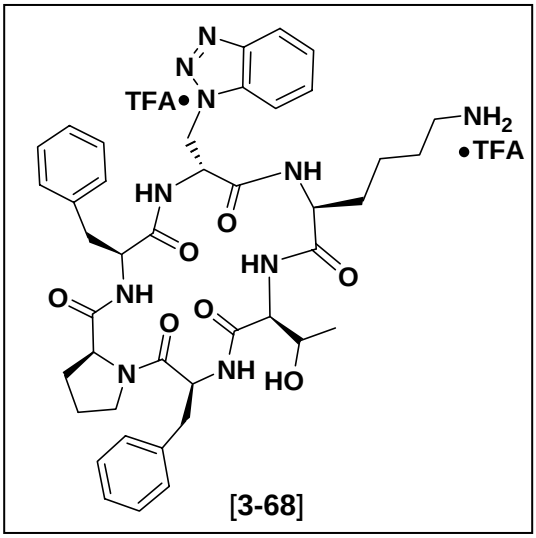

c[(D-1*H*-Benzotriazole-Ala)-Lys-Thr-Phe-Pro-Phe] [3-68]: 124 mg (quantitative yield). Analytical RP-HPLC: 90A:10B → 10A:90B / 30 min. r_t = 18.26 min (75%); MS (ESI) 809 $[M+H]^+$, 831 $[M+Na]^+$.

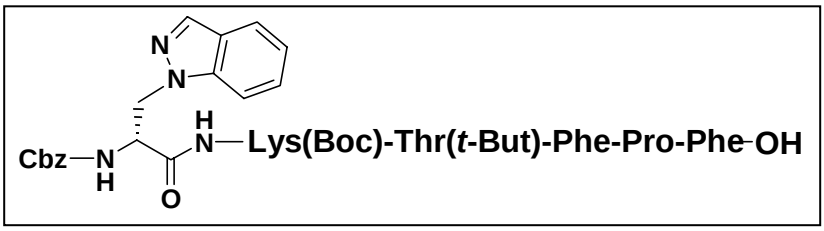

Z-D-1*H*-Indazole-Ala-Lys(Boc)-Thr(*t*-But)-Phe-Pro-Phe-OH: 281 mg (83% based on the calculated loading of the first amino acid onto the resin). R_f = 0.26 in solvent system (F), R_f = 0.72 in solvent system (H); Analytical RP-HPLC: 60A:40B → 10A:90B / 30 min. r_t = 26.27 min (90%); MS (ESI) 1114 $[M-H]^-$.

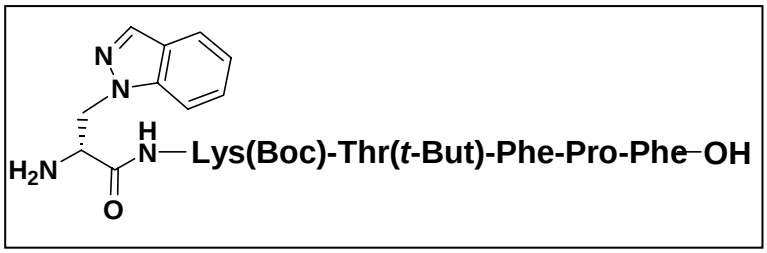

H-D-1*H*-Indazole-Ala-Lys(Boc)-Thr(*t*-But)-Phe-Pro-Phe-OH: 196 mg (80% yield). R_f = 0.13 in solvent system (F), R_f = 0.26 in solvent system (H); Analytical RP-HPLC: 60A:40B → 10A:90B / 30 min. r_t = 15.64 min (83%), 23.26 min (17%); MS (ESI) 980 $[M-H]^-$.

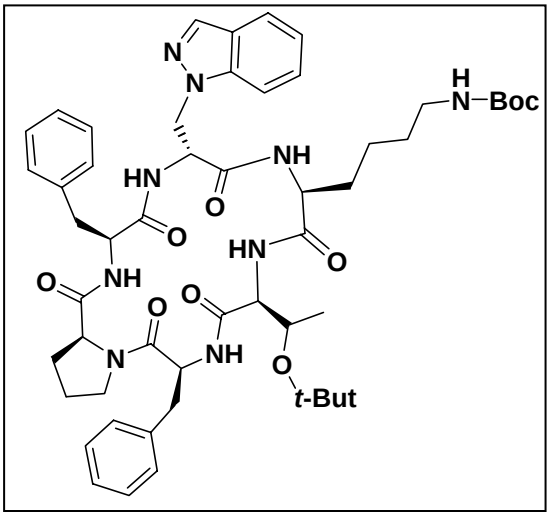

c[D-1*H*-Indazole-Ala-Lys(Boc)-Thr(*t*-But)-Phe-Pro-Phe]: 134 mg (70% yield). R_f = 0.70 in solvent system (F); Analytical RP-HPLC: 60A:40B → 10A:90B / 30 min. r_t = 23.65 min (85%), 90A:10B → 10A:90B / 30 min. r_t = 27.89 min (85%); MS (ESI) 986 $[M+Na]^+$.

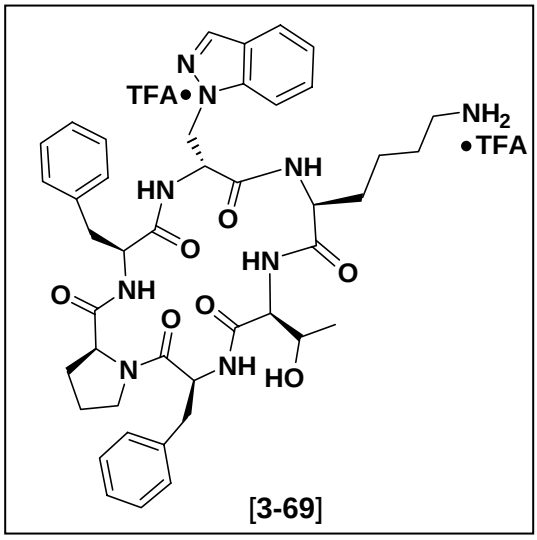

c[D-1*H*-Indazole-Ala-Lys-Thr-Phe-Pro-Phe] [3-69]: 145 mg (quantitative yield). Analytical RP-HPLC: 90A:10B → 10A:90B / 30 min. r_t = 19.00 min (75%); MS (ESI) 808 $[M+H]^+$, 830 $[M+Na]^+$.

3.6 References

1. Vale, W.; Brazeau, P.; Rivier, C.; Brown, M.; Boss, B.; Rivier, J.; Burgus, R.; Ling, N.; Guillemin, R. *Recent Progr. Horm. Res.*, **1975**, *31*, 365-397.

2. Brown, M.; Rivier, J.; Vale, W. *Endocrinology*, **1976**, *98*, 336-343.

3. Rivier, J.; Brown, M.; Rivier, C.; Ling, N.; Vale, W. In *Peptides 1976*; Loffet, A., Ed. Editions de l'Uniuversite de Bruxelles, Brussels, 1976, p 427-449.

4. Ohashi, S.; Sawano, S.; Kokubu, T.; Gondo, M.; Sakakibara, K. *Endocrinol. Jpn.*, **1976**, *23*, 435-438.

5. Rivier, J.; Brown, M.; Vale, W. *J. Med. Chem*, **1976**, *19*, 1010-1013.

6. Holladay, L. A.; Puett, D. In *57th Annual Meeting of the Endocrine Society* New York, NY, 1975, p Abs. # 402.

7. Rivier, J.; Brown, M.; Vale, W. *Biochem. Biophys. Res. Commun.*, **1975**, *65*, 746-751.

8. Brown, M.; Coy, D. H.; Gomez-Pan, A.; Hirst, B. H.; Hunter, M.; Meyers, C.; Reed, J. D.; Schally, A. V.; Shaw, B. *J. Physiol. (London)*, **1978**, *277*, 1-14.

9. Konturek, S. J.; Tasler, J.; Krol, R.; Pawlik, W.; Tasler, J.; Thor, P.; Walus, K.; Schally, A. V. *Proc. Soc. Exp. Biol. Med.*, **1977**, *155*, 519-522.

10. Roze, C.; Chariot, J.; Vaille, C. *Acad. Sci. Ser. D.*, **1978**, *287*, 281-284.

11. Hirst, B. H.; Shaw, B.; Meyers, C.; Coy, D. H. *Regul. Pept.*, **1980**, *1*, 97-113.

12. Meyers, C.; Coy, D. H.; Huang, W. Y.; Schally, A. V.; Redding, T. W. *Biochemistry*, **1978**, *17*, 2326-2331.

13. Nutt, R. F.; Saperstein, R.; Veber, D. F. In *Peptides: Structure and Function. Proceeding of the 8th American Peptide Symposium*; Hruby, V. J., Rich, D. H., Eds.; Pierce Chem. Co.; Rockford, Il.: 1983, p 345-348.

14. Murphy, W. A.; Lance, V. A.; Moreau, J. P.; Coy, D. H. *Life Sci.*, **1987**, *40*, 2515-2522.

15. Erchegyi, J.; Hoeger, C. A.; Low, W.; Hoyer, D.; Waser, B.; Eltschinger, V.; Schaer, J.-C.; Cescato, R.; Reubi, J. C.; Rivier, J. *J. Med. Chem*, **2004**, *48*, 507-514.

16. Reubi, J. C.; Schaer, J.-C.; Wenger, S.; Hoeger, C. A.; Erchegyi, J.; Waser, B.; Rivier, J. *PNAS*, **2000**, *97*, 13973-13978.

17. Huang, Z. W.; He, Y. B.; Raynor, K.; Tallent, M.; Reisine, T.; Goodman, M. *J. Am. Chem. Soc.*, **1992**, *114*, 9390-9401.

18. Moore, S. B.; Grant, M.; Rew, Y.; Bosa, E.; Fabbri, M.; Kumar, U.; Goodman, M. *J. Peptide Res.*, **2005**, *66*, 404-422.

19. Tanaka, H.; Tanizawa, K.; Arai, T.; Saito, K.; Arai, T.; Soda, K. *FEBS*, **1986**, *196*, 257-360.

20. Rew, Y.; Malkmus, S.; Svensson, C.; Yaksh, T. L.; Cheung, N. N.; Schiller, P. W.; Casse, J. A.; DeHaven, R. N.; Goodman, M. *J. Med. Chem*, **2002**, *45*, 3746-3754.

21. Corey, E. J.; Raju, N. *Tetrahedron Lett.*, **1983**, *24*, 5571-5574.

22. Greene, T. W.; Wuts, P. G. M. *Protective Groups in Oganic Synthesis, 3rd Edition*; John Wiley & Sons, Inc., NY, NY, 1999.

23. Herr, R. J. *Albany Molecular Research, Inc, Technical Reports*, **1999**, *3*, 4-5.

24. Eicher, T.; Hauptmann *The Chemistry of Heterocycles*; Georg Thieme Verlag Sittgart; New York, NY, 1995.

25. Garner, P. *Tetrahedron Lett.*, **1984**, *25*, 5855-5858.

26. Tan, K. L.; Bergman, R. G.; Ellman, J. A. *J. Am. Chem. Soc.*, **2001**, *123*, 2685-2686.

27. Zhao, M.; Li, J.; Mano, E.; Song, Z.; Tschaen, D. M.; Grabowski, E. J. J.; Reider, P. *J. Org. Chem.*, **1999**, *64*, 2564-2566.

28. Katritzky, A. R.; Kuzmierkiewicz, W.; Greenhill, J. V. *Rec. Trav. Chim. Pays-Bas.*, **1991**, *110*, 359-373.

29. Katritzky, A. R.; Lan, X.; Yang, J. Z.; Denisko, O. V. *Chem. Rev.*, **1998**, *98*, 409-548.

30. Palmer, M. H.; Findlay, R. H.; Kennedy, S. M. F.; McIntyre, P. S. *J. Chem. Soc., Perkin Trans. II*, **1975**, 1695-1700.

31. Kjellberg, J.; Johansson, N. G. *Tetrahedron Lett.*, **1986**, *42*, 6541-6544.

CHAPTER 4

4. THIOETHER-BRIDGED AMINO ACIDS AND THEIR INCORPORATION INTO CYCLIC RGD-CONTAINING INTEGRIN PEPTIDE LIGANDS

4.1 Introduction

4.1.1 The integrin cell surface receptors

There are four major classes of receptors involved in cell-cell and cell-matrix interactions: cadherins, selectins, receptors of the immunoglobuline superfamily, and integrins.[1] The integrins are a large family of heterodimeric glycoprotein cell surface receptors[2,3] which mediate a variety of cell adhesion events and signal transduction processes[4-6] such as embryonic development, the inflammatory response, angiogenesis and wound healing.[2] The integrins are also responsible for an array of pathological events including tumor metastasis, thrombosis and osteoporosis.[7-10] Several integrins, such as $\alpha v\beta 3$, $\alpha 5\beta 1$, and $\alpha IIb\beta 3$, recognize the tripeptide sequence Arg-Gly-Asp, RGD (Figure 4-1) which is found in many extracellular matrix proteins including fibronectin, vitronectin, and fibrinogen.

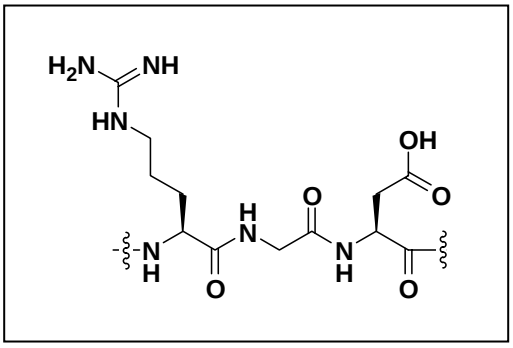

Figure 4-1: The tripeptide integrin recognition sequence Arg-Gly-Asp, or RGD.

While some integrins selectively recognize a single extracellular membrane (ECM) protein ligand (e.g. $\alpha 5\beta 1$ primarily recognizes fibronectin), others can bind

several ligands (e.g. $\alpha v\beta 3$ binds vitronectin, fibronectin, fibrinogen, denatured or proteolysed collagen, and other matrix proteins).

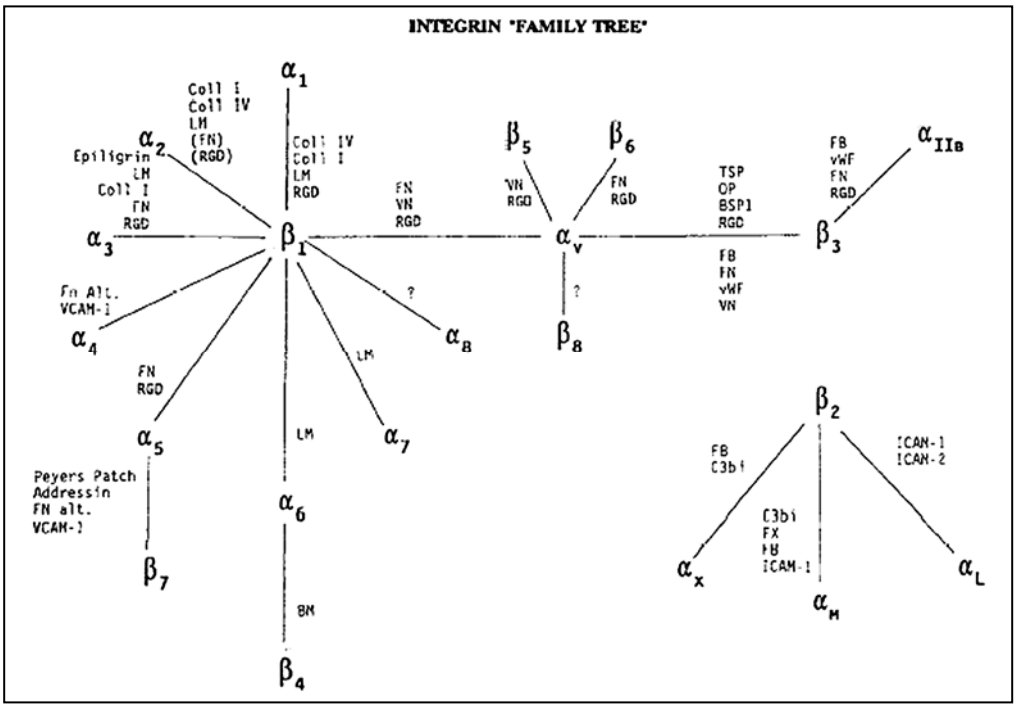

Figure 4-2: Diagram of the integrin family showing subunit associations and known ligand specificities.[11]

The transmembrane integrins contain two subunits called α and β. There are 19 known integrins, each comprised of one of eight separate β-subunits and one of 13 α-subunits and each $\alpha\beta$ combination has its own binding specificity. Some α-subunits, such as αv can associate with a range of β-subunits, while others, such as α3, only associate with one. As depicted in Figure 4-2, it is clear that integrin ligand binding

specificity is quite complex, for one integrin can bind more than one ECM protein and a single ECM protein can bind to more than one integrin.

The larger α-subunit (approximately 1100 residues) is often processed to form two disulfide-bridged chains of different lengths. The extracellular region of the α-subunit is characterized by three to four regions near the *N*-terminus that contain 12 to 15 amino acid residues which are capable of binding bivalent cations such as Ca^{2+} and Mg^{2+}. X-ray structure investigations of the α-subunit indicated the importance of the metal-binding sites for ligand binding.[12,13] This theory was confirmed by observing that integrins depend on the presence of bivalent metal ions, and the addition of Mn^{2+} increases the binding affinity of certain integrins for their ligands.[14-17]

The β-subunit is comprised of about 800 amino acid residues. There are four highly conserved cysteine-rich regions of 40 residues near the transmembrane domain and there is a large loop at the *N*-terminus of the extracellular region.[18]

Electron microscopy[19] and chemical cross-linking experiments have suggested that the amino-terminal globular domains of the α- and β-subunits associate to form an extracellular ligand binding domain.[20] Photo-crosslinking experiments have suggested that the actual binding occurs at the amino terminal end of the β-subunit, but that both subunits are required for ligand binding. Figure 4-3 is a schematic illustration of integrins and depicts some of their known characteristics.

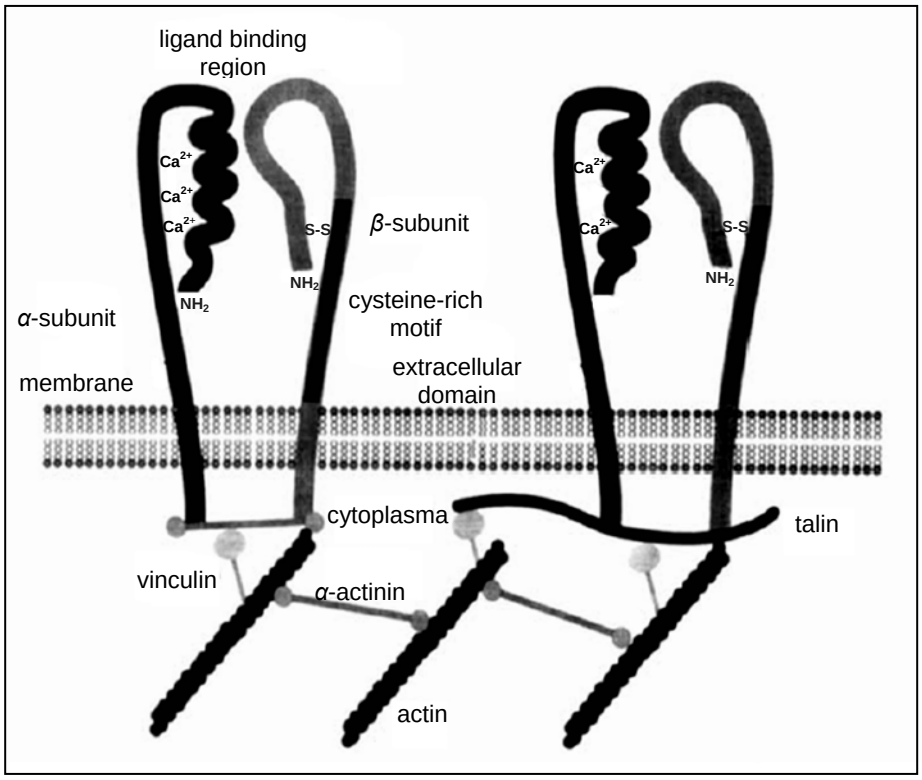

Figure 4-3: Schematic illustration of integrins and their interactions with some proteins within the cellular domain.[1]

4.1.2 Discussion of specific integrins

In conjunction with Integra Life Sciences, integrin research in the Goodman laboratories aimed to develop small, potent, peptidic ligands which were selective for integrin $\alpha v\beta 3$ over integrins $\alpha v\beta 5$, $\alpha 5\beta 1$, and $\alpha IIb\beta 3$.

The platelet glycoprotein receptor, $\alpha IIb\beta 3$, is primarily expressed on megakaryocyte-derived cells, such as platelets, and binds with different affinities to a large number of extracellular matrix proteins including fibrinogen, fibronectin, vitronectin, von Willibrand factor, and thrombospondin.[7,21] The binding of ligands,

such as fibrinogen, has been shown to be an important event in cell adhesion and aggregation phenomena.[22] The αIIbβ3 receptor is involved in primary and secondary hemostasis. It allows aggregation of platelets at sites of vascular injuries by binding to collagen filaments in the connective tissues at the edge of wounds. Aggregation of platelets by fibrinogen then forms a blood clot and seals the injured tissue. Defective formation of these clots or undesired platelet aggregation caused by receptor agonists could lead to embolies, stroke, unstable angina, or myocardial infarction.[23-25] Antagonists of this receptor inhibit clot formation.

The vitronectin receptor, αvβ3, has been extensively studied[26] because of its role in a number of cell adhesion processes including tumor metastasis,[27] phagocytosis of cells undergoing apoptosis,[28] bone remodeling,[29,30] acute renal failure,[31] adhesion of osteoclasts to the bone matrix, and angiogenesis.[32-35]

Angiogenesis is a process of migration and proliferation of smooth muscle and endothelial cells by which new blood vessels develop. New vessels grow by spouting from pre-existing vessels[36] or by recruitment of bone marrow-derived endothelial progenitor cells.[37] While growth factors and their receptors play key roles in angiogenic sprouting, adhesion to the ECM also regulates angiogenesis. Adhesion promotes endothelial cell survival[38,39] as well as endothelial cell proliferation and molitity[40] during new blood vessel growth. The growth of new blood vessels promotes embryonic development, wound healing, and the female reproductive cycle.

Formation of new blood vessels is also involved in many diseases where angiogenesis is misregulated. For example, in rheumatoid arthritis the cartilage of

joints is destroyed by invasion of new blood vessels. In diabetic retinopathy blood vessels grow into the retina and the vitreous body of the eye which leads to bleeding and, as a consequence, blindness.[33,41] Angiogenesis also plays a key role in the pathological development of solid tumor cancers,[32] and age-related macular degeneration.[36]

In earlier studies, it was discovered that endothelial cells actively involved in angiogenesis express integrin $\alpha v\beta 3$ but the integrin was not found to be expressed in mature vasculature.[33,42] Thus, antagonists to $\alpha v\beta 3$ should selectively inhibit angiogenesis without disrupting mature vascular tissue.

In addition to $\alpha v\beta 3$,[32] the expression of $\alpha 5\beta 1$ is significantly up-regulated on endothelium during angiogenesis.[43] Antagonizing integrins inhibits cell migration. The inhibition of integrin $\alpha 5\beta 1$ negatively regulates fibroblast, endothelial cell and tumor cell migration even when other integrin receptors for provisional matrix proteins are ligated. Antagonists of integrin $\alpha 5\beta 1$ suppress cell migration on vitronectin, but not cell attachment to vitronectin, indicating that these antagonists affect the migration machinery rather than the integrin receptors for vitronectin.[40] Once $\alpha v\beta 3$ and $\alpha 5\beta 1$ are expressed, angiogenesis depends on both integrins, as antagonists of each have been shown to block angiogenesis *in vivo*.[32,43] Integrin $\alpha v\beta 5$ has also been shown to regulate angiogenesis. This integrin promotes VEGF-, but not bFGF-mediated angiogenesis.[34,44]

Several anti-angiogenesis related integrin inhibitors are currently under investigation as therapeutics for cancer. Increased levels of expression of integrin

$\alpha v\beta 3$ are closely associated with increased cell invasion and metastasis.[45] Notably, integrin $\alpha v\beta 3$ is expressed on invasive melanoma, but not benign nevi nor normal melanocytes.[46,47] The $\alpha v\beta 3$ receptor's role in angiogenesis is important for the development of metastatic colonies. Humanized antibody antagonists of integrins $\alpha 5\beta 1$ and $\alpha v\beta 3$ as well as peptide inhibitors of integrins $\alpha v\beta 3$ and $\alpha v\beta 5$ are under evaluation as angiogenesis-inhibiting therapeutics in cancer clinical trials.[48,49] These integrin-based anti-angiogenesis therapeutics hold great promise as powerful treatments for cancer.[50] Because antagonists of $\alpha v\beta 3$, $\alpha 5\beta 1$ and $\alpha v\beta 5$ selectively inhibit angiogenesis without disrupting mature vascular tissue, they also have the potential to be useful in treating rheumatoid arthritis and diabetic retinopathy.[51-53]

4.1.3 Structure-activity relationship studies of the RGD tripeptide

The recognition site for many of the integrins that bind to the extracellular matrix is the tripeptide sequence, Arg-Gly-Asp (RGD). The sequence was first identified in fibronectin where the cell binding domain was narrowed down to the shortest sequence that could still compete with fibronectin for binding to its cell surface receptor.[54] The RGD sequence has been shown to be a recognition sequence in ECM proteins such as vitronectin and fibrinogen[7] and has since been found to inhibit other extracellular matrix proteins such as vitronectin, osteopontin, collagens, thrombospondin, fibrinogen, and von Willebrand factor from binding to their cell surface receptors.[7,8]

While numerous integrin receptors are believed to recognize RGD sequences, integrins are nonetheless, ligand specific. The mechanism by which different adhesion proteins are selected, however, is not well understood. Additional binding sites as well as different conformations of the RGD sequence in different proteins have been discussed.[55]

The discovery that cell attachment activity could be mimicked by short, immobilized, synthetic peptides containing the RGD sequence was significant, as was the observation that these same peptides were capable of inhibiting cell attachment to RGD-containing ligands in solution.[56] These findings meant that the potential existed to develop RGD-based therapeutics that functioned as either agonists to promote the interaction of cells and tissues with matrices, or as antagonists to control the nature of cell-cell and cell-ECM interactions. In addition, the pharmacophore was small enough to encourage broad analog development and held the promise of the development of small nonpeptide molecules.

Since integrins participate in a wide range of biological processes, much effort has been spent on the design of RGD-containing peptides and peptidomimetics of potential therapeutic use. Very early it was discovered that modifications such as replacement of Asp with Glu or Gly with D-Ala or L-Ala resulted in total loss of binding affinity.[57,58] Additional SAR studies of synthetic RGD peptides indicated that minor changes in and around the RGD sequence could alter integrin antagonist activity.[8] The RGD sequence was embedded in small cyclic peptides with restricted conformational flexibility which then exhibited varying integrin specificities. The

results of these SAR studies indicated that the information needed for a peptide to bind to an integrin resides in the RGD sequence and one of the roles of the surrounding residues is to force the RGD tripeptide into an appropriate conformation. The nature of the residues flanking the RGD sequence also directly influence receptor affinity, receptor selectivity, and other biological properties. The side chains and backbone elements of flanking residues may play very important roles in recognition as well.

Because there are many types of RGD ligands, each with a specific biological function, studies of structure-activity relationships of bioactive analogs provided insight into the requirements for binding specificity to a given receptor. In an effort to develop anti-angiogenesis therapeutics for the treatment of diabetic retinopathy, we hoped to utilize the information harvested from previous SAR studies to develop small, cyclic peptides which would selectively bind to integrin $\alpha v\beta 3$ over integrin $\alpha IIb\beta 3$, thus eliminating blood clot-associated side effects.

4.2 The incorporation of thioether building blocks into *αvβ*3-specific peptides

4.2.1 Design of the thioether building blocks

In the last few years, a number of potent peptide antagonists to the *α*v receptors have been reported.[1,59-64] We have developed cyclic peptides which contain the pentapeptide sequence Arg-Gly-Asp-Asp-Val (RGDDV) and exhibit selectivity for integrin *αvβ*3compared to *αvβ*5, *α*5*β*1, and *α*IIb*β*3.[65] Our collaborators at Integra Life Sciences discovered the pentapeptide pharmacophore RGDDV. Peptides containing the sequence were found during a random screening of the Integra peptide database for an osteoporosis program. It was discovered that when a heterogeneous population of cells isolated from neonatal rat bone marrow was seeded onto bone slices, cyclic peptides with the RGDDV sequence selectively inhibited osteoclast attachment without affecting the other cell types present. Those peptides were found to selectively antagonize *αvβ*3[66-70]and became the basis for rational peptidomimetic anti-angiogenesis drug design.[65]

The initial findings lead to the development of peptide c[(Mpa)-RGDDVC]-NH_2 [**4-1**] (Figure 4-4). The pharmacophoric sequence is cyclized via a disulfide bridge between the 3-mercaptopropionic acid (Mpa) and the cysteine side chain. Compound [**4-1**] exhibits increased selectivity for integrin *αvβ*3 over integrins *αvβ*5, *α*5*β*1, and *α*IIb*β*3. Substitution of the valine residue with the more hydrophobic amino acid, L-*tert*-butylglycine (*t*BuG) provided compound [**4-2**] which displayed a 4-fold increase in potency for binding to integrin *αvβ*3.[71]

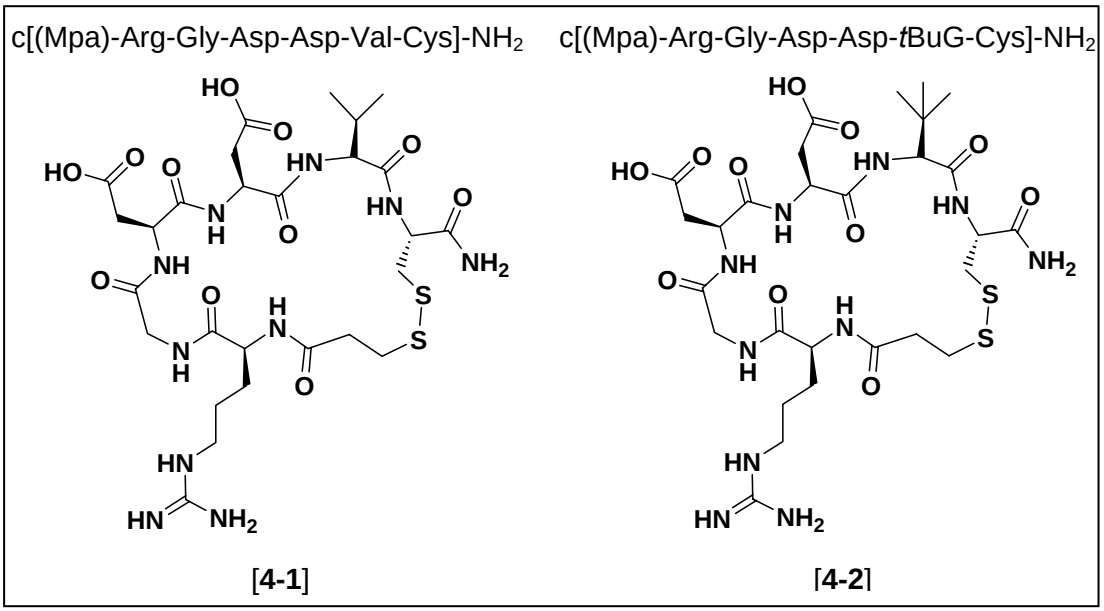

Figure 4-4: Structures of disulfide-bridged RGD peptides which selectively bind to integrin $\alpha v\beta 3$.

To increase the enzymatic stability of disulfide containing peptides, our group has successfully substituted disulfide bridges with lanthionine and thioether structures in various families of compounds including enkephalins,[72] somatostatin,[73-75] and a cell adhesion modulator.[76] *In vivo* experiments in animal models have shown that thioether bridges provide greater stability toward enzymatic degradation over disulfides.[74] As part of the current studies, we have designed and synthesized scalable thioether-bridged building blocks based on cysteine (*S*-acetyl analog [**4-3**] and *S*-propionyl analog [**4-4**], Figure 4-5) and homocysteine (*S*-acetyl analog [**4-5**] and *S*-propionyl analog [**4-6**], Figure 4-5). We incorporated these building blocks into analogs of peptide c[(Mpa)-RGDD(*t*BuG)C]-NH_2 [**4-2**] using solid phase peptide synthesis techniques.

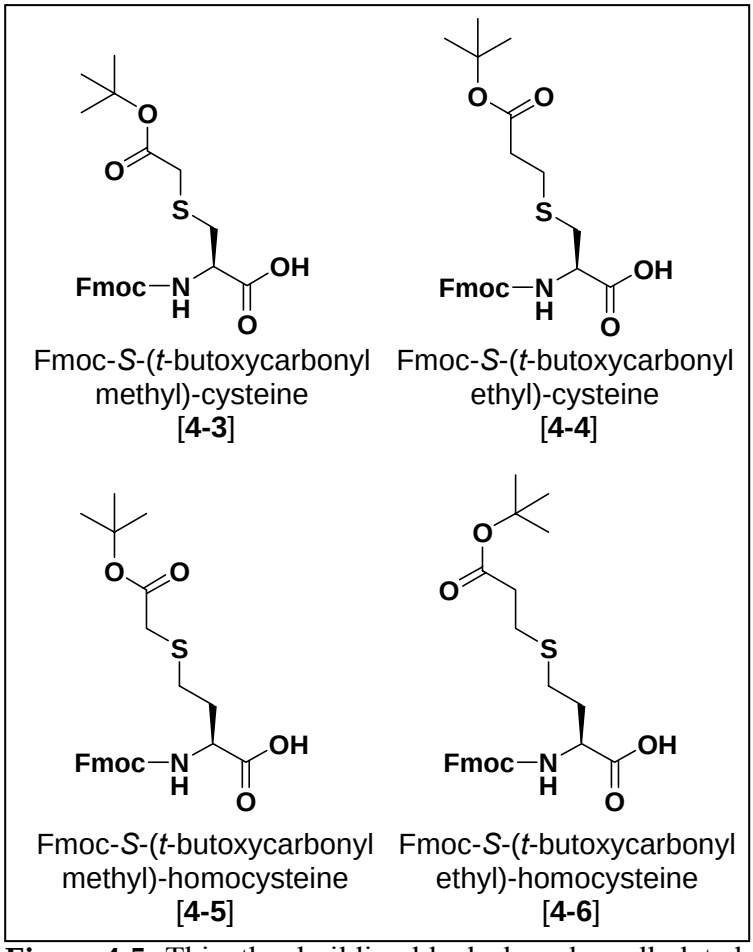

Figure 4-5: Thioether building blocks based on alkylated cysteine and homocysteine.

Peptides [**4-7**], [**4-8**], [**4-9**], and [**4-10**] (Figure 4-6) are examples of thioether-bridged analogs of the disulfide-bridged parent compound c[(Mpa)-RGDD(*t*BuG)C]-NH_2 [**4-2**] (Figure 4-4). These cyclic peptides were designed to increase the bioavailability and stability of parent compound [**4-2**]. Each of the four thioether building blocks pictured in Figure 4-5 was incorporated in place of the cysteine and Mpa residues of the parent molecule.

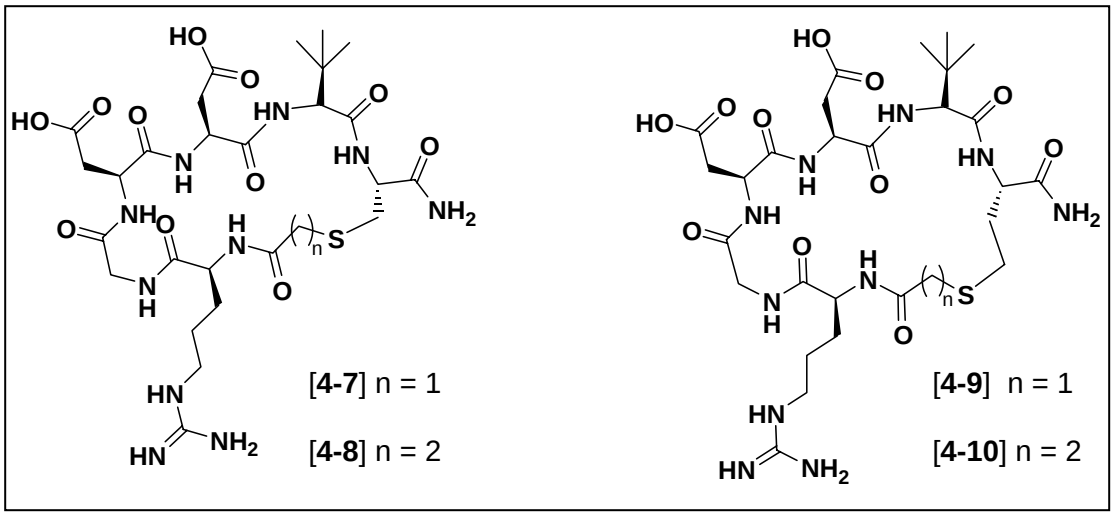

Figure 4-6: Thioether bridged RGD peptide analogs:
c[(*S*-MeCO-C)RGDD(*t*BuG)C]-NH_2 [**4-7**],
c[(*S*-EtCO-C)RGDD(*t*BuG)C]-NH_2 [**4-8**],
c[(*S*-MeCO-hC)RGDD(*t*BuG)C]-NH_2 [**4-9**],
c[(*S*-EtCO-hC)RGDD(*t*BuG)C]-NH_2 [**4-10**].

4.2.2 Methods to synthesize thioether bridges

Several methods have been developed to prepare thioether bridged peptides. Sulfur extrusion and Michael addition of cysteine to dehydroalanine are well established methods but unfortunately lack regio- and stereo-selectivity.[77-81] The β-lactone developed by Vederas,[82] and related synthetic routes developed in our laboratories,[83] are very useful to obtain orthogonally protected lanthionines with high stereoselectivity but can suffer from low regioselectivity, and do not provide building blocks which are suitably protected for Fmoc-protected solid phase synthesis. These methods are depicted in Figure 4-7.

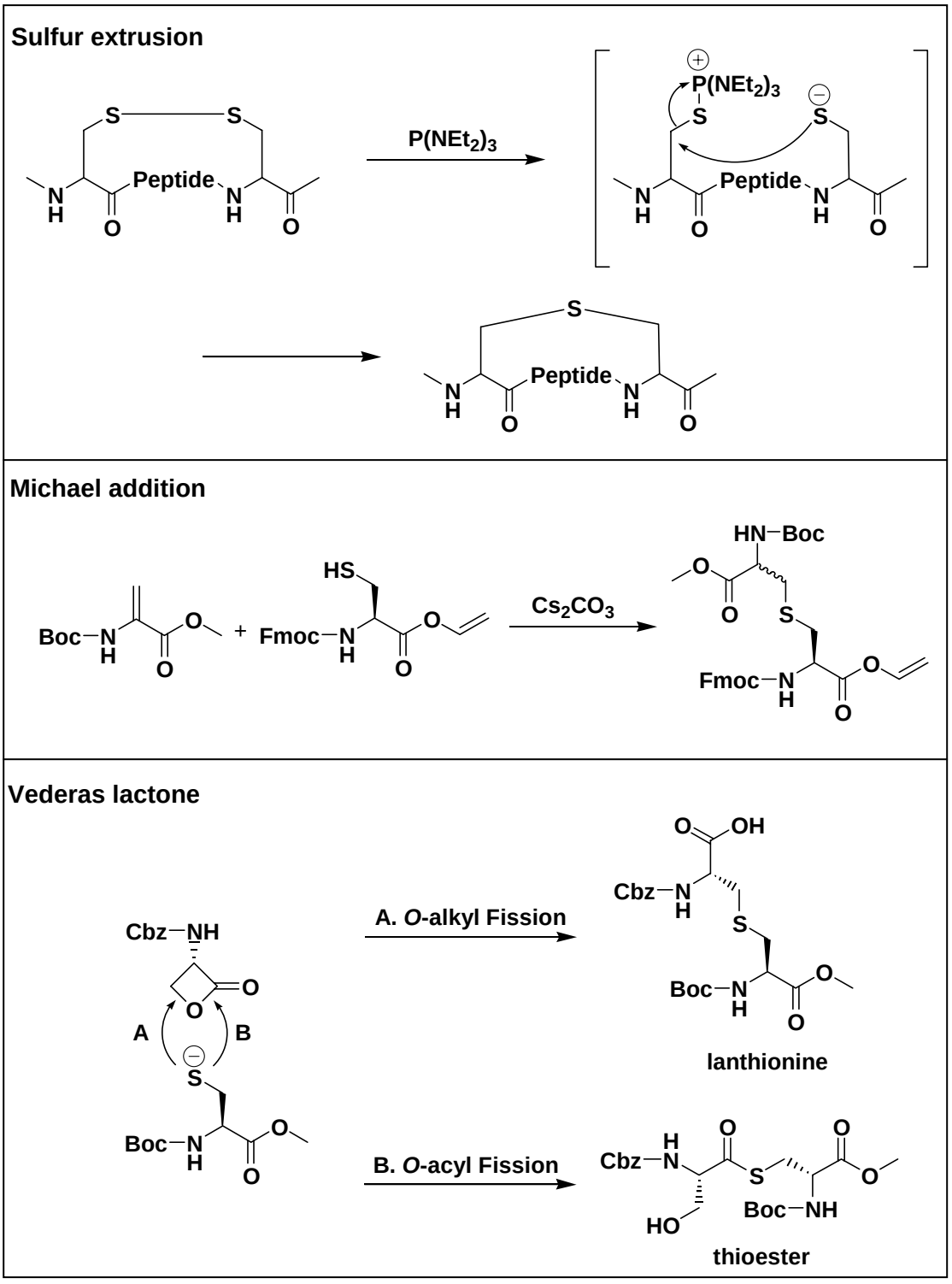

Figure 4-7: Problematic methods for the synthesis of thioether bridges include sulfur extrusion, Michael addition of cysteine to dehydroalanine, and the Vederas lactone.

Other known methods for the synthesis of thioether bridges involve the nucleophilic attack by cysteine derivatives on β-haloalanines, β-tosylated serine and β-tosylated threonine.[81,84-88] These syntheses proved to be problematic in solution because of difficult purifications, poor yields and lack of stereochemical control. Menez[89] avoided epimerization, a common side reaction, by using *N*-trityl-3-iodoalanine benzyl ester as a hindered electrophile and was able to successfully synthesize Fmoc-protected lanthionines (Figure 4-8). One of the major by-products in solution was the aziridine which was formed in significant amounts. By applying this method to solid phase peptide synthesis, where an excess of electrophile and the ability to remove the by-products overcomes the short comings of the solution synthesis, researchers in our laboratory were successful in synthesizing lanthionine bridged enkephalins.[72]

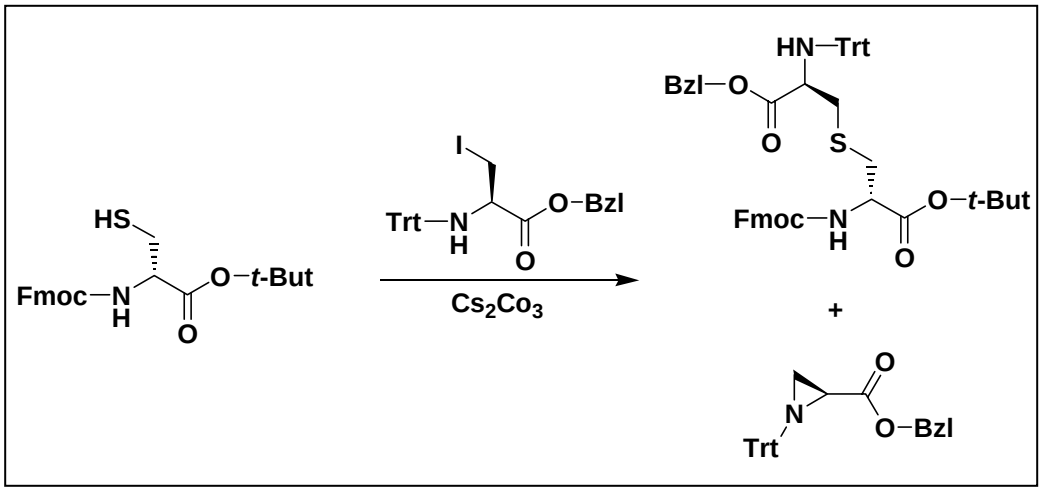

Figure 4-8: Attack of *N*-trityl-3-iodoalanine benzyl ester by cysteine derivatives in solution provides lanthionines and an aziridine by-product.

Unfortunately, none of these described methods provide appropriately protected building blocks for the synthesis of the desired RGD-containing peptides. In addition, we wanted to design thioether bridged analogs of peptide c[(Mpa)-RGDD(*t*BuG)C]-NH_2 [**4-2**] which were not lanthionine derivatives, and thus lacked an amine function as well as an additional stereocenter. We also sought to vary the number of carbons in the thioether bridge and wanted a synthetic method which would provide the thioethers in multigram, and would allow us to monitor the reactions in order to maximize the yields.

4.2.3 The syntheses of the thioether building blocks and their incorporation into peptides

The *S*-*t*-butyl acetyl cysteine [**4-3**] and the *S*-*t*-butyl propionyl cysteine [**4-4**] building blocks were synthesized as outlined in Scheme 4-1. The synthesis of *S*-alkylated cysteine building blocks [**4-3**] and [**4-4**] commenced with the esterification of bis-Fmoc-L-cystine [**4-11**] and provided fully protected cystine [**4-12**] in quantitative yield. Reduction of the disulfide bond of cystine [**4-12**] was achieved quantitatively with zinc powder in TFA/ MeOH under argon atmosphere and yielded key intermediate Fmoc-cysteine methyl ester [**4-13**]. Thiol [**4-13**] was then alkylated with *tert*-butyl bromoacetate in the presence of TEA to afford *S*-(*t*-butoxycarbonylmethyl)-cysteine methyl ester [**4-14**] in 90% yield. Alternately, a Michael addition of Fmoc-cysteine methyl ester [**4-13**] with *tert*-butyl acrylate provided *S*-(*t*-butoxycarbonylethyl)-cysteine methyl ester [**4-15**] in 93% yield**.**

Saponification of the methyl ester of each building block with lithium hydroxide in the presence of calcium chloride retained the Fmoc-protecting group and provided the free acids *S*-(*t*-butoxycarbonylmethyl)-cysteine [**4-4**] and *S*-(*t*-butoxycarbonylethyl)-cysteine [**4-5**] in 75% and 80% yield, respectively.

The *S*-(*t*-butoxycarbonylmethyl)- and *S*-(*t*-butoxycarbonylethyl)-homocysteines [**4-6**] and [**4-7**] were synthesized as shown in Scheme 4-2. Homocystine [**4-16**] was esterified with thionyl chloride and methanol in quantitative yield. Subsequent bis-Fmoc-protection was achieved with 9-fluorenylmethoxycarbonyl chloride (Fmoc-Cl) and potassium carbonate to provide the fully protected homocystine [**4-17**] in 95% yield. The remainder of the syntheses of *S*-(*t*-butoxycarbonylmethyl)-homocysteine [**4-6**] and *S*-(*t*-butoxycarbonylethyl)-homocysteine [**4-7**] were analogous to those of the previously described *S*-alkylated cysteine building blocks.

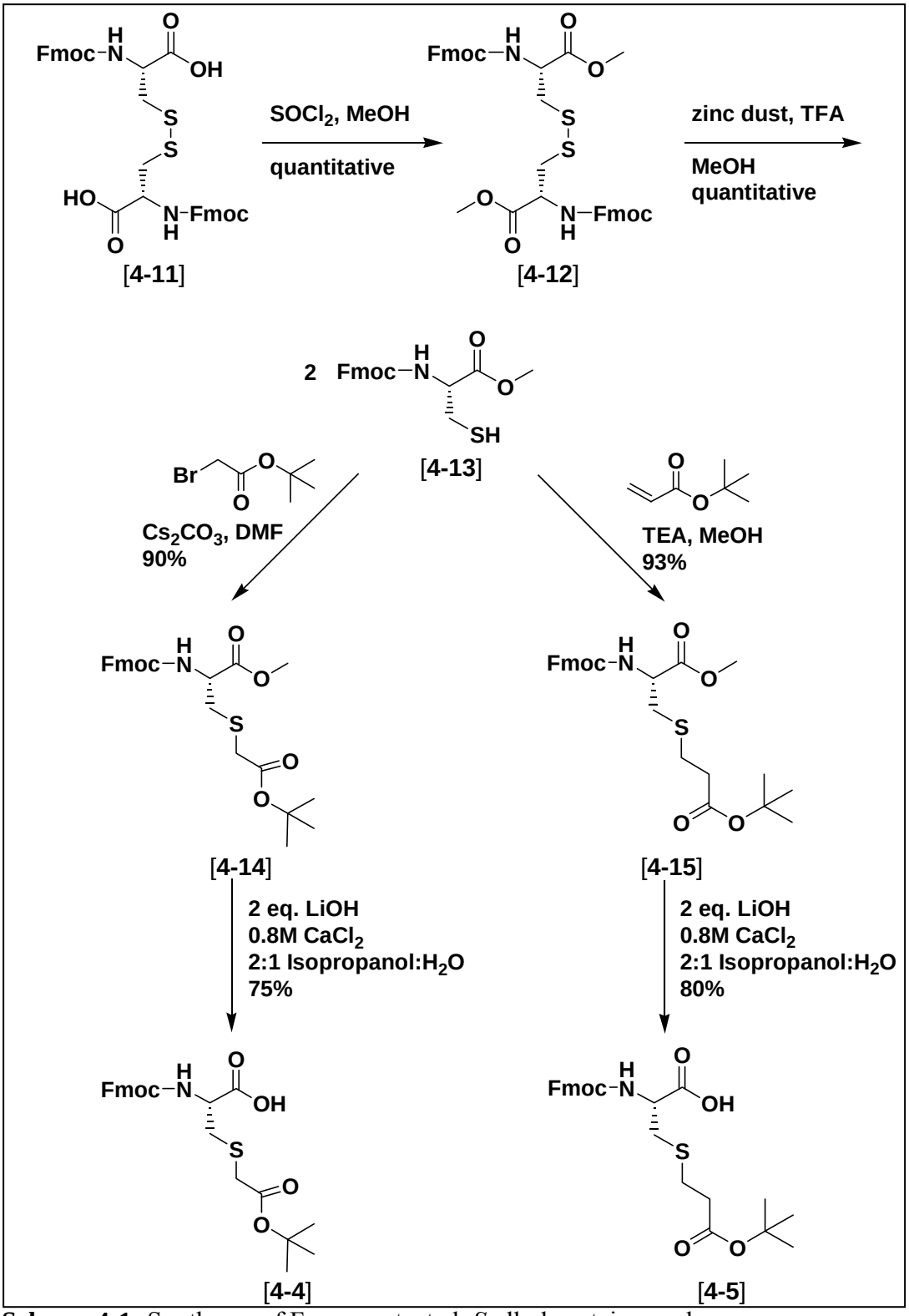

Scheme 4-1: Syntheses of Fmoc-protected, *S*-alkyl cysteine analogs.

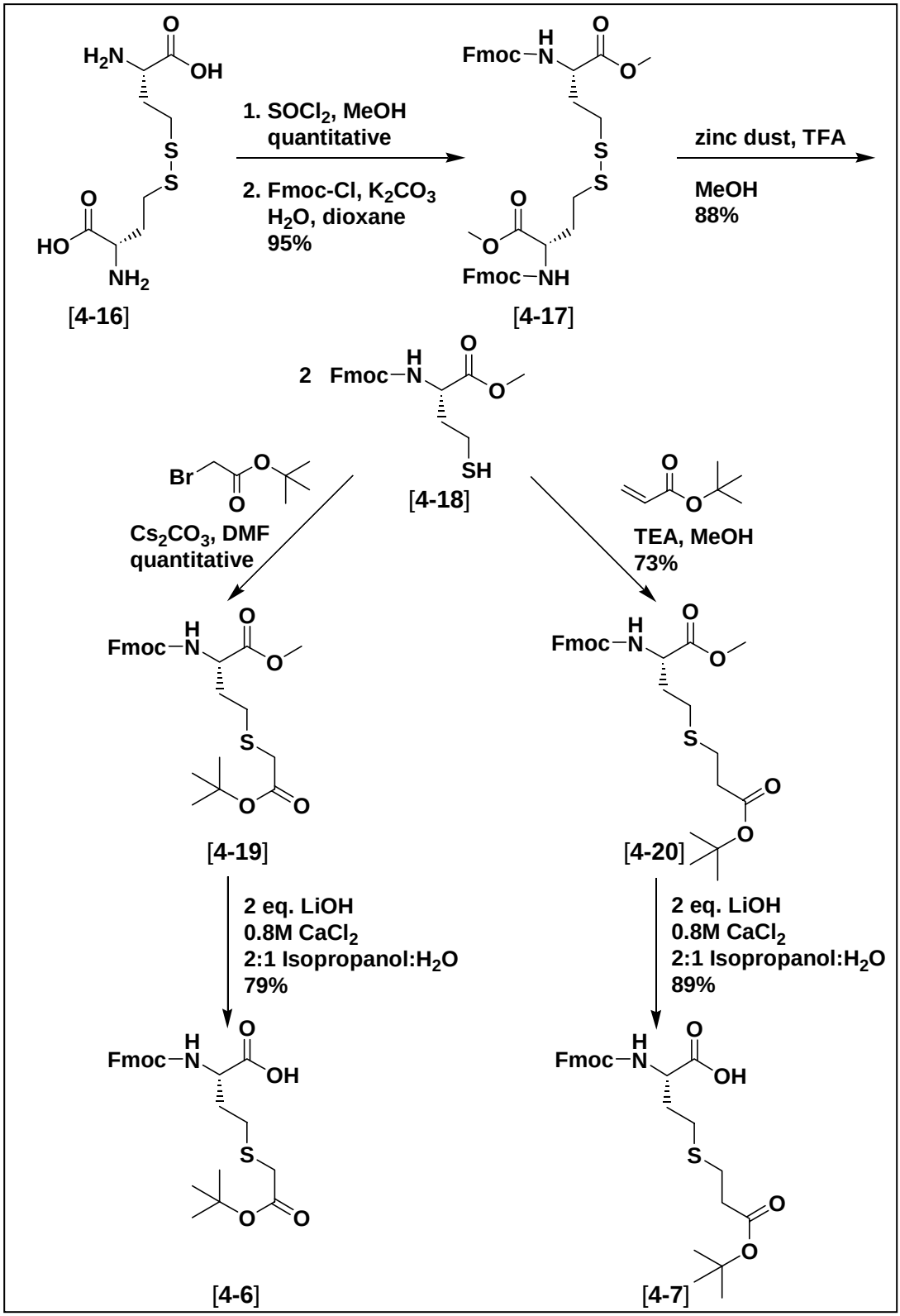

Scheme 4-2: Syntheses of Fmoc-protected, *S*-alkylated homocysteine analogs.

Each of the four building blocks was loaded onto Rink amide MBHA resin using DIC/ HOBt as demonstrated in Scheme 4-3 where *S*-(*t*-butoxycarbonylmethyl)-cysteine [**4-4**] is used as an example. The peptide was elongated by stepwise coupling of Fmoc-amino acid derivatives using DIC/ HOBt under standard coupling procedures. Resin bound peptide [**4-22**] was cleaved from the solid support by treatment with TFA which simultaneously removed the *tert*-butyl ester from the building block thioether side chain. The resulting side-chain carboxylic acid of linear peptide [**4-23**] was then cyclized to the *N*-terminal amino group in 1mM DMF using HATU and *N*-methyl morpholine as reagents. The remaining cyclohexylester protecting groups on the aspartic acid residues were removed using HF to provide *S*-acetyl cysteine thioether bridged peptide [**4-7**]. Final purification was carried out by preparative RP-HPLC on a flanged MODcol C18 column using a gradient of acetonitrile in water with 0.3% acetic acid. The *S*-(*t*-butoxycarbonylethyl)-cysteine [**4-8**], *S*-(*t*-butoxycarbonylmethyl)-homocysteine [**4-9**], and *S*-(*t*-butoxycarbonylethyl)-homocysteine [**4-10**] peptide analogs were synthesized in an analogous manner.

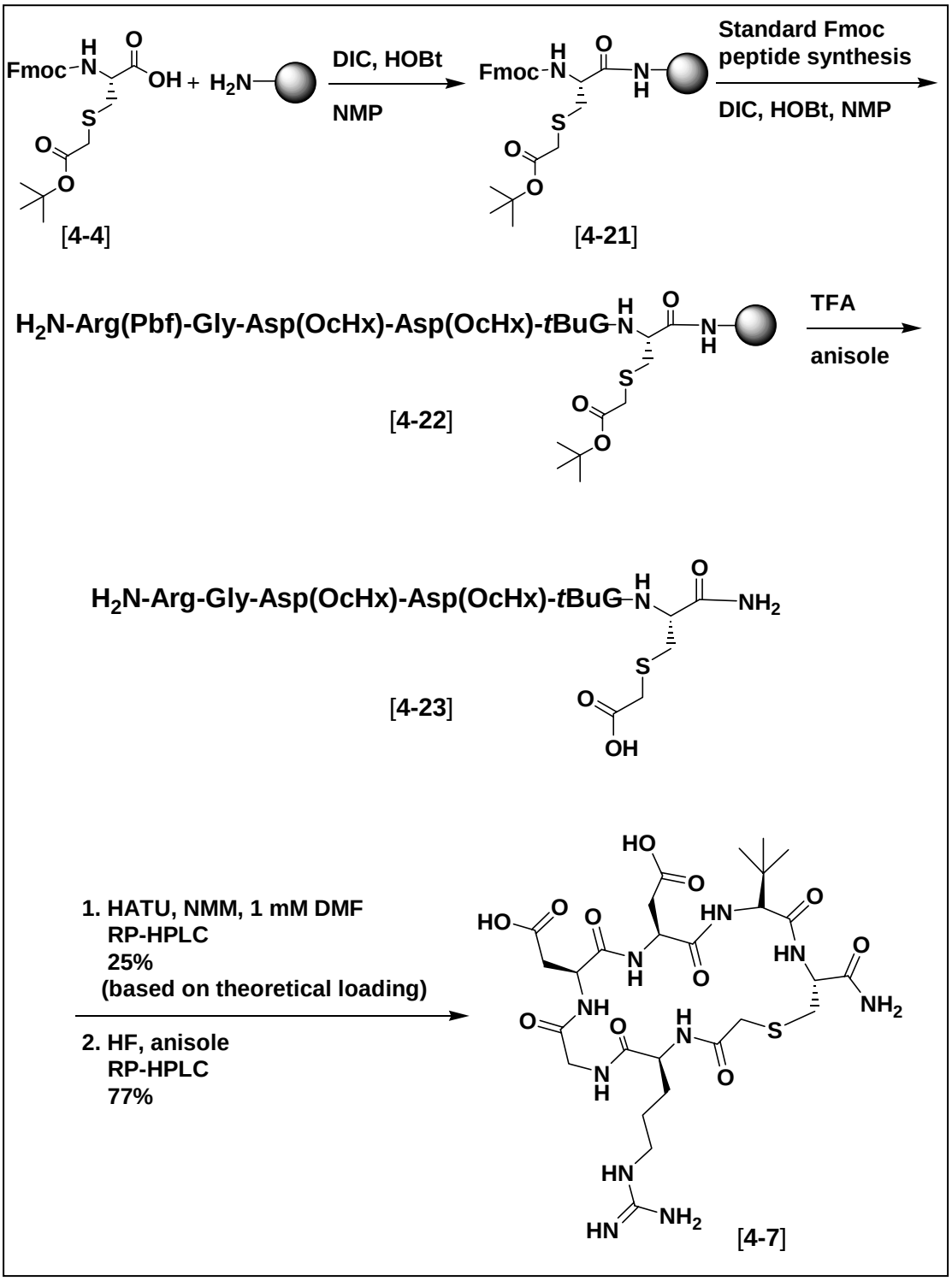

Scheme 4-3: Synthesis of *S*-*t*-butyl acetyl cysteine peptide [**4-4**] is representative of the syntheses of all four thioether-bridged peptide analogs.

4.2.4 Results of receptor binding assays

The binding affinities of the synthesized thioether bridged RGD peptides c[(*S*-MeCO-C)RGDD(*t*BuG)C]-NH_2 [**4-7**], c[(*S*-EtCO-C)RGDD(*t*BuG)C]-NH_2 [**4-8**], c[(*S*-MeCO-hC)RGDD(*t*BuG)C]-NH_2 [**4-9**], and c[(*S*-EtCO-hC)RGDD(*t*BuG)C]-NH_2 [**4-10**] for integrins $\alpha v\beta 3$, $\alpha v\beta 5$, $\alpha 5\beta 1$, and $\alpha IIb\beta 3$ were determined by biologists at Integra Life Sciences using an ELISA assay format. The data shown in Table 4-1 demonstrates that peptides [**4-7**], [**4-8**], [**4-9**], and [**4-10**], bind potently to integrin $\alpha v\beta 3$ with affinities which are comparable to the parent compound, c[(Mpa)RGDD(*t*BuG)C]-NH_2 [**4-2**]. The peptides [**4-7**], [**4-8**], and [**4-9**], which contain *S*-(carboxymethyl)-cysteine, *S*-(carboxyethyl)-cysteine, and *S*-(carboxy-methyl)-homocysteine, respectively, all also bind with similar affinities to integrin $\alpha 5\beta 1$ compared to c[(Mpa)RGDD(*t*BuG)C]-NH_2 [**4-2**], while the *S*-(carboxyethyl)-homocysteine analog [**4-10**] was an order of magnitude less potent at that integrin.

Table 4-1: Binding affinities of the parent compound and the thioether-bridged RGD peptides for integrins $\alpha v\beta 3$, $\alpha v\beta 5$, $\alpha 5\beta 1$, and $\alpha IIb\beta 3$ (IC_{50}, nM).

Compound	$\alpha v\beta 3$	$\alpha v\beta 5$	$\alpha 5\beta 1$	$\alpha IIb\beta 3$
c[(Mpa)RGDD(*t*BuG)C]-NH_2 [**4-2**]	10	210	390	70
c[(*S*-MeCO-C)RGDD(*t*BuG)C]-NH_2 [**4-7**]	34	380	37	748
c[(*S*-EtCO-C)RGDD(*t*BuG)C]-NH_2 [**4-8**]	16	271	41	149
c[(*S*-MeCO-hC)RGDD(*t*BuG)C]-NH_2 [**4-9**]	19	220	31	85
c[(*S*-EtCO-hC)RGDD(*t*BuG)C]-NH_2 [**4-10**]	32	1179	172	121

The *S*-(carboxyethyl)-homocysteine bridged peptide [**4-10**] maintained potent binding to integrin $\alpha v\beta 3$ and had affinities for integrins $\alpha 5\beta 1$ and $\alpha IIb\beta 3$ which were comparable to the parent peptide [**4-2**]. However, the binding of this compound to integrin $\alpha v\beta 5$ was an order of magnitude lower in potency than that of c[(Mpa)RGDD(*t*BuG)C]-NH_2 [**4-2**].

The most interesting result from the binding assays was that *S*-(carboxymethyl)-cysteine analog [**4-7**] exhibited 10-fold reduced binding affinity for integrin $\alpha IIb\beta 3$ compared to parent compound [**4-2**]. Because integrin $\alpha IIb\beta 3$ is involved in blood clot formation and platelet activities, compounds which bind to this integrin, as well as the integrins involved in angiogenesis, could display unwanted side effects. While we could not predict it, we had hoped that including the thioether building blocks in the peptides would reduce binding affinity for integrin $\alpha IIb\beta 3$. Because compound [**4-7**] displayed equipotent affinities for integrins $\alpha v\beta 3$ and $\alpha 5\beta 1$, with reduced affinity for integrin $\alpha IIb\beta 3$, it shows the most promise for effective blocking of angiogenesis.

As has been shown with other thioether-bridged analogs of disulfide bridged peptides, [72-76] we anticipate that thioether-bridged peptides [**4-7**], [**4-8**], [**4-9**], and [**4-10**], will exhibit much greater stability toward disulfide reductases as compared to disulfide-bridged parent compound [**4-2**].

4.3 Conclusions

The design and synthesis of the appropriately protected thioether building blocks was accomplished in multigram scale and in good yields. The syntheses of these building blocks are suitable to variations in chain length and can produce a variety of different thioether bridges. Our building blocks were incorporated into the RGDD(*t*BuG) sequence on solid supports, followed by cleavage from the resin and cyclization in solution. Evaluation of the binding affinities of the peptides to the isolated integrin receptors, $\alpha v\beta 3$, $\alpha v\beta 5$, $\alpha 5\beta 1$, and αIIb$\beta 3$, revealed that peptides [**4-7**], [**4-8**], and [**4-9**] bind with equal potency to the integrin $\alpha v\beta 3$ receptor as compared to parent compound [**4-2**]. However, the binding affinity of these three compounds to integrin $\alpha 5\beta 1$ is enhanced. Furthermore, peptide [**4-7**] exhibits a 10-fold reduced binding affinity for integrin αIIb$\beta 3$. The RGD cyclic peptide c[(*S*-MeCO-C)RGDD(*t*BuG)C]-NH_2 [**4-7**], binds potently to both integrins $\alpha v\beta 3$ and $\alpha 5\beta 1$. This finding could be of substantial interest for mechanistic investigations which are aimed toward the elucidation of the role of integrin receptors in models for diseases. The fact that integrins $\alpha v\beta 3$ and $\alpha 5\beta 1$ are involved in tumor angiogenesis and integrin $\alpha 5\beta 1$ is believed to be important for tumor metastasis could make a peptide that is a potent antagonist to those receptors an interesting drug candidate. The reduced affinity of compound [**4-7**] for integrin αIIb$\beta 3$ makes it of further interest.

Peptide analog [**4-10**] maintains binding affinities similar to that of parent compound [**4-2**] toward integrins $\alpha v\beta 3$, αIIb$\beta 3$, and $\alpha 5\beta 1$, but exhibits reduced binding to the $\alpha v\beta 5$ receptor. These results show once again that relatively subtle

changes to a molecule can lead to substantial changes in binding affinity and selectivity profiles of compounds.

Future work will explore the conformational analysis of these peptides to investigate the topochemical variations that might be responsible for the observed differences in binding affinity and receptor selectivity. The thioether bridged compounds should be subjected to enzymatic stability studies to verify that they are more stable than the disulfide bridged parent compound.

Because it bound with equal potency to integrins $\alpha v\beta 3$ and $\alpha 5\beta 1$, and exhibited decreased affinity for integrin αIIb$\beta 3$, peptide c[(*S*-MeCO-C)RGDD(*t*BuG)C]-NH_2 [**4-7**] was the most promising candidate for further biological investigation. There are several well defined animal models for testing the efficacy of compounds against angiogenesis. Further evaluation of compound [**4-7**] in animal models would help to determine if it is effective at inhibiting angiogenesis, and worthy of further investigation as a clinical candidate. These assays include: the murine hypoxia-induced retinal neovascularization assay,[42] the rabbit corneal pocket assay,[90] the *in ovo* chick chlorioallantoic membrane angiogenesis assay,[43] the chick chlorioallantoic membrane tumor assay,[43] and the SCID mouse model of human angiogenesis assay.[43]

4.4 Acknowledgements

Chapter 4 is based upon material in: Incorporation of thioether building blocks into an $\alpha_v\beta_3$-specific RGD peptide: synthesis and biological activity. Kelleman, Audrey; Mattern, Ralph-Heiko; Pierschbacher, Michael D.; Goodman, Murray. *Biopolymers*. **2003**, *71*, 686-695. The dissertation author was the primary investigator and author of this paper.

4.5 Experimental

4.5.1 General

Reactions in solution were monitored by thin-layer chromatography (TLC) carried out on 0.25 mm E. Merck silica gel plates (60F-254) using UV light as the visualization agent in the following solvent systems: (A) 1:1 EtOAc:hexanes, (B) DCM, (C) 10% MeOH/ DCM, (D) 5% MeOH/ DCM.

The NMR spectra were obtained on a Varian HG-400 (400 MHz) spectrometer. Chemical shifts (δ) are reported in parts per million (ppm) relative to residual undeuterated solvent as an internal standard. The following abbreviations were used to explain the multiplicities: s = singlet, d = doublet, t = triplet, q = quartet, m = multiplet, bs = broad singlet, dd = doublet of doublets, dt = doublet of triplets, dm = doublet of multiplets.

Analytical RP-LCMS was carried out at Integra Life Sciences on a Thermo Finnigan LCQ Advantage LC/MS/MS ion trap mass spectrometer in conjunction with

a Waters Alliance 2695 separation module and 2487 UV detector using Xcalibur software. Solvents used were as follows: solvent A = 0.01% TFA in H_2O, solvent B = 0.01% TFA in ACN. The flow rate was 0.25 mL/min using an XTerra MS C18 column (#1860000446, 2.1 x 50 mm, 5 μm particle diameter).

Preparative RP-HPLC purification was carried out on a Waters Prep LC 4000 with a Waters 2487 UV detector. Solvents used were as follows: solvent A = 0.3% AcOH in H_2O; solvent B = 0.3% AcOH in 80:20 ACN: H_2O. The flow rate was 40 mL/min using a flanged MODcol Kromasil C18 column (#PA0000-050025, 50.8 x 250 mm, 10 μm particle diameter, 100 Å pore size).

Analytical RP-HPLC was carried out on a Perkin-Elmer series 410 with a Perkin-Elmer LC 235 array detector. Solvents used were as follows: solvent A = 0.1% TFA in H_2O; solvent B = 0.1% TFA in ACN. The flow rate was 1 mL/min using a Vydac C18 column (#218TP5405, 4.6 x 50 mm, 5 μm particle diameter, 300 Å pore size).

4.5.2 Syntheses of building blocks

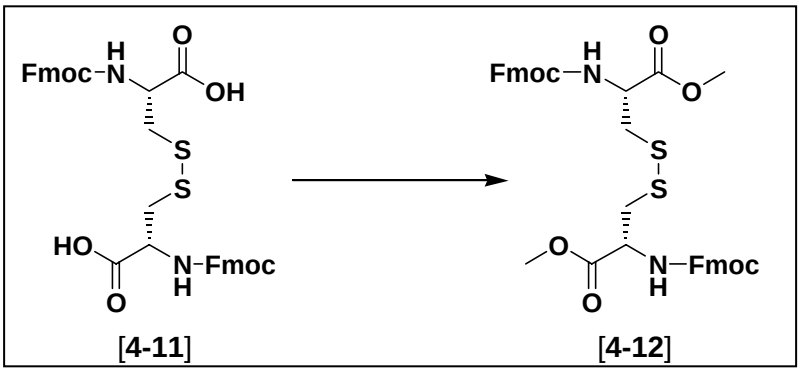

Bis-Fmoc-L-Cystine bis-methyl ester [4-12]: Bis-Fmoc-L-Cystine [**4-11**] (3.0 g, 4.38 mmol) was dissolved in a mixture of DCM (50 mL) and MeOH (150 mL). $SOCl_2$ (1.28 mL, 17.52 mmol) was added, drop-wise, over 30 min. The reaction was stirred over night under Ar. It became milky white with precipitate. The solid was filtered off and dried under reduced pressure (3.12 g, quantitative yield). R_f = 0.33 in solvent system (A); ^{1}H NMR ($CDCl_3$, 400 MHz) δ 7.75 (d, 4 H, *J* = 7.3 Hz, arom H), 7.59 (d, 4 H, *J* = 7.3 Hz, arom H), 7.40 (t, 4 H, *J* = 7.3 Hz, arom H), 7.30 (t, 4 H, *J* = 7.3 Hz, arom H), 5.71 (d, 2 H, *J* = 8.1 Hz, NH), 4.68 (dd, 2 H, *J* = 7.3, 16.8 Hz, α-H), 4.40 (m, 4 H, Fmoc CH_2), 4.20 (t, 1 H, *J* = 6.6 Hz, Fmoc CH), 3.80 (s, 6 H, OMe), 3.19 (m, 4 H, β-CH_2).

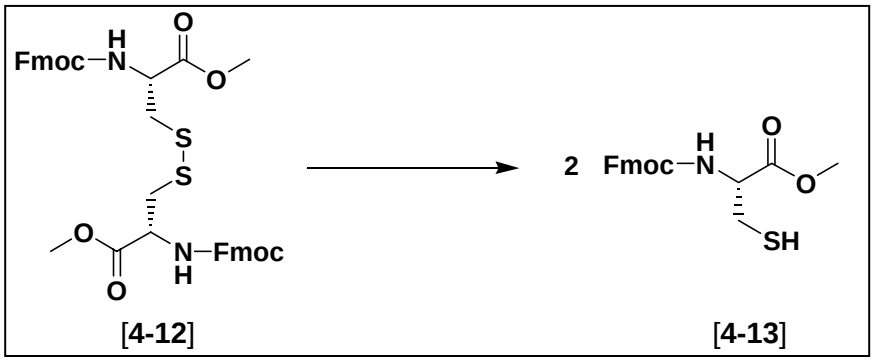

[**4-12**] [**4-13**]

Fmoc-L-Cysteine methyl ester [4-13]: Bis-Fmoc-L-Cystine bis-methyl ester [**4-12**] (0.500 g, 0.70 mmol) was dissolved in a mixture of DCM (20 mL) and MeOH (60 mL). The flask was then flushed with Ar. TFA (2.16 mL, 28 mmol) was added, followed by zinc dust (0.10 g, 1.40 mmol). The flask was flushed with Ar and stirred under Ar over night. The colorless solution was filtered to remove the zinc metal and then concentrated under reduced pressure. The residue was dissolved in EtOAc and washed with 1N HCl (3 x 10 mL), 1N NaOH (3 x 10 mL), and brine (1 x 10 mL). It was dried over $MgSO_4$, filtered, and the filtrate concentrated under reduced pressure to afford a white solid (0.50 g, quantitative yield). R_f = 0.46 in solvent system (A), R_f = 0.23 in solvent system (B); ^{1}H NMR ($CDCl_3$, 400 MHz) δ 7.76 (d, 2 H, *J* = 7.3 Hz, arom H), 7.60 (d, 2 H, *J* = 7.3 Hz, arom H), 7.40 (t, 2 H, *J* = 7.3 Hz, arom H), 7.32 (t, 2 H, *J* = 7.3 Hz, arom H), 5.66 (d, 1 H, *J* = 6.6 Hz, NH), 4.43 (m, 1 H, α-H), 4.40 (d, 2 H, *J* = 7.3 Hz, Fmoc CH_2), 4.22 (t, 1 H, *J* = 6.8 Hz, Fmoc CH), 3.81 (s, 3 H, OMe), 3.01 (m, 2 H, β-CH_2), 1.37 (t, 1 H, *J* = 8.8 Hz, SH).

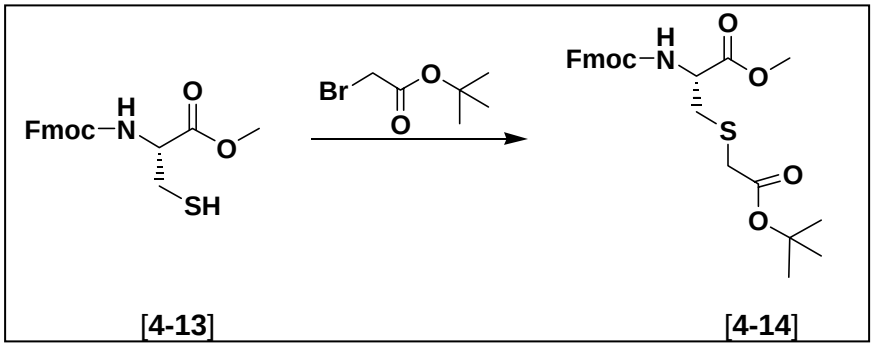

***N*-Fmoc-*S*-(*tert*-Butoxycarbonylmethyl)-L-Cysteine methyl ester [4-14]:** Fmoc-L-Cysteine methyl ester [**4-13**] (1.00 g, 2.80 mmol) and *t*-butyl bromoacetate (0.68 mL, 4.20 mmol) were dissolved in DMF (15 mL). Cesium carbonate (1.09 g, 3.36 mmol) was added and the reaction was stirred over night under Ar. The solvents were removed under reduced pressure, and the residue partitioned between DCM and 1N HCl. The layers were separated and the aqueous layer was washed with DCM (4 x 15 mL). The combined cloudy organic extracts were washed with 1N HCl (2 x 10 mL) and brine (1 x 15 mL). The solution was dried over $MgSO_4$, filtered, and the filtrate concentrated to 1.19 g of a white solid (90% yield). R_f = 0.44 in solvent system (A), R_f = 0.14 in solvent system (B), R_f = 0.78 in solvent system (C); ^{1}H NMR ($CDCl_3$, 400 MHz) δ 7.76 (d, 2 H, *J* = 7.3 Hz, arom H), 7.63 (d, 2 H, *J* = 7.3 Hz, arom H), 7.40 (t, 2 H, *J* = 7.3 Hz, arom H), 7.32 (t, 2 H, *J* = 7.3 Hz, arom H), 5.95 (d, 1 H, *J* = 8.0 Hz, NH), 4.65 (dd, 1 H, *J* = 5.1, 18.3 Hz, α-H), 4.40 (d, 2 H, *J* = 7.3 Hz, Fmoc CH_2), 4.25 (t, 1 H, *J* = 7.3 Hz, Fmoc CH), 3.79 (s, 3 H, OMe), 3.16 (m, 4 H, β-CH_2, S-CH_2), 1.50 (s, 9 H, *t*-But H).

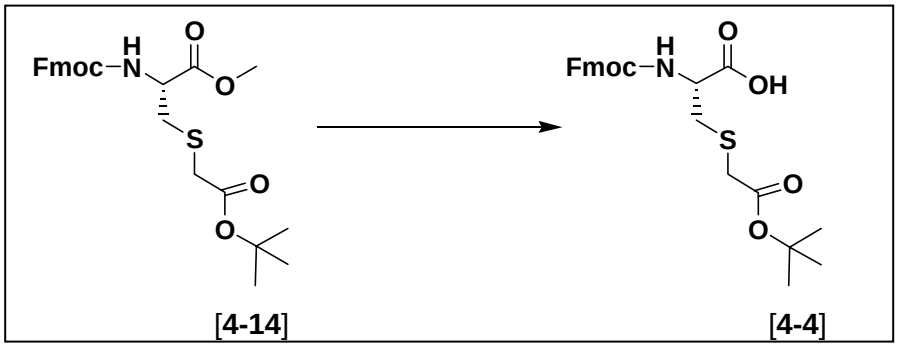

***N*-Fmoc-*S*-(*tert*-Butoxycarbonylmethyl)-L-Cysteine [4-4]:** *N*-Fmoc-*S*-(*tert*-butoxycarbonylmethyl)-L-Cysteine methyl ester [**4-14**] (2.18 g, 4.62 mmol) was dissolved in a mixture of isopropanol (65 mL) and THF (20 mL). Calcium chloride was added (8.32 g, 74.97 mmol). Separately, $LiOH \cdot H_2O$ (0.78 g, 18.48 mmol) was dissolved in H_2O (28 mL). The aqueous solution was added to the reaction mixture and stirred as a cloudy white solution for 45 min. The organic solvents were removed under reduced pressure and the resulting residue was dissolved in 10% K_2CO_3 (350 mL) as a cloudy white suspension. The aqueous layer was partitioned against Et_2O (3 x 75 mL) to remove the Fmoc deprotection side products, after which it was acidified to pH = 2 with concentrated HCl. It was then extracted with DCM (5 x 100 mL). The combined organic layers were then washed with 1N HCl (1 x 100 mL) and brine (1 x 100 mL), dried over $MgSO_4$, filtered, and the filtrate concentrated to a white solid. The solid was dissolved in DCM and purified by column chromatography using 6% MeOH/ DCM as an eluent. A white solid was obtained (1.58 g, 75% yield). R_f = 0.08 in solvent system (A), R_f = 0.23 in solvent system (C); ^1H NMR ($CDCl_3$, 400 MHz) δ 7.75 (d, 2 H, *J* = 7.3 Hz, arom H), 7.60 (d, 2 H, *J* = 7.3 Hz, arom H), 7.39 (t, 2 H, *J* = 7.3 Hz, arom H), 7.30 (t, 2 H, *J* = 7.3 Hz, arom H), 6.12 (d, 1 H, *J* = 6.60 Hz,

NH), 4.58 (m, 1H, α-H), 4.42 (d, J = 7.3 Hz, 2H, Fmoc CH_2), 4.24 (t, 1 H, J = 7.3 Hz, Fmoc CH), 3.29 (s, 2 H, S-CH_2), 3.10 (qd, 2 H, J = 5.8, 14.7 Hz, β-CH_2), 1.50 (s, 9 H, *t*-But H)

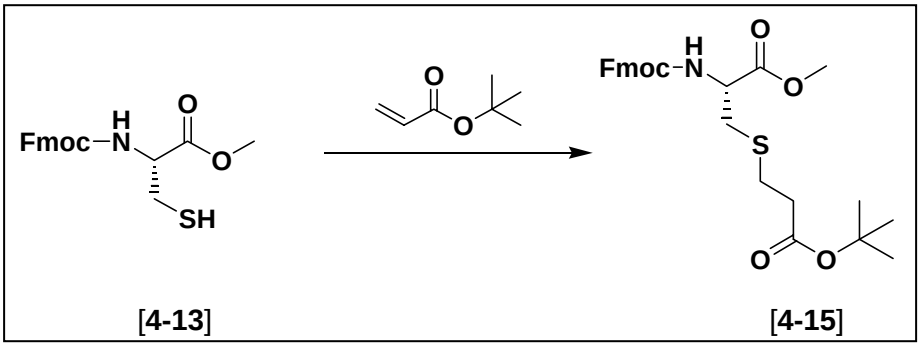

[**4-13**] [**4-15**]

***N*-Fmoc-*S*-(*tert*-Butoxycarbonylethyl)-L-Cysteine methyl ester [4-15]:** *t*-Butyl acrylate (1.14 mL, 7.80 mmol) and TEA (0.72 mL, 5.20 mL) were added to a stirred solution of Fmoc-L-Cysteine methyl ester [**4-13**] (1.86g, 5.20 mmol) in MeOH (40 mL). The reaction was stirred under Ar for 3 h. It was then concentrated under reduced pressure and the residue dissolved in DCM. It was washed with 1N HCl (3 x 10 mL), conc. $NaHCO_3$ (3 x 10 mL), and brine (1 x 15 mL), dried over Na_2SO_4. The solution was filtered and the filtrate concentrated to give a slightly yellow gel (2.36 g, 93% yield). R_f = 0.56 in solvent system (A), R_f = 0.21 in solvent system (B); ^{1}H NMR ($CDCl_3$, 400 MHz) δ 7.76 (d, 2 H, J = 7.3 Hz, arom H), 7.62 (d, 2 H, J = 7.3 Hz, arom H), 7.40 (t, 2 H, J = 7.3 Hz, arom H), 7.31 (t, 2 H, J = 7.3 J Hz, arom H), 5.85 (d, 1 H, J = 7.3 Hz, NH), 4.64 (m, 1 H, α-H), 4.40 (d, 2 H, J = 7.3 Hz, Fmoc CH_2), 4.22 (t, 1 H, J = 7.3 Hz, Fmoc CH), 3.78 (s, 3 H, OMe), 3.02 (d, 2 H, J = 3.7 Hz, β-CH_2), 2.77 (t, 2 H, J = 7.3 Hz, CH_2COO), 2.50 (t, 2 H, J = 7.3 Hz, S-CH_2), 1.50 (s, 9 H, *t*-But H).

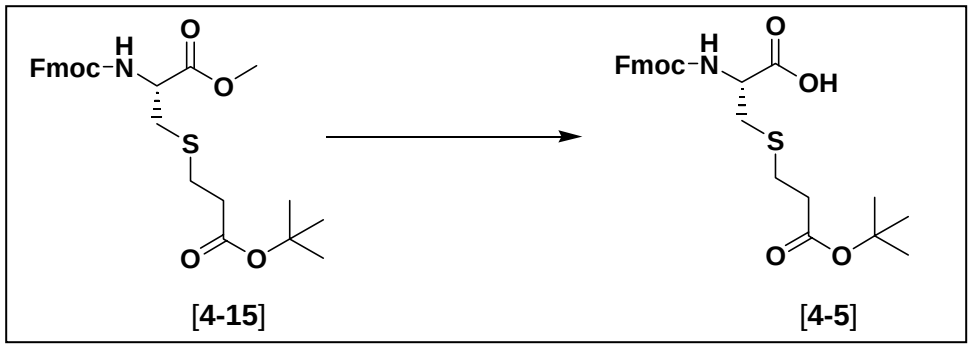

***N*-Fmoc-*S*-(*tert*-Butoxycarbonylethyl)-L-Cysteine [4-5]:** *N*-Fmoc-*S*-(*tert*-butoxycarbonylethyl)-L-Cysteine methyl ester [**4-15**] (2.36g, 4.86 mmol) was dissolved in isopropanol (68 mL). Calcium chloride was added (8.73 g, 78.66 mmol). Separately, $LiOH{\cdot}H_2O$ (0.82 g, 19.44 mmol) was dissolved in H_2O (29 mL). The aqueous solution was then added to the reaction mixture and stirred as a cloudy white suspension for 40 min. The organic solvents were then removed under reduced pressure and the residue dissolved in 10% K_2CO_3 (350 mL) as a cloudy white suspension. It was partitioned against Et_2O (3 x 75 mL) to remove the Fmoc deprotection side products. The aqueous layer was then acidified to pH = 2 with concentrated HCl. It was extracted with DCM (5 x 100 mL). The combined organic extracts were washed with 1N HCl (1 x 100 mL) and brine (1 x 100 mL), dried over $MgSO_4$, filtered, and the filtrate concentrated to a white solid (1.84g, 80% yield). R_f = 0.08 in solvent system (A); ^{1}H NMR ($CDCl_3$, 400 MHz) δ 9.38 (bs, 1 H, COOH), 7.75 (d, 2 H, *J* = 7.3 Hz, arom H), 7.61 (d, 2 H, *J* = 7.3 Hz, arom H), 7.39 (t, 2 H, *J* = 7.3 Hz, arom H), 7.31 (t, 2 H, *J* = 7.3 Hz, arom H), 5.85 (d, 1 H, *J* = 7.3 Hz, NH), 4.67 (m, 1 H, α-H), 4.40 (d, 2 H, *J* = 7.3 Hz, Fmoc CH_2), 4.23 (t, 1 H, *J* = 7.3 Hz, Fmoc CH),

3.06 (d, 2 H, J = 5.1 Hz, β-CH_2), 2.80 (t, 2 H, J = 7.3 Hz, CH_2COO), 2.51 (t, 2 H, J = 7.3 Hz, S-CH_2), 1.50 (s, 9 H, *t*-But H).

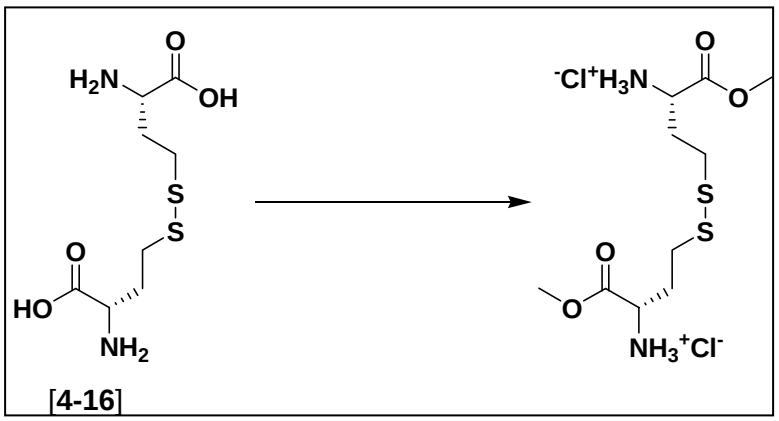

[**4-16**]

L-Homocystine bis-methyl ester·2HCl: L-Homocystine [**4-16**] (1.0 g, 3.75 mmol) was dissolved in MeOH (25 mL). $SOCl_2$ (1.09 mL, 15.02 mmol) was added, drop wise, over 20 min. The reaction was stirred under Ar over night. The reaction was concentrated under reduced pressure to a pale yellow solid (1.39g, quantitative yield): ^{1}H NMR ($CDCl_3$, 400 MHz) δ 4.17 (t, 2 H, J = 6.6 Hz, α-H), 3.82 (s, 6 H, NH_3), 3.69 (s, 6 H, OMe), 2.81 (t, 4 H, J = 7.3 Hz, γ-CH_2), 2.37 (m, 4 H, β-CH_2).

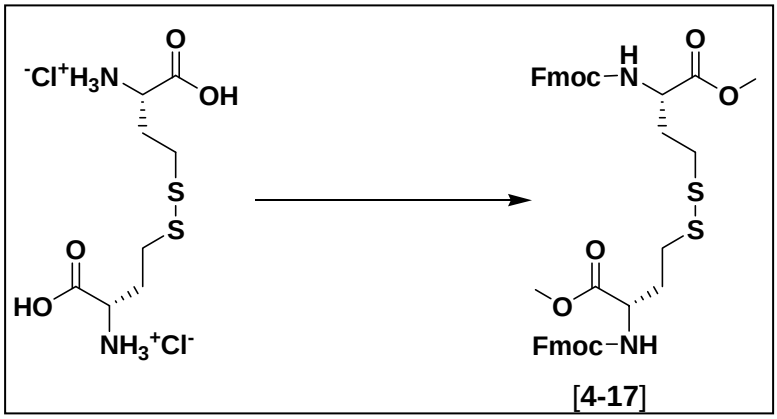

[**4-17**]

Bis-Fmoc-L-Homocystine bis-methyl ester [4-17]: L-Homocystine bis-methyl ester (1.11 g, 3.75 mmol) was placed into a flask. A solution of K_2CO_3 (3.11 g, 22.5 mmol) in H_2O (32 mL) and then added. Fmoc-Cl (1.94 g, 7.5 mmol) was dissolved in dioxane (10 mL) and added to the reaction which became cloudy. After 20 min. a clumpy white solid was floating in the reaction which was broken up with a spatula. It was stirred over night. The reaction was cloudy with fine particles and large chunks of white solid on the bottom. The reaction was sonicated to break up the solid which was then filtered off, washed with MeOH (3 x 15 mL), and dried under reduced pressure to afford a fine white solid (2.65 g, 95% yield). R_f = 0.33 in solvent system (A); ^{1}H NMR ($CDCl_3$, 400 MHz) δ 7.74 (d, 4 H, *J* = 7.3 Hz, arom H), 7.57 (d, 4 H, *J* = 7.3 Hz, arom H), 7.39 (t, 4 H, *J* = 7.3 Hz, arom H), 7.23 (t, 4 H, *J* = 7.3 Hz, arom H), 5.50 (d, 2 H, *J* = 8.0 Hz, NH), 4.49 (m, 2 H, α-H), 4.39 (m, 4 H, Fmoc CH_2), 4.19 (t, 2 H, *J* = 6.6 Hz, Fmoc CH), 3.75 (s, 6 H, OMe), 2.70 (t, 4 H, *J* = 7.3 Hz, γ-CH_2), 2.17 (dm, 4 H, β-CH_2).

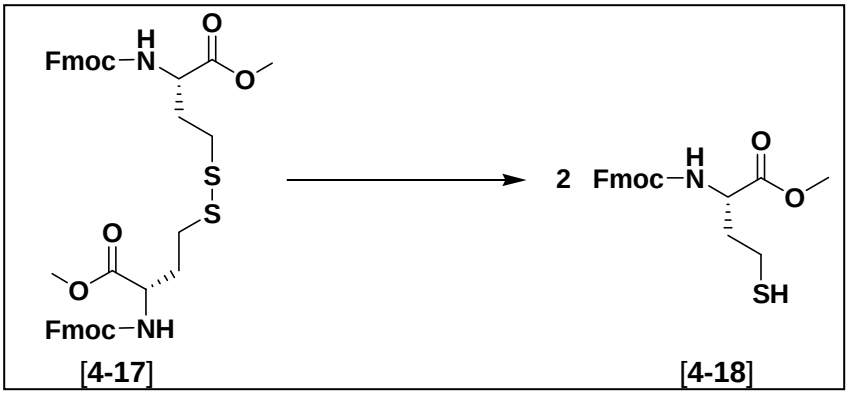

Fmoc-L-Homocysteine methyl ester [4-18]: Bis-Fmoc-L-Homocystine bis-methyl ester [**4-17**] (2.78 g, 3.75 mmol) was dissolved in a mixture of MeOH (150 mL), DCM (40 mL), and TFA (11.56 mL, 150 mmol). Zinc dust (0.74 g, 11.25 mmol) was added and the cloudy white reaction was stirred under Ar over night. The colorless solution was filtered to remove the zinc and the filtrate was concentrated to a white foam. The foam was dissolved in EtOAc and washed with 1N HCl (3 x 10 mL), 1N NaOH (3 x 10 mL), and brine (1 x 10 mL), dried over $MgSO_4$, filtered, and the filtrate concentrated to a white solid (2.45 g, 88% yield). R_f = 0.44 in solvent system (A), R_f = 0.21 in solvent system (B); ^{1}H NMR ($CDCl_3$, 400 MHz) δ 7.75 (d, 2 H, *J* = 7.3 Hz, arom H), 7.59 (d, 2 H, *J* = 7.3 Hz, arom H), 7.39 (t, 2 H, *J* = 7.3 Hz, arom H), 7.23 (t, 2 H, *J* = 7.3 Hz, arom H), 5.34 (d, 1 H, *J* = 8.0 Hz, NH), 4.54 (m, 1 H, α-H), 4.44 (m, 2 H, Fmoc CH_2), 4.22 (t, 1 H, *J* = 6.6 Hz, Fmoc CH), 3.77 (s, 3 H, OMe), 2.55 (m, 2 H, γ-CH_2), 2.05 (dm, 2 H, β-CH_2), 1.55 (t, 1 H, *J* = 8.0 Hz, SH).

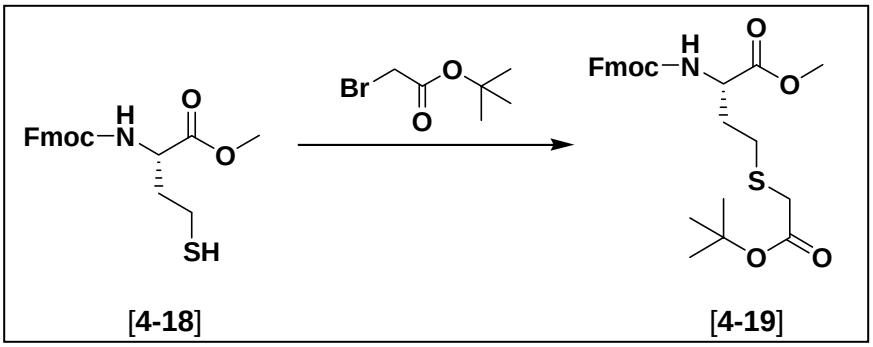

[**4-18**] [**4-19**]

***N*-Fmoc-*S*-(*tert*-Butoxycarbonylmethyl)-L-Homocysteine methyl ester [4-19]:** Fmoc-L-Homocysteine methyl ester [**4-18**] (1.22 g, 3.28 mmol) was dissolved in DMF (20 mL). *t*-Butyl-bromoacetate (0.80 mL, 4.92 mmol) was added followed by Cs_2CO_3 (1.28 g, 3.94 mmol). It was stirred under Ar for 3 h. The reaction was concentrated and the residue partitioned between 1N HCl (25 mL) and DCM (50 mL). The layers were separated and the organic layer was washed with 1N HCl (2 x 15 mL), conc. $NaHCO_3$ (3 x 15 mL), and brine (1 x 20mL), dried over Na_2SO_4, filtered, and the filtrate concentrated to a slightly yellow solid (1.59 g, quantitative yield). R_f = 0.39 in solvent system (B); ^{1}H NMR ($CDCl_3$, 400 MHz) δ 7.76 (d, 2 H, *J* = 7.3 Hz, arom H), 7.60 (d, 2 H, *J* = 7.3 Hz, arom H), 7.40 (t, 2 H, *J* = 7.3 Hz, arom H), 7.31 (t, 2 H, *J* = 7.3 Hz, arom H), 5.49 (d, 1 H, *J* = 8.8 Hz, NH), 4.49 (m, 1 H, α-H), 4.40 (d, 2 H, *J* = 7.3 Hz, Fmoc CH_2), 4.23 (t, 1 H, *J* = 6.6 Hz, Fmoc CH), 3.77 (s, 3 H, OMe), 3.13 (s, 2 H, S-CH_2), 2.67 (t, 2 H, *J* = 7.3 Hz, γ-CH_2), 2.10 (dm, 2 H, β-CH_2), 1.47 (s, 9 H, *t*-But H).

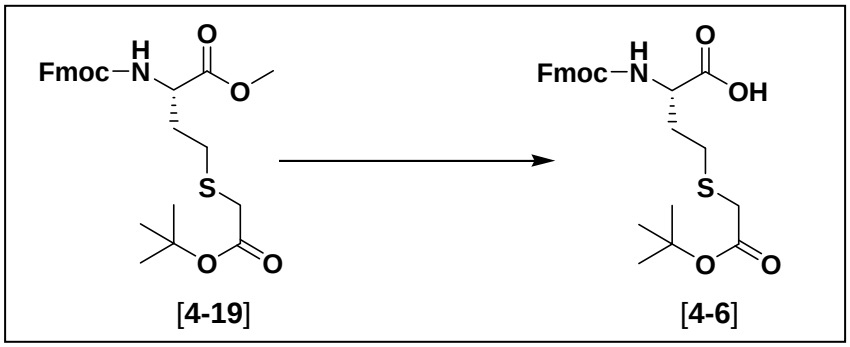

***N*-Fmoc-*S*-(*tert*-Butoxycarbonylmethyl)-L-Homocysteine [4-6]:** *N*-Fmoc-*S*-(*tert*-butoxycarbonylmethyl)-L-Homocysteine methyl ester [**4-19**] (1.59 g, 3.28 mmol) was dissolved in isopropanol (47 mL) and $CaCl_2$ was added (5.94 g, 53.52 mmol). Separately, $LiOH{\cdot}H_2O$ (0.56g, 13.12 mmol) was dissolved in H_2O (20 mL). The aqueous solution was then added to the reaction mixture and stirred as a cloudy white suspension for 2 h. The organic solvents were removed under reduced pressure and the resulting residue dissolved in 10% K_2CO_3 (100 mL) which produced a cloudy white suspension. It was partitioned against Et_2O (3 x 50 mL) to remove the Fmoc-deprotection side products. The aqueous layer was acidified to pH = 2 with concentrated HCl and was then washed with DCM (5 x 75 mL). The combined organic layers were then washed with 1N HCl (1 x 75 mL) and brine (1 x 75 mL), dried over Na_2SO_4, filtered, and the filtrate concentrated to a white solid (1.23 g, 79% yield). R_f = 0.10 in solvent system (A); ^{1}H NMR ($CDCl_3$, 400 MHz) δ 10.03 (bs, 1 H, COOH), 7.76 (d, 2 H, *J* = 7.3 Hz, arom H), 7.60 (d, 2 H, *J* = 7.3 Hz, arom H), 7.40 (t, 2 H, *J* = 7.3 Hz, arom H), 7.31 (t, 2 H, *J* = 7.3 Hz, arom H), 5.49 (d, 1 H, *J* = 8.8 Hz, NH), 4.49 (m, 1 H, α-H), 4.40 (d, 2 H, *J* = 7.3 Hz, Fmoc CH_2), 4.21 (t, 1 H, *J* =

6.6 Hz, Fmoc CH), 3.13 (s, 2 H, S-CH_2), 2.70 (t, 2 H, J = 7.3 Hz, γ-CH_2), 2.10 (dm, 2 H, β-CH_2), 1.47 (s, 9 H, *t*-But H).

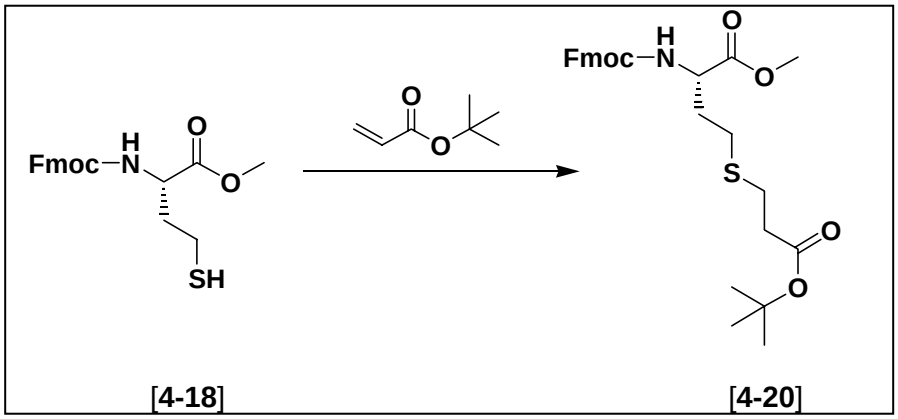

***N*-Fmoc-*S*-(*tert*-Butoxycarbonylethyl)-L-Homocysteine methyl ester [4-20]:** Fmoc-L-Homocysteine methyl ester [**4-18**] (1.00 g, 2.69 mmol) was dissolved in a mixture of MeOH (30 mL) and THF (15 mL). *t*-Butyl acrylate was added (0.59 mL, 4.04 mmol) followed by TEA (0.37 mL, 2.69 mL). It was stirred under Ar for 3 h. The reaction was then concentrated under reduced pressure and the residue dissolved in DCM. It was washed with 1N HCl (3 x 10 mL), conc. $NaHCO_3$ (3 x 10 mL), and brine (1 x 15 mL), dried over Na_2SO_4, filtered, and the filtrate concentrated to a pale yellow solid. The solid was dissolved in DCM and purified by column chromatography using DCM as the eluent. A colorless gel was obtained (0.98 g, 73% yield). R_f = 0.49 in solvent system (A), R_f = 0.10 in solvent system (B), R_f = 0.76 in solvent system (C); ^{1}H NMR ($CDCl_3$, 400 MHz) δ 7.76 (d, 2 H, J = 7.3 Hz, arom H), 7.60 (d, 2 H, J = 7.3 Hz, arom H), 7.40 (t, 2 H, J = 7.3 Hz, arom H), 7.32 (t, 2 H, J = 7.3 Hz, arom H), 5.49 (d, 1 H, J = 6.6 Hz, NH), 4.49 (m, 1 H, α-H), 4.40 (d, 2 H, J = 7.3 Hz, Fmoc

CH_2), 4.21 (t, 1 H, *J* = 7.3 Hz, Fmoc CH), 3.75 (s, 3 H, OMe), 2.74 (t, 2 H, *J* = 7.3 Hz, CH_2COO), 2.53 (m, 4 H, γ-CH_2, S-CH_2), 2.07 (dm, 2 H, β-CH_2), 1.46 (s, 9 H, *t*-But H).

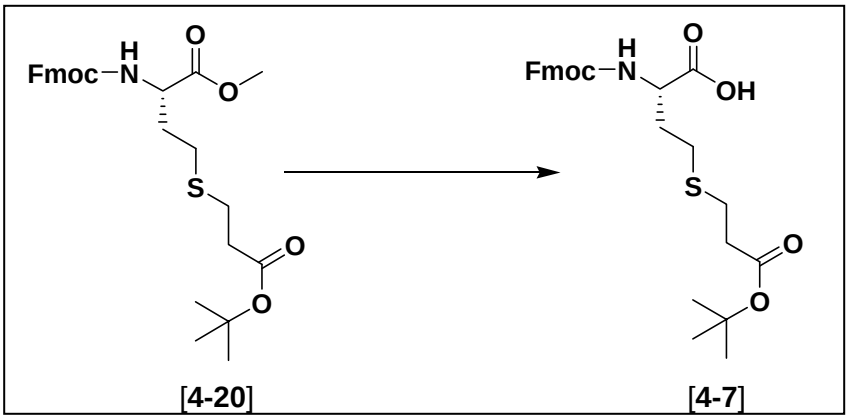

***N*-Fmoc-*S*-(*tert*-Butoxycarbonylethyl)-L-Homocysteine [4-7]** *N*-Fmoc-*S*-(*tert*-butoxycarbonylethyl)-L-Homocysteine methyl ester [**4-20**] (0.56 g, 1.12 mmol) was dissolved in isopropanol (16 mL). Calcium chloride was added (2.02 g, 18.20 mmol). Separately, $LiOH{\cdot}H_2O$ (0.19 g, 4.48 mmol) was dissolved in H_2O (6 mL). The aqueous solution was added to the reaction mixture and then stirred as a cloudy white suspension for 40 min. The organic solvents were removed under reduced pressure and the resulting residue was dissolved in 10% K_2CO_3 (100 mL) which produced a cloudy white suspension. It was partitioned against Et_2O (3 x 25 mL) to remove the Fmoc deprotection side products. The aqueous layer was then acidified to pH = 2 with concentrated HCl and was extracted with DCM (5 x 50 mL). The combined organic extracts were washed with 1N HCl (1 x 25 mL) and brine (1 x 15 mL), dried over

$MgSO_4$, filtered, and the filtrate concentrated to a white solid (0.48 g, 89% yield). R_f = 0.11 in solvent system (A), R_f = 0.20 in solvent system (C), R_f = 0.16 in solvent system (D); ^{1}H NMR ($CDCl_3$, 400 MHz) δ 8.89 (bs, 1 H, COOH), 7.74 (d, 2 H, *J* = 7.3 Hz, arom H), 7.59 (d, 2 H, *J* = 7.3 Hz, arom H), 7.38 (t, 2 H, *J* = 7.3 Hz, arom H), 7.30 (t, 2 H, *J* = 7.3 Hz, arom H), 5.49 (d, 1 H, *J* = 6.6 Hz, NH), 4.49 (m, 1 H, α-H), 4.40 (d, 2 H, *J* = 7.3 Hz, Fmoc CH_2), 4.21 (t, 1 H, *J* = 7.3 Hz, Fmoc CH), 2.74 (t, 2 H, *J* = 7.3 Hz, CH_2COO), 2.60 (t, 2 H, *J* = 6.6 Hz, γ-CH_2), 2.52 (t, 2 H, *J* = 7.3 Hz, S-CH_2), 2.09 (dm, 2 H, β-CH_2), 1.46 (s, 9 H, *t*-But H).

4.5.3 Peptide Synthesis

The peptides were synthesized by stepwise coupling of Fmoc-amino acid derivatives (Fmoc-*t*-Butyl-Glycine, Fmoc-Asp(β-cyclohexyl ester)-OH, Fmoc-Glycine, and Fmoc-Arg(Pbf)-OH) using standard coupling procedures on solid phase Rink amide MBHA resin. Specifically, DIC (3 eq.) and HOBt (3 eq.) in NMP were used as activation reagents for peptide bond formation using 3 equivalents of each amino acid (in relation to the theoretical loading of the resin). Cleavage from the resin, as well as removal of the *t*-butyl esters from the side-chain of the building blocks, was accomplished by treatment with TFA for 1 h. The resin was filtered off and washed with MeOH (5 x 25 mL). The filtrate was concentrated under reduced pressure to a solid, washed with Et_2O (3 x 20 mL), and dried under reduced pressure. The linear peptides were then cyclized using HATU (3 eq.) as an activating agent, in the presence of N-methyl morpholine (7 eq.) in DMF (1 mM) over night. The cyclic peptides were

purified by preparative RP-HPLC using a gradient of ACN in water with 0.3% AcOH. The side-chain cyclohexyl esters were removed by treatment with HF for 1 h in the presence of methyl anisole as a scavenger. The crude peptides were dissolved in H_2O, washed with Et_2O (3 x 50 mL), and lyophilized. The deprotected peptides were purified by preparative RP-HPLC using a gradient of ACN in water with 0.3% AcOH.

c[NH-Arg-Gly-Asp(OcHx)-Asp(OcHx)-tBuG-Cys(S-CH_2-CO)]-NH_2: Purified via preparative HPLC, 90A:10B → 0A:100B/ 100 min; $C_{39}H_{64}N_{10}O_{11}S$ (881 g/mol); LCMS (ES) *m/e* M+H 882, r_t = 9.99 min (90A:10B → 10A:90B/ 12 min) or r_t = 13.45 min (90A:10B → 10A:90B/ 23 min).

c[NH-Arg-Gly-Asp-Asp-tBuG-Cys(S-CH_2-CO)]-NH_2 [4-7]: Purified via preparative HPLC, 100A:0B → 70A:30B, 80 min; $C_{27}H_{44}N_{10}O_{11}S$ (716 g/mol); LCMS (ES) *m/e* M+H 717, r_t = 8.17 min (90A:10B → 10A:90B/ 12 min); Analytical HPLC r_t = 12.61 min (100A:0B → 60A:40B/ 30 min).

c[NH-Arg-Gly-Asp(OcHx)-Asp(OcHx)-tBuG-Cys(S-CH_2-CH_2-CO)]-NH_2: Purified via preparative HPLC, 90A:10B → 0A:100B/ 100 min; $C_{40}H_{66}N_{10}O_{11}S$ (895 g/mol); LCMS (ES) *m/e* M+H 896, r_t = 9.87 min (90A:10B → 10A:90B/ 12 min) or r_t = 13.67 min (90A:10B → 10A:90B/ 23 min).

c[NH-Arg-Gly-Asp-Asp-tBuG-Cys(S-CH_2-CH_2-CO)]-NH_2 [4-8]: Purified via preparative HPLC, 100A:0B → 70A:30B/ 80 min; $C_{28}H_{46}N_{10}O_{11}S$ (730 g/mol); LCMS (ES) *m/e* M+H 731, r_t = 8.46 min (90A:10B → 10A:90B/ 12 min); Analytical HPLC r_t = 12.78 min (100A:0B → 60A:40B/ 30 min).

c[NH-Arg-Gly-Asp(OcHx)-Asp(OcHx)-tBuG-HomoCys(S-CH_2-CO)]-NH_2: Purified via preparative HPLC, 90A:10B → 0A:100B/ 100 min; $C_{40}H_{66}N_{10}O_{11}S$ (895 g/mol); LCMS (ES) *m/e* M+H 896, r_t = 9.93 min (90A:10B → 10A:90B/ 12 min) or r_t = 13.47 min (90A:10B → 10A:90B/ 23 min).

c[NH-Arg-Gly-Asp-Asp-tBuG-HomoCys(S-CH_2-CO)]-NH_2 [4-9]: Purified via preparative HPLC, 100A:0B → 70A:30B/ 80 min; $C_{28}H_{46}N_{10}O_{11}S$ (730 g/mol); LCMS (ES) *m/e* M+H 731, r_t = 9.01 min (90A:10B → 10A:90B/ 12 min); Analytical HPLC r_t = 12.80 min (100A:0B → 60A:40B/ 30 min).

c[NH-Arg-Gly-Asp(OcHx)-Asp(OcHx)-tBuG-HomoCys(S-CH_2-CH_2-CO)]-NH_2: Purified via preparative HPLC, 90A:10B → 0A:100B/ 100 min; $C_{41}H_{68}N_{10}O_{11}S$ (909 g/mol); LCMS (ES) *m/e* M+H 910, r_t = 9.84 min (90A:10B → 10A:90B/ 12 min) or r_t = 13.70 min (90A:10B → 10A:90B/ 23 min).

c[NH-Arg-Gly-Asp-Asp-tBuG-HomoCys(S-CH_2-CH_2-CO)]-NH_2 [4-10]: Purified via preparative HPLC, 100A:0B → 70A:30B/ 80 min; $C_{29}H_{48}N_{10}O_{11}S$ (744 g/mol); LCMS (ES) *m/e* M+H 745, r_t = 8.66 min (90A:10B → 10A:90B/ 12 min); Analytical HPLC r_t = 13.72 min (100A:0B → 60A:40B/ 30 min).

4.5.4 Binding assays

Each well of a microtiter plate (Nunc MaxiSorp) was coated with 120 μL of purified receptor (0.5 μg/mL in assay buffer (2 mM $CaCl_2$, 1 mM $MgCl_2$, 50mM TRIS, 150mM NaCl at pH 7.4)) with 4 mM octyl glucoside overnight at room temperature with shaking. The receptor solution was removed, and each well was washed with 200 μL of 0.5% bovine serum albumin in assay buffer for ten minutes. This step was repeated for a total of three washes. Fifty micro liters of ten-fold dilutions (from 0.0002 to 200 μg/mL) of the inhibitory compounds in assay buffer was added to the wells. Fifty μL of biotinylated ligand (fibrinogen for $\alpha_{IIb}\beta_3$, fibronectin for $\alpha_5\beta_1$, and vitronectin for $\alpha_v\beta_3$, and $\alpha_v\beta_5$) in assay buffer was added to the wells. The plates were sealed and incubated overnight at room temperature with shaking.

The ligand / competitor solution was removed, then each well was washed with 250 μL wash buffer (0.05 % Tween 20, 50 mM TRIS, 150 mM $NaCl_2$, pH 7.4) for five minutes. This step was repeated for a total of three washes. One hundred micro liters of an Avidin Biotin Peroxidase Complex (Pierce Chemical ABC kit 32050) in wash buffer was added to each well. The plates were incubated for 30 minutes at room temperature with shaking. The ABC solution was removed and each well was washed

with 250 μl wash buffer for five minutes. This step was repeated for a total of three washes. One hundred micro liters of a peroxidase substrate (3, 3', 5, 5' tetramethylbenzidine, Pierce Chemical TMB substrate kit 34021) was added to each well.

The conversion of the substrate was monitored kinetically in a microtiter plate reader (Molecular Devices) at 650 nm. Optical density readings were made of each well at 12 second intervals for 10 minutes. The software for the plate reader was used to calculate the concentration at which 50% of the binding of the ligand to the receptor was inhibited (IC_{50}). The maximal velocity of the enzymatic conversion (V_{max}) was calculated for each well and expressed in milli-optical density units per minute (mOD/min). The V_{max} values were plotted as a function of inhibitor concentration, and a four parameter logistic curve was fitted to the data. The inflection point of this curve is the IC_{50}.

4.6 References

1. Haubner, R.; Finsinger, D.; Kessler, H. *Angew. Chem. Int. Ed. Engl.*, **1997**, *36*, 1374-1389.

2. Hynes, R. O. *Cell*, **1987**, *48*, 549-554.

3. Ruoslahti, E. *J. Clin. Invest.*, **1991**, *87*, 1-5.

4. Buck, C. A.; Horowitz, A. F. *Annu. Rev. Cell. Biol.*, **1987**, *3*, 179-205.

5. Hynes, R. O. *Trends Cell Biol.*, **1999**, *9*, M33-37.

6. Giancotti, F. G.; Ruoslahti, E. I. *Science*, **1999**, *285*, 1028-1032.

7. Ruoslahti, E.; Pierschbacher, M. D. *Science*, **1987**, *238*, 491-497.

8. Pierschbacher, M. D.; Ruoslahti, E. *Nature*, **1984**, *309*, 30-33.

9. Carlsson, R.; Engvall, E.; Freeman, A.; Ruoslahti, E. *Proc. Natl. Acad. Sci. U.S.A.*, **1981**, *78*, 2403-2406.

10. Hayman, E. G.; Pierschbacher, M. D.; Ohgren, Y.; Ruoslahti, E. *Proc. Natl. Acad. Sci. U.S.A.*, **1983**, *80*, 4003-4007.

11. Craig, W. S.; Cheng, S.; Mullen, D.; Blevitt, J. M.; Pierschbacher, M. D. *Biopolym. Pept. Sci. Sect.*, **1995**, *37*, 157-175.

12. Lee, J.-O.; Rieu, P.; Bankston, L. A.; Arnaout, M. A.; Liddington, R. *Structure*, **1995**, *3*, 1333-1340.

13. Lee, J.-O.; Rieu, P.; Arnaout, M. A.; Liddington, R. *Cell*, **1995**, *80*, 631-638.

14. Dransfield, I.; Cabanas, C.; Craig, A.; Hogg, N. *J. Cell Biol.*, **1992**, *116*, 219-226.

15. SBusk, M.; Pytela, R.; Sheppard, D. *267*, **1992**.

16. Yanai, T.; Shimooka, T.; Li, I. *Cell Struct. Func.*, **1991**, *16*, 149-156.

17. Altieri, D. C. *J. Immunol.*, **1991**, *147*, 1891-1898.

18. Hemler, M. E. *Annu. Rev. Immunol.*, **1990**, *8*, 365-400.
19. D'Souza, S. E.; Ginsberg, M. H.; Lam, S. C.-T.; Plow, E. F. *Science*, **1988**, *242*, 91-93.

20. Burridge, K.; Fath, K.; Kelly, T.; Nuckolis, B.; Turner, C. *Annu. Rev. Cell. Biol.*, **1988**, *4*, 487-525.

21. Adbelda, S. M.; Buck, C. A. *FASEB J.*, **1990**, *48*, 2868-2880.

22. Kieffer, N.; Phillips, D. R. *Annu. Rev. Cell. Biol.*, **1990**, *6*, 329-357.

23. Cook, N. S.; Kottirsch, G.; Zerwes, H.-g. *Drug Future*, **1994**, *19*, 135-159.

24. Gould, R. J. *Perspect. Drug Discovery Des.*, **1994**, *1*, 537-548.

25. Hawiger, J. *Atheroscler. Rev.*, **1990**, *21*, 165-186.

26. Horton, M. A. *Int. J. Biochem. Cell Biol.*, **1997**, *29*, 721-725.

27. Liotta, L. A.; Steeg, P. S.; Stetler-Stevenson, W. G. *Cell*, **1991**, *327-336*.

28. Savill, J.; Dransfield, I.; Hogg, N.; Haslett, C. *Nature*, **1990**, *343*, 170-173.

29. Grano, M.; Zigrino, P.; Colucci, S.; Zambonin, G.; Trusolino, L.; Serra, M.; Baldini, N.; Teti, A.; Marchisio, P. C.; Zambonin Zallone, A. *Exp. Cell Res.*, **1994**, *212*, 209-218.

30. Horton, M. A.; Taylor, M. L.; Arnett, T. R.; Helfrich, M. H. *Exp. Cell Res.*, **1991**, *195*, 368-375.

31. Noiri, E.; Gailit, J.; Sheth, D.; Magazine, H.; Gurrath, M.; Muller, G.; Kessler, H.; Goligorsky, M. S. *Kidney Int.*, **1994**, *46*, 1050-1058.

32. Brooks, P. C.; Clark, R. A. F.; Cheresh, D. A. *Science*, **1994**, *264*, 569-571.

33. Brooks, P. C.; Montgomery, A. M. P.; Rosenfeld, M.; Reisfeld, R. A.; Hu, T.; Klier, G.; Cheresh, D. A. *Cell*, **1994**, *79*, 1157-1164.

34. Friedlander, M.; Brooks, P. C.; Shaffer, R. W.; Kincaid, C. M.; Varner, J. A.; Cheresh, D. A. *Science*, **1995**, *270*, 1500-1502.

35. Duggan, M. E.; Hutchinson, J. H. *Exp. Opin. Ther. Pat.*, **2000**, *10*, 1367-1383.

36. Carmeliet, P.; Jain, R. K. *Nature*, **2000**, *407*, 249-257.

37. Asahara, T.; Murohara, T.; Sullivan, A.; Silver, M.; van der Zee, R.; Li, T.; Witzenbichker, B.; Shattermann, G.; Isner, J. M. *Science*, **1997**, *275*, 964-967.

38. Kim, S.; Bakre, M.; Yin, H.; Varner, J. A. *J. Clin. Invest.*, **2002**, *110*, 933-941.

39. Cheresh, D. A.; Stupack, D. G. *Nat. Med.*, **2002**, *8*, 193-194.

40. Kim, H. S.; Harris, M.; Varner, J. A. *J. Biol. Chem.*, **2000**, *275*, 33920-33928.

41. Folkman, J.; Shing, Y. *J. Biol. Chem.*, **1992**, *267*, 10931-10934.

42. Luna, J.; Tobe, T.; Mousa, S. A.; Reilly, T. M.; Compochiaro, P. A. *Laboratory Invest.*, **1996**, *75*, 563-573.

43. Kim, S.; Bell, K.; Mousa, S. A.; Varner, J. A. *Am. J. Path.*, **2000**, *156*, 1345-1362.

44. Varner, J. A. In *Cell Adhesion Molecules and Matrix Proteins*; Mousa, S. A., Ed.; Springer: Berlin, Germany, 1998, p 71-84.

45. Felding-Habermann, B.; Fransvea, E.; O'toole, T. E.; Manzuk, L.; Faha, B.; Hensler, M. *Clin. Exp. Metast.*, **2002**, *19*, 427-436.

46. Gehlsen, K. R.; Davis, G. E.; Sriramarao, P. *Clin. Exp. Metast.*, **1992**, *10*, 111-120.

47. Adbelda, S. M.; Motto, S. A.; Elder, D. E.; Stewart, R.; Damjianovich, L.; Herlyn, M.; Buck, C. A. *Cancer. Res.*, **1990**, *50*, 6757-6764.

48. Jin, H.; Varner, J. A. *British J. Cancer*, **2004**, *90*, 561-565.

49. Kerr, J. S.; Slee, A. M.; Mousa, S. A. *Expert Opin. Investig. Drugs*, **2002**, *11*, 1765-1774.

50. Chio, E. T.; Engel, L.; Callow, A. D.; Sun, S.; Trachtenberg, J.; Santoro, S. A.; Ryan, U. S. *J. Vasc. Surg.*, **1994**, *19*, 125-127.

51. Drake, C. J.; Cheresh, D. A.; Little, C. D. *J. Cell Sci.*, **1995**, *108*, 2655-2661.

52. Chorev, M.; Dresner-Pollak, R.; Eshel, Y.; Rosenblatt, M. *Biopolym. Pept. Sci. Sect.*, **1995**, *37*, 367-375.

53. Nicosia, R. F.; Bonanno, E. *Am. J. Path.*, **1991**, *138*, 829-833.

54. Gartner, T. K.; Bennet, J. S. *J. Biol. Chem.*, **1985**, *260*, 11891-11894.

55. Gilmore, A. P.; Burridge, K. *Structure*, **1996**, *4*, 647-651.

56. Ruoslahti, E. *Cell Biology of Extracellular Matrix*; Plenum Press, New York, 1991.

57. Ali, F. E.; Calvo, R.; Romoff, T.; Samanen, J.; Nichols, A.; Store, B. In *Pepties: Chemistry, Structure, and Biology. Proceedings of the 11th American Peptide Symposium*; Rivier, J. E., Marshall, G. R., Eds.; ESCOM: Leiden, Netherlands: 1990, p 94-96.

58. Nutt, R. F.; Brady, S. F.; Sisko, J. T.; Ciccarone, T. M.; Colton, C. D.; Levy, M. R.; Gould, R. J.; Zhang, G.; Friedman, P. A.; Veber, D. F. In *Pept. Proc. Eur. Pept. Symp. 21th*; Giralt, E., Andreu, D., Eds.; ESCOM: Leiden, Neth.: 1991, p 784-786.

59. Dechantsreiter, M. A.; Planker, E.; Mathae, B.; Lohof, E.; Hoelzemann, G.; Jonczyk, A.; Goodman, S. L.; Kessler, H. *J. Med. Chem.*, **1999**, *42*, 3033-3040.

60. Schabbert, S.; Pierschbacher, M. D.; Mattern, R. H.; Goodman, M. *Bioorg. Med. Chem.*, **2002**, *10*, 3331-3337.

61. Aumailley, M.; Gurrath, M.; Mueller, G.; Calvete, J.; Timpl, R.; Kessler, H. *FEBS Lett.*, **1991**, *291*, 50-54.

62. Haubner, R.; Schmitt, W.; Hoelzemann, G.; Goodman, S. L.; Jonczyk, A.; Kessler, H. *J. Am. Chem. Soc.*, **1996**, *118*, 7881-7891.

63. Haubner, R.; Gratias, R.; Diefenbach, B.; Goodman, S. L.; Jonczyk, A.; Kessler, H. *J. Am. Chem. Soc.*, **1996**, *118*, 7461-7472.

64. Burgess, K.; Lim, D.; Mousa, S. A. *J. Med. Chem.*, **1996**, *39*, 4520-4526.

65. Mullen, D. G.; Cheng, S.; Ahmed, S.; Blevitt, J. M.; Bonnin, D.; Craig, W. S.; Ingram, R. T.; Minasyan, R.; Tolley, J. O.; Tschopp, J. F.; Pierschbacher, M. D. In *Peptides: Chemistry, Structure, and Biology. Proceedings of the 14th American Peptide Symposium*; Kaumaya, P. T. P., Hodges, R. S., Eds.; Mayflower Scientific Ltd: West Midlands, UK: 1996, p 207-208.

66. Jennings, L. K.; Phillips, D. R. *J. Biol. Chem.*, **1982**, *257*, 10458-10466.

67. Coller, B. S.; Peerschke, E. I.; Scudder, L. E.; Sullivan, C. A. *J. Clin. Invest.*, **1983**, *72*, 325-338.
68. Shadle, P. J.; Ginsberg, M. H.; Plow, E. F.; Barondes, S. H. *J. Cell Biol.*, **1984**, *99*, 2056-2060.

69. Tschopp, J. F.; Driscoll, E. M.; Mu, D. X.; Black, S. C.; Pierschbacher, M. D.; Lucchesi, B. R. *Coron. Artery Dis.*, **1993**, *4*, 809-817.

70. Cheng, S.; Craig, W. S.; Mullen, D.; Tschopp, J. F.; Dixon, D.; Pierschbacher, M. D. *J. Med. Chem.*, **1994**, *37*, 1-8.

71. Locardi, E.; Mullen, D. G.; Mattern, R. H.; Goodman, M. *J. Pept. Sci.*, **1999**, *5*, 491-506.

72. Rew, Y.; Malkmus, S.; Svensson, C.; Yaksh, T. L.; Chung, N. N.; Schiller, P. W.; Cassel, J. A.; DeHaven, R. N.; Goodman, M. *J. Med. Chem.*, **2002**, *45*, 3746-3754.

73. Li, H.; Jiang, X.; Howell, S. B.; Goodman, M. *J. Pept. Sci.*, **2000**, *6*, 26-35.
74. Osapay, G.; Prokai, L.; Kim, H. S.; Medzihradszky, K. F.; Coy, D. H.; Liapakis, G.; Reisine, T.; Melacini, G.; Zhu, Q.; Wang, S. H.; Mattern, R. H.; Goodman, M. *J. Med. Chem.*, **1997**, *40*, 2241-2251.

75. Melacini, G.; Zhu, Q.; Osapay, G.; Goodman, M. *J. Med. Chem.*, **1997**, *40*, 2252-2258.

76. Li, H.; Jiang, X.; Goodman, M. *J. Pept. Sci.*, **2001**, *7*, 82-91.

77. Harpp, D. N.; Gleason, J. G. *J. Org. Chem.*, **1971**, *36*, 73-80.

78. Kitazawa, M.; Fukase, K.; Wakamiya, T.; Shiba, T. *Pept. Chem.*, **1987**, *24*, 317-322.

79. Osapay, G.; Wang, S.; Comer, D. D.; Toy-Palmer, A.; Zhu, Q.; Goodman, M. In *Peptides: Chemistry, Structure, and Biology. Proceedings of the 13th American Peptide Symposium*; Hodges, R. S., Smith, J. A., Eds.; ESCOM: Leiden, Neth.: 1993, p 435-437.

80. Polinsky, A.; Cooney, M. G.; Toy-Palmer, A.; Osapay, G.; Goodman, M. *J. Med. Chem.*, **1992**, *35*, 4185-4194.

81. Cavelier-Frontin, F.; Daunis, J.; Jacquier, R. *Tetrahedron Asymm.*, **1992**, *3*, 85-94.

82. Pu, Y.; Martin, F. M.; Vederas, J. C. *J. Org. Chem.*, **1991**, *56*, 1280-1283.
83. Shao, H.; Wang, S. H. H.; Lee, C. W.; Osapay, G.; Goodman, M. *J. Org. Chem.*, **1995**, *60*, 2956-2957.

84. Photaki, I. *J. Am. Chem. Soc.*, **1963**, *85*, 1123-1126.

85. Nakajima, K.; Oda, H.; Okawa, K. *Bull. Chem. Soc. Jpn.*, **1983**, *56*, 520-522.

86. Photaki, I.; Samouilidis, I.; Caranikas, S.; Zervas, L. *J. Chem. Soc., Perkin Trans, 1*, **1979**, 2599-2605.

87. Wakamiya, T.; Oda, Y.; Fukase, K.; Shiba, T. *Bull. Chem. So. Jpn*, **1985**, *58*.

88. Fukase, K.; Kitazawa, M.; Sano, A.; Shimbo, K.; Horimoto, S.; Fujita, H.; Kubo, A.; Wakamiya, T.; Shiba, T. *Bull. Chem. Soc. Jpn.*, **1992**, *65*, 2227-2240.

89. Dugave, C.; Menez, A. *Tetrahedron Asymm.*, **1997**, *8*, 1453-1465.

90. Gimbrone, M. A.; Cotran, R. S.; Leapman, S. B.; Folkman, J. *J. Natl. Cancer Inst.*, **1974**, *52*, 413-419.